



# THE UNIVERSITY *of* EDINBURGH

This thesis has been submitted in fulfilment of the requirements for a postgraduate degree (e.g. PhD, MPhil, DClInPsychol) at the University of Edinburgh. Please note the following terms and conditions of use:

This work is protected by copyright and other intellectual property rights, which are retained by the thesis author, unless otherwise stated.

A copy can be downloaded for personal non-commercial research or study, without prior permission or charge.

This thesis cannot be reproduced or quoted extensively from without first obtaining permission in writing from the author.

The content must not be changed in any way or sold commercially in any format or medium without the formal permission of the author.

When referring to this work, full bibliographic details including the author, title, awarding institution and date of the thesis must be given.

# The Three-Loop Soft Anomalous Dimension of Massless Multi-Leg Scattering

Øyvind Almelid



Doctor of Philosophy  
The University of Edinburgh  
April 2016



# Abstract

Infrared (IR) singularities are a salient feature of any field theory containing massless fields. In Quantum Chromodynamics (QCD), such singularities give rise to logarithmic corrections to physical observables. For many interesting observables, these logarithmic corrections grow large in certain areas of phase space, threatening the stability of perturbative expansion and requiring resummation.

It is known, however, that IR singularities are universal and exponentiate, allowing one to study their all-order behaviour in any gauge theory by means of so-called webs: specific linear combinations of Feynman diagrams with modified colour factors corresponding to those of fully connected trees of gluons.

Furthermore, infrared singularities factorise from the hard cross-section into soft and jet functions. The soft function may be calculated as a correlator of Wilson lines, vastly simplifying the computation of IR poles and allowing analytic computation at high loop order. Renormalisation group equations then allow the definition of a soft anomalous dimension, which may then be directly computed either through differential equations or by a direct, diagrammatic method.

Soft singularities are highly constrained by rescaling symmetry, factorisation, Bose symmetry, and high energy- and collinear limits. In the case of light-like external partons, this leads directly to a set of constraint equations for the soft anomalous dimension, the simplest solution of which is a sum over colour dipoles. At two loops, this so-called dipole formula is the only admissible solution, leading to the complete cancellation of any tripole colour structure. Corrections beyond the dipole formula may first be seen at three loops, and must take the form of weight five polylogarithmic functions of conformal invariant cross-ratios, correlating four hard jets through a quadrupole colour structure.

In this thesis we calculate this first correction beyond the dipole formula by considering three-loop multiparton webs in the asymptotic limit of light-like

external partons. We do this by computing all relevant webs correlating two, three and four lines at three loop order by means of an asymptotic expansion of Mellin-Barnes integrals near the limit of light-like external partons.

We find a remarkably simple result, expressible entirely in terms of Brown's single-valued harmonic polylogarithms, consistent with high-energy and forward scattering limits.

Finally, we study the behaviour of this correction in the limit of two partons becoming collinear, and discuss collinear factorisation properties.

# Lay Summary

Because of the high level of specialisation needed to do research in particle physics, people who work on experiments very rarely also work on theory, and vice versa. Furthermore, taking a complex theory of fundamental particles – be it the standard model or some more exotic theory of new physics – and producing predictions which can be tested in an experiment like the Large Hadron Collider is a large and complicated task, involving large amounts of mathematics, computer simulation and statistics. Indeed, taking a theory from an equation on a blackboard and bringing it to the stage where it can be tested requires the work of researchers with a great many different specialisations, loosely gathered under the umbrella term of “phenomenology”. Physicists in this field tend to concern themselves with a few key questions:

- How can I tell different theories of particle physics apart in an experiment?
- What do these theories have in common, and what sets them apart?
- In this theory, what is the probability of producing particle X in a collider experiment at energy Y?
- What are the error bars on this prediction, and how can I get a more precise prediction?

In addition, some physicists are interested in understanding the mathematical properties of theories, in the hopes that this will lead to better ways of either performing these calculations, or a better understanding of the theory itself.

In this thesis, I study a feature shared by all theories of particle physics: so-called infrared singularities. Infrared singularities are a mathematical property of any theory which contains massless particles, and the exact behaviour of these particles makes a large difference to predictions for experiments. I calculate these

singularities at higher precision than has been done before, and in a way such that it can be applied to any theory of particle physics. This is interesting both for understanding the mathematics of particle physics, and hopefully it will also help contribute to higher precision predictions for experimental results.

# Declaration

I declare that this thesis was composed by myself, that the work contained herein is my own except where explicitly stated otherwise in the text, and that this work has not been submitted for any other degree or professional qualification except as specified.

Parts of this work have been published in [1].

*(Øyvind Almelid, April 2016)*





# Acknowledgements

I wish to thank my supervisor Einan Gardi, for many useful discussions, guidance, and for his time and patience. His enthusiasm for physics and dedication to detail has been of enormous value to me throughout my PhD. Many thanks also go to Claude Duhr for all his help and collaboration, without which this work would not have been possible. I also wish to thank Vittorio Del Duca for welcoming me to Rome and letting me work at La Sapienza, and Lorenzo Magnea for his hospitality in letting me visit Turin.

Special thanks also go to everyone else whose work on three-loop multiparton webs has been used in this thesis: Chris White, Jennifer Smillie, Mark Harley, Giulio Falcioni, Lorenzo Magnea, Mairi McKay, Alastair Heffernan, Rebecca Lodin. Without your contributions it would not have been possible to perform this calculation.

Special thanks go to Mark Harley and Samuel Abreu for many useful discussions on soft singularities, polylogarithms and other things. Thanks to James Carrington for help with Mathematica and programming. To Anne Pawsey, Ben Wynne, Catherine Lee, Kym Eden, Robert Concannon: thanks for all the fish. To Ömer Gurdogan, Hjalte Frellesvig, Francesco Moriello who made my stay in Rome so very fun. To Kristel Torokoff for all her guidance and support in my teaching work.

I also wish to thank my many office mates: Enrico Rinaldi, Pan Kessel, Nico Kronberg, Valentina Verducci, Samuel Abreu, Eliana Lambrou, Vladimir Prochazka, Sam Bartrum, Jack Medley, Andries Waelkens, Ava Khamseh and Gustav Mogull.

Thanks to my family: Ragnhild, Kaare, Janos, Marianne, Fridtjof, Jannike. Your support means a lot to me. Special thanks to Ragna, for her never-ending enthusiasm.

Many thanks also to the many other people on the PPT corridor, in condensed matter, particle physics experiment and elsewhere who have made the last four years in Edinburgh fun.

Finally, huge thanks to my girlfriend Hannah. Words cannot describe how grateful

I am for all her love, support and patience.

# Contents

<b>Abstract</b>	i
<b>Lay Summary</b>	iii
<b>Declaration</b>	v
<b>Acknowledgements</b>	vii
<b>Contents</b>	ix
<b>List of Figures</b>	xv
<b>List of Tables</b>	xix
<b>Glossary</b>	xxi
<b>1 Introduction and Background</b>	1
1.1 A One-Loop Example .....	5
1.2 The Soft Anomalous Dimension.....	9
1.2.1 IR-UV Connection and The Soft Anomalous Dimension .....	12
1.2.2 Colour Algebra .....	13
1.2.3 Constraint Equations and The Dipole Formula.....	13
1.2.4 Kinematic Dependence of Three-loop Corrections to the Dipole Formula .....	17

1.2.5	The Soft Anomalous Dimension on Massive Wilson Lines ...	18
1.2.6	Exponentiation and Renormalisation of the Multi-Parton Soft Anomalous Dimension .....	19
1.2.7	Feynman Rules for Multi-Parton Webs in Configuration Space.....	22
1.2.8	Regge Limits .....	24
1.2.9	Collinear Factorisation.....	25
1.3	Mellin-Barnes Integration and Asymptotic Expansion.....	25
1.3.1	Integration Contours .....	28
1.3.2	Parametrising Mellin-Barnes integrals.....	30
1.3.3	Asymptotic Expansions.....	32
1.4	Polylogarithms .....	33
1.4.1	Multiple Polylogarithms .....	34
1.4.2	Algebra and Coalgebra.....	35
1.4.3	Parameter Integrals.....	36
1.4.4	Single-Valued Harmonic Polylogarithms.....	38
<b>2</b>	<b>The Soft Anomalous Dimension at Two Loops</b>	<b>41</b>
2.1	Two-loop Calculation of the Three-line Two-loop Web.....	41
2.1.1	The Scalar Three-mass Triangle .....	44
2.1.2	Feynman Parameters.....	45
2.1.3	Alpha Parameters.....	47
2.2	The Two-loop Soft Anomalous Dimension in the limit of Light-Like External Partons.....	48
<b>3</b>	<b>Colour Conservation at Three Loops</b>	<b>51</b>
3.1	$\Gamma^S$ on Four Lines .....	52

3.2	Four-Line Webs .....	52
3.3	Three-Line Webs.....	54
3.3.1	Colour Conservation.....	54
3.4	Two-Line Webs .....	55
3.4.1	Colour Conservation.....	56
3.5	Colour Conservation in $\Gamma^S$ .....	57
3.6	$\Gamma^S$ on Three Lines.....	59
<b>4</b>	<b>Computing Webs at Three Loops</b>	<b>61</b>
4.1	General Overview.....	62
4.2	Webs Containing Gluon-Gluon Interactions.....	66
4.2.1	Vertex Integrals and Dual Momentum Space Representations.....	68
4.2.2	Vertex Differentiation and Parameter Integration.....	71
4.2.3	Asymptotic Expansion .....	73
4.2.4	Parametrisation.....	74
4.2.5	Numerical Evaluation of MB Integrals.....	74
4.3	Collinear Reduction.....	75
<b>5</b>	<b>Results for Three-loop Webs in Lightlike Kinematics</b>	<b>77</b>
5.1	Four-line webs.....	79
5.1.1	The Four-Line Four-Gluon Vertex .....	79
5.1.2	The Four-Line Double Three-Gluon Vertex.....	79
5.1.3	The 1121-web .....	80
5.1.4	Multiple Gluon Exchange Webs .....	82

5.2	Three-line webs .....	83
5.2.1	Fully connected graphs .....	84
5.2.2	Webs Containing a Single Three Gluon Vertex .....	88
5.2.3	Webs with Vertex Corrections .....	91
5.2.4	Three-line Multiple Gluon Exchange Webs .....	93
5.3	Two-Line Webs .....	95
5.3.1	Fully Connected Webs .....	95
5.3.2	Webs Containing Three Gluon Vertices.....	97
5.3.3	Webs With Vertex Corrections.....	98
5.3.4	Multiple Gluon Exchange Webs .....	99
<b>6</b>	<b>The Quadrupole Correction to the Soft Anomalous Dimension</b>	<b>101</b>
6.1	Assembling all two-line diagrams .....	101
6.2	Assembling all three-line diagrams .....	102
6.3	Combining Two-Line and Three-Line Webs.....	103
6.4	Four-line diagrams .....	104
6.4.1	Combining all fully connected diagrams. ....	105
6.4.2	The 1221-web and the 1121-web.....	107
6.4.3	The 1113-web .....	108
6.4.4	Combining all Four-Line Diagrams .....	110
6.5	Assembling all diagrams .....	111
<b>7</b>	<b>The Regge Limit</b>	<b>113</b>
<b>8</b>	<b>Collinear Limits</b>	<b>121</b>

<b>9</b>	<b>Concluding Remarks and Outlook</b>	127
	<b>Appendices</b>	129
<b>A</b>	<b>Full Calculation of the Four-Line Four-Gluon Vertex Diagram</b>	131
<b>B</b>	<b>Full Calculation of the Four-Line Double Three-Gluon Vertex Diagram</b>	137
<b>C</b>	<b>Full Calculation of the Three-Line Four-Gluon Vertex Diagram</b>	143
<b>D</b>	<b>Full Calculation of the Three-Line Double Three-Gluon Vertex Diagram</b>	149
<b>E</b>	<b>Full Calculation of the 311-Web</b>	155
<b>F</b>	<b>Collinear reduction of the 23-Web</b>	159
	<b>Bibliography</b>	161





# List of Figures

1.1	Single emission of soft gluon from an external parton emerging from an arbitrary process $P$ . . . . .	5
1.2	One-loop QCD correction to the gluon-fermion coupling. . . . .	7
1.3	Schematic depiction of factorisation, as in eq. (1.16). . . . .	10
1.4	Examples of color-connected and disconnected two-line diagrams. . . . .	19
1.5	Example of effective vertex diagrams contributing to different exponentiated colour factors (ECFs) in $w_{(33)}$ . . . . .	21
1.6	A scalar triangle with powers $\nu_i$ of the propagators and incoming off-shell momenta $p_i$ , as in eq. (1.68) . . . . .	26
1.7	Contour shift to regulate $z_2$ . From the initial contour (a), crossing the pole at $z_2 = -\epsilon - z_1$ (b) causes us to pick up its residue (c). . . . .	29
2.1	Web topologies correlating three lines at two loops. . . . .	42
2.2	A three-mass scalar triangle. . . . .	43
3.1	Maximally Non-Abelian Colour Structure on Four Lines . . . . .	53
4.1	Four-line webs containing gluon-gluon interactions. . . . .	61
4.2	Representative diagrams for each four-line multiple gluon exchange-web. . . . .	62
4.3	Web with tripole colour factor, which we discard. . . . .	63
4.4	Fully connected three-line webs contribution to $H_3$ . . . . .	63
4.5	Representative diagrams of three-line webs contributing to $H_3$ which contain a single three-gluon vertex. . . . .	64

4.6	Representative diagram of web with vertex correction contributing to $H_3$ . . . . .	64
4.7	Representative diagrams of three-line multiple gluon exchange webs (MGEWs) contributing to $H_3$ . . . . .	65
4.8	Fully connected two-line webs contributing to $H_2$ . . . . .	65
4.9	The 23-web, which contributes to $H_2$ . . . . .	65
4.10	Representative diagrams of MGEWs with and without vertex corrections that contribute to $H_2$ . . . . .	66
4.11	Gluon vertex integrals and corresponding dual diagrams. . . . .	69
4.12	Collinear reduction of $w_{(1112)}$ to $w_{122}$ . . . . .	76
5.1	Fully connected webs connecting four lines. . . . .	78
5.2	One of two graphs with single three gluon vertex contributing to $w_{1112}$ . . . . .	78
5.3	Representative diagrams of four-line MGEWs. . . . .	78
5.4	Fully connected three-line diagrams contributing to $H_3$ . . . . .	84
5.5	Representative diagrams of three-line webs containing a single three-gluon vertex. . . . .	88
5.6	Collinear reduction of $w_{(1112)}$ , to $w_{(221)}$ . . . . .	89
5.7	Representative diagram of the 411-web: $w_{(411)}$ . . . . .	91
5.8	Three-line MGEWs. . . . .	92
5.9	Fully connected two-line webs. . . . .	96
5.10	Representative diagram from the 32-web, $w_{32}$ . . . . .	98
5.11	Representative diagram of the 24-web, $w_{42}$ . . . . .	98
5.12	$w_{33}(\alpha_{12})$ . . . . .	99
5.13	Collinear reduction of $w_{1221}$ to $w_{33}$ , note the symmetry $\beta_1 \leftrightarrow \beta_2$ in $w_{33}$ , not present in $w_{123}$ . . . . .	100
7.1	Analytic continuation contours for $z$ and $\bar{z}$ for the case of $\beta_1$ and $\beta_2$ incoming, both contours are continuing in the clockwise direction.	114
7.2	Example t-channel exchange in clockwise labelling convention. . .	117

A.1	The four-gluon vertex web $w_{4g}$ . . . . .	132
A.2	The four mass box, $\text{Box}(\{p_i\})$ . . . . .	133
B.1	$w_{(12)(34)}$ . . . . .	137
B.2	The slashed four mass box $S(\{p_i^2\}, s, t)$ . . . . .	139
C.1	Three-line four-gluon vertex $w_{(4g),3}(\alpha_{12}, \alpha_{13}, \alpha_{23})$ . . . . .	144
D.1	Hard three-line double three gluon vertex . . . . .	150
F.1	Representative diagram of the 23-web. . . . .	159



# List of Tables

1.1	Some examples of Brown's single-valued harmonic polylogarithms.	40
7.1	Analytic continuation of $u$ , $v$ , $z$ , and $\bar{z}$ to the forward scattering region. We give the total phase change of $u$ and $v$ , and the corresponding transformation of $z$ and $\bar{z}$ , where we have abbreviated the direction of the contours as c. for clockwise and c.c. for counterclockwise. . . . .	114



# Glossary

**CICR** conformal invariant cross ratio. 3, 15–17, 79, 106, 113

**ECF** exponentiated colour factor. xv, 20, 21

**IR** infrared. 1–3, 5, 7–9, 11–13, 22, 127

**MB** Mellin-Barnes. 4, 18, 25–28, 30–33, 36, 66, 70, 71, 74, 87, 128, 150, 151

**MGEW** multiple gluon exchange webs. xvi, 63, 65, 66, 78–80, 82, 83, 89, 90, 92, 99, 106, 157

**MPL** multiple polylogarithms. 34–38

**RG** renormalisation group. 1, 2, 12–14

**SVHPL** single-valued harmonic polylogarithm. 114

**UV** ultraviolet. 1, 2, 7, 8, 12





# Chapter 1

## Introduction and Background

The study and treatment of singularities is an integral part of perturbative quantum field theory. In the case of ultraviolet (UV) singularities, the process of renormalisation has both cured the singularities and provided us with a new understanding of quantum field theories through renormalisation group (RG) equations (see e.g. [2], a concise modern introduction is given in [3], or in e.g. [4, 5]).

In addition to UV singularities, any theory with massless fields also has infrared (IR) singularities, i.e. singularities associated with the emission and re-absorption of one or more low-energy particles. The existence of such IR singularities is thus a general property of gauge theories with massless gauge bosons, such as Quantum Electrodynamics or Quantum Chromodynamics.

IR singularities may arise in two distinct, but overlapping regions of phase space. Firstly, massless particles give rise to singularities when their energy becomes small, we refer to such singularities as *soft* singularities. Secondly, when two massless particles become *collinear*, they give rise to so-called collinear singularities, resulting in *jets*. A key distinction is whether a scattering amplitude has massless or massive external states, since the latter only contains soft singularities, not collinear ones.

IR singularities are treated in cross-sections through the sum of virtual corrections and diagrams containing real emissions, integrated over some appropriate region

of phase space (see e.g. [6]). Schematically this looks like

$$\underbrace{\frac{1}{\epsilon}}_{\text{virtual}} - \underbrace{Q^{2\epsilon} \int_0^{m^2} \frac{dk^2}{(k^2)^{1+\epsilon}}}_{\text{real}} \propto \log\left(\frac{m^2}{Q^2}\right) + \mathcal{O}(\epsilon), \quad (1.1)$$

where  $Q$  is some hard scale associated with the relevant observable (e.g. the center-of-mass energy of a scattering event), and  $m^2$  is some small scale which depends on the observable (e.g. a jet mass).

Treatment and cancellation of IR singularities was first understood in the context of QED by Bloch and Nordsieck [7]. More generally, the safe treatment of IR singularities is guaranteed for so-called infrared safe observables by the Kinoshita-Lee-Nauenberg (KLN) theorem [8, 9]. However, if a process has a large *hierarchy of scales*, i.e.  $\alpha_s \log(Q^2/m^2) \sim 1$ , perturbative expansion breaks down. For this reason, it is vital to calculate, classify and resum (see e.g. [10, 11]) IR singular contributions to scattering amplitudes.

The history of IR singularities dates back over three decades, from early treatments in quantum electrodynamics (see e.g. [12]), to more general treatments in a variety of non-Abelian gauge theories [6, 13–34]. Apart from the direct need to compute and resum IR singularities for phenomenological reasons, they also have a number of features which make them interesting from a purely theoretical standpoint. For one thing, they are universal [13], enabling computation for a general scattering process in a given field theory.

Furthermore, we will see in section 1.2.6 that certain IR-singular contributions share kinematic structure in a way which enables their computation in a general gauge theory. For these contributions, useful constraints may be obtained by requiring compatibility with different theories. Notably, compatibility with  $\mathcal{N} = 4$  Super Yang-Mills will require that our final result in chapter 6 must be composed of polylogarithms of uniform transcendental weight  $2l + 1$  [35]<sup>1</sup>.

Secondly, an observation was made in [18], which relates the structure of soft singularities to those of UV singularities of a correlator of Wilson lines. This enables us to study the structure of IR singularities by means of RG equations. Such RG considerations have led to the ability to directly compute a *soft anomalous dimension* (defined in section 1.2), which simplifies the process of exponentiating IR poles. This RG approach has been studied extensively and yields insights into

---

<sup>1</sup>We will discuss polylogarithms and transcendental weight in section 1.4

the all-order structure generated by soft gluons [18, 27–33, 35–61].

Exponentiation can also be achieved through the study of so-called webs, which enables the direct diagrammatic computation of the soft anomalous dimension [15–17, 19–26]. The study of such webs is of mathematical interest, as they reveal a rich, iterative structure of the exponentiated IR poles.

Furthermore, both of these methods reveal a startling simplicity in taking the soft limit, which both motivates and enables analytic computation. Thus, IR singularities are known in general at two-loop accuracy for both light-like [27] and massive [28–31] external partons.

Both direct calculation [27–31] and theoretical considerations [32, 33, 35, 50, 62, 63] reveal a startling simplicity in the structure of IR singularities. This is understood as a consequence of rescaling invariance, Bose symmetry, high-energy limits other general considerations which serve to constrain the structure of soft singularities.

A direct study of these constraints revealed a possible all-order solution for the soft singularities of massless external partons to be a sum over colour dipoles (which we will outline in section 1.2.3) [32, 33, 37]. This solution is the only permissible solution at two loops. At three loops, there may be corrections composed of specific kinematic invariants known as conformal invariant cross ratios (CICRs), and at four loops we may see contributions arise due to quartic casimir operators. Indeed, theoretical considerations have shown that the so-called sum-over-dipole formula receives corrections at four loops [34], though as yet no complete analytic computation has been performed beyond two loops.

Besides the clear interest in understanding soft singularities at three loops for theoretical reasons, a full three-loop calculation would also be useful for practical applications. Firstly, understanding the complete structure of soft singularities at three loops will serve as a check of any three-loop calculation. Since parts of the work in this thesis were published in [1], such a calculation has in fact been performed [64], and the results confirm our findings.

Furthermore, a complete three-loop calculation is of relevance to resummation of observables involving three or more hard external partons (see e.g. [10, 11]). Such resummation involves also the real (and process-specific) terms, which would have to be computed and taken into account to the same order in perturbation theory. Nonetheless, a full three-loop calculation of the soft anomalous dimension would eventually be applicable at a sufficiently high logarithmic order to many processes

(see e.g. [65–68]).

In this thesis, we will aim to calculate the three-loop contributions to the exponent for soft singularities containing massless external partons. Our general strategy will be to work on a process containing only massive external partons, thus avoiding the issue of collinear divergences. We will then perform an asymptotic expansion around the limit of massless external states in order to obtain the required corrections to the dipole formula.

We will begin by considering a simple one-loop example in section 1.1. We will then take some time to study the soft anomalous dimension in section 1.2: starting from soft-collinear-hard factorisation we will define the soft anomalous dimension in section 1.2.1. We will then discuss the constraint equations and the sum-over-dipole formula of [32, 33, 37] in section 1.2.3. Following on from this, we will look at the kinematic and colour structure of any corrections to the dipole formula, before briefly discussing constraints provided by the Regge limit (section 1.2.8) and collinear limits (section 1.2.9).

Having thus introduced the main theoretical concepts, we will briefly cover two calculational tools of importance. We will begin with Mellin-Barnes (MB) integration techniques (section 1.3), which will enable us to perform asymptotic expansions near the limit of light-like external partons. Finally, we will conclude this chapter with a discussion of parameter integration and polylogarithms in section 1.4.

After defining our main concepts and tools, we will consider an example two-loop calculation and discuss the implications of the sum-over-dipole formula at two loops in the limit of massless external partons (chapter 2). We will then proceed to consider the colour structure of any results of our calculation in chapter 3, and outline our general method of computation in chapter 4. Finally, we will present our results for each individual diagram in chapter 5, before assembling the full correction to the dipole formula in chapter 6. We will then consider the Regge limit of our result in chapter 7 before discussing collinear factorisation in chapter 8.

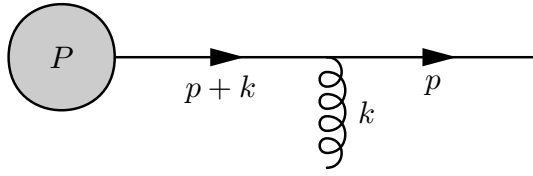


**Figure 1.1** *Single emission of soft gluon from an external parton emerging from an arbitrary process  $P$ .*

## 1.1 A One-Loop Example

Before we consider IR singularities in more general terms, it is perhaps useful to consider a simple example. We begin by investigating the Feynman rule for the emission of a soft gluon from a fermion. Consider the diagram snippet in fig. 1.1 where we take the momentum of the fermion –  $p$  – to be external and hence on-shell. The vertex then contributes the following factor to the Feynman diagram

$$V^\mu(p, k, a) = ig_s \bar{u}(p) \gamma^\mu \frac{\not{p} + \not{k} + m}{(p+k)^2 - m^2} \mathbf{T}^a. \quad (1.2)$$

The colour matrix  $\mathbf{T}^a$  is here the usual emission matrix for an outgoing fermion  $\mathbf{T}^a = t_{\alpha\beta}^{(a)}$ . The purpose of writing  $\mathbf{T}^a$  is to later generalise to arbitrary colour representations, independent of the specific gauge group or representation of the particle emitting a gluon. Full details on this notation are given in section 1.2.2.

Taking  $k \ll p$ , we neglect  $k^2$  in the denominator and  $\not{k}$  in the numerator, since  $p$  is on-shell the denominator then simplifies

$$V^\mu(p, k, a) \underset{k \ll p}{\approx} ig_s \bar{u}(p) \gamma^\mu \frac{\not{p} + m}{2(p \cdot k)} \mathbf{T}^a. \quad (1.3)$$

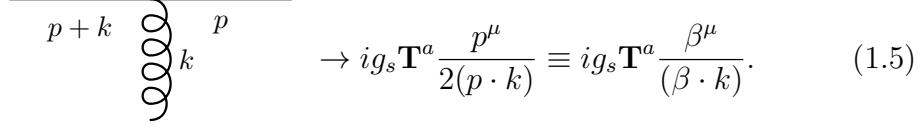
We may now utilise the anticommutator to exchange  $\not{p}$  and  $\gamma^\mu$ , the Dirac equation then immediately tells us that  $\bar{u}(p)\not{p} = \bar{u}(p)m$ . When the dust settles, we have obtained the following expression for the vertex and the internal propagator

$$V^\mu(p, k, a) \underset{k \ll p}{\approx} ig_s \bar{u}(p) \frac{p^\mu}{(p \cdot k)} \mathbf{T}^a. \quad (1.4)$$

It is notable that the emission vertex has become invariant under rescalings of

the four-momentum  $p^\mu$ . Furthermore, the spin-dependence of the gluon emission has entirely vanished from the vertex in the soft limit. This is convenient, since it allows us to generalise this result to any number of gluon emissions inductively.

To be more precise, we define the *eikonal Feynman rule* for the emission of a soft gluon from an external parton as



$$\begin{array}{c} \text{---} p+k \quad \text{---} p \\ \quad \quad \quad \left. \begin{array}{c} \text{ } \\ \text{ } \\ \text{ } \end{array} \right) k \\ \rightarrow ig_s \mathbf{T}^a \frac{p^\mu}{2(p \cdot k)} \equiv ig_s \mathbf{T}^a \frac{\beta^\mu}{(\beta \cdot k)}. \end{array} \quad (1.5)$$

Note the appearance of  $\beta \equiv p/Q$ , which represents an arbitrary rescaling of the momentum  $p$ , under which the eikonal Feynman rule is invariant. Furthermore, the eikonal Feynman rule can be entirely reproduced by a Wilson line operator, written in configuration space as

$$\Phi(0, \infty) = \mathcal{P} \exp \left( ig_s \int_0^\infty ds \beta^\mu A_\mu(s\beta^\mu) \right). \quad (1.6)$$

To see this, we Fourier transform to momentum space

$$\begin{aligned} ig_s \int_a^b ds \beta^\mu A_\mu(s\beta^\mu) &= ig_s \int \frac{d^d k}{(2\pi)^d} \beta^\mu \tilde{A}_\mu(k) \int_0^\infty ds e^{is\beta \cdot k} \\ &= g_s \int \frac{d^d k}{(2\pi)^d} \tilde{A}_\mu(k) \frac{\beta^\mu}{(\beta \cdot k)}. \end{aligned} \quad (1.7)$$

The Wilson line thus captures the fact that the emission of a soft gluon causes no recoil to the emitting particle, and does not resolve its spin.

We may now apply these tools to an example. Consider a QCD correction to the gluon-fermion coupling, as in fig. 1.2.

$$\begin{aligned} \mathcal{M}^{\mu a}(p_1 + p_2) &= -g_s^3 \mathbf{T}^b \mathbf{T}^a \mathbf{T}^b \\ &\times \int \frac{d^d k}{(2\pi)^d} \bar{u}(p_1) \gamma^\nu \frac{\not{p}_1 + \not{k} + m}{(p_1 + k)^2 - m^2} \gamma^\mu \frac{\not{p}_2 - \not{k} + m}{(p_2 - k)^2 - m^2} \gamma_\nu \frac{1}{k^2} v(p_2) \end{aligned} \quad (1.8)$$

The expression above is clearly not gauge invariant. However, it does serve to illustrate some of the concepts we will introduce in the following chapter. Taking

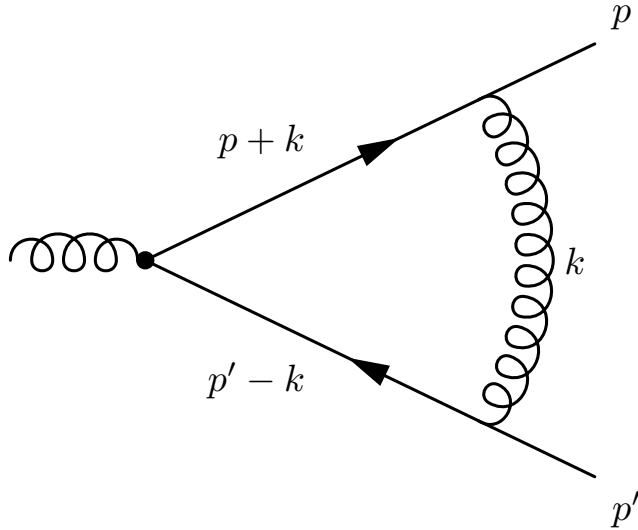


**Figure 1.2** *One-loop QCD correction to the gluon-fermion coupling.*

the soft limit of eq. (1.8) we find

$$\mathcal{M}^{\mu a}(p + p_2) \underset{k^2 \ll p_1^2, p_2^2}{\propto} g_s^3 \mathbf{T}^b \mathbf{T}^a \mathbf{T}^b \bar{u}(p) \gamma^\mu v(p_2) \int \frac{d^d k}{(2\pi)^d} \frac{p_1 \cdot p_2}{k^2 (p_1 \cdot k) (p_2 \cdot k)}. \quad (1.9)$$

The tree-level amplitude has factorised out of the loop integral in the soft limit. This property is a general property of IR singularities, and one we will return to in section 1.2.

A few observations are in order: firstly, the expression in eq. (1.9) is divergent both for  $k \ll p$  and for  $k \gg p$ , in spite of eq. (1.8) being UV-finite. Furthermore, the rescaling invariance of the eikonal emission means that the whole integral is scaleless, and hence zero in dimensional regularisation. The reason for this is that taking the soft limit has introduced UV poles which precisely cancel the IR poles [53]. This enables us to compute the IR pole of eq. (1.8) in terms of the UV pole in eq. (1.9). We will discuss this in more detail in section 1.2.1.

We also note that while the kinematics have factorised, the colour factor of this diagram differs from the tree-level vertex, albeit in a fairly simple manner for this example. This is hardly surprising, since the soft gluon does carry colour, and we would in general expect it to thus affect the colour flow of the hard interaction vertex between the gluon and fermion in eq. (1.8). Thus, when we consider soft factorisation more generally in section 1.2, we will have to choose a basis for the possible colour flows in the hard part of the amplitude, whereupon soft singularities will be some matrix in this colour flow space (see e.g. [11] for a



much more thorough treatment of factorisation).

In the next section we will define all the tools needed to understand and handle these issues, and we will show that we may capture the soft singularity in eq. (1.8) in the following configuration-space diagram by utilising our Wilson lines:

$$w_{(11)}(\gamma_{ij}, \epsilon) \equiv (\mathbf{T}_1 \cdot \mathbf{T}_2) (ig_s \mu^\epsilon)^2 (\beta_1 \cdot \beta_2) \mathcal{N} \times \int_0^\infty ds_1 ds_2 \frac{e^{-im(s_1 \sqrt{\beta_1^2 - i0} + s_2 \sqrt{\beta_2^2 - i0})}}{(-(s_1 \beta_1 - s_2 \beta_2))^{1-\epsilon}}. \quad (1.10)$$

In the above, we have utilised the Feynman rules for Wilson lines which we will give in full in section 1.2.7. For now, we note that we have introduced the rescaling-invariant angle  $\gamma_{ij} \equiv \frac{\beta_1 \cdot \beta_2}{\sqrt{\beta_1^2} \sqrt{\beta_2^2}}$ , a normalisation associated with the configuration space propgataor  $\mathcal{N} \equiv \frac{\Gamma(1-\epsilon)}{4\pi^{2-\epsilon}}$  and an exponential regulator which regulates away the IR pole (we may utilise the UV counterterm to recover it) in a manner which obeys the rescaling invariance of the Wilson lines. The advantage to working in configuration space is the immediate reduction from  $d$ -dimensional momentum integrals to scalar ones. For this reason, we will work exclusively in configuration space for the remainder of the thesis.

Having highlighted most of the properties we need for section 1.2, we are now more or less done with our one-loop example. For completeness, we note that the integrations over the Wilson line parameters  $s_i$  may be performed by the following rescaling

$$s_1 = \frac{\alpha x}{\sqrt{\beta_1^2}}, \quad (1.11)$$

$$s_2 = \frac{\alpha(1-x)}{\sqrt{\beta_2^2}}, \quad (1.12)$$

where we have  $\alpha \in [0, \infty)$  and  $x \in [0, 1]$ . Performing the integral over  $\alpha$  then yields

$$w_{(11)}(\gamma_{ij}, \epsilon) = -(\mathbf{T}_1 \cdot \mathbf{T}_2) (g_s)^2 \left( \frac{\mu^2}{m^2} \right) \frac{\gamma_{12}}{2} \mathcal{N} \Gamma(2\epsilon) \times \int_0^1 dx (-x^2 - (1-x)^2 + x(1-x)\gamma_{12})^{1-\epsilon}. \quad (1.13)$$

This integral may then be recast in terms of a hypergeometric function [17]:

$$\begin{aligned}
w_{(11)}(\gamma_{ij}, \epsilon) = & -(\mathbf{T}_1 \cdot \mathbf{T}_2) \frac{g_s^2}{2} \gamma_{12} \left( \frac{\mu^2}{m^2} \right) \mathcal{N}\Gamma(2\epsilon) \\
& \times {}_2F_1 \left( [1, 1 - \epsilon], [3/2], \frac{1}{2} + \frac{\gamma_{12}}{4} \right).
\end{aligned}
\tag{1.14}$$

Thus, the one-loop two-line soft pole may be found order-by-order through an expansion of the hypergeometric function in  $\epsilon$ .

This concludes our one-loop example. In the next section we will look at IR singularities more generally, and define the tools we need for our three-loop calculation.

## 1.2 The Soft Anomalous Dimension

Having seen an example of an IR singularity, we now turn to the broader study of such singularities in the context of a general gauge theory. As we have already seen, the Eikonal approximation leads to a significant simplification of the Feynman rule for the emission of a soft photon. This property extends beyond QCD: it is universal to all massless particles and enables a succinct and simple description of IR singularities in any gauge theory, and to all orders in perturbation theory. The basis for this is soft-collinear factorisation, which enables the separation of the soft and collinear modes from the hard scattering event [11, 13, 14, 27, 33, 49, 50, 69]. On an intuitive level, the energy scales of the hard scattering and any soft gluons dictate a significant difference in the compton wavelength, which prohibits the soft gluons from resolving the hard interaction. While a two-leg amplitude in a non-Abelian gauge theory is necessarily a colour singlet, a multi-leg amplitude allows many different colour flows through the amplitude. It is convenient to explicitly define this decomposition: let  $\mathcal{M}$  be an amplitude with  $n$  partonic legs: we denote the colour index of leg  $i$  with  $\alpha_i$  and pick a linearly independent basis of colour tensors  $(C_L)_{\{\alpha_i\}}$  for the amplitude:

$$\mathcal{M} \left( \frac{p_i}{\mu}, \alpha_s(\mu), \epsilon \right) \equiv \sum_L \mathcal{M}_L \left( \frac{p_i}{\mu}, \alpha_s(\mu), \epsilon \right) (C_L)_{\{\alpha_i\}}.
\tag{1.15}$$

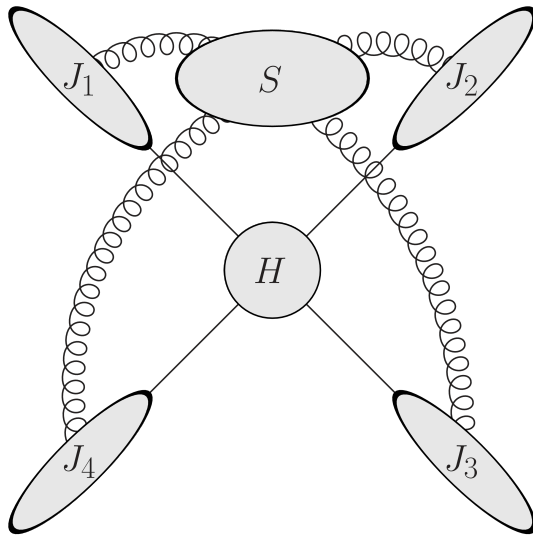


**Figure 1.3** Schematic depiction of factorisation, as in eq. (1.16).

We will follow [33, 50] and define a factorised amplitude  $\mathcal{M}$  as follows:

$$\mathcal{M}_L \left( \frac{p_i}{\mu}, \alpha_s(\mu), \epsilon \right) = \sum_K \mathcal{S}_{LK}(\beta_i \cdot \beta_j, \alpha_s(\mu^2), \epsilon) H_K \left( \frac{2p_i \cdot p_j}{\mu^2}, \frac{(2p_i \cdot n_I)^2}{n_i^2 \mu^2}, \alpha_s(\mu^2) \right) \times \prod_{i=1}^n \frac{J_i \left( \frac{(2p_i \cdot n_i)^2}{n_i^2 \mu^2}, \alpha_s(\mu^2), \epsilon \right)}{\mathcal{J}_i \left( \frac{(2\beta_i \cdot n_i)^2}{n_i^2}, \alpha_s(\mu^2), \epsilon \right)}. \quad (1.16)$$

Fig. 1.3 provides a schematic depiction of the formula. We have thus defined four quantities: the hard function  $H$ , the soft function  $S$ , a jet function  $J$  and the so-called eikonal jet  $\mathcal{J}$ . The hard function is finite after the usual UV renormalisation, and we have defined it with an index  $K$  to allow for different process-dependent colour flows through the amplitude in a manner analogous to eq. (1.15). Since soft gluons carry colour, the soft function  $\mathcal{S}_{LK}$  then mixes the colour flows of the hard interaction, producing  $\mathcal{M}_L$ . Finally, the jet functions are unique to massless external partons, and carry information about collinear singularities.

The soft function is of primary interest to us: its definition is motivated by the eikonal Feynman rule we defined in eq. (1.5), and is defined in terms of the Wilson line in eq. (1.6):

$$\Phi_{\beta_i}(a, b) \equiv \mathcal{P} \exp \left( i \int_a^b dx^\mu A_\mu(x) \right), \quad (1.17)$$

where the operator  $\mathcal{P}$  is a path-ordering operator.

We may define the soft function as a vacuum expectation value of multiple such Wilson lines, extending from the hard interaction at the origin to infinity in directions  $\beta_i$

$$(C_L)_{\{\alpha_i\}} \mathcal{S}_{LK}(\beta_i \cdot \beta_j, \alpha_s(\mu^2), \epsilon) = \sum_{\{n_i\}} \langle 0 | \Phi_{\beta_1}(0, \infty) \cdots \Phi_{\beta_n}(0, \infty) | 0 \rangle. \quad (1.18)$$

The jet functions capture collinear singularities, and their definition depends on the partonic content of the various external lines. For instance, an outgoing fermionic jet is defined as

$$\bar{u}(p_i) J \left( \frac{(2p_i \cdot n_i)^2}{n_i^2 \mu^2}, \alpha_s(\mu^2), \epsilon \right) = \langle p | \bar{\psi}(0) \Phi_n(0, -\infty) | 0 \rangle \quad (1.19)$$

The Wilson line simulates interactions with other external partons, the direction of  $n$  is arbitrary, but off the light-cone in order to avoid incurring further spurious collinear singularities.

Finally, the so-called Eikonal jet has been introduced to deal with the region of phase space which is both soft and collinear. It shares the kinematic structure of the partonic jet, but with a Wilson line replacing the partonic line as follows

$$\mathcal{J}_i \left( \frac{(2\beta_i \cdot n_i)^2}{n_i^2}, \alpha_s(\mu^2), \epsilon \right) = \langle 0 | \Phi_{\beta_i}(0, \infty) \Phi_n(0, -\infty) | 0 \rangle. \quad (1.20)$$

The jet functions are of primary importance in understanding the IR singularity structure of amplitudes with massless external partons. In particular, note the dependence of the eikonal jet on both  $\beta$  and  $n$ . This dependence, coupled with the way in which the eikonal jet serves the dual purpose of either cancelling soft singularities from the jet function, or collinear singularities from the soft function, strongly constrain the structure of the soft function, as we will see in section 1.2.1.

Before we do, however, we note that the jet functions only appear for Wilson lines with massless external partons. For massive external partons, the factorisation formula becomes

$$\mathcal{M}_L \left( \frac{p_i}{\mu}, \alpha_s(\mu), \epsilon \right) = \sum_K \mathcal{S}_{LK}(\gamma_{ij}, \alpha_s(\mu^2), \epsilon) H_K \left( \frac{2p_i \cdot p_j}{\mu^2}, \alpha_s(\mu^2) \right). \quad (1.21)$$

Note in particular the dependence on the spacetime angle  $\gamma_{ij}$ :

$$\gamma_{ij} \equiv \frac{\beta_i \cdot \beta_j}{\sqrt{\beta_i^2} \sqrt{\beta_j^2}}. \quad (1.22)$$

This quantity captures the rescaling invariance of the Wilson lines, and is therefore the invariant which the massive soft function depends on.

The absence of collinear singularities in the case of massive external partons will enable us to avoid directly working with jet functions. We will work with amplitudes containing only massive external partons, where  $\beta_i^2 \neq 0$ . However, we are ultimately interested in corrections to the dipole formula (which we will discuss shortly in section 1.2.3), which is a purely massless phenomenon. Hence, we will later perform an asymptotic expansion around the massless limit  $\beta_i^2 \rightarrow 0$  in order to recover the massless soft anomalous dimension, where we may directly compare our result with the constraints which we will derive in section 1.2.3.

### 1.2.1 IR-UV Connection and The Soft Anomalous Dimension

Since it only depends on the momenta of the external partons through  $\beta_i$ , the soft function as defined in eq. (1.16) is scaleless, and hence zero in dimensional regularisation. This is not due to a lack of IR singularities, but rather due to the introduction of spurious ultraviolet singularities when taking the eikonal approximation [53]. These UV singularities must then precisely cancel the IR poles present in  $S$ . This presents us with the opportunity to utilise UV renormalisation group considerations to study IR singularities [18, 32, 40, 53, 56]. The argument is based on multiplicative renormalisability [70], which enables us to write a UV counterterm which obeys the standard RG equations. The soft function is then nonzero after renormalising the UV terms. The fact that the soft function is scaleless thus enables us to identify the IR poles of the soft function with the UV poles in the multiplicative counterterm, which ultimately enables us to define the soft anomalous dimension  $\Gamma^S$ :

$$\begin{aligned} \mu \frac{d}{d\mu} S_{IK}(\beta_i \cdot \beta_j, \alpha_s(\mu^2), \epsilon) = \\ - \Gamma_{IJ}^S(\beta_i \cdot \beta_j, \alpha_s(\mu^2), \epsilon) S_{JK}(\beta_i \cdot \beta_j, \alpha_s(\mu^2), \epsilon). \end{aligned} \quad (1.23)$$

We note here that  $\Gamma^S$  is a pure counterterm: it only depends on the renormalisation scale  $\mu$  through the running coupling.

In section 1.2.6 we will review how we may obtain a direct diagrammatic description of  $\Gamma^S$ , which we will use for our calculations. However, the ability to use RG equations to study  $\Gamma^S$  directly also yields some interesting constraints which we will summarise shortly. First, however, we must make a slight digression to make a full exposition of our colour algebra notation, which we briefly introduced in section 1.1.

## 1.2.2 Colour Algebra

Throughout this thesis, we will be utilising Catani-Seymour notation for the colour algebra. Our aim is to work with a general, representation-independent colour structure, which may later be specialised to a specific process. Thus, we operate with the colour factors  $\mathbf{T}_i$ , where  $i$  indexes an external parton in  $S$ , and is taken to be in the relevant representation for parton  $i$ . This means that  $\mathbf{T}_i^a = t_{\alpha\beta}^a$  for a final state-quark or an initial-state antiquark,  $\mathbf{T}_i^a = -t_{\beta\alpha}^a$  for an initial-state quark or a final-state antiquark, and  $\mathbf{T}_i^a = if_{\alpha\alpha\beta}$  for a gluon. As an example, this enables to write the quadratic Casimir in an arbitrary colour representation as follows

$$C_i \mathbb{1} = \mathbf{T}_i^a \mathbf{T}_i^a. \quad (1.24)$$

For a quark in  $SU(N_c)$ , this yields  $C_F = t_{\alpha\beta}^a t_{\beta\gamma}^a = (N_c^2 - 1)/(2N_c)\delta_{\alpha\gamma}$ .

## 1.2.3 Constraint Equations and The Dipole Formula

The massless two-loop soft anomalous dimension was calculated in 2006 [27]. The result was found to be proportional to the one-loop result, specifically, if we label the  $l$ -loop soft anomalous dimension as  $\Gamma^{(l)}$ , then we have

$$\Gamma^{(2)} = \frac{\gamma_K^{(2)}}{2} \Gamma^{(1)}, \quad (1.25)$$

where  $\gamma_K^{(2)}$  is the two-loop coefficient of the well-known cusp anomalous dimension: the coefficient of the IR pole of a Wilson loop with a single cusp [18, 71]. This result confirmed an earlier prediction [6], and prompted a review of the general structure of IR singularities [32, 33]. We will utilise the notation of [33] and summarise the main results in this section. The key component in deriving the

constraint equations is the eikonal jet. Since it is a pure counterterm and depends on no scale, it only depends on  $\mu$  through the running coupling, allowing the immediate integration of its RG equation, i.e. we have the standard RG equation

$$\frac{d}{d \log(\mu)} \mathcal{J}_i(w_i, \alpha_s(\mu^2), \epsilon) = -\gamma_{\mathcal{J}_i}(w_i, \alpha_s(\mu^2), \epsilon), \quad (1.26)$$

where we have defined the shorthand  $w_i \equiv \frac{(\beta_i \cdot n)^2}{n^2}$ . Upon integration, this yields

$$\mathcal{J}_i(w_i, \alpha_s(\mu^2), \epsilon) = \exp \left[ -\frac{1}{2} \int_0^{\mu^2} \frac{d\xi^2}{\xi^2} \gamma_{\mathcal{J}_i}(w_i, \alpha_s(\xi^2, \epsilon), \epsilon) \right]. \quad (1.27)$$

The anomalous dimension  $\gamma_{\mathcal{J}_i}$  is singular due to the cusp anomaly. In the same manner as for the Sudakov form factor [72], the singular contribution is then governed by  $\gamma_K$ , and can be separated out as a pure counterterm with no kinematic dependence, into a so-called  $K+G$ -equation. This results in a factorised expression for the eikonal jet:

$$\begin{aligned} \mathcal{J}_i(w_i, \alpha_s(\mu^2), \epsilon) = \\ \exp \left[ \frac{1}{2} \int_0^{\mu^2} \frac{d\xi^2}{\xi^2} \left( \frac{1}{2} G_{\mathcal{J}}(w_i, \alpha_s(\xi^2, \epsilon)) - \frac{1}{4} \gamma_K(\alpha_s(\xi^2, \epsilon)) \log \left( \frac{\mu^2}{\xi^2} \right) \right) \right]. \end{aligned} \quad (1.28)$$

However, the dependence of  $\mathcal{J}_i$  on  $w_i$  is known from [50]:

$$\frac{\partial}{\partial \log(w_i)} \log(\mathcal{J}_i(w_i, \alpha_s(\mu^2), \epsilon)) = -\frac{1}{8} \int_0^{\mu^2} \frac{d\xi^2}{\xi^2} \gamma_K(\alpha_s(\xi^2, \epsilon)) \quad (1.29)$$

Comparing the eq. (1.29) to eq. (1.28) we may deduce the dependence of  $G_{\mathcal{J}}$  on  $w_i$ . Ultimately, this yields the following result for the eikonal jet

$$\begin{aligned} \mathcal{J}_i(w_i, \alpha_s(\mu^2), \epsilon) = \\ \exp \left[ \frac{1}{2} \int_0^{\mu^2} \frac{d\xi^2}{\xi^2} \left( \frac{1}{2} \delta_{\mathcal{J}}(\alpha_s(\xi^2, \epsilon)) - \frac{1}{4} \gamma_K(\alpha_s(\xi^2, \epsilon)) \log \left( \frac{w_i \mu^2}{\xi^2} \right) \right) \right]. \end{aligned} \quad (1.30)$$

The solution obtained in eq. (1.30) directly enables us to derive the constraint equations for  $\Gamma^S$ . The crucial observation which enables this is that while  $\Gamma^S$  contains collinear singularities, and hence has a singular contribution, this singularity is cancelled by the eikonal jet. We define the so-called reduced soft

function  $\bar{S}$ :

$$\bar{S}_{IJ}(\rho_{ij}, \alpha_s(\mu^2)) = \frac{S_{IJ}(\beta_i \cdot \beta_j, \alpha_s(\mu^2), \epsilon)}{\prod_{i=1}^n \mathcal{J}_i(w_i, \alpha_s(\mu^2), \epsilon)}. \quad (1.31)$$

The reduced soft function also has an associated reduced soft anomalous dimension  $\Gamma^{\bar{S}}$ , defined in the same way as we defined  $\Gamma^S$ . However, this reduced soft anomalous dimension is free of cusp singularities, and eq. (1.16) implies that it must be manifestly rescaling invariant in both  $\beta$  and  $n$ , hence we have defined the invariants

$$\rho_{ij} = \frac{(\beta_i \cdot \beta_j)^2 n_i^2 n_j^2}{4 (\beta_i \cdot n_i)^2 (\beta_j \cdot n_j)^2}. \quad (1.32)$$

Differentiating eq. (1.31), we obtain a relationship between  $\Gamma^{\bar{S}}$ ,  $\Gamma^S$  and  $\gamma_{\mathcal{J}_i}$  which upon inserting eq. (1.30) yields

$$\begin{aligned} \Gamma_{IJ}^{\bar{S}}(\rho_{ij}, \alpha_s(\mu^2)) &= \Gamma^S(\beta_i \cdot \beta_j, \alpha_s(\mu^2), \epsilon) - \delta_{IJ} \sum_{k=1}^n \left[ -\frac{1}{2} \delta_{\mathcal{J}_k}(\alpha_s(\mu^2), \epsilon) \right. \\ &\quad \left. + \frac{1}{4} \gamma_K^{(k)}(\alpha_s(\mu^2), \epsilon) \log(w_i) + \frac{1}{4} \int_0^{\mu^2} \frac{d\xi^2}{\xi^2} \gamma_K^{(k)}(\alpha_s(\xi^2), \epsilon) \right]. \end{aligned} \quad (1.33)$$

At this point we may observe a few things which will be of primary importance to the structure of our calculation in later chapters. Firstly, any off-diagonal elements in  $\Gamma^S$  are equal to those of  $\Gamma^{\bar{S}}$ , and are hence finite and invariant of any rescaling of  $\beta_i$ . Thus, they must be composed entirely of so-called CICRs, defined as

$$\rho_{ijkl} = \frac{(\beta_i \cdot \beta_j) (\beta_k \cdot \beta_l)}{(\beta_i \cdot \beta_k) (\beta_j \cdot \beta_l)}. \quad (1.34)$$

We note the need for at least four distinct partons in order to define a CICR, this means that such terms can first appear at three-loop order. This fact provides a strong motivation for studying the light-like soft anomalous dimension at three loops.

Turning to the diagonal elements of  $\Gamma^S$ , it is clear that in order to obtain only finite contributions to  $\Gamma^{\bar{S}}$ , the singular terms must cancel between  $\Gamma^S$  and the eikonal jet terms  $\gamma_{\mathcal{J}_i}$ . Thus, any singular terms must be proportional to  $\gamma_K$ , and any finite terms which are not CICR-dependent must combine with  $\log(w_i)$  in eq. (1.33) to produce the appropriate dependence on  $\rho_{ij}$ . Considering the  $w$ -dependence of



eq. (1.33), one then arrives at [32, 33]

$$\sum_{j \neq i} \rho_{ij} \frac{\partial}{\partial \rho_{ij}} \Gamma_{IJ}^{\bar{S}}(\rho_{ij}, \alpha_s) = \delta_{IJ} \frac{1}{4} \gamma_K^{(i)}(\alpha_s). \quad (1.35)$$

Eq. (1.35) ultimately leads to the promised sum-over-dipoles formula. However, a few remarks with regards to the colour structure of the soft anomalous dimension are required in order to obtain it. Specifically, the non-Abelian exponentiation theorem implies that up to and including three loops, the cusp anomalous dimension is only proportional to the quadratic Casimir operator  $C_i$  of the relevant parton, so-called Casimir scaling. Utilising our notation for the colour factors outlined in section 1.2.2, we then define

$$\gamma_K^{(i)}(\alpha_s) = \mathbf{T}_i^a \mathbf{T}_i^a \hat{\gamma}_K(\alpha_s) + \tilde{\gamma}_K^{(i)}(\alpha_s), \quad (1.36)$$

where we take  $\tilde{\gamma}_K^{(i)}$  to be  $\mathcal{O}(\alpha_s^4)$ . Considering the solution to eq. (1.35) for  $\hat{\gamma}_K$  and excluding any contributions which are separately rescaling invariant then ultimately yield [32, 33]

$$\begin{aligned} \Gamma_{\text{dip.}}^S(\beta_i \cdot \beta_j, \alpha_s(\mu^2)) &= -\frac{1}{4} \hat{\gamma}_K(\alpha_s(\mu^2)) \sum_{i \neq j} \log(\beta_i \cdot \beta_j) \mathbf{T}_i^a \mathbf{T}_j^a \\ &+ \left[ -\frac{1}{2} \hat{\delta}_S(\alpha_s(\mu^2)) + \frac{1}{4} \int_0^{\mu^2} \frac{d\lambda^2}{\lambda^2} \hat{\gamma}_K(\alpha_s(\lambda^2, \epsilon)) \right] \sum_{i=1}^n \mathbf{T}_i^a \mathbf{T}_i^a. \end{aligned} \quad (1.37)$$

The dipole formula is arrived at as the unique solution to eq. (1.35) under the requirement that the kinematic function does not explicitly depend on CICRs, as well as the assumption of Casimir scaling. These assumptions then naturally yield two potential sources of corrections to the dipole formula.

As we mentioned, Casimir scaling may first be broken at four loops, by the appearance of quartic Casimir operators. Secondly CICR-dependent terms may arise at three loops, and recent considerations in  $\mathcal{N} = 4$  Super Yang-Mills demonstrated that such terms will exist at four loops [34]. To date, no complete calculation of any such corrections exists. We will therefore attempt a complete calculation at three loops of any CICR-dependent corrections to the dipole formula in chapter 5.

## 1.2.4 Kinematic Dependence of Three-loop Corrections to the Dipole Formula

As we mentioned, contributions to  $\Gamma^S$  beyond the dipole formula (eq. (1.37)) at three loops can be exclusively composed of CICRs as in eq. (1.34). This motivates a particular interest in diagrams connecting four Wilson lines by a single connected tree of gluons. The reason for this is that these diagrams are the only ones which depend on the complete set of angles  $\beta_i \cdot \beta_j$  connecting all four lines, and hence the only diagrams which may directly depend on CICRs. All other diagrams may produce dependence on CICRs only through sums of permutations of the external legs.

Since we wish to study corrections to the dipole formula in more detail, we define the function  $\Delta$  according to

$$\Gamma^S(\beta_i \cdot \beta_j, \alpha_s(\mu^2)) \equiv \Gamma_{\text{dip.}}^S(\beta_i \cdot \beta_j, \alpha_s(\mu^2)) + \Delta(z, \bar{z}). \quad (1.38)$$

Our results will often depend on Källén functions, hence we have used the kinematic invariants  $z$  and  $\bar{z}$  in eq. (1.38). They are defined by

$$\rho_{1234} = \frac{(\beta_1 \cdot \beta_2)(\beta_3 \cdot \beta_4)}{(\beta_1 \cdot \beta_3)(\beta_2 \cdot \beta_4)} \equiv z\bar{z}, \quad (1.39a)$$

$$\rho_{1432} = \frac{(\beta_1 \cdot \beta_4)(\beta_2 \cdot \beta_3)}{(\beta_1 \cdot \beta_3)(\beta_2 \cdot \beta_4)} \equiv (1-z)(1-\bar{z}). \quad (1.39b)$$

Their utility is made clear if we explicitly solve for  $z$  and  $\bar{z}$

$$z = 1 - \rho_{1234} + \rho_{1432} + \sqrt{\lambda(1, \rho_{1234}, \rho_{1432})} \quad (1.40a)$$

$$\bar{z} = 1 - \rho_{1234} + \rho_{1432} - \sqrt{\lambda(1, \rho_{1234}, \rho_{1432})}, \quad (1.40b)$$

where  $\lambda$  is the familiar Källén function

$$\lambda(a, b, c) = a^2 + b^2 + c^2 - 2ab - 2ac - 2bc. \quad (1.41)$$

Bose symmetry constrains the kinematic behaviour of  $\Delta$ . We will return to this matter when we consider the specific combinations of kinematic functions and colour factors which may appear in chapter 3. However, it is convenient to consider how permutations affect  $z$  and  $\bar{z}$ . Following [35], we observe that swapping Wilson lines yield transformations that affect  $z$  and  $\bar{z}$  in the same way. Specifically, we

find the following effects on  $z$  and  $\bar{z}$

$$z \xrightarrow{1\leftrightarrow 2 \vee 3\leftrightarrow 4} \frac{z}{1-z} \quad (1.42)$$

$$z \xrightarrow{1\leftrightarrow 3 \vee 2\leftrightarrow 4} 1-z \quad (1.43)$$

$$z \xrightarrow{1\leftrightarrow 4 \vee 2\leftrightarrow 3} \frac{1}{1-z}. \quad (1.44)$$

These symmetries will be useful in chapter 3 and later in expressing our results in a manner which makes Bose symmetry explicit.

## 1.2.5 The Soft Anomalous Dimension on Massive Wilson Lines

Our aim in this thesis is to compute  $\Delta(z, \bar{z})$ , as defined in eq. (1.38). However, we wish to avoid the thorny issue of collinear singularities and the overlapping singularities in the soft-collinear region. As we mentioned at the beginning of this chapter, we will avoid collinear singularities by working explicitly with non-lightlike Wilson lines, whereupon the factorisation formula reduces to the one in eq. (1.21).

For the remainder of this chapter we will therefore work exclusively with non-lightlike Wilson lines. Using eq. (1.21), we may then define a soft anomalous dimension for massive external partons in analogy to eq. (1.23) [17]

$$\mu \frac{d}{d\mu} S_{IK}(\gamma_{ij}, \alpha_s(\mu^2)) = -\Gamma_{IJ}^S(\gamma_{ij}, \alpha_s(\mu^2)) S_{JK}(\gamma_{ij}, \alpha_s(\mu^2)). \quad (1.45)$$

In the next section, we will look at how we may directly compute  $\Gamma^S$  diagrammatically, we will then turn our eyes to the tool we will ultimately use to recover the light-like behaviour of  $\Gamma^S$ : MB integration in section 1.3. Finally, in section 1.4 we will discuss the analytic structure of our results in the context of multiple polylogarithms.

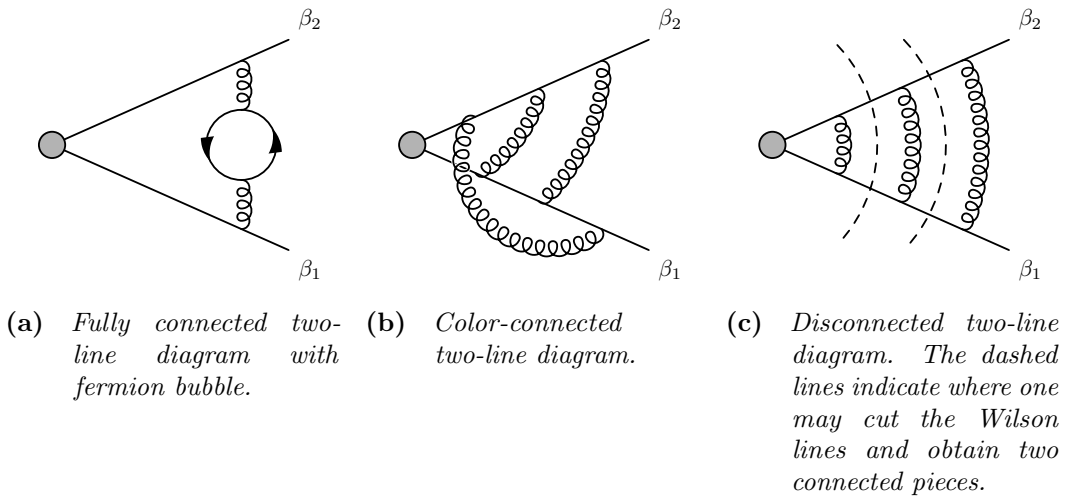


**Figure 1.4** Examples of color-connected and disconnected two-line diagrams.

## 1.2.6 Exponentiation and Renormalisation of the Multi-Parton Soft Anomalous Dimension

The calculation of soft singularities can be significantly simplified by the fact that soft singularities *exponentiate*. That is, we may not only write the soft matrix as some exponential, but we can in fact find a diagrammatic interpretation of this exponential. This fact has been known in the context of Abelian theories (it was first shown in [12]), where the exponent receives contributions only from fully connected diagrams.

However, the Abelian case is vastly simplified by the ability to interchange the points of emission and absorption of photons without it affecting the charge flow. For a non-Abelian theory this is no longer possible, leading to some complications in defining the exponentiated soft function. In the case of two-parton diagrams, one finds that the exponent receives contributions from all color-connected diagrams [15, 19, 22, 73]. These are diagrams where there is no way to cut the Wilson lines and obtain two disjoint, connected diagrams. Put differently: the colour flow of the diagram, as dictated by the ordering of the gluons, does not allow one to decompose the diagram into separate pieces. An example of both color-connected and color-disconnected diagram is given in fig. 1.4.

Extending this notion to diagrams with more than two external partons presents a challenge: since gluons may now attach to multiple different lines, the notion of color-connected does not easily extend to multi-leg diagrams. Instead, one finds [20] that sets of diagrams contribute to the exponent in very specific

linear combinations. These linear combinations are collectively referred to as webs, and are defined as follows.

Consider a set of  $n$  Feynman diagrams –  $\{\mathcal{D}_i\}$ ,  $i \in \{1, \dots, n\}$  – contributing to the soft function, where the diagrams in the set differ only by permutations of the orderings of emissions of gluons along the Wilson lines. Each diagram has a colour and kinematic component, labelled  $\mathcal{C}_i$  and  $\mathcal{F}_i$ . These diagrams then contribute to the exponent only in specific linear combinations dictated by the *web mixing-matrix*  $R_{ij}$  as follows

$$W = \sum_{i,j} \mathcal{C}_i R_{ij} \mathcal{F}_j. \quad (1.46)$$

The web-mixing matrix can be found either by means of the *replica trick*[20], or more directly by means of *web effective vertices*[16], the latter of which we will discuss later in this section.

The mixing matrix has some interesting properties. Firstly, it is idempotent, i.e. it has eigenvalues  $\lambda_i \in \{0, 1\}$ , making it a projection matrix. Furthermore, the sum of any row or column in  $R_{ij}$  is zero.

The role of  $R$  is to project out specific linear combinations of Feynman diagrams with modified colour factors, which we refer to as ECFs, which we will label  $\tilde{\mathcal{C}}$ . To see this, we diagonalise the web mixing matrix as  $R = Y^{-1}DY$ .  $D$  is then a diagonal matrix with all diagonal entries being either 0 or 1. The number of nonzero diagonal entries in  $D$  are  $r = \text{Rank}(R)$ , and we may choose to work in a basis such that  $D$  is simply an identity matrix in the upper left corner, and zero everywhere else, yielding

$$W = \sum_{i=1}^r (\mathcal{C}Y^{-1})_i (Y\mathcal{F})_i \equiv \sum_{i=1}^r \tilde{\mathcal{C}}_i \tilde{\mathcal{F}}_i. \quad (1.47)$$

It then transpires that the ECFs in  $\tilde{\mathcal{C}}$ , are *fully connected*, i.e. they are colour factors corresponding to connecting the same attachments of Wilson lines to a single graph of gluons, internally connected by three-gluon vertices[16].

As mentioned before, the precise expressions for these linear combinations may be derived in a few different ways. One method, which is largely diagrammatic is the method of effective vertices [16], which in turn is derived from the replica trick method [20]. To do this, a set of effective vertices which attaches  $n$  gluons to a Wilson line –  $V_{n,k}$  – are defined. We will not give details of the definition,

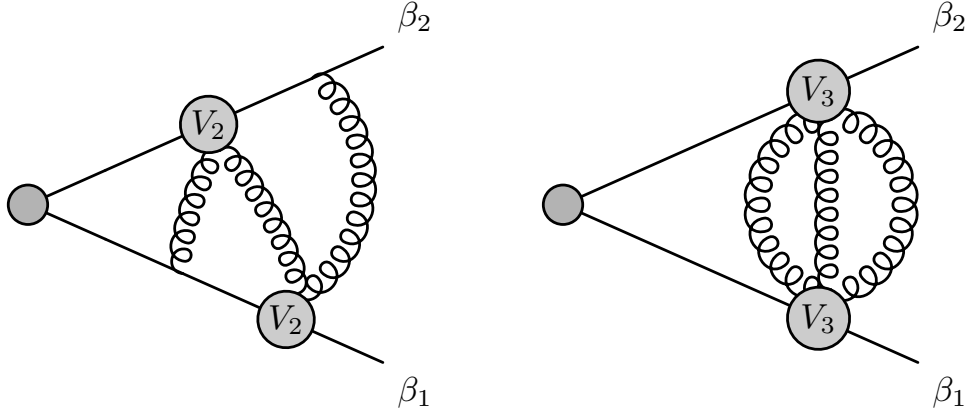


**Figure 1.5** *Example of effective vertex diagrams contributing to different ECFs in  $w_{(33)}$*

but merely note that in terms of colour and kinematics, these vertices correspond to antisymmetric permutations of the points of emission along the Wilson line, both in terms of colour and kinematics. For instance, the colour component of the effective vertex attaching two gluons to a Wilson line is given by

$$V_{2\mathcal{C}}^{a,b} \propto [\mathbf{T}^a, \mathbf{T}^b] = if^{abc}\mathbf{T}^c, \quad (1.48)$$

And the corresponding kinematic factor would then take the difference between the two potential orderings of the gluons on the Wilson line.

$$V_{2\mathcal{F}} \propto \theta(x_a > x_b) - \theta(x_b < x_a). \quad (1.49)$$

A web in this notation is defined by a group of gluons attached to effective vertices in such a way that if the Wilson lines were removed entirely, the graph of gluons and effective vertices is singly connected. This somewhat formalises the notion of web colour factors being fully connected. We emphasise that a Wilson line may have more than a single effective vertex attached to it. In such cases, we take the symmetric sum over all permutations of the effective vertices along the Wilson line.

Finally, we may now turn to the topic of renormalisation of multi-parton webs. Our goal is to directly compute  $\Gamma^S$ , which as we have seen consists of particular linear combinations of kinematic factors, with ECFs. It is also notable that while individual diagrams may have subdivergences, higher-order poles are always determined by the exponent, implying an intricate cancellation of subdivergences

between webs and lower-order counterterms. This complex interplay means that one may directly compute  $\Gamma^S$  as a specific linear combination of webs, and lower-order pole terms. Labelling the  $n$ -loop web contribution at order  $\epsilon^k$  as  $w^{(n,k)}$ , and  $\Gamma^{(n)}$  as the corresponding  $n$ -loop contribution to  $\Gamma^S$ , it has been shown that [17]

$$\Gamma^{(1)} = -2w^{(1,-1)}, \quad (1.50)$$

$$\Gamma^{(2)} = -4w^{(2,-1)} - 2[w^{(1,-1)}, w^{(1,0)}], \quad (1.51)$$

$$\begin{aligned} \Gamma^{(3)} = & -6w^{(3,-1)} + \frac{3}{2}b_0 [w^{(1,-1)}, w^{(1,1)}] + 3[w^{(1,0)}, w^{(2,-1)}] \\ & + 3[w^{(2,0)}, w^{(1,-1)}] + [w^{(1,0)}, [w^{(1,-1)}, w^{(1,0)}]] \\ & + [w^{(1,-1)}, [w^{(1,-1)}, w^{(1,1)}]]. \end{aligned} \quad (1.52)$$

In the above we have the constant  $b_0$ , being the first coefficient of the beta function of  $\alpha_s$ , i.e.  $\frac{d\alpha_s}{d\log(\mu^2)} = -\alpha_s (\epsilon + \sum_{i=0}^{\infty} \alpha_s^{n+1} b_i)$ .

The specific linear combinations of webs and counterterms in eqs. (1.50) to (1.52) thus are ultimately the objects we wish to compute. We refer to them as *reduced webs* and denote them  $\bar{w}$ .

Having thus defined our objects of interest, we will now look at how to calculate them by setting up the Feynman rules. We will then return to a few additional constraints which will be of interest after we have completed our calculations.

## 1.2.7 Feynman Rules for Multi-Parton Webs in Configuration Space

Now that we have a complete picture of the various components of  $\Gamma^S(\gamma_{ij}, \alpha(\mu^2))$  with non-lightlike external partons, the associated Feynman rules are as follows.

Each attachment of a gluon to a Wilson line is associated with the term

$$D_{\Phi}^a(\beta^\mu) = ig_s \mu^\epsilon \mathbf{T}^a \beta^\mu \int_0^\infty ds e^{-ims\sqrt{\beta^2 - i0}}. \quad (1.53)$$

The exponential regulator is there to eliminate IR singularities, leaving only UV poles. We explicitly indicated the sign of the  $i0$ -prescription, which corresponds to  $\beta^2$  being interpreted as a square mass. This prescription guarantees the convergence of the integral at  $s \rightarrow \infty$  for both space-like and time-like Wilson lines, and is in accordance with the convention chosen in [16]. In particular,

note that the analytic continuation of the  $i0$ -term is  $\beta^2 - i0 = |\beta^2| \exp(-i\theta)$  with  $\theta > 0$ . For timelike Wilson lines we then have  $\theta \rightarrow 0^+$ , this results in  $\sqrt{\beta^2 - i0} = \sqrt{|\beta^2|} - i0/2$ . Conversely, in the case of spacelike Wilson lines we have  $\theta = \pi$  and consequently obtain  $\sqrt{\beta^2 - i0} = -i\sqrt{|\beta^2|}$ . While our prescription works in both of these regions, we will for the sake of convenience limit ourselves to the case of spacelike Wilson lines.

The rescaling invariance of the Wilson lines manifests itself as the ability to rescale the integration measure  $s$ . We will be utilising this property when integrating over the exponential regulator. We recall that a natural invariant to express  $\Gamma^S$  for non-lightlike external partons is the spacetime angle  $\gamma_{ij}$ , we also define a normalised  $\hat{\beta}_i$

$$\hat{\beta} \equiv \frac{\beta}{\sqrt{|\beta^2|}} \quad (1.54)$$

$$\gamma_{ij} \equiv 2 \frac{\beta_i \cdot \beta_j}{\sqrt{\beta_i^2} \sqrt{\beta_j^2}} = -2 \hat{\beta}_i \cdot \hat{\beta}_j \quad (1.55)$$

The definition of  $\gamma_{ij}$  in terms of  $\hat{\beta}$  is specific to spacelike Wilson lines, as is the fact that  $\hat{\beta}^2 = -1$ .

One further convenient parametrisation, and one we will use when writing our results is given by:

$$\gamma_{ij} \equiv -\alpha_{ij} - \frac{1}{\alpha_{ij}}. \quad (1.56)$$

In the above, we have the choice of  $|\alpha_{ij}| > 1$  or  $|\alpha_{ij}| < 1$ . In this work, we will always choose  $|\alpha_{ij}| < 1$ , thus placing  $\alpha_{ij}$  within the unit circle.

The light-like limit of these parameters are given by  $\beta_i^2 \rightarrow 0$ , this implies

$$\lim_{\beta_i^2 \rightarrow 0} \gamma_{ij} = -\infty \quad (1.57)$$

$$\lim_{\beta_i^2 \rightarrow 0} \alpha_{ij} = 0^+ \quad (1.58)$$



The gluon propagators are given by

$$D_g^{\mu\nu}(x) = -\mathcal{N} \frac{g^{\mu\nu}}{(-x^2 + i0)^{1-\epsilon}}, \quad (1.59)$$

$$\mathcal{N} \equiv \frac{\Gamma(1-\epsilon)}{4\pi^{2-\epsilon}}. \quad (1.60)$$

A three-gluon vertex is given by

$$G_{3\mu\nu\sigma}^{abc}(x_1, x_2, x_3) = -ig_s \mu^\epsilon f^{abc} \int d^d z \Gamma_{\mu\nu\sigma}(\partial_{x_1}, \partial_{x_2}, \partial_{x_3}), \quad (1.61)$$

$$\Gamma^{\mu\nu\sigma}(\partial_{x_1}, \partial_{x_2}, \partial_{x_3}) \equiv [g^{\mu\nu}(\partial_{x_1}^\sigma - \partial_{x_2}^\sigma) + g^{\nu\sigma}(\partial_{x_2}^\mu - \partial_{x_3}^\mu) + g^{\mu\sigma}(\partial_{x_3}^\nu - \partial_{x_1}^\nu)]. \quad (1.62)$$

Similarly, a four-gluon vertex is defined as

$$G_{4\mu\nu\rho\sigma}^{abcd} = -ig_s^2 \mu^{2\epsilon} \int d^d z [f^{abe} f^{cde} (g_{\mu\rho} g_{\nu\sigma} - g_{\mu\sigma} g_{\nu\rho}) + f^{ace} f^{bde} (g_{\mu\nu} g_{\rho\sigma} - g_{\mu\sigma} g_{\nu\rho}) + f^{ade} f^{bce} (g_{\mu\nu} g_{\rho\sigma} - g_{\mu\rho} g_{\nu\sigma})]. \quad (1.63)$$

## 1.2.8 Regge Limits

A further constraint can be found for any non-dipole contributions to  $\Gamma^S$  by considering the Regge limit of forward scattering [62, 63, 74]. This limit of two-to-two scattering is characterised by  $s \gg t$ , and has the effect of dressing the gluon propagators as follows

$$\frac{s}{t} \rightarrow \left(\frac{s}{t}\right)^{\alpha(t)}, \quad (1.64)$$

where  $\alpha(t)$  is the so-called Regge trajectory. This process of dressing the propagators is referred to as Reggeisation.

Reggeisation is an infrared phenomenon, and it has been found in [62, 63, 74] that its behaviour is entirely accounted for by the sum-over-dipoles formula in eq. (1.37). This directly provides a constraint on any corrections beyond the dipole formula, since these corrections cannot contribute to leading or subleading contributions in the Regge limit. Thus, for any contributions beyond the dipole formula, we may not have any higher powers of  $\log(t/s)$  than  $\log(t/s)$  for the real part, and  $i \log^2(t/s)$  in the imaginary part of the correction upon taking the Regge limit.

In chapter 7 we will see that this provides a strong constraint and check on our calculation of corrections beyond the dipole formula.

### 1.2.9 Collinear Factorisation

It is expected that amplitudes with external gluon jets should obey so-called collinear splitting factorisation [32, 35, 69, 75]. The basic tenet of collinear splitting factorisation is that if we take an  $n$ -leg amplitude  $\mathcal{M}_n$  and consider the limit of two legs parallel, the amplitude should factorise according to

$$\mathcal{M}_n(p_1, \dots, p_n) \xrightarrow{1||2} \text{Sp}(p_1, p_2) \mathcal{M}_{n-1}(p_1 + p_2, p_3, \dots, p_n). \quad (1.65)$$

This should apply also to the soft components of  $\mathcal{M}_n$ , hence we are led to define a soft anomalous dimension for the splitting function  $\text{Sp}(p_1, p_2)$ . It has been shown that this  $\Gamma_{\text{Sp}}$  can then be written in terms of the soft anomalous dimension on  $n$  and  $n - 1$  lines as [32, 35]

$$\Gamma_{\text{Sp}}(\beta_1, \beta_2) = \Gamma_n(\beta_1, \beta_2, \dots, \beta_n) - \Gamma_{n-1}(\beta_1 + \beta_2, \beta_3, \dots, \beta_n). \quad (1.66)$$

Thus, an important consistency check on our result is that we must find the same result for  $\Gamma_{\text{Sp}}$  for any  $n$ , and that this result can only depend on  $p_1, p_2$ , and the associated colour factors  $\mathbf{T}_1$  and  $\mathbf{T}_2$ . We will return to this assertion in chapter 8, after we have calculated the relevant contributions.

This concludes our review of the soft anomalous dimension. Next, we will turn our attention to the mathematical tools of our calculation. First, we will review MB integration techniques, which will enable us to perform an asymptotic expansion near the limit of light-like external partons. In section 1.4 we will then review the algebra of polylogarithms, which will provide us both with a tool for computing MB integrals, and with a means for simplifying and understanding our results.

## 1.3 Mellin-Barnes Integration and Asymptotic Expansion

Mellin-Barnes integration techniques are of primary interest as a tool for performing integrals, as well as asymptotic expansion. A review of MB integrals can be found

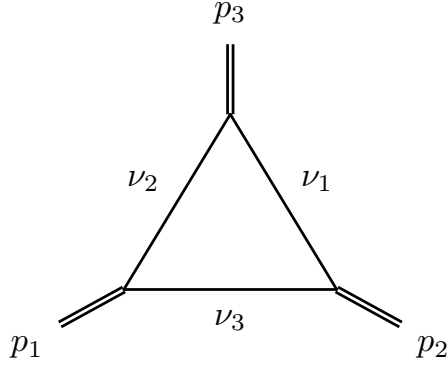


**Figure 1.6** *A scalar triangle with powers  $\nu_i$  of the propagators and incoming off-shell momenta  $p_i$ , as in eq. (1.68)*

in [76], we will limit ourselves to a brief overview. The basis of MB integration is the identity

$$\frac{1}{(A+B)^\lambda} = \frac{1}{\Gamma(\lambda)} \frac{1}{2\pi i} \int_C dz \Gamma(-z) \Gamma(z+\lambda) \frac{A^z}{B^{\lambda+z}}, \quad (1.67)$$

where the integration contour  $C$  runs from  $-i\infty$  to  $+i\infty$  between the poles of the two gamma functions, that is when  $\text{Im}(z) = 0$  we have  $\text{Re}(z) < 0$  and  $\text{Re}(z) > -\lambda$ . Our goal in utilising this formula is similar to the reason for utilising Feynman parameters: by swapping the order of integration we may reduce loop integrations in a Feynman diagram to simpler known integrals, namely Beta functions in the case of MB. There are some advantages to this. First and foremost, the asymptotic behaviour of MB integrals is well understood, which gives us a simple way to expand the integrand around the limit of light-like external partons. In a similar vein, it is relatively straightforward to resolve the pole structure of MB integrals and expand in  $\epsilon$  under the integral sign without incurring spurious singularities. We will discuss these matters in detail later on, but it is convenient to consider an example parametrisation for clarification. If we consider the massless triangle diagram in fig. 1.6 we obtain the following Feynman integral:

$$T(\{p_i^2\}, \{\nu_i\}, d) = \frac{1}{\pi^{d/2}} \int \frac{d^d k}{(-k^2)^{\nu_2} (-(k+p_1)^2)^{\nu_3} (-(k+p_1+p_2)^2)^{\nu_1}} \quad (1.68)$$

Recasting this in terms of Feynman parameters, we obtain

$$\begin{aligned}
T(\{p_i^2\}, \{\nu_i\}, d) = & i \frac{\Gamma(\sum_i \nu_i - d/2)}{\prod_i \Gamma(\nu_i)} \left[ \prod_{i=1}^3 \int_0^\infty d\alpha_i \alpha_i^{\nu_i-1} \right] \\
& \times \delta\left(1 - \sum_{\{i\}} \alpha_i\right) \frac{(\sum_i \alpha_i)^{\sum_i \nu_i - d}}{(-\alpha_2 \alpha_3 p_1^2 - \alpha_1 \alpha_3 p_2^2 - \alpha_1 \alpha_2 p_3^2)^{\sum_i \nu_i - d/2}} \quad (1.69)
\end{aligned}$$

We are now ready to introduce MB-parameters. We utilise the Cheng-Wu theorem to set  $\alpha_3 = 1$ , then

$$\begin{aligned}
T(\{p_i^2\}, \{\nu_i\}, d) = & i \frac{\Gamma(\sum_i \nu_i - d/2)}{\prod_i \Gamma(\nu_i)} \int_0^\infty d\alpha_1 d\alpha_2 \alpha_1^{\nu_1-1} \alpha_2^{\nu_2-1} \\
& \times \frac{(1 + \alpha_1 + \alpha_2)^{\sum_i \nu_i - d}}{(-\alpha_2 p_1^2 - \alpha_1 p_2^2 - \alpha_1 \alpha_2 p_3^2)^{\sum_i \nu_i - d/2}}. \quad (1.70)
\end{aligned}$$

We now use eq. (1.67) to split the two brackets and introduce the MB integration parameters  $z_1$  and  $z_2$ :

$$\begin{aligned}
T(\{p_i^2\}, \{\nu_i\}, d) = & i \frac{1}{\Gamma(d - \sum_i \nu_i) \prod_i \Gamma(\nu_i)} \\
& \times \frac{1}{(2\pi i)^2} \int_{C_1} dz_1 \int_{C_2} dz_2 (-p_1^2)^{z_1} \Gamma(-z_1) \Gamma(-z_2) \\
& \times \Gamma(z_1 - \sum_i \nu_i - d/2) \Gamma(z_2 + d - \sum_i \nu_i) \\
& \times \int_0^\infty d\alpha_1 \frac{\alpha_1^{d/2 - \nu_2 - \nu_3 - z_1 - 1}}{(1 + \alpha_1)^{-\sum_i \nu_i + d + z_2}} \\
& \times \int_0^\infty d\alpha_2 \frac{\alpha_2^{z_1 + z_2 + \nu_2 - 1}}{(-p_2^2 - \alpha_2 p_3^2)^{-d/2 + \sum_i \nu_i + z_1}}, \quad (1.71)
\end{aligned}$$

where the contours  $C_i$  fulfill the implicit requirement that the real part of all Gamma functions must be positive when  $z_i$  are on the real axis. If we rescale  $\alpha_2$  by  $p_2^2/p_3^2$ , we obtain the standard semi-infinite integral representation of the Beta function, yielding

$$\begin{aligned}
T(\{p_i^2\}, \{\nu_i\}, d) = & i \frac{1}{\Gamma(d - \sum_i \nu_i) \prod_i \Gamma(\nu_i)} \frac{1}{(2\pi i)^2} \int_{C_1} dz_1 \int_{C_2} dz_2 \\
& \times (-p_1^2)^{z_1} (-p_2^2)^{d/2 - \nu_1 - \nu_3 + z_2} (-p_3^2)^{-\nu_2 - z_1 - z_2} \Gamma(-z_1) \Gamma(-z_2) \\
& \times \Gamma(d/2 - \nu_2 - \nu_3 - z_1) \Gamma(-\nu_1 + d/2 + z_2 + z_1) \\
& \times \Gamma(z_1 + z_2 + \nu_2) \Gamma(\nu_1 + \nu_3 - d/2 - z_2). \quad (1.72)
\end{aligned}$$

Finally, cleaning up a bit we may shift  $z_2 \rightarrow z_2 + \nu_1 + \nu_3 - d/2$ , such that the dimension of the MB integral is entirely carried in the term proportional to  $p_3^2$ . This of course also modifies the contour  $C_2 \rightarrow C'_2$ , a matter which we will discuss shortly. The end result is

$$\begin{aligned}
T(\{p_i^2\}, \{\nu_i\}, d) = & i \frac{1}{\Gamma(d - \sum_i \nu_i) \prod_i \Gamma(\nu_i)} \frac{1}{(2\pi i)^2} \int_{C_1} dz_1 \int_{C_2} dz_2 \\
& \times \left( \frac{-p_1^2}{-p_3^2} \right)^{z_1} \left( \frac{-p_2^2}{-p_3^2} \right)^{z_2} (-p_3^2)^{d/2 - \sum_i \nu_i} \Gamma(-z_1) \Gamma(-z_2) \\
& \times \Gamma(d/2 - \nu_2 - \nu_3 - z_1) \Gamma(d/2 - z_2 - \nu_1 - \nu_3) \\
& \times \Gamma(z_1 + z_2 + \sum_i \nu_i - d/2) \Gamma(\nu_3 + z_2 + z_1). \tag{1.73}
\end{aligned}$$

This triangle will be useful to us later on in considering webs at two and three loops containing a single three-gluon vertex. For now, we merely note that at this point the kinematic structure of  $T$  has been entirely decomposed into a sum of relatively simple residues. This is the key advantage to utilising MB integration techniques: both expanding in  $\epsilon$  and more general asymptotic expansions are easy to express and understand as residues of gamma functions.

In order to resolve the singularities in  $\epsilon$ , however, we must first choose our contours such that we do not incur any unregulated poles when we expand in  $\epsilon$ . In the next section, we will consider this issue a little more thoroughly.

### 1.3.1 Integration Contours

We initially required that the contours, extending from  $-i\infty$  to  $+i\infty$  must be such that the real part of the Gamma functions is positive when  $z$  is on the real axis. However, in order for the integrals over  $\alpha_i$  to be convergent, we must impose the same requirement for the Gamma functions produced by the Feynman parameter integrals. Thus, the procedure for deriving an MB integral leads us to require that the contour must pass to the right of all Gamma functions with poles extending towards  $-\infty$  and to the left of any Gamma functions with poles extending towards  $+\infty$ . Furthermore, this requirement is invariant of any translation or rescaling of the integration parameters. We will therefore omit the specific contours from now on and take their behaviour as implicit in any future calculation until such a time as it becomes necessary to specify their real parts.

The integration contour of an MB integral is intricately linked to its singularity

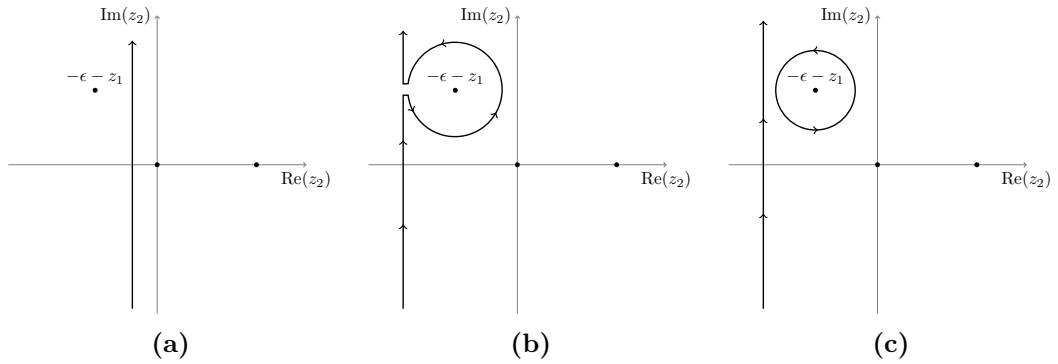


**Figure 1.7** *Contour shift to regulate  $z_2$ . From the initial contour (a), crossing the pole at  $z_2 = -\epsilon - z_1$  (b) causes us to pick up its residue (c).*

structure. Recall that we have worked with the implicit requirement that the integration contour should be to the left of all gamma functions where the residues extend to  $+\infty$ , and vice versa. A pole in  $\epsilon$  then manifests as a “pinch” on the MB contour, where taking the limit  $\epsilon \rightarrow 0$  causes the contour to run straight across one or more poles. For example, our triangle integral is divergent in  $d = 6$  dimensions for  $\nu_i = 1$ , so if we consider  $d = 6 - 2\epsilon$  we have

$$\begin{aligned}
T(\{p_i^2\}, \{1, \dots\}, 6 - 2\epsilon) &= i \left( -\frac{\mu^2}{p_3^2} \right)^\epsilon \frac{1}{\Gamma(3 - \epsilon)} \frac{1}{(2\pi i)^2} \int_{-i\infty}^{+i\infty} dz_1 dz_2 \\
&\times \left( \frac{p_1^2}{p_3^2} \right)^{z_1} \left( \frac{p_2^2}{p_3^2} \right)^{z_2} \Gamma(-z_1) \Gamma(1 - \epsilon - z_1) \Gamma(-z_2) \Gamma(1 - \epsilon - z_2) \\
&\times \Gamma(1 + z_1 + z_2) \Gamma(\epsilon + z_1 + z_2).
\end{aligned} \tag{1.74}$$

Considering straight-line contours, we have the requirements  $\text{Re}(z_i) < 0, i = 1, 2$  and  $\text{Re}(z_1) + \text{Re}(z_2) > -\epsilon$ . For our initial contours, we then have to choose something like  $z_i = -\epsilon/4$ , which makes it clear that when we take  $\epsilon \rightarrow 0$ , we have  $\text{Re}(z_i) \rightarrow 0$ , running over the left-most pole of  $\Gamma(-z_i)$ .

There are now two known approaches to expanding in  $\epsilon$  under the integral sign [77, 78]. While we will largely be dealing with finite MB representations in this thesis, it is worth noting that when necessary we will utilise the methods of [77].

The basic idea is that we may resolve the pole in  $\epsilon$  by shifting the contour out of the pinch, incurring a residue, as illustrated in fig. 1.7. Having done so, we may then simply expand in  $\epsilon$  under the integral sign.

### 1.3.2 Parametrising Mellin-Barnes integrals

Performing the residue sums of MB integrals can be prohibitively complicated, particularly for many-fold integrals, where the residues typically depend on other MB integration parameters. In recent years, a new method has been found to convert MB integrals to parametric integrals [79]. This is advantageous to us since we anticipate that our calculations will yield polylogarithmic results with relatively simple rational prefactors.

The basic idea is as follows: the main complication of performing the residue sums of an MB integral comes from when residues of one MB-integrand depends on another. In such circumstances, one quickly obtains a complicated nested sum, which can be hard to do in practice. What we wish to achieve is a factorised form of the integral, where the argument of each Gamma function depends on one and only one MB parameter. To achieve this, we require that our MB integrals must be “balanced”. By this we mean that for each MB integrand  $z_i$ , there are as many Gamma functions depending on  $z_i$  as there are which depend on  $-z_i$ . The advantage of this is that we may rewrite  $\Gamma(a-z_i)\Gamma(b+z_i) = B(a-z_i, b+z_i)\Gamma(a+b)$ , and then utilise the standard parametrisation formula for the Beta function to insert a parameter integral representation. If we then choose which Gamma functions to parametrise in such a way that we may ultimately factorise our MB integrals into products of independent integrals, this would drastically simplify the residue sum.

As an example, consider the scalar triangle of eq. (1.73) in  $d = 4$  dimensions with  $\nu_i = 1$ , we have

$$T(\{p_i\}, \{1\}, 4) = i \frac{1}{(2\pi i)^2} \int_{-i\infty}^{+i\infty} dz_1 dz_2 (p_1^2)^{z_1} (p_2^2)^{z_2} (p_3^2)^{-1-z_1-z_2} \times \Gamma^2(-z_1)\Gamma^2(-z_2)\Gamma^2(1+z_1+z_2), \quad (1.75)$$

where we have chosen  $\text{Re}(z_1) = -\frac{1}{3}$  and  $\text{Re}(z_2) = -\frac{1}{5}$  for convenience. We now wish to factorise this integral by introducing some Beta functions, we must eliminate the Gamma functions which depend on  $1+z_1+z_2$ , so we parametrise

them as follows

$$\begin{aligned}
T(\{p_i\}, \{1\}, 4) &= i \frac{1}{(2\pi i)^2} \int_{-i\infty}^{+i\infty} dz_1 dz_2 (p_1^2)^{z_1} (p_2^2)^{z_2} (p_3^2)^{-1-z_1-z_2} \\
&\quad \times \Gamma(-z_1)\Gamma(1+z_1)\Gamma(-z_2)\Gamma(1+z_2) \\
&\quad \times B(-z_1, 1+z_1+z_2)B(-z_2, 1+z_1+z_2).
\end{aligned} \tag{1.76}$$

If we wish to utilise the standard semi-infinite parameter integral representation of the beta function, we must have positive real parts of all arguments of the Beta function, however this argument is equivalent to the requirement made on the Gamma functions in the first place, so it is already guaranteed by our choice of contours. We have the following representation of the Beta function

$$B(a, b) = \int_0^\infty \frac{dx x^{a-1}}{(1+x)^{a+b}}. \tag{1.77}$$

We furthermore introduce the invariants  $u = p_1^2/p_3^2$  and  $v = p_2^2/p_3^2$ , this yields

$$\begin{aligned}
T(\{p_i\}, \{1\}, 4) &= i (p_3^2)^{-1} \frac{1}{(2\pi i)^2} \int_0^\infty dx_1 dx_2 \\
&\quad \times \int_{-i\infty}^{+i\infty} dz_1 \Gamma(-z_1)\Gamma(1+z_1) \frac{u^{z_1}}{(x_1(1+x_2))^{z_1+1}} \\
&\quad \times \int_{-i\infty}^{+i\infty} dz_2 \Gamma(-z_2)\Gamma(1+z_2) \frac{v^{z_2}}{(x_2(1+x_1))^{z_2+1}}
\end{aligned} \tag{1.78}$$

The MB integrals are now trivial to do, we may take the residue sum and simply perform the geometric series we obtain, however this representation is simply the standard MB parametrisation formula in eq. (1.67). Thus, we have the following parameter integral representation

$$T(\{p_i\}, \{1\}, 4) = i (p_3^2)^{-1} \frac{1}{(2\pi i)^2} \int_0^\infty \frac{dx_1 dx_2}{(u+x_1(1+x_2))(v+x_2(1+x_1))}. \tag{1.79}$$

At this point, we are done with utilising MB integration techniques for this integral. We will see in section 1.4 that the parameter integral above is expressible in terms of multiple polylogarithms, and we will derive an analytic result for the integral then.



### 1.3.3 Asymptotic Expansions

A related issue to that of regulation is one of asymptotically expanding a MB integral around some small parameter. This has been studied previously, resulting in an algorithm and a software package which we will use extensively [80].

The algorithm in [80] requires that the expansion parameter in the MB integrand –  $\lambda$  – is written as a pure power dependence on the MB integration parameters. Let us take a concrete example: suppose we wish to expand our three-mass triangle integral,  $T(\{p_i\}, \{1\}, 4)$  near the limit of taking  $p_1$  and  $p_2$  on-shell at the same rate. We recall eq. (1.75), and introduce an expansion parameter  $\lambda$  by rescaling  $p_1^2 \rightarrow \lambda p_1^2$  and  $p_2^2 \rightarrow \lambda p_2^2$ :

$$T_a(\{p_i\}, \{1\}, 4, \lambda) = i \frac{1}{(2\pi i)^2} \int_{-i\infty}^{+i\infty} dz_1 dz_2 \lambda^{z_1+z_2} (p_1^2)^{z_1} (p_2^2)^{z_2} (p_3^2)^{-1-z_1-z_2} \times \Gamma^2(-z_1)\Gamma^2(-z_2)\Gamma^2(1+z_1+z_2). \quad (1.80)$$

The introduction of  $\lambda$  is only intended as a means of book-keeping. That is, we now have a single parameter which captures the asymptotic behaviour of the integrand near  $p_1^2$  and  $p_2^2$  approaching zero at the same rate. The intention is to power expand around  $\lambda = 0$  to obtain this behaviour, and subsequently set  $\lambda = 1$ .

We will perform this power expansion by explicitly considering the residue sum generated by closing the contours in eq. (1.80). We take the contours to be straight lines in the complex plane with  $\text{Re}(z_1) = -\frac{1}{3}$  and  $\text{Re}(z_2) = -\frac{1}{5}$ . Since we are considering small  $\lambda$ , we must close the contours in the right half-plane to obtain a convergent series of residues. Considering  $z_1$ , we then have residues at  $z_1 = 0, 1, 2, \dots$ . Writing the integral over  $z_1$  as a residue sum, we then have

$$T_a(\{p_i\}, \{1\}, 4, \lambda) = -\frac{i}{p_3^2} \frac{1}{(2\pi i)^2} \int_{-i\infty}^{+i\infty} dz_2 \left(\frac{p_2^2}{p_3^2}\right)^{z_2} \lambda^{z_2} \Gamma^2(-z_2) \times \sum_{n=0}^{\infty} \left(\frac{p_1^2}{p_3^2}\right)^n \lambda^n \frac{\Gamma^2(1+n+z_2)}{(n!)^2} \times \left( \log\left(\frac{p_1^2 \lambda}{p_3^2}\right) + 2\psi(1+n+z_2) - 2\psi(1+n) \right). \quad (1.81)$$

The residue sum is now a power series in  $\lambda$ . The leading term in the expansion of  $T_a$  in  $\lambda$  must thus be given by the first term in the sum over  $n$ , all other terms

are power-suppressed in  $\lambda$ . Retaining only this term yields

$$T_a(\{p_i\}, \{1\}, 4, \lambda) \underset{\lambda \ll 1}{\approx} -\frac{i}{p_3^2} \frac{1}{(2\pi i)^2} \int_{-i\infty}^{+i\infty} dz_2 \left(\frac{p_2^2}{p_3^2}\right)^{z_2} \lambda^{z_2} \Gamma^2(-z_2) \Gamma^2(1+z_2) \times \left( \log\left(\frac{p_1^2 \lambda}{p_3^2}\right) + 2\psi(1+z_2) + 2\gamma_E \right). \quad (1.82)$$

The process may be repeated for  $z_2$ , in the end we obtain

$$T_a(\{p_i\}, \{1\}, 4, \lambda) = \frac{i}{p_3^2} \left( 2\zeta_2 + \log\left(\frac{p_1^2}{p_3^2}\right) \log\left(\frac{p_2^2}{p_3^2}\right) \right) + \frac{i}{p_3^2} \log(\lambda) \left( \log\left(\frac{p_1^2}{p_3^2}\right) + \log\left(\frac{p_2^2}{p_3^2}\right) + \log(\lambda) \right) + \mathcal{O}(\lambda) \quad (1.83)$$

Our expansion parameter  $\lambda$  has served its purpose, we may set it to 1, we conclude that

$$T(\{p_i\}, \{1\}, 4) \xrightarrow[\substack{p_i^2 \rightarrow 0 \\ i \in \{1,2\}}]{\frac{i}{p_3^2}} \left( 2\zeta_2 + \log\left(\frac{p_1^2}{p_3^2}\right) \log\left(\frac{p_2^2}{p_3^2}\right) \right). \quad (1.84)$$

The process we just outlined by example readily generalises to more intricate MB integrals by means of recursion. We will utilise it to expand around  $\beta_i^2 \rightarrow 0 \forall i$ , i.e.  $\gamma_{ij} \rightarrow -\infty$ , or  $\alpha_{ij} \rightarrow 0$ .

## 1.4 Polylogarithms

A great many Feynman integrals – and all the ones we will concern ourselves with in this thesis – are expressible order by order in  $\epsilon$  as a sum of generalised polylogarithms<sup>2</sup>. Furthermore, it is known that polylogarithms satisfy the structures of a Hopf algebra [81], allowing for both significant simplification, and the calculation of many Feynman integrals. In this thesis we will mostly be utilising this algebraic structure explicitly to compute Feynman integrals [82]. We will therefore not spend much time on the mathematics of polylogarithms, though an overview can be found in [83].

---

<sup>2</sup>Recently it has become clear that certain Feynman integrals (most notably the three-mass sunset diagram) cannot be described in terms of polylogarithms, but rather seem to belong to some larger family of *elliptic* integrals, of which polylogarithms form a subset. However, such functions will not appear in our calculations.

## 1.4.1 Multiple Polylogarithms

Our results will be expressible in terms of so-called multiple polylogarithms (MPLs). Throughout this thesis, we will use the notation of Goncharov and define recursively [84, 85]

$$G(a_1, a_2, \dots, a_n; z) \equiv \int_0^z \frac{dt}{t - a_1} G(a_2, \dots, a_n; t), \quad (1.85)$$

$$G(; z) = 1, \quad (1.86)$$

$$G(\underbrace{0, \dots, 0}_{n \text{ times}}; z) \equiv \frac{1}{n!} \log^n(z), \quad (1.87)$$

where the last definition is to regulate the end-point divergence at  $t=0$  of integrals like  $G(0; z) = \int_0^z \frac{dt}{t}$ . The number of integrations in a given polylogarithm is referred to as the *weight* of the polylogarithm<sup>3</sup>, thus the weight of eq. (1.85) is  $n$ .

Apart from the special case of eq. (1.87), it is also worth defining the classical polylogarithm

$$\text{Li}_n(z) \equiv -G(\underbrace{0, \dots, 0}_{n-1 \text{ times}}, 1; z), \quad (1.88)$$

thus we have  $\text{Li}_1(z) = -\log(1-z)$ . This definition is somewhat unorthodox, since the classical polylogarithm is normally defined as a sum, namely

$$\text{Li}_n(z) \equiv \sum_{i=1}^{\infty} \frac{z^i}{i^n}. \quad (1.89)$$

However, the equivalence can easily be shown by induction starting from  $\text{Li}_1(z) = -G(1, z)$ . We also note that the Riemann zeta numbers  $-\zeta_n \equiv \text{Li}_n(1)$  are included in our definition of the classical polylogarithm. These numbers thus have transcendental weight  $n$ , and are the only non-rational constants which will appear in our Feynman integrals<sup>4</sup>.

---

<sup>3</sup>It is also sometimes referred to as the transcendental weight, or the transcendentality.

<sup>4</sup>More generally, so-called multiple zeta values may also appear, however we will not encounter them.

## 1.4.2 Algebra and Coalgebra

One very useful property of MPLs is that they form what is known as a Hopf algebra [81]. The basis of this algebra is the shuffle product, which is defined for words  $a = a_1, a_2, \dots, a_n$  and  $b = b_1, b_2, \dots, b_m$  as follows

$$G(a; z)G(b; z) = \sum_{w \in a \sqcup b} G(w; z), \quad (1.90)$$

where  $\sqcup$  denotes the shuffle product, that is any way of interleaving  $a$  and  $b$  which preserves their internal ordering. It is worth noting that the shuffle product has weight  $n + m$ , thus making the shuffle algebra a *graded* algebra.

Another convenient component of the Hopf algebra of polylogarithms is the coproduct [81]. The coproduct enables one to decompose polylogarithms into products of logarithms of lower weight in a uniquely defined manner. We denote the coproduct  $\Delta$ , we have schematically

$$\Delta G(a_1, \dots, a_n, z) = \sum G(b_1, \dots, b_i, z) \otimes G(c_1, \dots, c_{n-i}, z). \quad (1.91)$$

Furthermore, the coproduct is coassociative, meaning that no matter which order one performs these decompositions, the result is unique, i.e. applying the coproduct again to the above, we have

$$\begin{aligned} \Delta (\Delta G(a_1, \dots, a_n, z)) &= \sum (\Delta G(b_1, \dots, b_i, z)) \otimes G(c_1, \dots, c_{n-i}, z) \\ &= \sum G(b_1, \dots, b_i, z) \otimes (\Delta G(c_1, \dots, c_{n-i}, z)). \end{aligned} \quad (1.92)$$

We will not give a complete definition of the coproduct here. A thorough discussion can again be found in [83]. However, it is notable that the coproduct has the property that discontinuities act only on the first component of the coproduct, and derivatives only on the last component

$$\Delta (\text{Disc}(F)) = (\text{Disc} \otimes \mathbb{1}) \cdot (\Delta F), \quad (1.93)$$

$$\Delta \left( \frac{d}{dx} F \right) = \left( \mathbb{1} \otimes \frac{d}{dx} \right) \cdot (\Delta F). \quad (1.94)$$

These properties have particular implications for Feynman integrals, and have played an important role in formulating a diagrammatic interpretation of the coproduct of Feynman diagrams [86], as well as establishing a basis of functions for multiple-gluon-exchange webs [26].

One other property of importance is that  $\pi$  and even zeta-values are only allowed in the first entry of the coproduct, this is in order to avoid an inconsistency related to the fact that  $\zeta_{2n} \propto \pi^2 \zeta_{2n-2}$ .

We label particular components of the iterated coproduct as  $\Delta_{i_1, i_2, \dots, i_n}$ , where  $i_k$  are the weight of the  $k^{\text{th}}$  term in the co-product, i.e.  $\Delta_{1,2,3}$  will produce a co-product where the first entry is weight 1, the second is weight 2 and the third and final entry is weight 3. Since Zeta values are irreducible, information about  $\zeta_n$  is not present in a specific component of the coproduct unless that component has a part which has weight  $k \geq n$ . In the case of even  $n$ , the *first* entry in the coproduct must be weight  $k \geq n$  for  $\zeta_n$  to appear.

### 1.4.3 Parameter Integrals

The coproduct and the algebra of polylogarithms is primarily of interest to us for two purposes: to perform parameter integrals, and to simplify our results. From eq. (1.85), it is clear that at each step in our integration, we require a denominator which is linear in at least one integration parameter, and then to be able to rewrite the numerator in terms of polylogarithms whose last argument is this same integration parameter. The ability to do this is related to the property of linear reducibility. Assuming that our integral has this property an algorithm for performing the integration – which uses numerical fitting to determine the dependence on  $\zeta_n$  – is presented in [83]. A completely analytic method is presented in [87], however we will only utilise the methods in [83] in this thesis.

The algorithm works by repeatedly taking the coproduct until one obtains the component of the coproduct where every term is weight 1. The algebraic properties of logarithms may then be utilised on this component to re-write the coproduct and match it to a trial function on the level of the co-product. Having obtained such a trial function, the terms proportional to  $\zeta_i$  must then be reconstructed, since such terms are invariably lost when taking the  $1, 1, \dots, 1$ -component of the coproduct.

As a simple example, we may consider a scalar three-mass triangle in  $d = 4$ . We saw in the previous section that its MB representation may be parametrised as in eq. (1.79). The form is already conducive to writing the result in terms of MPLs, since the integrand consists of linear denominators in the two integration

parameters:

$$T(\{p_i\}, \{1\}, 4) = i (p_3^2)^{-1} \frac{1}{(2\pi i)^2} \int_0^\infty \frac{dx_1 dx_2}{(u + x_1(1 + x_2))(v + x_2(1 + x_1))}. \quad (1.95)$$

Our first step is to part the integral into fractions, which enables us to do one integral immediately

$$T(\{p_i\}, \{1\}, 4) = i (p_3^2)^{-1} \int_0^\infty \frac{dx_2}{x_2^2 + (1 - u + v)x_2 + v} \quad (1.96)$$

$$\times \left( \log\left(\frac{v}{u}\right) + \log\left(1 + \frac{x_2}{v}\right) - \log(x_2) + \log(x_2 + 1) \right) \quad (1.97)$$

The denominator is quadratic in  $x_2$ , its roots contain a Källén function,  $\lambda(1, u, v)$ , as in eq. (1.41). It is convenient to introduce new invariants  $z$  and  $\bar{z}$  as follows

$$u = z\bar{z}, \quad (1.98)$$

$$v = (1 - z)(1 - \bar{z}). \quad (1.99)$$

We then also transform  $x_2$  according to  $x_2 = 1/t_2 - 1$ , to obtain

$$T(\{p_i\}, \{1\}, 4) = i (p_3^2)^{-1} \int_0^1 \frac{dt_2}{(1 - t_2 z)(1 - t_2 \bar{z})} \\ \times [\log(1 - t_2(1 - (1 - z)(1 - \bar{z}))) - \log(1 - t_2) - \log(t_2) - \log(z\bar{z})] \quad (1.100)$$

We have  $G(a, z) = \log(1 - z/a)$ , which we may use to re-write the integrand in terms of MPLs. Integrating over  $t_2$  is then a simple matter of parting into fractions and utilising eq. (1.85) to obtain

$$T(\{p_i\}, \{1\}, 4) = i \frac{1}{(p_3^2)} \frac{1}{z - \bar{z}} \left[ \log(z\bar{z}) \log\left(\frac{1 - z}{1 - \bar{z}}\right) \right. \\ \left. + G\left(\frac{1}{z}, 0, 1\right) + G\left(\frac{1}{z}, 1, 1\right) - G\left(\frac{1}{\bar{z}}, 0, 1\right) - G\left(\frac{1}{\bar{z}}, 1, 1\right) \right. \\ \left. - G\left(\frac{1}{z}, \frac{1}{z + \bar{z} - z\bar{z}}, 1\right) + G\left(\frac{1}{\bar{z}}, \frac{1}{z + \bar{z} - z\bar{z}}, 1\right) \right] \quad (1.101)$$

Thus far we have utilised the algebraic properties of logarithms to re-cast our integral, we now wish to do the same to this weight two expression. The algorithm outlined in [83] does this by utilising the (1, 1)-component ( $\delta_{11}$ ) of the coproduct to find an expression with the same decomposition in terms of simple logarithms. Numerics are then utilised to fix the constants  $\zeta_n$  which are left out by the

coproduct. In this manner, it can be shown that

$$T(\{p_i\}, \{1\}, 4) = i \frac{1}{(p_3^2)} \frac{1}{z - \bar{z}} \left[ \log(z\bar{z}) \log\left(\frac{1-z}{1-\bar{z}}\right) + \text{Li}_2(z) - \text{Li}_2(\bar{z}) \right]. \quad (1.102)$$

#### 1.4.4 Single-Valued Harmonic Polylogarithms

The branch cut structure of a MPL  $G(\cdots, a_i, \cdots, z)$  is dictated by its branch points  $z = a_i$ . However, in many applications, specific kinematic regions might be free of branch cuts in spite of  $a_i = z$  being present in the region. This is possible if the result is constructed of specific linear combinations of polylogarithms of the various invariants, such that any branch cut of a single polylogarithm is cancelled by an equal and opposite branch cut. The simplest example of such a linear combination can be given for  $z$  a complex invariant and  $\bar{z}$  being its complex conjugate<sup>5</sup>. We then have the linear combination

$$\mathcal{L}_0(z) = \log(z\bar{z}) = \log(z) + \log(\bar{z}). \quad (1.103)$$

The argument of the combined logarithm is manifestly real, and it is clear that when  $z$  crosses the branch cut in one direction,  $\bar{z}$  crosses it in the other direction, cancelling out any contribution from crossing the branch cut.

This is clearly a simple example, however such polylogarithms have been found to exist at higher weights. They are generally called Brown's single-valued harmonic polylogarithms, and further details can be found in [88]. Some further discussion of their applications to physics are given in [89, 90]. Some examples of such polylogarithms, which we will use later are provided in table 1.1.

A few properties are worth noting: firstly, the indices  $a_i$  in  $\mathcal{L}_{a_1 \cdots a_n}$  are either 0 or 1, reflecting the fact that single-valued harmonic polylogarithms only have branch points at  $z = 0, 1$ . Secondly, like MPLs, single-valued harmonic polylogarithms obey a shuffle relation, i.e.

$$\mathcal{L}_{a_1 \cdots a_n}(z) \mathcal{L}_{b_1 \cdots b_m}(z) = \sum_{w \in a \sqcup b} \mathcal{L}_w(z). \quad (1.104)$$

---

<sup>5</sup>These invariants appeared in section 1.3.2, if we choose the region of  $\lambda(1, u, v) < 0$ , where  $\lambda$  is the Källén function (eq. (1.41)).

Lastly, there's an index reversal identity as follows

$$\mathcal{L}_{a_1 \dots a_n}(z) = (-1)^{n+1} \mathcal{L}_{a_n \dots a_1}(\bar{z}) \quad (1.105)$$

Finally, we note that the three-mass triangle in eq. (1.102) may be written more succinctly in terms of single-valued harmonic polylogarithms:

$$T(\{p_i\}, \{1\}, 4) = i \frac{1}{(p_3^2)} \frac{1}{z - \bar{z}} [\mathcal{L}_{0,1}(z) - \mathcal{L}_{1,0}(z)]. \quad (1.106)$$

This concludes our overview of polylogarithms. In what follows, we will first consider a two-loop calculation of a single fully connected web. This calculation will provide us with a background example for the three-loop calculation which follows, and will allow us to directly obtain a full non-lightlike result, which will enable us to discuss the light-like limit of  $\Gamma^S$  at two loops in more detail.



Weight	$\mathcal{L}$	
1	$\mathcal{L}_0(z)$	$\log(z) + \log(\bar{z})$
1	$\mathcal{L}_1(z)$	$\log(1-z) + \log(1-\bar{z})$
2	$\mathcal{L}_{0,1}(z)$	$\frac{1}{2} \log(z\bar{z}) \log\left(\frac{1-z}{1-\bar{z}}\right) - \text{Li}_2(z) + \text{Li}_2(\bar{z})$
3	$\mathcal{L}_{1,0,0}(z)$	$\begin{aligned} & \text{Li}_3(z) + \text{Li}_3(\bar{z}) - \frac{1}{2} \log(z) \text{Li}_2(\bar{z}) - \frac{1}{2} \text{Li}_2(z) \log(\bar{z}) \\ & - \frac{1}{2} \text{Li}_2(\bar{z}) \log(\bar{z}) - \frac{1}{4} \log^2(z) \log(1-\bar{z}) \\ & - \frac{1}{4} \log(1-z) \log^2(\bar{z}) - \frac{1}{4} \log(1-z) \log^2(z) \\ & - \frac{1}{4} \log(1-\bar{z}) \log^2(\bar{z}) - \frac{1}{2} \log(1-z) \log(z) \log(\bar{z}) \\ & - \frac{1}{2} \log(z) \log(1-\bar{z}) \log(\bar{z}) - \frac{1}{2} \text{Li}_2(z) \log(z) \end{aligned}$
5	$\mathcal{L}_{1,0,1,0,1}(z)$	$\begin{aligned} & 4\zeta(3)G(1,z)G(1,\bar{z}) - G(1,\bar{z})G(0,1,0,1,\bar{z}) \\ & - G^2(0,1,z)G(1,\bar{z}) - G(0,z)G(1,z)G(0,1,z)G(1,\bar{z}) \\ & - G(1,z)G(0,1,z)G(0,\bar{z})G(1,\bar{z}) \\ & + G(0,1,z)G(1,\bar{z})G(0,1,\bar{z}) - 2G(0,1,z)G(0,1,1,\bar{z}) \\ & - G(0,z)G(1,z)G(1,\bar{z})G(0,1,\bar{z}) - G(1,z)G^2(0,1,\bar{z}) \\ & - G(1,z)G(0,\bar{z})G(1,\bar{z})G(0,1,\bar{z}) \\ & + 2G(1,z)G(0,0,1,z)G(1,\bar{z}) \\ & + 2G(1,z)G(1,\bar{z})G(0,0,1,\bar{z}) \\ & + 2G(0,z)G(0,1,1,z)G(1,\bar{z}) \\ & + G(1,z)G(0,1,z)G(0,1,\bar{z}) \\ & + 2G(0,1,1,z)G(0,\bar{z})G(1,\bar{z}) - 2G(0,1,1,z)G(0,1,\bar{z}) \\ & + 2G(0,z)G(1,z)G(0,1,1,\bar{z}) \\ & + 2G(1,z)G(0,\bar{z})G(0,1,1,\bar{z}) + G(0,1,0,1,z)G(1,\bar{z}) \\ & + G(1,z)G(0,1,0,1,\bar{z}) + 2G(0,1,0,1,1,\bar{z}) \\ & + 2G(0,1,1,0,1,\bar{z}) - G(1,z)G(0,1,0,1,z) \\ & + 2G(0,1,0,1,1,z) + 2G(0,1,1,0,1,z) \end{aligned}$

**Table 1.1** Some examples of Brown's single-valued harmonic polylogarithms.

# Chapter 2

## The Soft Anomalous Dimension at Two Loops

We now turn our attention to the two-loop soft anomalous dimension. A full calculation has been performed in [28–31].

Our goal in this section, however, is to outline and demonstrate the methods we will later apply to three loops, as well as to examine in further detail the relationship between  $\Gamma^S$  for lightlike and non-lightlike external partons, and the dipole formula (eq. (1.37)). For this reason, we will focus only on fully connected diagrams, then simply state the full result and discuss the lightlike limit.

### 2.1 Two-loop Calculation of the Three-line Two-loop Web

At this loop order, we have two diagrams to consider, one consisting of single gluon exchanges (fig. 2.1b), and one fully connected graph (fig. 2.1a). For our purposes, we will only focus on the fully connected diagram containing a single three gluon vertex, as it gives a concise introduction to the techniques we will ultimately apply at three loops. Due to its connected nature, the diagram only has a single  $\frac{1}{\epsilon}$  pole, and we do not need to concern ourselves with subdivergences, which only arise in the multiple gluon exchange diagrams at this loop order. While our starting point will differ from that of [30, 31], our calculation will eventually

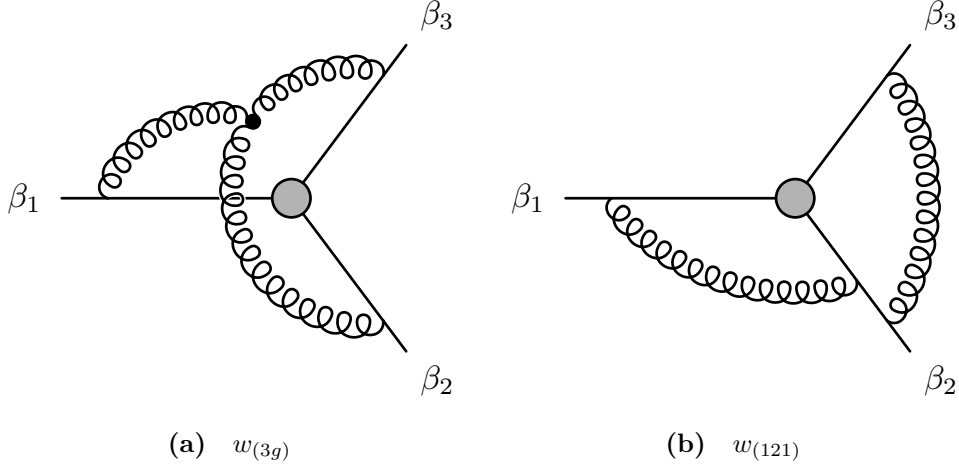


**Figure 2.1** Web topologies correlating three lines at two loops.

converge on the same integral, and we will follow their calculation from that point on.

Hence, considering the three-gluon vertex diagram, the Feynman rules yield the following expression for the full diagram

$$w_{(3g)}(\alpha_{12}, \alpha_{13}, \alpha_{23}) \equiv \mathcal{C}_{(3g)} \mathcal{F}_{(3g)}(\alpha_{12}, \alpha_{13}, \alpha_{23}), \quad (2.1)$$

$$\mathcal{C}_{3g} \equiv i f^{abc} \mathbf{T}_1^a \mathbf{T}_2^b \mathbf{T}_3^c, \quad (2.2)$$

$$\begin{aligned} \mathcal{F}_{(3g)}(\alpha_{12}, \alpha_{13}, \alpha_{23}) &\equiv -i \mu^{4\epsilon} g_s^4 \mathcal{N}^3 \int d^d z \int_0^\infty ds_1 ds_2 ds_3 \hat{\beta}_1^\mu \hat{\beta}_2^\nu \hat{\beta}_3^\sigma, \\ &\times \Gamma_{\mu\nu\sigma} \left( \partial_{s_1 \hat{\beta}_1 - z}, \partial_{s_2 \hat{\beta}_2 - z}, \partial_{s_3 \hat{\beta}_3 - z} \right) \\ &\times \left[ \prod_{i=1}^3 \left( -(s_i \hat{\beta}_i - z)^2 \right)^{\epsilon-1} \right] e^{-i(m-i0)\sum_i s_i}. \end{aligned} \quad (2.3)$$

Where as before, we have taken the convention of normalised, spacelike  $\hat{\beta}_i$ , i.e.  $\hat{\beta}_i^2 = -1$ .

Our first order of business is to isolate the UV pole of this diagram by means of the following reparametrisation

$$\begin{aligned} s_i &= \alpha y_i, \\ \sum_{i=1}^3 y_i &= 1. \end{aligned} \quad (2.4)$$

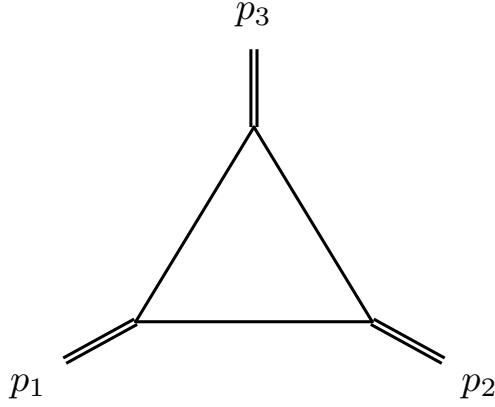


**Figure 2.2** *A three-mass scalar triangle.*

Performing the integration over  $\alpha$  then yields

$$\mathcal{F}_{(3g)} = -ig_s^4 \left(\frac{\mu^2}{m^2}\right)^{2\epsilon} \mathcal{N}^3 \Gamma(4\epsilon) \int d^d z \int_0^\infty dy_1 dy_2 dy_3 \delta\left(1 - \sum_i y_i\right) \hat{\beta}_1^\mu \hat{\beta}_2^\nu \hat{\beta}_3^\sigma \Gamma_{\mu\nu\sigma}\left(\partial_{y_1 \hat{\beta}_1 - z}, \partial_{y_2 \hat{\beta}_2 - z}, \partial_{y_3 \hat{\beta}_3 - z}\right) \left[ \prod_{i=1}^3 \left(- (y_i \hat{\beta}_i - z)^2 + i0\right)^{\epsilon-1} \right]. \quad (2.5)$$

Note that we have transferred the  $i0$ -prescription to its usual place in the propagator, since it will be important when we Wick-rotate  $z$ .

Next we turn our attention to the integration over the vertex,  $z$ . Our aim is to substitute an MB representation of this vertex by means of simply inserting that of a known one-loop integral. The  $z$ -dependence in the differentiation is redundant, and we may simply rewrite the vertex factor  $\Gamma$  such that it acts on the Wilson line parameters. Doing so, we extract the  $z$ -integration entirely and obtain

$$\mathcal{F}_{(3g)} = -ig_s^4 \left(\frac{\mu^2}{m^2}\right)^{2\epsilon} \mathcal{N}^3 \Gamma(4\epsilon) \int_0^\infty dy_1 dy_2 dy_3 \delta\left(1 - \sum_i y_i\right) \hat{\beta}_1^\mu \hat{\beta}_2^\nu \hat{\beta}_3^\sigma \Gamma_{\mu\nu\sigma}\left(\partial_{y_1 \hat{\beta}_1}, \partial_{y_2 \hat{\beta}_2}, \partial_{y_3 \hat{\beta}_3}\right) \int d^d z \left[ \prod_{i=1}^3 \left(- (y_i \hat{\beta}_i - z)^2\right)^{\epsilon-1} \right]. \quad (2.6)$$

## 2.1.1 The Scalar Three-mass Triangle

Turning our attention to the integration over  $z$ , we observe that if we define auxiliary momenta  $p_i \equiv y_i \hat{\beta}_i - y_{i-1} \hat{\beta}_{i-1}$ , cyclically – i.e.  $y_0 \hat{\beta}_0 \equiv y_3 \hat{\beta}_3$  – this integral is simply a scalar triangle (fig. 2.2), which we defined in eq. (1.68). Inserting this into  $\mathcal{F}_{(3g)}$ , we obtain

$$\mathcal{F}_{(3g)} = -g_s^4 \pi^{d/2} \left( \frac{\mu^2}{m^2} \right)^{2\epsilon} \mathcal{N}^3 \Gamma(4\epsilon) \int_0^\infty dy_1 dy_2 dy_3 \delta \left( 1 - \sum_i y_i \right) \quad (2.7)$$

$$\hat{\beta}_1^\mu \hat{\beta}_2^\nu \hat{\beta}_3^\sigma \Gamma_{\mu\nu\sigma} \left( \partial_{y_1 \hat{\beta}_1}, \partial_{y_2 \hat{\beta}_2}, \partial_{y_3 \hat{\beta}_3} \right) T(\{p_i^2\}, \{1 - \epsilon\}, d).$$

The one-loop scalar triangle  $T(\{p_i^2\}, \{\nu_i\}, d)$  has been studied extensively. We will make use of the Mellin-Barnes representation in eq. (1.73), inserting this into eq. (2.7) and defining  $y_{ij} \equiv y_i \hat{\beta}_i - y_j \hat{\beta}_j$  we then obtain

$$\mathcal{F}_{(3g)} = -4 \left( \frac{\alpha_S}{4\pi} \right)^2 \left( \frac{\tilde{\mu}^2}{m^2 e^{\gamma_E}} \right)^{2\epsilon} \frac{\Gamma(4\epsilon)}{\Gamma(1 + \epsilon)} \int_0^\infty dy_1 dy_2 dy_3 \delta \left( 1 - \sum_i y_i \right)$$

$$\hat{\beta}_1^\mu \hat{\beta}_2^\nu \hat{\beta}_3^\sigma \Gamma_{\mu\nu\sigma} \left( \partial_{y_1 \hat{\beta}_1}, \partial_{y_2 \hat{\beta}_2}, \partial_{y_3 \hat{\beta}_3} \right) \int_{-i\infty}^{+i\infty} dz_1 dz_2 (-y_{13}^2)^{z_1} (-y_{12}^2)^{z_2} (-y_{23}^2)^{-1+2\epsilon-z_1-z_2}$$

$$\Gamma^2(-z_1) \Gamma^2(-z_2) \Gamma(1 - \epsilon + z_1 + z_2) \Gamma(1 - 2\epsilon + z_1 + z_2), \quad (2.8)$$

where for convenience we have rescaled the renormalisation scale  $\tilde{\mu} = \mu e^{\gamma_E} / \pi$ .

In order to calculate the two-loop contribution to  $\Gamma_S$ , it is sufficient to compute the pole term of  $\mathcal{F}_{(3g)}$ , hence we now expand in  $\epsilon$  to obtain

$$\mathcal{F}_{(3g)}^{(2,-1)} = - \left( \frac{1}{4\pi} \right)^2 \int_0^\infty dy_1 dy_2 dy_3 \delta \left( 1 - \sum_i y_i \right)$$

$$\hat{\beta}_1^\mu \hat{\beta}_2^\nu \hat{\beta}_3^\sigma \Gamma_{\mu\nu\sigma} \left( \partial_{y_1 \hat{\beta}_1}, \partial_{y_2 \hat{\beta}_2}, \partial_{y_3 \hat{\beta}_3} \right) \quad (2.9)$$

$$\int_{-i\infty}^{+i\infty} dz_1 dz_2 (-y_{13}^2)^{z_1} (-y_{12}^2)^{z_2} (-y_{23}^2)^{-1-z_1-z_2}$$

$$\Gamma^2(-z_1) \Gamma^2(-z_2) \Gamma^2(1 + z_1 + z_2).$$

We turn next to the differentiation term  $\Gamma_{\mu\nu\sigma}$ , and rewrite it in terms of derivatives

with respect to  $y_{ij}^2$ , we obtain

$$\hat{\beta}_1^\mu \hat{\beta}_2^\nu \hat{\beta}_3^\sigma \Gamma_{\mu\nu\sigma} \left( \partial_{y_1 \hat{\beta}_1}, \partial_{y_2 \hat{\beta}_2}, \partial_{y_3 \hat{\beta}_3} \right) = -\frac{1}{2} \sum_{(i,j,k)} \epsilon_{ijk} y_j (\gamma_{ij} \gamma_{jk} - 2\gamma_{ik}) \partial_{y_{ij}^2}. \quad (2.10)$$

Inserting this into our MB integral, and taking advantage of the fact that  $T(\{p_i^2\}, \{1\}, 4)$  is symmetric under the interchange of any momenta, we obtain

$$\begin{aligned} \mathcal{F}_{(3g)}^{(2,-1)} &= \frac{1}{2} \left( \frac{1}{4\pi} \right)^2 \sum_{(i,j,k)} \epsilon_{ijk} (\gamma_{ij} \gamma_{jk} - 2\gamma_{ik}) \frac{1}{(2\pi i)^2} \int_{-i\infty}^{+i\infty} dz_1 dz_2 \\ &\quad \Gamma^2(-z_1) \Gamma(-z_2) \Gamma(1-z_2) \Gamma^2(1+z_1+z_2) \int_0^\infty dy_i dy_j dy_k \quad (2.11) \\ &\quad \delta \left( 1 - \sum_l y_l \right) y_j (-y_{ik}^2)^{z_1} (-y_{ij}^2)^{z_2-1} (-y_{jk}^2)^{-1-z_1-z_2}. \end{aligned}$$

Note here that we have used the identity  $z_2 \Gamma(-z_2) = -\Gamma(1-z_2)$  to absorb the stray factor of  $z_2$  resulting from the differentiation. At this point, our expression exactly matches the momentum-space calculation using Feynman parameters [31].

## 2.1.2 Feynman Parameters

We now wish to perform the remaining two integrations over the Wilson lines. To do this, we first observe  $-y_{ij}^2 = (y_i^2 + y_j^2 - \gamma_{ij} y_i y_j)$ , and we use the standard MB parametrisation formula of eq. (1.67) to extract the terms containing  $\gamma_{ij}$

$$\begin{aligned} \mathcal{F}_{(3g)}^{(2,-1)} &= \frac{1}{2} \left( \frac{1}{4\pi} \right)^2 \sum_{(i,j,k)} \epsilon_{ijk} (\gamma_{ij} \gamma_{jk} - 2\gamma_{ik}) \frac{1}{(2\pi i)^5} \int_{-i\infty}^{+i\infty} dz_1 dz_2 \\ &\quad \left[ \prod_{l=1}^3 \int_{-i\infty}^{+i\infty} dw_l \Gamma(-w_l) \right] (-\gamma_{ij})^{w_3} (-\gamma_{ik})^{w_2} (-\gamma_{jk})^{w_1} \\ &\quad \Gamma(-z_1) \Gamma(-z_2) \Gamma(w_2 - z_1) \Gamma(1 - z_2 + w_3) \quad (2.12) \\ &\quad \Gamma(1 + z_1 + z_2) \Gamma(1 + z_1 + z_2 + w_1) \\ &\quad \int_0^\infty dy_i dy_j dy_k \delta \left( 1 - \sum_l y_l \right) y_i^{w_2+w_3} y_j^{w_1+w_3+1} y_k^{w_1+w_2} \\ &\quad (y_i^2 + y_j^2)^{z_2-1-w_3} (y_i^2 + y_k^2)^{z_1-w_2} (y_j^2 + y_k^2)^{-1-z_1-z_2-w_1} \end{aligned}$$

We are now ready to do the parameter integrals. It is convenient to separate out the parameter integrals themselves, we define

$$I_{(3)} \equiv \int_0^\infty dy_i dy_j dy_k \delta \left( 1 - \sum_l y_l \right) y_i^{w_2+w_3} y_j^{w_1+w_3+1} y_k^{w_1+w_2} \quad (2.13)$$

$$(y_i^2 + y_j^2)^{z_2-1-w_3} (y_i^2 + y_k^2)^{z_1-w_2} (y_j^2 + y_k^2)^{-1-z_1-z_2-w_1} .$$

We then perform the following transformations

$$\begin{pmatrix} y_i \\ y_j \\ y_k \end{pmatrix} = \begin{pmatrix} (1-x)y \\ (1-x)(1-y) \\ x \end{pmatrix}, \quad (2.14)$$

followed by the transformation  $a = x/(1-x)$ , yielding

$$I_{(3)} = \int_0^1 dy \int_0^\infty da a^{w_1+w_2} y^{w_2+w_3} (1-y)^{w_1+w_3+1} \quad (2.15)$$

$$(y^2 + (1-y)^2)^{z_2-1-w_3} (y^2 + a^2)^{z_1-w_2}$$

$$((1-y)^2 + a^2)^{-1-z_1-z_2-w_1} .$$

We now rescale  $a \rightarrow a(1-y)$  and introduce  $b = y/(1-y)$  to obtain

$$I_{(3)} = \int_0^\infty da a^{w_1+w_2} (1+a^2)^{-1-z_1-z_2-w_1} \quad (2.16)$$

$$\int_0^\infty db b^{w_2+w_3} (1+b^2)^{z_2-1-w_3} (a^2 + b^2)^{z_1-w_2} .$$

We are almost ready to do the integral. We introduce one more MB parameter to get

$$I_{(3)} = \frac{1}{\Gamma(w_2 - z_1)} \frac{1}{(2\pi i)} \int_{-i\infty}^{+i\infty} dz_3 \Gamma(-z_3) \Gamma(z_3 + w_2 - z_1)$$

$$\int_0^\infty da a^{2z_1-2z_3+w_1-w_2} (1+a^2)^{-1-z_1-z_2-w_1} \quad (2.17)$$

$$\int_0^\infty db b^{w_2+w_3+2z_3} (1+b^2)^{z_2-1-w_3} .$$

Performing the integration now produces

$$\begin{aligned}
I_{(3)} &= \frac{1}{4} \frac{1}{\Gamma(w_2 - z_1) \Gamma(1 + z_1 + z_2 + w_1) \Gamma(1 + w_3 - z_2)} \\
&\quad \frac{1}{(2\pi i)} \int_{-i\infty}^{+i\infty} dz_3 \Gamma(-z_3) \Gamma(z_3 + w_2 - z_1) \\
&\quad \Gamma\left(\frac{1}{2} + \frac{w_1}{2} - \frac{w_2}{2} + z_1 - z_3\right) \Gamma\left(\frac{1}{2} + \frac{w_1}{2} + \frac{w_2}{2} + z_2 + z_3\right) \\
&\quad \Gamma\left(\frac{1}{2} + \frac{w_2}{2} + \frac{w_3}{2} + z_3\right) \Gamma\left(\frac{1}{2} - \frac{w_2}{2} + \frac{w_3}{2} - z_2 - z_3\right)
\end{aligned} \tag{2.18}$$

Inserting this into eq. (2.12), we obtain

$$\begin{aligned}
\mathcal{F}_{(3g)}^{(2,-1)} &= \frac{1}{8} \left(\frac{1}{4\pi}\right)^2 \sum_{(i,j,k)} \epsilon_{ijk} (\gamma_{ij}\gamma_{jk} - 2\gamma_{ik}) \frac{1}{(2\pi i)^6} \int_{-i\infty}^{+i\infty} dz_1 dz_2 dz_3 \\
&\quad \left[ \prod_{l=1}^3 \int_{-i\infty}^{+i\infty} dw_l \Gamma(-w_l) \right] (-\gamma_{ij})^{w_3} (-\gamma_{ik})^{w_2} (-\gamma_{jk})^{w_1} \\
&\quad \Gamma(-z_1) \Gamma(-z_2) \Gamma(-z_3) \Gamma(z_3 + w_2 - z_1) \Gamma(1 + z_1 + z_2) \\
&\quad \Gamma\left(\frac{1}{2} + \frac{w_1}{2} - \frac{w_2}{2} + z_1 - z_3\right) \Gamma\left(\frac{1}{2} + \frac{w_1}{2} + \frac{w_2}{2} + z_2 + z_3\right) \\
&\quad \Gamma\left(\frac{1}{2} + \frac{w_2}{2} + \frac{w_3}{2} + z_3\right) \Gamma\left(\frac{1}{2} - \frac{w_2}{2} + \frac{w_3}{2} - z_2 - z_3\right)
\end{aligned} \tag{2.19}$$

### 2.1.3 Alpha Parameters

We have thus obtained a representation of the three-gluon vertex in the form of a six-fold Mellin-Barnes integral. The expression is rather large, and impractical to compute as is, so we need to apply Barnes' lemmas [91, 92] in order to reduce the complexity<sup>1</sup>. One such application is immediately possible to perform, reducing the integral to five-fold. However, further progress is hampered by the factors of  $\frac{1}{2}$  in the arguments of the gamma functions. To alleviate this, we once again introduce alpha parameters according to eq. (1.56). We then introduce three new MB parameters to split the brackets containing alphas, and repeatedly apply

---

<sup>1</sup>For a good overview of these methods, see e.g. Ch. 4 and App. D of [76].



Barnes' lemmas. The result is a three-fold MB integral

$$\begin{aligned}
\mathcal{F}_{(3g)}^{(2,-1)} &= \frac{1}{8} \left( \frac{1}{4\pi} \right)^2 \sum_{(i,j,k)} \epsilon_{ijk} \left( \left( \alpha_{ij} + \frac{1}{\alpha_{ij}} \right) \left( \alpha_{jk} + \frac{1}{\alpha_{jk}} \right) + 2 \left( \alpha_{ik} + \frac{1}{\alpha_{ik}} \right) \right) \\
&\quad \frac{1}{(2\pi i)^6} \int_{-i\infty}^{+i\infty} dr_1 dr_2 dr_3 \alpha_{ij}^{2r_3+1} \alpha_{ik}^{2r_2} \alpha_{jk}^{2r_1+1} \\
&\quad \Gamma^2(1+r_1+r_2) \Gamma^2(-r_1-r_2) \Gamma^2(1+r_1-r_2) \Gamma^2(-r_1+r_2) \\
&\quad \Gamma(1+r_2+r_3) \Gamma(-r_2-r_3) \Gamma(1-r_2+r_3) \Gamma(r_2-r_3)
\end{aligned} \tag{2.20}$$

This three-fold MB integral has a remarkably simple structure.

Utilising the parametrisation procedure outlined in section 1.3.2, we obtain

$$\begin{aligned}
\mathcal{F}_{(3g)}^{(2,-1)} &= \frac{1}{2} \left( \frac{1}{4\pi} \right)^2 \sum_{(i,j,k)} \epsilon_{ijk} \left( \left( \alpha_{ij} + \frac{1}{\alpha_{ij}} \right) \left( \alpha_{jk} + \frac{1}{\alpha_{jk}} \right) + 2 \left( \alpha_{ik} + \frac{1}{\alpha_{ik}} \right) \right) \\
&\quad \int_0^\infty \frac{dx_1 dx_2 dx_3 x_3}{\left( x_1 + \alpha_{jk} \right) \left( x_1 + \frac{x_3}{\alpha_{ik}} \right) \left( x_2 + \alpha_{ik} \right) \left( \frac{x_2}{\alpha_{jk}} + x_3 \right) \left( x_3 + \alpha_{ij} \right) \left( x_3 + \frac{1}{\alpha_{ij}} \right)}.
\end{aligned} \tag{2.21}$$

Performing the integration, we obtain a fairly large result with a complex rational prefactor. However, due to the sum over a totally antisymmetric tensor, most such terms cancel. What remains is simply

$$\mathcal{F}_{(3g)}^{(2,-1)}(\alpha_{12}, \alpha_{13}, \alpha_{23}) = 2 \left( \frac{1}{4\pi} \right)^2 \sum_{(i,j,k)} \epsilon_{ijk} \frac{1 + \alpha_{ij}^2}{1 - \alpha_{ij}^2} \log \alpha_{ij} \log^2 \alpha_{ik}. \tag{2.22}$$

The result is manifestly antisymmetric in swapping any two Wilson lines, as one would expect and require in order to satisfy Bose symmetry.

## 2.2 The Two-loop Soft Anomalous Dimension in the limit of Light-Like External Partons

A complete calculation of  $\Gamma^S$  at two loops involves the computation of the web composed of diagrams like the one in fig. 2.1b. We will not show this computation here, however a complete calculation can be found in [28–31].

The result obtained in eq. (2.22) has a *tripole* colour structure, i.e. its colour factor is proportional to  $f^{abc}\mathbf{T}_1^a\mathbf{T}_2^b\mathbf{T}_3^c$ . As discussed in section 1.2.3, such colour structures must vanish in the limit of lightlike external partons, leaving behind only  $\Gamma^{\text{dip.}}$ . However, it is clear that near the light-like limit of  $\alpha_{ij} \rightarrow 0$ , we have

$$\begin{aligned} \mathcal{F}_{(3g)}^{(2,-1)}(\{\alpha_{ij}\}) &= 2\frac{1}{(4\pi)^2}(\log(\alpha_{12}) - \log(\alpha_{13}))(\log(\alpha_{13}) - \log(\alpha_{23})) \\ &\quad \times (\log(\alpha_{23}) - \log(\alpha_{12})) + \mathcal{O}(\alpha_{ij}) \end{aligned} \quad (2.23)$$

This contribution, however, is exactly cancelled in the light-like limit by the contribution from the 1-2-1 web (fig. 2.1b)[30, 31], leaving behind simply

$$\Gamma^{(2,-1)}(\{\hat{\beta}_i\}) = \Gamma^{\text{dip.},(2,-1)}(\{\hat{\beta}_i\}). \quad (2.24)$$

This cancellation only occurs in the limit of light-like external partons, and the case of massive external partons is necessarily more complex. For a complete calculation and complete results, see [28–31].



# Chapter 3

## Colour Conservation at Three Loops

Having seen how the dipole formula manifests itself in the light-like limit at two loops, we now turn our attention to three loops. As we have discussed in section 1.2.3, three loops is the first occasion for any corrections beyond the dipole formula to occur. Such corrections can only depend on conformal invariant cross-ratios, which implies kinematic dependence on at least four Wilson lines. However, since the dipole formula only applies once colour conservation is taken into account, this does not necessarily imply the cancellation of any webs connecting two or three lines. In this chapter – however – we will see that the form of such contributions are highly constrained by Bose symmetry, and will develop the formalism required to assemble all diagrams contributing at three loops to four lines beyond the dipole formula.

The layout of this chapter is as follows: we will start by discussing how to assemble the soft anomalous dimension at four lines, and the kinematic structure of these contributions. We will then discuss in turn the colour basis and structure of four-, three- and two-line webs contributing to  $\Gamma^S$  before and after colour conservation, as well as how these contributions may satisfy the requirements of the dipole formula. Finally, we will assemble a sum of all diagrams contributing to  $\Gamma^S$ .

We work with four lines since this is the maximal number of Wilson lines it is possible to connect at three loops. For the purposes of colour conservation, we assume four Wilson lines, though our result is readily extensible to more than four lines. We make no assumptions about momentum conservation at the origin, allowing for any number of non-QCD particles.

### 3.1 $\Gamma^S$ on Four Lines

We know from the dipole formula (1.37) that the form of  $\Gamma^S$  at three loops for four Wilson lines is of the form

$$\Gamma^S(\{\alpha_{ij}\}) = \Delta(z, \bar{z}) + \Gamma_{\text{dip.}}(\{\alpha_{ij}\}). \quad (3.1)$$

A priori, these contributions arise from webs connecting two, three and four lines which we will denote by  $\Gamma_n$ , where  $n$  is the number of Wilson lines. Schematically, we have

$$\Gamma^S(\{\alpha_{ij}\}) = \Gamma_4(z, \bar{z}, \{\log(\alpha_{ij})\}) + \Gamma_3(\{\log(\alpha_{ij})\}) + \Gamma_2(\{\log(\alpha_{ij})\}). \quad (3.2)$$

We note that  $\Gamma_3$  and  $\Gamma_2$  are polynomial in  $\log(\alpha_{ij})$ . This is specifically because our asymptotic expansion near the light-like limit power-suppresses any non-logarithmic terms. The reasoning for this can also be understood by considering the dipole formula. Specifically, the contributions from webs connecting two and three lines are constructed by summing over all ways of choosing three or two lines out of the four, i.e.

$$\Gamma_3(\{\log(\alpha_{ij})\}) = \sum_{1 \leq i < j < k \leq 4} G_3(i, j, k) \quad (3.3)$$

$$\Gamma_2(\{\log(\alpha_{ij})\}) = \sum_{1 \leq i < j \leq 4} G_2(i, j) \quad (3.4)$$

Since we need four Wilson lines in order to construct a CICR, the only way we can obtain any CICR-dependence from such a sum is if terms depending on individual angles sum to something depending on their products. Thus, the CICR-dependence of the correction to the dipole formula implies that  $\Gamma_2$  and  $\Gamma_3$  must be polynomial in  $\log(\alpha_{ij})$ .

### 3.2 Four-Line Webs

We begin by presenting the most general Bose symmetric form of a four-line web contribution to  $\Gamma^S$ . Since all webs have maximally non-abelian colour factors, such a contribution must take the form of the colour factor associated with a double three gluon vertex diagram, as depicted in fig. 3.1. We define the kinematic

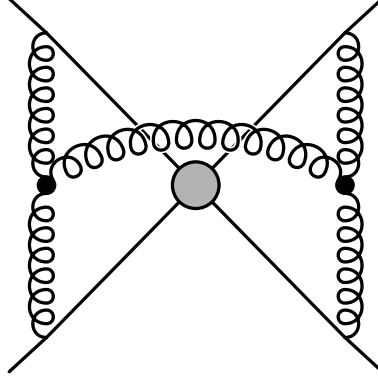


**Figure 3.1** *Maximally Non-Abelian Colour Structure on Four Lines*

function  $H_4 [(i, j), (k, l)]$  where the indices  $i, j, k, l$  label the colour and kinematic factors associated with each leg, and obtain

$$\begin{aligned} \Gamma_4(1, 2, 3, 4) \equiv & \mathbf{T}_1^a \mathbf{T}_2^b \mathbf{T}_3^c \mathbf{T}_4^d (f^{abe} f^{cde} H_4 [(1, 2); (3, 4)] \\ & + f^{ace} f^{bde} H_4 [(1, 3); (2, 4)] + f^{ade} f^{bce} H_4 [(1, 4); (2, 3)]) . \end{aligned} \quad (3.5)$$

Bose symmetry is realised by antisymmetry within the round brackets, and symmetry in swapping the round brackets, i.e.

$$H_4 [(1, 2); (3, 4)] = H_4 [(3, 4); (1, 2)] = -H_4 [(2, 1); (3, 4)] . \quad (3.6)$$

We now wish to see what happens when we apply colour conservation to this expression. We set  $\mathbf{T}_4 = -\sum_{i=1}^3 \mathbf{T}_i$  and then apply the identity  $\mathbf{T}_i^a \mathbf{T}_i^b = \frac{1}{2} \{\mathbf{T}_i^a, \mathbf{T}_i^b\} + \frac{i}{2} f^{abc} \mathbf{T}_i^c$ . All terms with a tripole colour factor<sup>1</sup> which are generated by applying colour conservation cancel due to the symmetries outlined in eq. (3.6), and what remains is simply

$$\begin{aligned} \Gamma_4(1, 2, 3, 4) = & -\frac{1}{2} f^{abe} f^{cde} \sum_{\substack{(i,j,k) \in (1,2,3) \\ j < k \\ i \neq j,k}} \{\mathbf{T}_i^a, \mathbf{T}_i^d\} \mathbf{T}_j^b \mathbf{T}_k^c \\ & \times (H_4 [(i, j), (k, 4)] + H_4 [(i, k), (j, 4)]) . \end{aligned} \quad (3.7)$$

<sup>1</sup>Colour factor associated with a three gluon vertex, such as the one in eq. (2.2)

### 3.3 Three-Line Webs

We now consider webs connecting three lines in the same manner as we did for four Wilson lines in the previous sections. We find our three-line maximally non-abelian colour basis to have the colour factors obtained from four lines in eq. (3.7) and a tripole term, in agreement with [16]. In general, the sum over all three-line webs must then be of the form

$$G_3(1, 2, 3) \equiv iN_c f^{abc} \mathbf{T}_1^a \mathbf{T}_2^b \mathbf{T}_3^c H_c [(1, 2, 3)] \\ + \sum_{\substack{(i,j,k) \in (1,2,3) \\ j < k}} f^{abe} f^{cde} \{ \mathbf{T}_i^a, \mathbf{T}_i^d \} \mathbf{T}_j^b \mathbf{T}_k^c H_3 [i, \{j, k\}], \quad (3.8)$$

where we again require total antisymmetry within the round brackets and symmetry within curly brackets. We now extend this to four lines by summing over all subsets of three Wilson lines

$$\Gamma_3(1, 2, 3, 4) = G_3(1, 2, 3) + G_3(1, 2, 4) + G_3(1, 3, 4) + G_3(2, 3, 4). \quad (3.9)$$

#### 3.3.1 Colour Conservation

Applying colour conservation to eq. (3.9), we obtain

$$\Gamma_3(1, 2, 3, 4) = \sum_{\substack{(i,j,k) \in (1,2,3) \\ j < k \\ i \neq j, k}} f^{abe} f^{cde} \{ \mathbf{T}_i^a, \mathbf{T}_i^d \} \mathbf{T}_j^b \mathbf{T}_k^c U(i, \{j, k\}, 4) \\ + \Gamma_T(1, 2, 3, 4) + \Gamma_D(1, 2, 3, 4) + \Gamma_{\text{Tripole}}(1, 2, 3, 4), \quad (3.10)$$

where we have defined  $\Gamma_T$  to contain all colour factors connecting two lines with anticommutators,  $\Gamma_D$  to contain all dipole terms, and  $\Gamma_{\text{Tripole}}$  to contain pure

tripole terms. In terms of kinematic functions, they are

$$U(i, \{j, k\}, 4) \equiv H_3 [i, \{j, k\}] - H_3 [i, \{j, 4\}] - H_3 [i, \{k, 4\}] - H_3 [4, \{i, j\}] - H_3 [4, \{i, k\}] + H_3 [4, \{j, k\}], \quad (3.11)$$

$$\Gamma_T(1, 2, 3, 4) \equiv \frac{1}{2} \sum_{1 \leq i < j \leq 3} f^{abe} f^{cde} \{\mathbf{T}_i^a, \mathbf{T}_i^c\} \{\mathbf{T}_j^b, \mathbf{T}_j^d\} \times (H_3 [i, \{j, 4\}] + H_3 [j, \{4, i\}] + H_3 [4, \{j, i\}]), \quad (3.12)$$

$$\Gamma_D(1, 2, 3, 4) \equiv \frac{N_c^2}{4} \sum_{1 \leq i < j \leq 3} (\mathbf{T}_i \cdot \mathbf{T}_j) \times (H_3 [i, \{j, 4\}] + H_3 [j, \{4, i\}] + H_3 [4, \{j, i\}]), \quad (3.13)$$

$$\Gamma_{\text{Tripole}}(1, 2, 3, 4) \equiv i N_c f^{abc} \mathbf{T}_1^a \mathbf{T}_2^b \mathbf{T}_3^c (H_c [(1, 2, 3)] - H_c [(1, 2, 4)] + H_c [(1, 3, 4)] - H_c [(2, 3, 4)]). \quad (3.14)$$

It follows from the constraint equations (eq. (1.35)) and Bose symmetry that we must require [32, 33]

$$\Gamma_{\text{Tripole}}(1, 2, 3, 4) = 0. \quad (3.15)$$

### 3.4 Two-Line Webs

Moving on to webs connecting two lines, we first need to establish a colour basis at three loops. Since exponentiated colour factors are of the form of fully connected diagrams, there are relatively few possible combinations. One obvious form is of course the dipole  $\mathbf{T}_i^a \mathbf{T}_j^a$ , which we will take as one element in our basis.

The only other maximally non-Abelian colour structure at this loop order is products of colour factors involving two structure constants, i.e.

$$C_2(x, y, z, w) \equiv f^{abe} f^{cde} \mathbf{T}_x^a \mathbf{T}_y^b \mathbf{T}_z^c \mathbf{T}_w^d. \quad (3.16)$$

Specifically, we consider  $C_2$  with all permutations of the sets  $\{i, i, i, j\}$  and  $\{i, i, j, j\}$  being the arguments as possible basis elements. We then apply the same commutator identity we utilised to calculate colour factors in the three- and four-line cases to reduce this set to a basis. Upon doing so, we find just one more



basis element composed of two anticommutator terms, our full basis is

$$c_1 = \mathbf{T}_i^a \mathbf{T}_j^a, \quad (3.17)$$

$$c_2 = f^{abe} f^{cde} \{ \mathbf{T}_i^a, \mathbf{T}_i^c \} \{ \mathbf{T}_j^b, \mathbf{T}_j^d \}. \quad (3.18)$$

Since  $c_1$  can only contribute to  $\Gamma_{\text{dip.}}$ , we will set it aside. We therefore define the quantities

$$\Gamma_2(1, 2, 3, 4) = \Gamma_{2C}(1, 2, 3, 4) + \Gamma_{2D}(1, 2, 3, 4), \quad (3.19)$$

$$\Gamma_{2C}(1, 2, 3, 4) = \sum_{1 \leq i < j \leq 4} f^{abe} f^{cde} \{ \mathbf{T}_i^a, \mathbf{T}_i^c \} \{ \mathbf{T}_j^b, \mathbf{T}_j^d \} H_2(\{i, j\}), \quad (3.20)$$

$$\Gamma_{2D}(1, 2, 3, 4) = \frac{N_c^2}{2} \sum_{i < j} (\mathbf{T}_i \cdot \mathbf{T}_j) H_{2D}[\{i, j\}]. \quad (3.21)$$

### 3.4.1 Colour Conservation

We are now ready to apply colour conservation to the two-line graphs. We first consider  $\Gamma_{2C}$  and find

$$\begin{aligned} \Gamma_{2C}(1, 2, 3, 4) &= -4 f^{abe} f^{cde} \sum_{\substack{(i,j,k) \in (1,2,3) \\ j < k}} \{ \mathbf{T}_i^a, \mathbf{T}_i^c \} \mathbf{T}_j^b \mathbf{T}_k^d H_2(\{i, 4\}) \\ &+ \sum_{1 \leq i < j \leq 3} f^{ace} f^{bde} \{ \mathbf{T}_i^a, \mathbf{T}_i^b \} \{ \mathbf{T}_j^c, \mathbf{T}_j^d \} \\ &\times (H_2(\{i, j\}) + H_2(\{i, 4\}) + H_2(\{j, 4\})) \\ &+ \frac{N_c^2}{2} \sum_i (\mathbf{T}_i \cdot \mathbf{T}_i) H_2(\{i, 4\}) \\ &+ N_c^2 \sum_{1 \leq i < j \leq 3} (\mathbf{T}_i \cdot \mathbf{T}_j) (H_2(\{i, 4\}) + H_2(\{j, 4\})) \end{aligned} \quad (3.22)$$

The latter two terms proportional to  $N_c^2$  are clearly dipole terms, contributing to  $\Gamma_{\text{dip.}}$ . For completeness, we also apply colour conservation to  $\Gamma_{2D}$ , yielding

$$\begin{aligned} \Gamma_{2D}(1, 2, 3, 4) &= -\frac{N_c^2}{2} \sum_{i=1}^3 (\mathbf{T}_i \cdot \mathbf{T}_i) H_{2D}[\{i, 4\}] \\ &+ \frac{N_c^2}{2} \sum_{1 \leq i < j \leq 3} (\mathbf{T}_i \cdot \mathbf{T}_j) (H_{2D}[\{i, j\}] - H_{2D}[\{i, 4\}] - H_{2D}[\{j, 4\}]). \end{aligned} \quad (3.23)$$

### 3.5 Colour Conservation in $\Gamma^S$

We now wish to put all this together into a final expression for  $\Gamma^S$  on four lines. As a first step, it is convenient to look at the expressions which come from two- and three-line diagrams separately. We find that if we define a combined function of two and three lines  $\bar{H}_3$  as follows

$$\bar{H}_3(i, \{j, k\}) \equiv H_3(i, \{j, k\}) + H_2(\{i, j\}) + H_2(\{i, k\}), \quad (3.24)$$

eq. (3.22) becomes

$$\begin{aligned} \Gamma_3(1, 2, 3, 4) + \Gamma_{2C}(1, 2, 3, 4) &= \sum_{\substack{(i,j,k) \in (1,2,3) \\ j < k}} f^{abe} f^{cde} \{\mathbf{T}_i^a, \mathbf{T}_i^d\} \mathbf{T}_j^b \mathbf{T}_k^c \bar{U}(i, \{j, k\}, 4) \\ &+ \bar{\Gamma}_T(1, 2, 3, 4) + \bar{\Gamma}_D(1, 2, 3, 4) + \frac{N_c^2}{2} \sum_i (\mathbf{T}_i \cdot \mathbf{T}_i) H_2(\{i, 4\}) \\ &- \frac{N_c^2}{2} \sum_{1 \leq i < j \leq 3} \mathbf{T}_i \cdot \mathbf{T}_j (H_2(\{i, j\}) - H_2(\{i, 4\}) - H_2(\{j, 4\})). \end{aligned} \quad (3.25)$$

Eqs. (3.11) to (3.13) with  $H_3$  replaced by  $\bar{H}_3$  define  $\bar{U}$ ,  $\bar{\Gamma}_T$  and  $\bar{\Gamma}_D$ , respectively. This definition of  $\bar{H}_3$  is unique: it is the only way to absorb the two-line function  $H_2$  into the definition of  $H_3$  in a manner which obeys Bose symmetry on three lines.

Next we consider the non-dipole colour factors on two lines, they are given by  $\bar{\Gamma}_T$ . The constraint equations in eq. (1.35) require that these terms may at most be constant, yielding the following requirement

$$\bar{H}_3[i, \{j, k\}] + \bar{H}_3[j, \{k, i\}] + \bar{H}_3[k, \{j, i\}] = 3C, \quad (3.26)$$

where  $C$  is a constant. This requirement also immediately yields  $\bar{\Gamma}_D(1, 2, 3, 4) \propto C$ , drastically simplifying our expression in eq. (3.25). In a similar vein, we find that the only way of defining a four-line function with the symmetries of  $H_4$  and which

reproduces  $\bar{U}$  is

$$\begin{aligned} \bar{H}_4 [(i, j), (k, l)] &\equiv H_4 [(i, j), (k, l)] \\ &- \frac{2}{3} (\bar{H}_3 [i, \{j, k\}] - \bar{H}_3 [i, \{j, l\}] - \bar{H}_3 [j, \{i, k\}] + \bar{H}_3 [j, \{i, l\}] \\ &+ \bar{H}_3 [k, \{i, l\}] - \bar{H}_3 [k, \{j, l\}] - \bar{H}_3 [l, \{i, k\}] + \bar{H}_3 [l, \{j, k\}]) . \end{aligned} \quad (3.27)$$

$$\bar{H}_{2D} [\{i, j\}] \equiv H_{2D} [\{i, j\}] - H_2 [\{i, j\}] \quad (3.28)$$

Utilising this definition along with eq. (3.26) yields the following result for  $\Delta(z, \bar{z})$  and  $\Gamma_{\text{dip}}$ .

$$\begin{aligned} \Delta(z, \bar{z}) &= -\frac{1}{2} \sum_{\substack{(i,j,k) \in (1,2,3) \\ j < k}} f^{abe} f^{cde} \{\mathbf{T}_i^a, \mathbf{T}_i^d\} \mathbf{T}_j^b \mathbf{T}_k^c \\ &\quad \times (\bar{H}_4 [(i, j), (k, 4)] + \bar{H}_4 [(i, k), (j, 4)] + 4C) \\ &\quad + \frac{3}{2} C \sum_{1 \leq i < j \leq 3} f^{abe} f^{cde} \{\mathbf{T}_i^a, \mathbf{T}_i^c\} \{\mathbf{T}_j^b, \mathbf{T}_j^d\}, \\ \Gamma_{\text{dip}}(1, 2, 3, 4) &= -\frac{N_c^2}{2} \sum_{i=1}^3 (\mathbf{T}_i \cdot \mathbf{T}_i) \bar{H}_{2D} [\{i, 4\}] \\ &\quad + \frac{N_c^2}{2} \sum_{1 \leq i < j \leq 3} (\mathbf{T}_i \cdot \mathbf{T}_j) \left( \bar{H}_{2D} [\{i, j\}] - \bar{H}_{2D} [\{i, 4\}] - \bar{H}_{2D} [\{j, 4\}] + \frac{3}{2} C \right). \end{aligned} \quad (3.29)$$

The result for  $\Delta$  is written here in terms of colour factors after applying colour conservation and removing the colour factor  $\mathbf{T}_4$ . However we could just as easily write it in a manifestly Bose symmetric fashion by re-introducing  $\mathbf{T}_4$  as follows

$$\begin{aligned} \Delta(z, \bar{z}) &= \mathbf{T}_1^a \mathbf{T}_2^b \mathbf{T}_3^c \mathbf{T}_4^d (f^{abe} f^{cde} \bar{H}_4 [(1, 2); (3, 4)] \\ &\quad + f^{ace} f^{bde} \bar{H}_4 [(1, 3); (2, 4)] + f^{ade} f^{bce} \bar{H}_4 [(1, 4); (2, 3)]) \\ &\quad + C \sum_{\substack{(i,j,k) \in (1,2,3,4) \\ j < k \\ i \neq j, k}} f^{abe} f^{cde} \{\mathbf{T}_i^a, \mathbf{T}_i^d\} \mathbf{T}_j^b \mathbf{T}_k^c. \end{aligned} \quad (3.31)$$

The inclusion of a constant term proportional to three-line colour factors differs from similar expressions given in [32, 33], where the term was excluded for reasons of symmetry as well as collinear limits. Contrary to expectations, we will find that such a term is in fact needed in order to satisfy collinear limits. We will defer further discussion of the matter until we have evaluated the limits in chapter 8.

### 3.6 $\Gamma^S$ on Three Lines

Now that we have found an explicit expression for  $\Delta$  in terms of our colour and kinematic basis, we need one more ingredient in order to consider collinear limits. Recall that the anomalous dimension of the splitting function  $\Gamma_{\text{Sp}}$  is defined as the difference between an  $n$ -leg and an  $(n - 1)$ -leg soft anomalous dimension

$$\Gamma_{\text{Sp}}(p_1, p_2) = \Gamma_n(\beta_1, \beta_2, \dots, \beta_n) - \Gamma_{n-1}(\beta_1 + \beta_2, \beta_3, \dots, \beta_n). \quad (3.32)$$

If we wish to compute  $\Gamma_{\text{Sp}}$ , we therefore need not only  $\Gamma_4$ , but also  $\Gamma_3$ . We utilise the same colour basis and find

$$\Gamma_3(1, 2, 3) = G_3(1, 2, 3) + G_2(1, 2) + G_2(1, 3) + G_2(2, 3). \quad (3.33)$$

Applying the same techniques as we did for four lines, and requiring the cancellation of tripole terms, we find that we may write

$$\Gamma_3(1, 2, 3) = \sum_{\substack{(i,j,k) \in (1,2,3) \\ j < k}} f^{abe} f^{cde} \{ \mathbf{T}_i^a, \mathbf{T}_i^d \} \mathbf{T}_j^b \mathbf{T}_k^c \bar{H}_3(i, \{j, k\}). \quad (3.34)$$

The  $\Gamma_3$  in  $\Gamma_{\text{Sp}}$  is in a four-line colour basis, i.e. it depends on  $\mathbf{T}_1 + \mathbf{T}_2$ ,  $\mathbf{T}_3$  and  $\mathbf{T}_4$ . We will therefore not apply colour conservation to eq. (3.34), but rather leave it like this until we consider a specific collinear limit in chapter 8.

Instead, the next chapter will cover the main techniques of our calculation in depth, before we proceed to give the full analytic result of all relevant webs in chapter 5.



# Chapter 4

## Computing Webs at Three Loops

Having established the general kinematic and colour structure at three loops, we now turn to computing three-loop webs in the asymptotic limit of lightlike Wilson lines. Our plan is to calculate all webs contributing to colour factors other than dipoles and tripoles, either by performing an expansion around the light-like limit of an already known result, or utilising Mellin-Barnes techniques to perform an asymptotic expansion near the light-like limit under the integral sign, as outlined in section 1.3.3.

Out of these two methods, the latter is by far the most time-consuming and intricate, and so we will dedicate a large portion of this chapter to the methodology we use to compute these webs, which have in common that they contain one or more gluon-gluon interaction vertices. Figure 4.1 shows the subset of these webs which connect four lines, and fig. 4.2 shows examples of specific permutations of

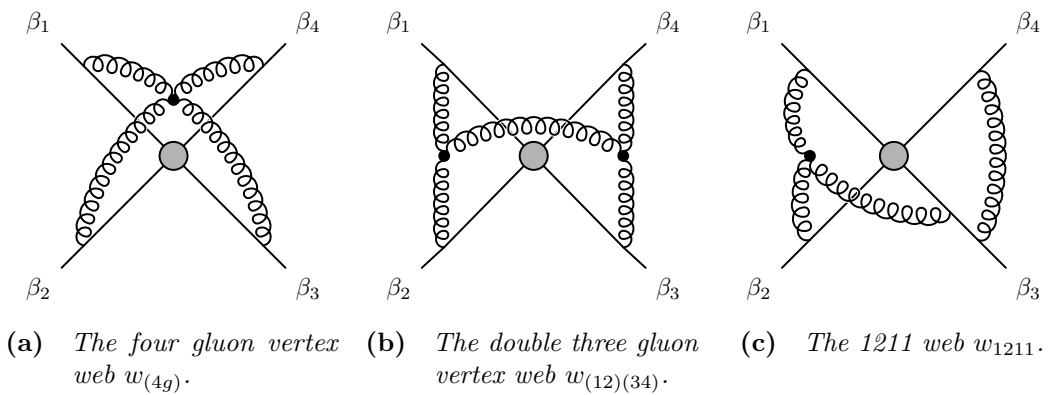


**Figure 4.1** *Four-line webs containing gluon-gluon interactions.*

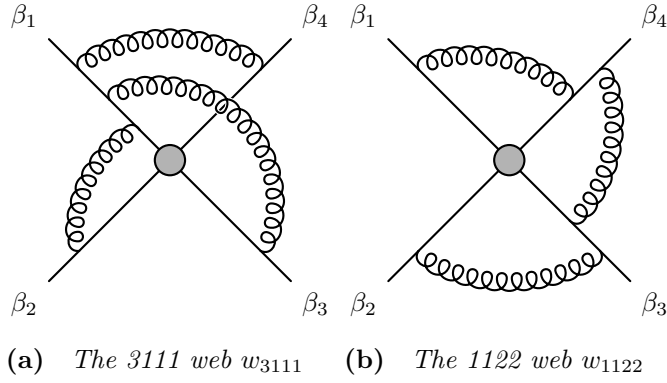


**Figure 4.2** *Representative diagrams for each four-line multiple gluon exchange web.*

the corresponding multiple gluon exchange webs.

Before we proceed, it is important to note that we must have full non-lightlike results for a web in order to utilise collinear reduction. The reason for this is clear if we consider the various kinematic limits involved. The light-like limit is characterised by  $\beta_i^2 \rightarrow 0$ , or equivalently  $\alpha_{ij} \rightarrow 0 \forall i, j$ . However, collinear reduction requires us to take two lines parallel, i.e  $\beta_i \parallel \beta_j$ , or equivalently  $\alpha_{ij} \rightarrow 1$ . Thus, in expanding around  $\alpha_{ij} = 0$ , we lose the ability to take the collinear limit in a consistent manner. This forces us to explicitly calculate all diagrams containing multiple gluon vertices, since we are not in possession of any results for these diagrams with non-lightlike external partons.

The layout of the chapter is as follows: We begin with a general overview of all the webs we wish to compute, and how we will compute each of them. We then discuss webs containing multiple gluon exchange vertices, outlining our methodology for calculating the contribution to the soft anomalous dimension near the asymptotic light-like limit. We then briefly discuss light-like limits of known results and the procedure of collinear reduction.

## 4.1 General Overview

We wish to calculate  $H_4$ ,  $H_3$  and  $H_2$ , as defined in eqs. (3.5), (3.10) and (3.20), respectively. These diagrams come with specific colour factors, and hence we will discard all webs which do not contribute to these colour factors (i.e webs which only contribute dipole or tripole colour factors, e.g. fig. 4.3).

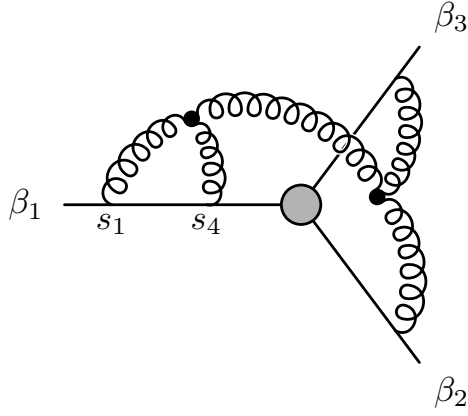
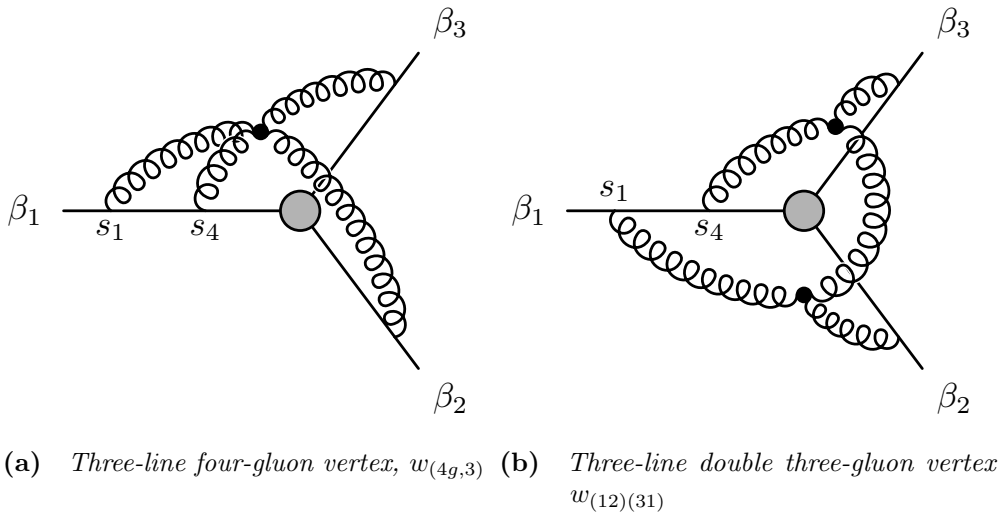


**Figure 4.3** Web with tripole colour factor, which we discard.



(a) Three-line four-gluon vertex,  $w_{(4g,3)}$  (b) Three-line double three-gluon vertex  $w_{(12)(31)}$

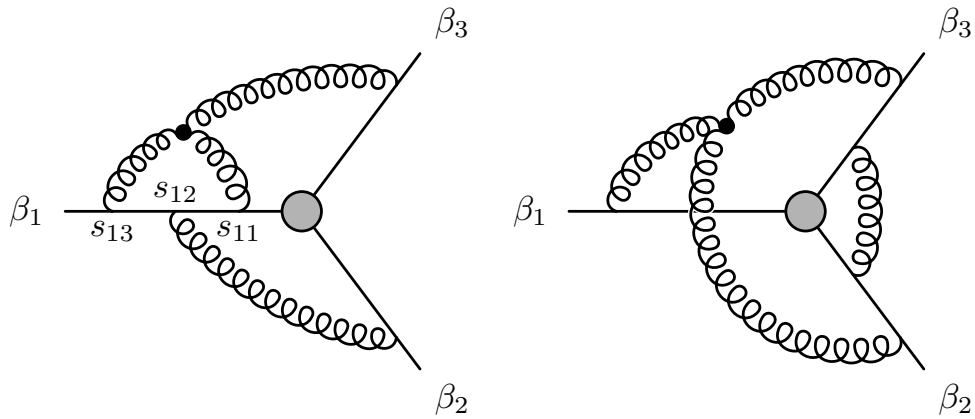
**Figure 4.4** Fully connected three-line webs contribution to  $H_3$

The four-line webs we will have to explicitly compute are depicted in fig. 4.1. In the case of fig. 4.1c, significant progress on the integration has been made in [93], which we will use our starting point. There are two other webs which contribute to  $H_4$ , these are the MGEWs in fig. 4.2, which have already been computed in [26].

For  $H_3$ , we need the diagrams in figs. 4.4 to 4.7. We will explicitly compute the webs in figs. 4.5a and 5.4, while the web in fig. 4.5b will be obtained by collinear reduction. The web containing a vertex correction in fig. 4.6 has been computed in [94], and the MGEWs in fig. 4.7 have been calculated in [95]. We will simply state their results here.

Finally, the webs contributing to  $H_2$  are given in figs. 4.8 to 4.10. Again, we will compute the fully connected webs in fig. 4.8 explicitly, the remaining webs will be





(a) Configuration of 311-web which contributes to  $H_3$ , other configurations only contribute tripole colour factors.

(b)  $w_{122}$

**Figure 4.5** Representative diagrams of three-line webs contributing to  $H_3$  which contain a single three-gluon vertex.

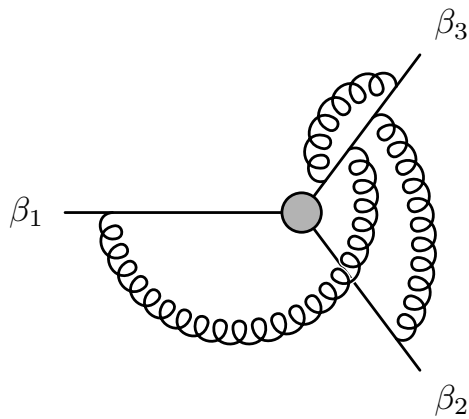


**Figure 4.6** Representative diagram of web with vertex correction contributing to  $H_3$ .

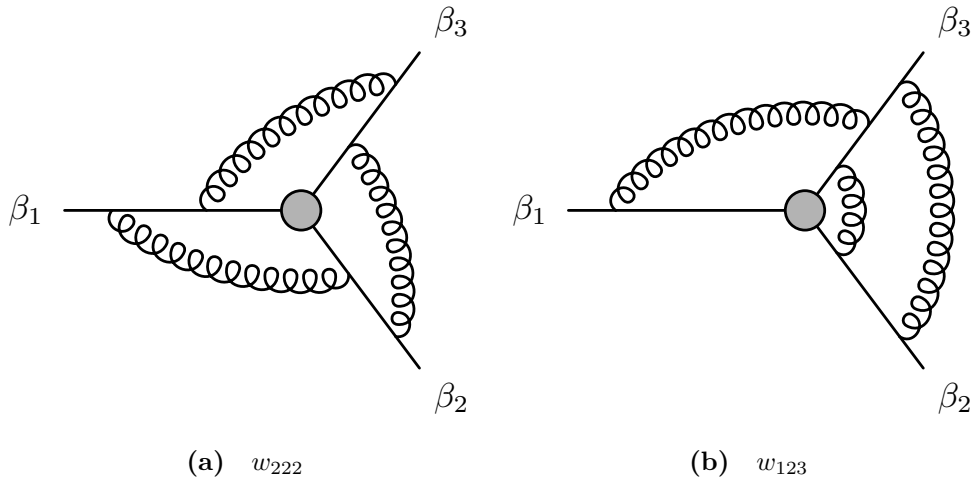


**Figure 4.7** Representative diagrams of three-line MGEWs contributing to  $H_3$ .

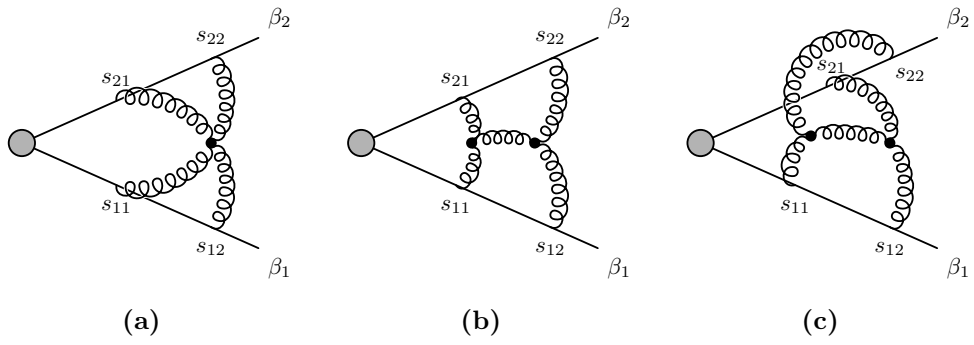


**Figure 4.8** Fully connected two-line webs contributing to  $H_2$ .

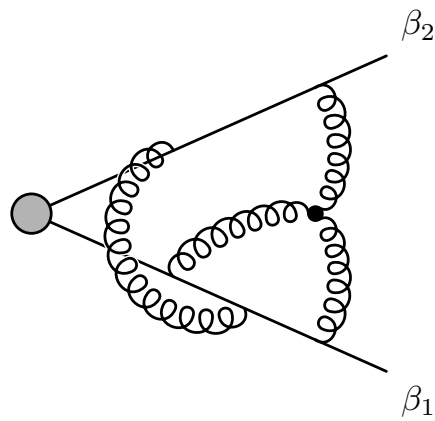
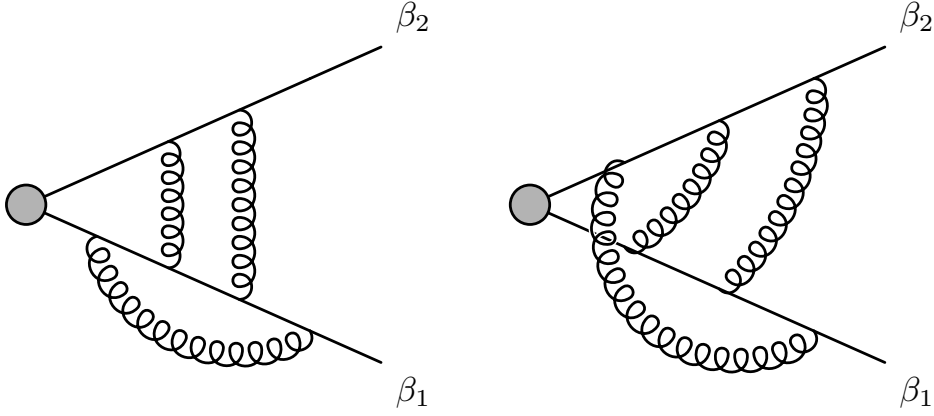


**Figure 4.9** The 23-web, which contributes to  $H_2$ .



(a) Representative diagram of the 24-web. (b) Representative diagram of the 33-web.

**Figure 4.10** Representative diagrams of MGEWs with and without vertex corrections that contribute to  $H_2$ .

computed by means of collinear reduction.

## 4.2 Webs Containing Gluon-Gluon Interactions

Arguably the most difficult webs to calculate at three loop order are webs containing gluon-gluon interactions. This owes largely to the complexity of their kinematic integrals, and to date no complete calculation of these webs has been performed. We will not attempt to calculate these diagrams in full, but rather we will focus on their behaviour near the asymptotic light-like limit.

To do this, we will find a Mellin-Barnes representation of the relevant integrals, and utilise the techniques in section 1.3.3 to perform an expansion around the asymptotic light-like limit.

Our procedure mirrors the one we employed to obtain a MB representation in section 2.1. We start with a Feynman integral on  $n_l$  Wilson lines and with  $n_v$  internal vertices, factorised into a kinematic factor  $\mathcal{F}_G$  and a corresponding colour factor  $\mathcal{C}_G$

$$w_G(\{\mathbf{T}_i\}, \{\gamma_{ij}\}, \epsilon) = \mathcal{C}_G(\{\mathbf{T}_i\}, \{\gamma_{ij}\}) \mathcal{F}_G(\{\gamma_{ij}\}, \epsilon). \quad (4.1)$$

The colour factor will be one of the basis elements discussed in chapter 3, attached to the relevant number of legs, and potentially with some polynomial dependence on  $\gamma_{ij}$ , to make the colour factor manifestly Bose symmetric. Focusing on the

kinematic factor, it has the general form

$$\begin{aligned} \mathcal{F}_G(\gamma_{ij}, \epsilon) = & \mathcal{A} \left[ \prod_{i=1}^{n_l} \int_0^\infty ds_i \beta_i^{\sigma_i} e^{-ims_i \sqrt{\beta_i^2 + i0}} \right] \\ & \times \left[ \prod_{j=1}^{n_v} \int d^d z_j \right] H_{\sigma_1 \dots \sigma_n}(s_i \beta_i, \{z_i\}, \epsilon), \end{aligned} \quad (4.2)$$

Where we have once again considered spacelike Wilson lines and have used the rescaling invariance of the Wilson lines to normalise them such that  $\beta_i^2 = -1$ .

$H$  is homogeneous such that at  $l$  loops, we have

$$H_{\sigma_1 \dots \sigma_n}(\alpha s_i \beta_i, \{\alpha z_i\}, \epsilon) = \alpha^{(2l+2n_v)\epsilon - n_l - 4n_v} H_{\sigma_1 \dots \sigma_n}(s_i \beta_i, \{z_i\}, \epsilon). \quad (4.3)$$

We therefore proceed as we did in eq. (2.4), by rescaling all integration parameters by a common scale  $\alpha$ , and integrating out this scale. The specific form of this parametrisation varies depending on the integral we intend to perform, generically we have

$$z_i = \alpha w_i, \quad (4.4)$$

$$s_i = \alpha \frac{f_i(\{x_j\})}{\sqrt{\beta_i^2}}, \quad (4.5)$$

where  $\sum_i f_i(\{x_j\}) = 1$ . This allows us to integrate over  $\alpha$  and obtain the full divergence of  $\mathcal{F}_G$ . For instance, we find in Appendix A that the four-gluon vertex diagram in fig. 4.1a has the kinematic factor

$$\begin{aligned} \mathcal{F}_{(4g)}(\{\beta_i\}, \epsilon) \equiv & -ig_s^6 \left( \frac{\mu^2}{m^2} \right)^{3\epsilon} \mathcal{N}^4(\beta_1 \cdot \beta_3)(\beta_2 \cdot \beta_4) \\ & \times \int d^d z \prod_{i=1}^4 \left[ \int_0^\infty ds_i \frac{e^{-ims_i \sqrt{\beta_i^2 - i0}}}{[-(s_i \beta_i - z)^2 + i0]^{1-\epsilon}} \right]. \end{aligned} \quad (4.6)$$

It is clear that if we rescale this expression according to eqs. (4.4) and (4.5), the denominator scales as  $\alpha^{8-8\epsilon}$ , and the combined integration measures rescale as  $\alpha^{8-2\epsilon}$ . We choose to rescale the integrand according to  $s_i = \alpha y_i / \sqrt{\beta_i^2}$  and  $z \rightarrow \alpha z$ ,

with the requirement that  $\sum_i y_i = 1$ . After integrating over  $\alpha$  we then obtain

$$\mathcal{F}_{(4g)}(\{\beta_i\}, \epsilon) = -ig_s^6 \left(\frac{\mu^2}{m^2}\right)^{3\epsilon} \mathcal{N}^4 \frac{\gamma_{13}\gamma_{24}}{4} \Gamma(6\epsilon) \int d^d z \int_0^1 \left(\prod_{i=1}^4 dy_i\right) \quad (4.7)$$

$$\times \delta\left(1 - \sum_{i=1}^4 y_i\right) \prod_{i=1}^4 \left[-\left(y_i \hat{\beta}_i - z\right)^2 + i0\right]^{\epsilon-1}. \quad (4.8)$$

With the exception of the 1211-web in fig. 4.1c – which has subdivergences – we may at this point expand in  $\epsilon$ , since there are no further divergences. Defining  $J[\{f_i(\{x_j\})\}]$  as the Jacobian of our generic transformations in eqs. (4.4) and (4.5), we then have

$$\begin{aligned} \mathcal{F}^{(l,-1)} &= \frac{\Omega}{(4\pi)^3} \frac{1}{(2l)} \left[ \prod_{i=1}^{n_l} \int_0^\infty dx_i \beta_i^{\sigma_i} \right] \left[ \prod_{j=1}^{n_v} \int d^d w_j \right] \\ &\times |J[\{f_i(\{x_j\})\}]| H_{\sigma_1 \dots \sigma_n} (f_i(\{x_j\}) \beta_i, \{w_i\}, \epsilon). \end{aligned} \quad (4.9)$$

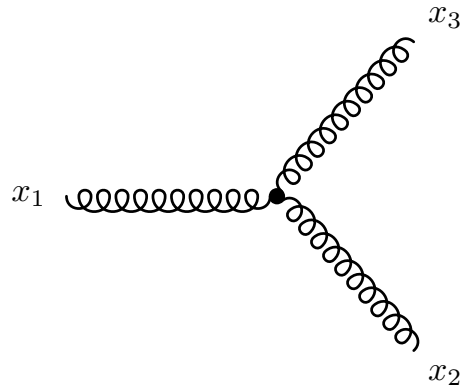
## 4.2.1 Vertex Integrals and Dual Momentum Space Representations

Next, we wish to perform the vertex integrals. This also resembles what we did in section 2.1, in that we insert an auxiliary momentum space integral. We have three topologies of gluon-gluon interactions to consider: a single three-gluon vertex, as we have in the 1211-web of fig. 4.1c, a four-gluon vertex as in fig. 4.1a, or a double three gluon vertex as in fig. 4.1b. In all these cases, regardless of the number of external partons, the vertex integrations correspond to the same dual diagrams. These vertices and their associated momentum-space diagrams are depicted in fig. 4.11.

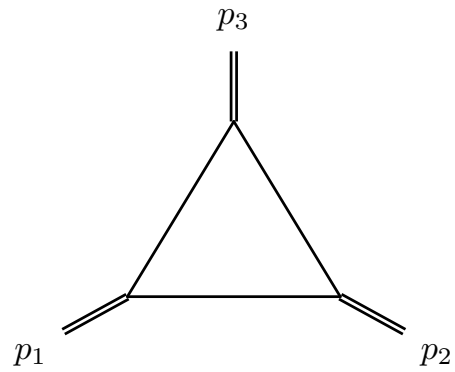
The mapping then proceeds as follows: consider a vertex  $V_f$ , we have  $n$  attachments of gluons to a Wilson line, label their positions in spacetime cyclically as  $x_i^\mu$ , call the integral over the vertex and associated propagators  $V_f(\{x_i\})$ . Introduce dual momenta according to

$$p_i \equiv x_i - x_{i-1}, \quad x_0 \equiv x_n, \quad (4.10)$$

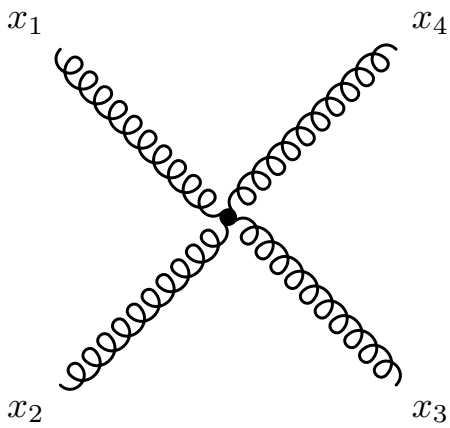
$$x_{ij} \equiv (x_i - x_j)^2. \quad (4.11)$$



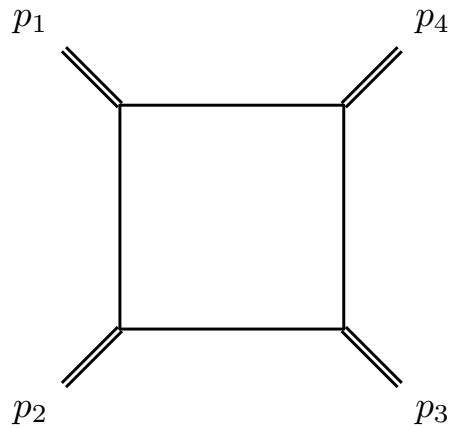
(a) Three gluon vertex integral.



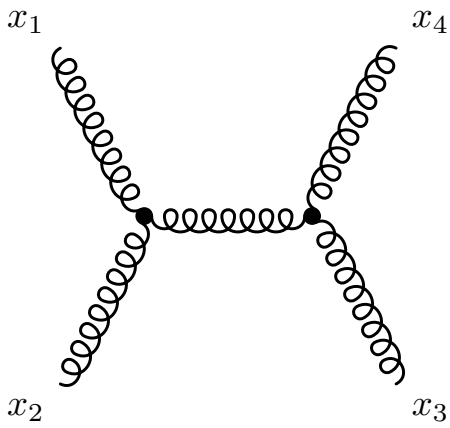
(b) Triangle diagram, dual to three gluon vertex.



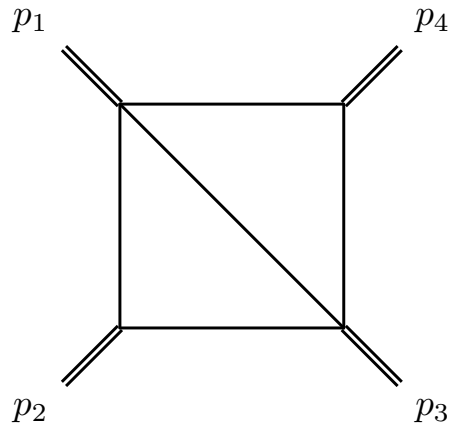
(c) Four gluon vertex integral.



(d) Box diagram, dual to four gluon vertex.



(e) Double three gluon vertex integral.



(f) Slashed box diagram, dual to double three gluon vertex.

**Figure 4.11** Gluon vertex integrals and corresponding dual diagrams.

We then have

$$V_f(\{x_i\}) = D_f(\{p_i\}) = D_f(\{x_{ij}\}), \quad (4.12)$$

where  $D_f$  is the auxiliary momentum diagram of  $V_f$ . We already have a MB representation of the three-gluon vertex,  $T(\{p_i\}, \{\nu_i\}, d)$ , as given in eq. (1.73), and we have seen an example of its application in eq. (2.7). In the case of the four-gluon vertex, its dual is a four-mass box, which is known in  $d = 4$  to have the same MB representation as the three-mass triangle [96]:

$$V_{(4g)}(\{x_i\}) \equiv \frac{i}{\pi^2} \int d^4 z \prod_{i=1}^4 [-(x_i - z)^2 + i0]^{-1} \quad (4.13)$$

$$D_{(4g)}(\{x_{ij}\}) = \frac{1}{x_{13}x_{24}} \frac{1}{(2\pi i)^2} \int_{-i\infty}^{+i\infty} dz_1 dz_2 \left( \frac{x_{12}x_{34}}{x_{13}x_{24}} \right)^{z_1} \left( \frac{x_{14}x_{23}}{x_{13}x_{24}} \right)^{z_1} \times \Gamma^2(-z_1) \Gamma^2(-z_2) \Gamma^2(1 + z_1 + z_2). \quad (4.14)$$

In the case of the double three gluon vertex, we have a two-loop slashed box diagram as its dual. Here, we derive a MB representation of the momentum dual diagram ourselves in Appendix B, it is

$$V_{(3g)^2}(\{x_i\}) \equiv \frac{1}{\pi^4} \int d^4 z d^4 w (-x_1 - z)^{-1} (-x_2 - z)^{-1} \times (-x_3 - w)^{-1} (-x_4 - w)^{-1} (-z - w)^{-1}, \quad (4.15)$$

$$D_{(3g)^2}(\{x_{ij}\}) = \left( \prod_{\substack{i < j \\ (i,j) \neq (1,4)}} \frac{1}{(2\pi i)} \int_{-i\infty}^{i\infty} dt_{ij} \left( \frac{x_{ij}}{x_{14}} \right)^{t_{ij}} \Gamma(-t_{ij}) \right) \times \Gamma(-t_{12} - t_{13} - t_{23}) \Gamma(-t_{23} - t_{24} - t_{34}) \times \Gamma(1 + t_{12} + t_{23} + t_{24}) \Gamma(1 + t_{13} + t_{23} + t_{34}) \times \Gamma(1 + t_{12} + t_{13} + t_{23} + t_{24} + t_{34}) \times \frac{\Gamma(t_{34} - t_{12})}{\Gamma(1 + t_{34} - t_{12})} (\psi(-t_{12}) - \psi(-t_{34})). \quad (4.16)$$

Thus, we have parametrised all of our vertex integrals in terms of three different dual momentum space diagrams. We next need to perform the integration over the Wilson lines.

## 4.2.2 Vertex Differentiation and Parameter Integration

Before we can perform any integration over the Wilson lines, we must perform the differentiations associated with any three-gluon vertices. The differentiation is straightforward, since the MB representations of our dual momentum diagrams always depend on the dual momenta simply as a power, and that there is always an accompanying gamma function, so we have  $(-p_i^2)^z \Gamma(-z)$ . We may rewrite our differentiations in terms of  $p_i^2$  as we did in section 2.1, we then observe

$$\partial_{p_i^2} (-p_i^2)^z \Gamma(-z) = (-p_i^2)^{z-1} \Gamma(1-z). \quad (4.17)$$

After this, we perform the integrals over the Wilson lines, introducing as many MB parameters as is necessary in order to ensure that each parameter integral only produces Gamma functions, and so we obtain a pure power dependence on  $\gamma_{ij}$ , which we need in order to perform an asymptotic expansion (see section 1.3.3). To obtain the latter, we observe that all of our propagators  $x_{ij}$  have their directions dictated by the four-momenta  $\hat{\beta}_i$ . If  $x_i \parallel x_j$ , the propagator reduces to  $(|x_i| - |x_j|)^2$  with no angular dependence. Otherwise, we have, say  $x_i \parallel \hat{\beta}_i$ , and similarly  $x_j \parallel \hat{\beta}_j$  which we then apply the standard MB parametrisation formula (eq. (1.67)) to

$$x_{ij}^p = (|x_i|^2 + |x_j|^2 - |x_i||x_j|\gamma_{ij})^p \quad (4.18)$$

$$= \frac{1}{\Gamma(-p)} \frac{1}{(2\pi i)} \int dz_{ij} \frac{(-|x_i||x_j|\gamma_{ij})^{z_{ij}}}{(|x_i|^2 + |x_j|^2)^{z_{ij}-p}}. \quad (4.19)$$

Thus, we now have a pure power dependence on  $\gamma_{ij}$  in our MB integral.

We then wish to perform the Wilson line integrals. These integrations vary greatly depending on each diagram, however there are some common traits. As an example, both of the fully connected four-line diagrams have Wilson line integrals of the form

$$I_4(\{a_i\}, \{b_{ij}\}) \equiv \left( \prod_{j=1}^4 \int_0^1 dy_j (y_j^2)^{a_j} \prod_{i=1}^{j-1} (y_i^2 + y_j^2)^{b_{ij}} \right) \delta \left( 1 - \sum_{i=1}^4 y_i \right). \quad (4.20)$$

Here  $a_i$  and  $b_{ij}$  are linear functions of the MB parameters, and  $I_4$  carries the overall mass dimension of the MB integral, i.e. we have  $2 \sum a_i + 2 \sum b_{ij} = -4$ . Three-line and two-line integrals will be similar, but with some propagators  $x_{ij}$  replaced by  $(|x_i| - |x_j|)^2$  and an accompanying Heaviside function  $\theta(|x_i| < |x_j|)$ , corresponding to the ordering of two points of emission on the same Wilson line.



We may perform this parameter integral by introducing the following reparametrisation:

$$\begin{pmatrix} y_1 \\ y_2 \\ y_3 \\ y_4 \end{pmatrix} = \begin{pmatrix} yx \\ (1-y)x \\ z(1-x) \\ (1-z)(1-x) \end{pmatrix}. \quad (4.21)$$

This yields

$$\begin{aligned} I_4(\{a_i\}, \{b_{ij}\}) &= \int_0^1 dx dy dz (1-x)^{2a_3+2a_4+2b_{34}+1} x^{2a_1+2a_2+2b_{12}+1} \\ &\quad \times y^{2a_1} (1-y)^{2a_2} z^{2a_3} (1-z)^{2a_4} (y^2 + (1-y)^2)^{b_{12}} \\ &\quad \times (x^2 y^2 + (1-x)^2 z^2)^{b_{13}} (x^2 y^2 + (1-x)^2 (1-z)^2)^{b_{14}} \\ &\quad \times (x^2 (1-y)^2 + (1-x)^2 z^2)^{b_{23}} \\ &\quad \times (x^2 (1-y)^2 + (1-x)^2 (1-z)^2)^{b_{24}} (z^2 + (1-z)^2)^{b_{34}}. \end{aligned} \quad (4.22)$$

Next, we transform to semi-infinite parameters

$$\begin{aligned} I_4(\{a_i\}, \{b_{ij}\}) &= \int_0^\infty d\alpha d\beta d\gamma (\alpha^2)^{a_1+a_2+b_{12}+\frac{1}{2}} \\ &\quad \times (\beta^2)^{a_1} (\beta^2 + 1)^{b_{12}} (\gamma^2)^{a_3} (\gamma^2 + 1)^{b_{34}} \\ &\quad \times ((\beta + 1)^2)^{-a_1-a_2-b_{12}-1} ((\gamma + 1)^2)^{-a_3-a_4-b_{34}-1} \\ &\quad \times \left( \frac{\alpha^2}{(\beta + 1)^2} + \frac{1}{(\gamma + 1)^2} \right)^{b_{24}} \left( \frac{\alpha^2 \beta^2}{(\beta + 1)^2} + \frac{1}{(\gamma + 1)^2} \right)^{b_{14}} \\ &\quad \times \left( \frac{\alpha^2}{(\beta + 1)^2} + \frac{\gamma^2}{(\gamma + 1)^2} \right)^{b_{23}} \left( \frac{\alpha^2 \beta^2}{(\beta + 1)^2} + \frac{\gamma^2}{(\gamma + 1)^2} \right)^{b_{13}}. \end{aligned} \quad (4.23)$$

We are now free to rescale  $\alpha \rightarrow \alpha\gamma(1+\beta)/(1+\gamma)$ , yielding

$$\begin{aligned} I_4(\{a_i\}, \{b_{ij}\}) &= \int_0^\infty d\alpha d\beta d\gamma (\alpha^2)^{a_1+a_2+b_{12}+\frac{1}{2}} (\alpha^2 + 1)^{b_{23}} (\beta^2)^{a_1} \\ &\quad \times (\beta^2 + 1)^{b_{12}} (\gamma^2)^{a_1+a_2+a_3+b_{12}+b_{13}+b_{23}+1} (\gamma^2 + 1)^{b_{34}} \\ &\quad \times (\alpha^2 \beta^2 + 1)^{b_{13}} (\alpha^2 \gamma^2 + 1)^{b_{24}} (\alpha^2 \beta^2 \gamma^2 + 1)^{b_{14}}. \end{aligned} \quad (4.24)$$

The three brackets depending on more than one MB parameter can now be opened using the standard MB parametrisation formula, doing this and performing the

subsequent parameter integrals yields

$$\begin{aligned}
I_4(\{a_i\}, \{b_{ij}\}) = & \\
& \frac{1}{8 \left( \prod_{i < j} \Gamma(-b_{ij}) \right)} \frac{1}{(2\pi i)^3} \int_{-i\infty}^{+i\infty} dz_3 dz_4 dz_5 \\
& \times \Gamma(-z_3) \Gamma(-z_4) \Gamma(-z_5) \Gamma(z_3 - b_{13}) \Gamma(z_4 - b_{24}) \Gamma(z_5 - b_{14}) \\
& \times \Gamma\left(a_1 + z_3 + z_5 + \frac{1}{2}\right) \Gamma\left(-a_1 - b_{12} - z_3 - z_5 - \frac{1}{2}\right) \\
& \times \Gamma(a_1 + a_2 + b_{12} + z_3 + z_4 + z_5 + 1) \\
& \times \Gamma(-a_1 - a_2 - b_{12} - b_{23} - z_3 - z_4 - z_5 - 1) \\
& \times \Gamma\left(a_1 + a_2 + a_3 + b_{12} + b_{13} + b_{23} + z_4 + z_5 + \frac{3}{2}\right) \\
& \times \Gamma\left(-a_1 - a_2 - a_3 - b_{12} - b_{13} - b_{23} - b_{34} - z_4 - z_5 - \frac{3}{2}\right).
\end{aligned} \tag{4.25}$$

We will utilise this result when computing the four-line fully connected webs. For other webs with multiple-gluon vertices, we will compute the requisite parameter integrals as needed, following the same procedure as we just used for the four-line webs above.

Having performed this integration step, we are ready to perform an asymptotic expansion.

### 4.2.3 Asymptotic Expansion

We now have a pure MB representation of our web, it is schematically of the form

$$\mathcal{F}^{(l,-1)} = \left[ \prod_i \int_{-i\infty}^{+i\infty} dr_i \right] \left[ \prod_{i \neq j} \int_{-i\infty}^{+i\infty} dz_{ij} (-\gamma_{ij})^{z_{ij}} \right] \prod_k \Gamma(g_k(\{z_{ij}\}, \{r_i\})), \tag{4.26}$$

We wish to expand around the limit of  $\beta_i^2$ , that is, recalling our definition of  $\gamma_{ij} \equiv -\frac{2\beta_i \beta_j}{\sqrt{|\beta_i|^2} \sqrt{|\beta_j|^2}}$ , we wish to study the asymptotic limit

$$\gamma_{ij} \rightarrow -\infty. \tag{4.27}$$

Thus, we introduce a parameter  $\lambda$  according to  $\gamma_{ij} \rightarrow -\gamma_{ij}/\lambda$  and apply the methods of asymptotic expansion outlined in section 1.3.3 to obtain the leading term in the expansion around  $\lambda = 0$ .

## 4.2.4 Parametrisation

Having performed the asymptotic expansion, we now need to compute the surviving MB integrals. To do so, we will utilise parametrisation and residue sums, as outlined in section 1.3.2. This process is highly individualised and can involve a large number of MB integrals and corresponding parametrisation. Ultimately, however, we obtain a result which can be compared numerically to our MB representation obtained immediately following asymptotic expansion. In the next chapter we will list the results for each web calculated in this manner, before finally assembling the full three-loop result in chapter 6.

## 4.2.5 Numerical Evaluation of MB Integrals

On a few occasions, we will be forced by the complexity of our integrals to compute some constant terms numerically. The reason for this is that the asymptotic expansion may produce a large number of integrals containing Gamma functions with non-integer constants or coefficients of the MB integration parameters (e.g.  $\int dz \Gamma^2(-z) \Gamma(2z)$ ). Such integrals are hard to compute algorithmically, since their residue sums depend on roots of unity, and in some cases they are difficult to parametrise. Furthermore, the sheer volume of such integrals produced by a single asymptotic expansion renders manual computation infeasible, whilst simultaneously reducing the precision of numerical computation.

Numerical integration will be performed using Monte Carlo techniques implemented in [77] with its default integration parameters. These Monte Carlo integrations are performed using the Vegas algorithm, as implemented in the Cuba library [97]. On these occasions, we will give errors in the form of the standard error as determined by Cuba.

Ultimately, we will have strong analytic reasons for deducing the overall result produced by any of these numeric computations. The numerics therefore serve to check our analytic answer, rather than as a means of deduction.

### 4.3 Collinear Reduction

For a lot of the MGEWs, we will not have to perform an explicit calculation. Rather, we will either rely on known results for four- and three-leg diagrams [26, 94, 95], or we will utilise these results to infer the contributions of legs correlating fewer lines through a process known as collinear reduction. The technique is outlined in detail in [95], which includes some examples.

For our purposes, we note that this procedure is most easily explained by means of effective vertices [16]. The effective vertex language provides an alternative way of obtaining the exponentiated colour factors and associated kinematic combinations of webs by means of a purely diagrammatic approach. For our purposes we simply note that the effective vertices represent a completely antisymmetrised set of both colour factors and their associated kinematic factors. For instance, the effective vertex  $V_2$  connecting two gluons to a single Wilson line has colour component  $C_{2,1} = [\mathbf{T}^a, \mathbf{T}^b]$ , and orders the points of emission along the Wilson line accordingly, i.e. if  $x_1$  and  $x_2$  are associated with the colour factors  $\mathbf{T}^a$  and  $\mathbf{T}^b$ , respectively, then kinematically,  $V_2$  produces the combination  $\theta(x_1 > x_2) - \theta(x_2 > x_1)$ .

The procedure of collinear reduction, then, stems from the observation that if we take two lines collinear in an  $n$ -line diagram, the corresponding effective vertices retain their internal ordering on the line, but we are integrating over all positions of these vertices along each line, and hence we obtain a kinematic factor corresponding to taking the symmetric sum of the ordering of points of emission on the two lines we take collinear.

An example is shown in fig. 4.12, where we take  $1||4$  in fig. 4.12a, to obtain a symmetrised colour factor on 1, as indicated by the dashed circle around the two vertices where we must sum over their orderings.

Taking the two lines collinear does not render the colour representations on each line to become the same, however the symmetrised kinematic combination can be obtained by taking such a collinear limit. According to the Feynman rules in [16], the corresponding exponentiated colour factor can then be read directly off the vertex, according to the rule that we take  $\frac{1}{2}\{\mathbf{T}^a, \mathbf{T}^b\}$  for the symmetric

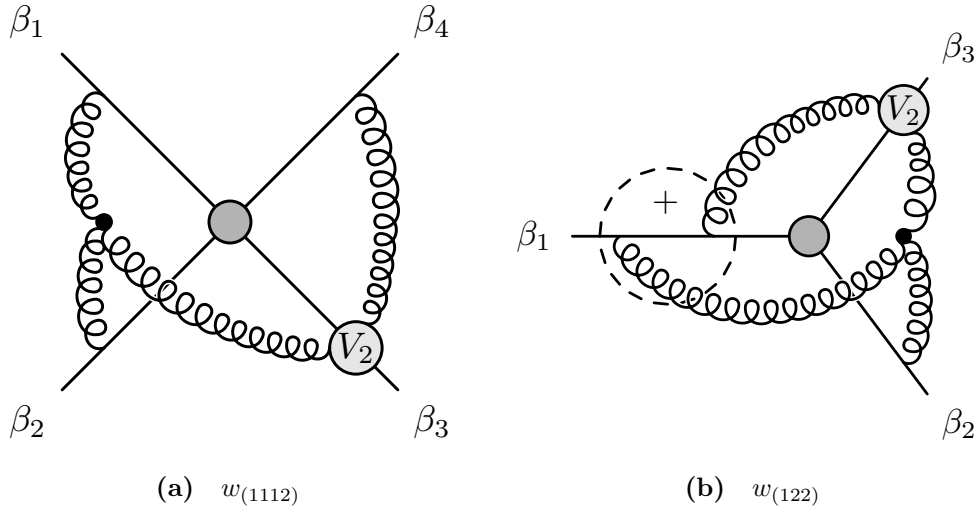


**Figure 4.12** Collinear reduction of  $w_{(1112)}$  to  $w_{122}$

combination. In the case of fig. 4.12b, we find

$$C_{122} = \{\mathbf{T}_1^a, \mathbf{T}_1^d\} \mathbf{T}_2^b \mathbf{T}_3^c f^{cde} f^{abe}, \quad (4.28)$$

$$\mathcal{F}_{(122)}(\alpha_{12}, \alpha_{13}, \alpha_{23}) = \frac{1}{2} \mathcal{F}_{(1112)}(\alpha_{12}, \alpha_{13}, \alpha_{23}; \alpha_{34}) \Big|_{4||1}. \quad (4.29)$$

More details on this calculation will be provided in section 5.2.2.

# Chapter 5

## Results for Three-loop Webs in Lightlike Kinematics

Having outlined our methods of calculation, we will proceed to present all the webs relevant for our calculation of  $\Delta(z, \bar{z})$ . In addition to explicit calculation, we utilise the results of [26, 94, 95], both directly and for the purpose of collinear reduction. Due to the lengthy nature of the calculation, most of the details have been relegated to the appendices, specifically Appendices A to E. The collinear reductions will however be performed in full in this chapter. In this chapter we will focus on summarising the main results, and any deviations from the methods outlined in chapter 4. We will begin with four-line webs, and then proceed to three and two lines, finally assembling the full result. In all cases we give our results factorised into colour and kinematic factors according to

$$w_f(\{\alpha_{ij}\}, \{\mathbf{T}_i\}) = \mathcal{C}_f(\{\mathbf{T}_i\}, \{\alpha_{ij}\}) \mathcal{F}_f(\{\alpha_{ij}\}). \quad (5.1)$$

Furthermore, we decompose  $\mathcal{F}$  according to its order in  $\alpha_s$  and  $\epsilon$ :  $\mathcal{F} = \sum_{i,j} \alpha_s^i \epsilon^j \mathcal{F}^{(i,j)}$ .

In the next chapter we will assemble all of these results into a single correction to the dipole formula.

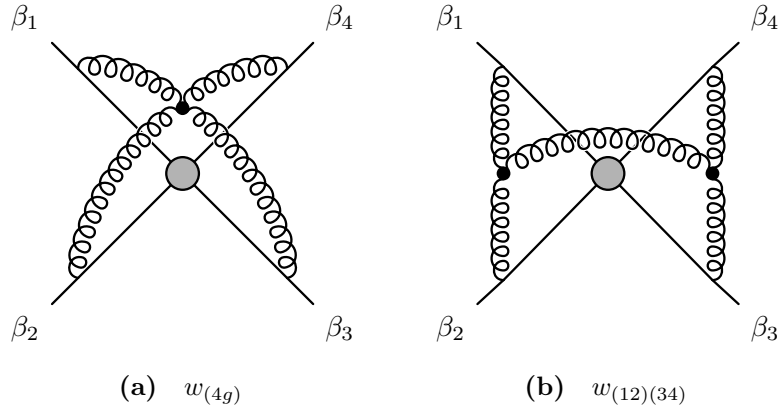


**Figure 5.1** Fully connected webs connecting four lines.

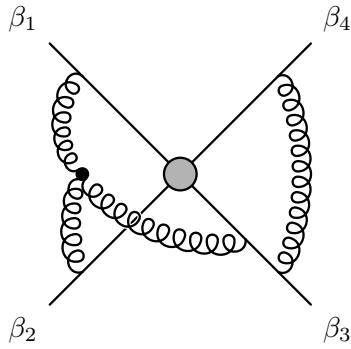


**Figure 5.2** One of two graphs with single three gluon vertex contributing to  $w_{1112}$

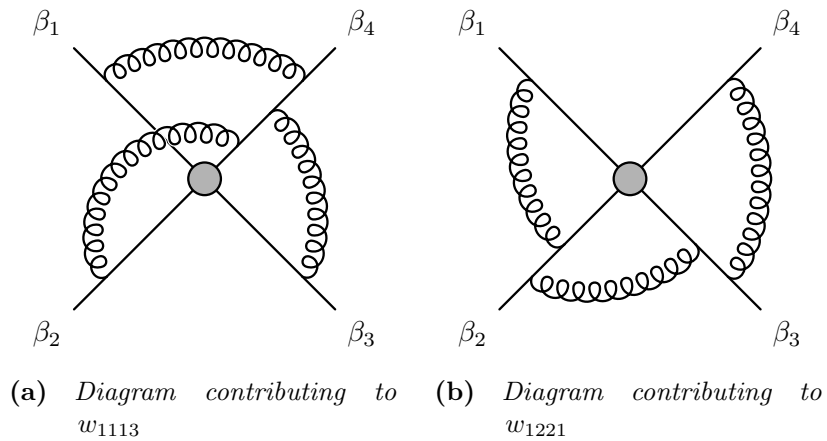


**Figure 5.3** Representative diagrams of four-line MGEWs.

## 5.1 Four-line webs

At four lines, we have three distinct sets of webs: fully connected graphs (fig. 5.1), a graph containing a single three gluon vertex and a single gluon exchange (fig. 5.2), and two MGEWs (fig. 5.3). As we discussed at the beginning of chapter 3, only the fully connected graphs may have non-logarithmic dependence on CICRs, and are hence of primary interest.

### 5.1.1 The Four-Line Four-Gluon Vertex

In the case of  $w_{(4g)}$  in fig. 5.1a, we have relegated the full calculation to Appendix A. We obtain a rather lengthy final result for  $w_{(4g)}$ , with the following form

$$\begin{aligned} \mathcal{C}_{(4g)} = & \mathbf{T}_1^a \mathbf{T}_2^b \mathbf{T}_3^c \mathbf{T}_4^d [f^{abe} f^{cde} (1 - (1 - z)(1 - \bar{z})) \\ & + f^{ace} f^{bde} (z\bar{z} - (1 - z)(1 - \bar{z})) + f^{ade} f^{bce} (z\bar{z} - 1)], \end{aligned} \quad (5.2)$$

$$\mathcal{F}_{(4g)}^{(3,-1)} = - \left( \frac{1}{4\pi} \right)^3 \frac{2}{3} \frac{1}{z - \bar{z}} f_1(z, \bar{z}, \{\alpha_{ij}\}), \quad (5.3)$$

where  $f_1$  is a pure weight five polylogarithmic function, satisfying Bose symmetry by being completely symmetric under the interchange of any two Wilson lines. The result for  $f_1$  is rather large, so we provide it as a supplement to this thesis in machine-readable format.

### 5.1.2 The Four-Line Double Three-Gluon Vertex

Turning our attention to  $w_{(12)(34)}$  in fig. 5.1b, we have again relegated its calculation to Appendix B. After asymptotic expansion and performing the MB integration, we obtain

$$\mathcal{C}_{(12)(34)} = f^{abe} f^{cde} \mathbf{T}_1^a \mathbf{T}_2^b \mathbf{T}_3^c \mathbf{T}_4^d, \quad (5.4)$$

$$\mathcal{F}_{(12)(34)}^{(3,-1)} = \left( \frac{1}{4\pi} \right)^3 \frac{2}{3} \left( f_0(z, \bar{z}, \{\alpha_{ij}\}) + \frac{1 - (1 - z)(1 - \bar{z})}{z - \bar{z}} f_1(z, \bar{z}, \{\alpha_{ij}\}) \right). \quad (5.5)$$

Note again the appearance of  $f_1(z, \bar{z}, \alpha_{ij})$ .  $f_0$  is a pure, weight five polylogarithmic function, satisfying all the symmetries of  $H_4$  in eq. (3.6), as Bose symmetry would require. We attach it in machine readable format as a supplement to this thesis,



though we will analyse its full form in more detail in section 6.4.1.

### 5.1.3 The 1121-web

For the web in fig. 5.2, it has been shown in [93] that after subtracting appropriate counterterms, it can be written as

$$\mathcal{C}_{1121} = f^{abe} f^{cde} \mathbf{T}_1^a \mathbf{T}_2^b \mathbf{T}_3^c \mathbf{T}_4^d \quad (5.6)$$

$$\begin{aligned} \mathcal{F}_{1121}^{(3,-1)}(\alpha_{12}, \alpha_{13}, \alpha_{23}, \alpha_{34}) &= \frac{1}{3} \frac{1}{(4\pi)^3} (M_{0,0,0}(\alpha_{34}) t_1(\alpha_{12}, \alpha_{13}, \alpha_{23}) \\ &\quad - 2M_{1,0,0}(\alpha_{34}) t_0(\alpha_{12}, \alpha_{13}, \alpha_{23})) \end{aligned} \quad (5.7)$$

The integrals  $t_0$  and  $t_1$  are integrations over Wilson lines connecting to a scalar triangle, much like was the case for the three gluon vertex in chapter 2. Note that  $t_0$  and  $t_1$  only depend on the three angles internal to the three-gluon vertex. All dependence on  $\alpha_{14}$  is captured by the MGEW basis functions [95]

$$\begin{aligned} t_0(\alpha_{12}, \alpha_{13}, \alpha_{23}) &= \int_0^1 dy_1 dy_2 dy_3 \delta \left( 1 - \sum_{i=1}^3 y_i \right) \\ &\quad \times \beta_1^\mu \beta_2^\nu \beta_3^\rho \Gamma_{\mu\nu\rho}(\partial_{y_1\beta_1}, \partial_{y_2\beta_2}, \partial_{y_3\beta_3}) \\ &\quad \times T^{(0)}(\{p_i\}, \{1\}, 4), \end{aligned} \quad (5.8)$$

$$\begin{aligned} t_1(\alpha_{12}, \alpha_{13}, \alpha_{23}) &= \int_0^1 dy_1 dy_2 dy_3 \delta \left( 1 - \sum_{i=1}^3 y_i \right) \\ &\quad \times \beta_1^\mu \beta_2^\nu \beta_3^\rho \Gamma_{\mu\nu\rho}(\partial_{y_1\beta_1}, \partial_{y_2\beta_2}, \partial_{y_3\beta_3}) \\ &\quad \times (T^{(1)}(\{p_i\}, \{1\}, 4) - 4 \log(y_3) T^{(0)}(\{p_i\}, \{1\}, 4)), \end{aligned} \quad (5.9)$$

where we define  $T^{(n)}$  as the  $\mathcal{O}(\epsilon^n)$  term in the expansion of the scalar triangle integral in eq. (2.7).  $t_0$  is then simply the three gluon vertex diagram, for which we have the full result in eq. (2.22). In order to calculate  $t_1$ , we need an MB representation of the  $\mathcal{O}(\epsilon)$  term of  $T$ . Since both the integration and  $T$  are finite in  $d = 4$  dimensions, we may expand in  $\epsilon$  under the integral sign. We insert

eq. (2.10) and write  $\log(y_3) = \frac{d}{da}\Big|_{a=0} y_3^a$ , all of this results in

$$\begin{aligned}
& t_1(\alpha_{12}, \alpha_{13}, \alpha_{23}) = \\
& -\frac{1}{2} \int_0^1 dy_1 dy_2 dy_3 \delta\left(1 - \sum_{i=1}^3 y_i\right) \sum_{(i,j,k)} \epsilon_{ijk} y_j (\gamma_{ij} \gamma_{jk} - 2\gamma_{ik}) \partial_{y_{ij}^2} \\
& \times \int dz_1 dz_2 \left(\frac{y_{ij}^2}{y_{ik}^2}\right)^{z_1} \left(\frac{y_{jk}^2}{y_{ik}^2}\right)^{z_2} \Gamma^2(-z_1) \Gamma^2(-z_2) \Gamma^2(1 - z_1 - z_2) \\
& \times \left(\gamma_E - 4 \frac{d}{da} \left((y_{ij}^2)^a + (y_3)^a\right)\Big|_{a=0} - \psi(-z_1) - \psi(-z_2) + 3\psi(1 + z_1 + z_2)\right).
\end{aligned} \tag{5.10}$$

We may now proceed to perform the integrals over  $y_i$  in exactly the same manner as we did in chapter 2. Performing an asymptotic expansion near the limit of light-like external partons and computing the surviving MB integrals, we obtain

$$\mathcal{C}_{(1121)} = f^{abe} f^{cde} \mathbf{T}_1^a \mathbf{T}_2^b \mathbf{T}_3^c \mathbf{T}_4^d \tag{5.11}$$

$$\begin{aligned}
& \mathcal{F}_{1121}(\alpha_{12}, \alpha_{13}, \alpha_{23}, \alpha_{34}) = \\
& -\frac{1}{3} \frac{1}{(4\pi)^3} [8(\log(\alpha_{12}) - \log(\alpha_{13}))(\log(\alpha_{12}) - \log(\alpha_{23})) \\
& \times (\log(\alpha_{13}) - \log(\alpha_{23}))(\log^2(\alpha_{34}) + \zeta_2) + 2\log(\alpha_{34}) \\
& \times \left[\frac{2}{3}(\log^4(\alpha_{13}) - \log^4(\alpha_{23}) - \log^3(\alpha_{12})(\log(\alpha_{13}) - \log(\alpha_{23}))) \right. \\
& + \frac{8}{3}(\log(\alpha_{13})\log^3(\alpha_{23}) - \log^3(\alpha_{13})\log(\alpha_{23})) \\
& + \frac{2}{3}(\log(\alpha_{12})\log^3(\alpha_{13}) - \log(\alpha_{12})\log^3(\alpha_{23})) \\
& + 2(\log^2(\alpha_{12})\log^2(\alpha_{23}) - \log^2(\alpha_{12})\log^2(\alpha_{13})) \\
& + 2(\log(\alpha_{12})\log^2(\alpha_{13})\log(\alpha_{23}) - \log(\alpha_{12})\log(\alpha_{13})\log^2(\alpha_{23})) \\
& - 4\zeta_2(\log(\alpha_{12})\log(\alpha_{13}) - \log(\alpha_{12})\log(\alpha_{23})) \\
& \left. + 4\zeta_2(\log^2(\alpha_{13}) - \log^2(\alpha_{23})) - 8\zeta_3(\log(\alpha_{13}) - \log(\alpha_{23}))\right]
\end{aligned} \tag{5.12}$$

Both the colour and kinematic factors are antisymmetric under the exchange of  $\beta_1$  and  $\beta_2$ , as one would expect from Bose symmetry. Furthermore, we note that the result is uniform weight five.

### 5.1.4 Multiple Gluon Exchange Webs

Finally, the two MGEWs in fig. 5.3 have been calculated in detail in [26] and subsequently expressed in terms of MGEW basis functions in [95], they are

$$\bar{w}_{(1221)}^{(3)}(\alpha_{12}, \alpha_{23}, \alpha_{34}) = -\frac{1}{6} \frac{1}{(4\pi)^3} f^{abe} f^{cde} \mathbf{T}_1^a \mathbf{T}_2^b \mathbf{T}_3^c \mathbf{T}_4^d \quad (5.13)$$

$$\times r(\alpha_{12}) r(\alpha_{23}) r(\alpha_{34}) G_{(1221)}(\alpha_{12}, \alpha_{23}, \alpha_{34})$$

$$G_{(1221)}(\alpha_{12}, \alpha_{23}, \alpha_{34}) = -\frac{1}{2} M_{2,0,0}(\alpha_{12}) M_{0,0,0}(\alpha_{23}) M_{0,0,0}(\alpha_{34})$$

$$-\frac{1}{2} M_{0,0,0}(\alpha_{12}) M_{0,0,0}(\alpha_{23}) M_{2,0,0}(\alpha_{34}) + M_{0,0,0}(\alpha_{12}) M_{2,0,0}(\alpha_{23}) M_{0,0,0}(\alpha_{34})$$

$$-M_{0,0,0}(\alpha_{12}) M_{1,0,0}(\alpha_{23}) M_{1,0,0}(\alpha_{34}) - M_{1,0,0}(\alpha_{12}) M_{1,0,0}(\alpha_{23}) M_{0,0,0}(\alpha_{34})$$

$$+2M_{1,0,0}(\alpha_{12}) M_{0,0,0}(\alpha_{23}) M_{1,0,0}(\alpha_{34}) + 4M_{0,0,0}(\alpha_{12}) M_{2,0,0}(\alpha_{23}) M_{1,0,0}(\alpha_{34}) \quad (5.14)$$

$$\bar{w}_{(1113)}^{(3)}(\alpha_{14}, \alpha_{24}, \alpha_{34}) = -\frac{1}{6} \frac{1}{(4\pi)^3} \mathbf{T}_1^a \mathbf{T}_2^b \mathbf{T}_3^c \mathbf{T}_4^d r(\alpha_{12}) r(\alpha_{13}) r(\alpha_{14}) \quad (5.15)$$

$$\times (f^{ade} f^{bce} G_{1113}(\alpha_{14}, \alpha_{24}, \alpha_{34}) + f^{ace} f^{bde} G_{1113}(\alpha_{24}, \alpha_{14}, \alpha_{34}))$$

$$G_{(1113)}(\alpha_{14}, \alpha_{24}, \alpha_{34}) =$$

$$\frac{1}{2} M_{2,0,0}(\alpha_{14}) M_{0,0,0}(\alpha_{24}) M_{0,0,0}(\alpha_{34}) + \frac{1}{2} M_{0,0,0}(\alpha_{14}) M_{0,0,0}(\alpha_{24}) M_{2,0,0}(\alpha_{34})$$

$$-M_{0,0,0}(\alpha_{14}) M_{2,0,0}(\alpha_{24}) M_{0,0,0}(\alpha_{34}) + M_{0,0,0}(\alpha_{14}) M_{1,0,0}(\alpha_{24}) M_{1,0,0}(\alpha_{34})$$

$$+M_{1,0,0}(\alpha_{14}) M_{1,0,0}(\alpha_{24}) M_{0,0,0}(\alpha_{34}) - 2M_{1,0,0}(\alpha_{14}) M_{0,0,0}(\alpha_{24}) M_{1,0,0}(\alpha_{34}) \quad (5.16)$$

In order to obtain the light-like limit of these webs, we only need to obtain light-like limit of the basis functions  $M_{0,0,0}$ ,  $M_{1,0,0}$  and  $M_{2,0,0}$ , they are

$$M_{0,0,0}(\alpha) = 2 \log(\alpha) \xrightarrow{\alpha \rightarrow 0} 2 \log(\alpha) \quad (5.17)$$

$$M_{1,0,0}(\alpha) = 2 \text{Li}_2(\alpha^2) + 4 \log(\alpha) \log(1 - \alpha^2) - 2 \log^2(\alpha) - 2\zeta_2 \quad (5.18)$$

$$\xrightarrow{\alpha \rightarrow 0} -2 \log^2(\alpha) - 2\zeta_2$$

$$M_{2,0,0}(\alpha) = -4 (\text{Li}_3(\alpha^2) + 2 \text{Li}_3(1 - \alpha^2)) - 8 \log(1 - \alpha^2) \log^2(\alpha)$$

$$+ \frac{8}{3} \log^3(\alpha) + 8\zeta_2 \log(\alpha) + 4\zeta_3 \quad (5.19)$$

$$\xrightarrow{\alpha \rightarrow 0} \frac{8}{3} \log^3(\alpha) + 8\zeta_2 \log(\alpha) - 4\zeta_3$$

Utilising these limits, we obtain

$$\begin{aligned}
G_{(1221)}(\alpha_{12}, \alpha_{23}, \alpha_{34}) &\xrightarrow{\alpha \rightarrow 0} -\frac{16}{3} \log^3(\alpha_{12}) \log(\alpha_{23}) \log(\alpha_{34}) \\
&- \frac{16}{3} \log(\alpha_{12}) \log(\alpha_{23}) \log^3(\alpha_{34}) + 16 \log^2(\alpha_{12}) \log(\alpha_{23}) \log^2(\alpha_{34}) \\
&- 8 \log^2(\alpha_{12}) \log^2(\alpha_{23}) \log(\alpha_{34}) - 8 \log(\alpha_{12}) \log^2(\alpha_{23}) \log^2(\alpha_{34}) \\
&\quad + 8\zeta_2 [2 \log(\alpha_{23}) \log^2(\alpha_{12}) + 2 \log(\alpha_{23}) \log^2(\alpha_{34}) \\
&\quad - \log(\alpha_{34}) \log^2(\alpha_{12}) - \log^2(\alpha_{23}) \log(\alpha_{12}) \\
&\quad - \log^2(\alpha_{34}) \log(\alpha_{12}) - \log^2(\alpha_{23}) \log(\alpha_{34}) \\
&\quad - 8 \log(\alpha_{23}) \log(\alpha_{34}) \log(\alpha_{12})] - 8\zeta_3 [2 \log(\alpha_{12}) \log(\alpha_{34}) \\
&\quad - \log(\alpha_{12}) \log(\alpha_{23}) - \log(\alpha_{34}) \log(\alpha_{23})] \\
&\quad + 20\zeta_4 [2 \log(\alpha_{23}) - \log(\alpha_{12}) - \log(\alpha_{34})]
\end{aligned} \tag{5.20}$$

$$\begin{aligned}
G_{(1113)}(\alpha_{14}, \alpha_{24}, \alpha_{34}) &\xrightarrow{\alpha \rightarrow 0} -\frac{32}{3} \log(\alpha_{14}) \log^3(\alpha_{24}) \log(\alpha_{34}) \\
&+ \frac{16}{3} \log^3(\alpha_{14}) \log(\alpha_{24}) \log(\alpha_{34}) + \frac{16}{3} \log(\alpha_{14}) \log(\alpha_{24}) \log^3(\alpha_{34}) \\
&+ 8 \log^2(\alpha_{14}) \log^2(\alpha_{24}) \log(\alpha_{34}) + 8 \log(\alpha_{14}) \log^2(\alpha_{24}) \log^2(\alpha_{34}) \\
&- 16 \log^2(\alpha_{14}) \log(\alpha_{24}) \log^2(\alpha_{34}) + 8\zeta_2 [\log(\alpha_{14}) \log^2(\alpha_{24}) \\
&\quad + \log^2(\alpha_{24}) \log(\alpha_{34}) + \log^2(\alpha_{14}) \log(\alpha_{34}) + \log(\alpha_{14}) \log^2(\alpha_{34}) \\
&\quad - 2 \log^2(\alpha_{14}) \log(\alpha_{24}) - 2 \log(\alpha_{24}) \log^2(\alpha_{34})] \\
&- 2\zeta_3 [\log(\alpha_{14}) \log(\alpha_{24}) + \log(\alpha_{24}) \log(\alpha_{34}) - 2 \log(\alpha_{14}) \log(\alpha_{34})] \\
&\quad + 20\zeta_4 [\log(\alpha_{14}) + 2 \log(\alpha_{24}) + \log(\alpha_{34})]
\end{aligned} \tag{5.21}$$

The results are once again uniform weight five.

## 5.2 Three-line webs

We now consider all three-loop webs connecting three Wilson lines. The topologies can be obtained by considering ways of identifying two Wilson lines in the four-loop topologies in section 5.1. Thus, the topologies fall broadly into three classes: fully connected diagrams, diagrams containing a three gluon vertex, and MGEWs. The MGEWs have been computed both directly and through collinear reduction in [95], and we will simply apply a light-like limit to their results.

We will systematically discard any contributions to tripole or dipole colour factors, retaining only contributions to  $H_3$ , described in detail in chapter 3. All relevant

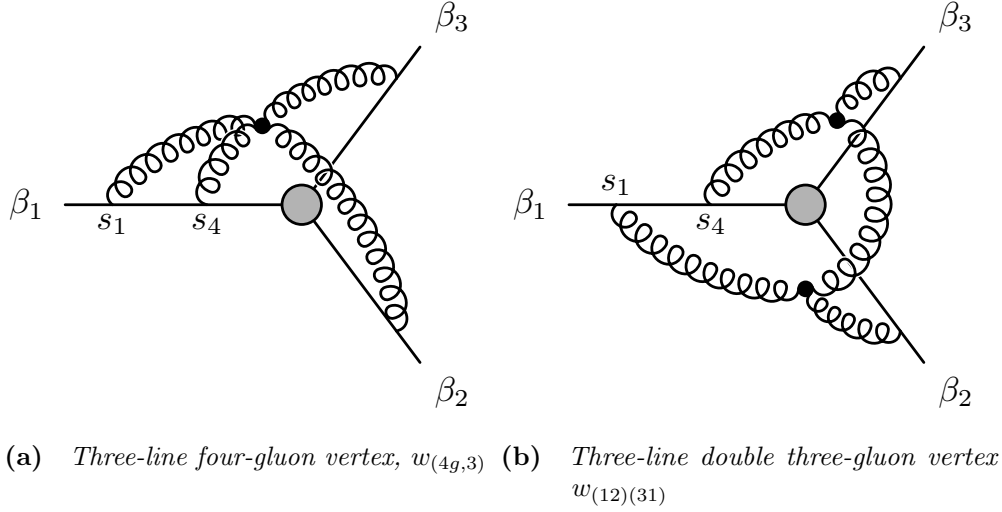


**Figure 5.4** Fully connected three-line diagrams contributing to  $H_3$

exponentiated colour factors have been computed in [16], so we only need to explicitly compute the colour factors of the fully connected diagrams.

### 5.2.1 Fully connected graphs

Among the fully connected graphs, we only need to compute the topologies in fig. 5.4.

We begin with the four gluon vertex diagram, we let  $\beta_4 = \beta_1$ , for ease of notation and obtain

$$\mathcal{C}_{(4g),3} = f^{abe} f^{cde} \{ \mathbf{T}_1^a, \mathbf{T}_1^d \} \mathbf{T}_2^b \mathbf{T}_3^c \quad (5.22)$$

$$\begin{aligned} \mathcal{F}_{(4g),3}(\alpha_{12}, \alpha_{13}, \alpha_{23}) &= -ig_s^6 \left( \frac{\mu^2}{m^2} \right)^{3\epsilon} \mathcal{N}^4 \Gamma(6\epsilon) \left( \frac{\gamma_{12}\gamma_{13}}{4} - \frac{\gamma_{23}}{2} \right) \\ &\times \int d^d z \prod_{i=1}^4 \left[ \int_0^\infty dy_i \frac{1}{[-(y_i \beta_i - z)^2 + i0]^{1-\epsilon}} \right] \\ &\times \delta \left( 1 - \sum_i y_i \right) \theta(y_4 < y_1). \end{aligned} \quad (5.23)$$

The calculation now proceeds in much the same way as it did for the four-gluon vertex, we give full details in Appendix C. The vertex integration still corresponds to a four-mass box diagram (as we saw in the previous section for the four-line four-gluon vertex), though the parameter integration proceeds slightly differently,

due to the inclusion of a Heaviside function. In the end, we find

$$\begin{aligned}
\mathcal{F}_{(4g),3}^{(3,-1)}(\alpha_{12}, \alpha_{13}, \alpha_{23}) = & \\
& -\frac{1}{(4\pi)^3} \frac{1}{3} \left( -\frac{1}{3} \log^4(\alpha_{12}) - \frac{1}{3} \log^4(\alpha_{13}) - \log^2(\alpha_{12}) \log(\alpha_{13}) \log(\alpha_{23}) \right. \\
& - \log(\alpha_{12}) \log^2(\alpha_{13}) \log(\alpha_{23}) + 4 \log(\alpha_{12}) \log(\alpha_{13}) \log(\alpha_{23}) \\
& + 2 \log^2(\alpha_{12}) \log^2(\alpha_{13}) - \log^2(\alpha_{12}) \log^2(\alpha_{23}) - \log^2(\alpha_{13}) \log^2(\alpha_{23}) \\
& + \frac{1}{3} \log(\alpha_{12}) \log^3(\alpha_{23}) + \frac{1}{3} \log(\alpha_{13}) \log^3(\alpha_{23}) + \frac{2}{3} \log(\alpha_{13}) \log^3(\alpha_{12}) \\
& + \frac{2}{3} \log^3(\alpha_{13}) \log(\alpha_{12}) + \log(\alpha_{23}) \log^3(\alpha_{12}) + \log^3(\alpha_{13}) \log(\alpha_{23}) \\
& - 6 \log(\alpha_{13}) \log^2(\alpha_{12}) - 6 \log^2(\alpha_{13}) \log(\alpha_{12}) - 2 \log(\alpha_{23}) \log^2(\alpha_{12}) \\
& - 2 \log^2(\alpha_{13}) \log(\alpha_{23}) + 2 \log^2(\alpha_{23}) \log(\alpha_{12}) + 2 \log(\alpha_{13}) \log^2(\alpha_{23}) \\
& + \frac{2}{3} \log^3(\alpha_{12}) + \frac{2}{3} \log^3(\alpha_{13}) - \frac{2}{3} \log^3(\alpha_{23}) + 24 \log(\alpha_{12}) \log(\alpha_{13}) \\
& + 4 \log^2(\alpha_{12}) + 4 \log^2(\alpha_{13}) - 4 \log^2(\alpha_{23}) - 32 \log(\alpha_{12}) - 32 \log(\alpha_{13}) \\
& - 24 \zeta_4 + \zeta_3 (12 \log(\alpha_{12}) + 12 \log(\alpha_{13}) - 24) + \zeta_2 (-6 \log^2(\alpha_{12}) \\
& - 6 \log^2(\alpha_{13}) + 6 \log(\alpha_{23}) \log(\alpha_{12}) + 6 \log(\alpha_{13}) \log(\alpha_{23}) \\
& \left. + 12 \log(\alpha_{12}) + 12 \log(\alpha_{13}) - 12 \log(\alpha_{23}) - 24) + 64 \right).
\end{aligned} \tag{5.24}$$

Note the appearance of many terms which have transcendental weight less than five. This is a general feature of three-line and two-line graphs, and the cancellation of all such terms will provide a strong consistency check on our calculation.

Turning our attention to the double three gluon vertex diagram  $w_{(12)(31)}$  in fig. 5.4b, we provide full details in Appendix D. There are two permutations contributing

to  $H_3$ , we compute them jointly and find

$$w_{(12)(31)}(\alpha_{12}, \alpha_{13}, \alpha_{23}) + w_{(12)(31)}(\alpha_{13}, \alpha_{12}, \alpha_{23}) \quad (5.25)$$

$$\equiv \mathcal{C}_{(12)(13),s} \mathcal{F}_{(12)(13),s}(\alpha_{13}, \alpha_{12}, \alpha_{23}) \quad (5.26)$$

$$\mathcal{C}_{(12)(31),s} = f^{abe} f^{cde} \{ \mathbf{T}_1^a, \mathbf{T}_1^d \} \mathbf{T}_2^b \mathbf{T}_3^c \quad (5.27)$$

$$\begin{aligned} \mathcal{F}_{(12)(31),s}^{(3,-1)}(\alpha_{13}, \alpha_{12}, \alpha_{23}) &= \frac{1}{(4\pi)^3} \frac{2}{3} \frac{1}{\pi^4} \int_0^\infty dy_1 dy_2 dy_3 dy_4 \\ &\times \delta \left( 1 - \sum_i y_i \right) \int d^4 z d^4 w \beta_1^\mu \beta_2^\nu \beta_3^\rho \beta_1^\sigma \\ &\times \Gamma_{\mu\nu\tau} (\partial_{y_1\beta_1}, \partial_{y_2\beta_2}, -\partial_{y_1\beta_1} - \partial_{y_2\beta_2}) \\ &\times \Gamma_{\rho\sigma\tau} (\partial_{y_3\beta_3}, \partial_{y_4\beta_1}, -\partial_{y_3\beta_3} - \partial_{y_4\beta_1}) \\ &\times (-(y_1\beta_1 - z)^2 + i0)^{-1} (-(y_2\beta_2 - z)^2 + i0)^{-1} \\ &\times (-(y_3\beta_3 - w)^2 + i0)^{-1} (-(y_4\beta_1 - w)^2 + i0)^{-1} \\ &\times (-(z - w)^2 + i0)^{-1} (\theta(y_4 < y_1) + \theta(y_1 < y_4)). \end{aligned} \quad (5.28)$$

The calculation proceeds much like that of  $\mathcal{F}_{(4g),3}^{(3,-1)}$ , however we find MB integrals to be prohibitively complex, hindering analytic computation of terms proportional to  $\log(\alpha_{12})$ ,  $\log(\alpha_{13})$ , and the constant term. We will compute these terms numerically, and compare their value to constraints derived from collinear factorisation and Regge limits in later chapters. We will relegate the independent result for  $\mathcal{F}_{(12)(31),s}^{(3,-1)}$  to Appendix D, for now it is notable that there is a significant cancellation of

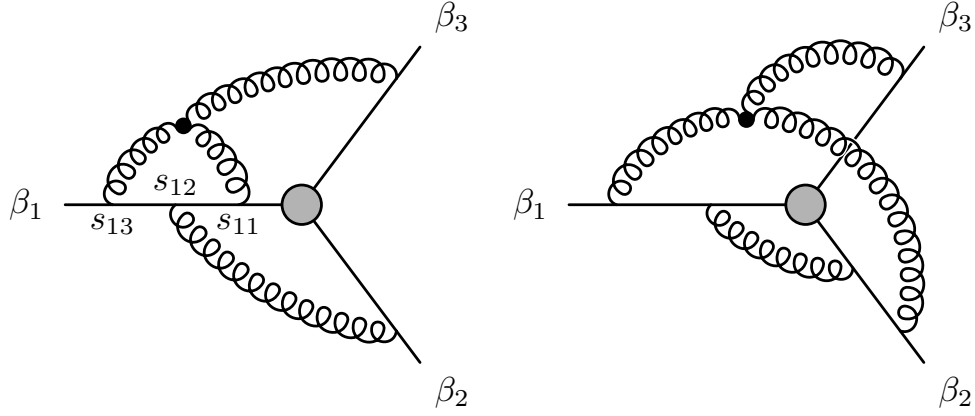
lower-weight terms between  $\mathcal{F}_{(12)(31),s}^{(3,-1)}$  and  $\mathcal{F}_{(4g,3)}^{(3,-1)}$ , we find

$$\begin{aligned}
& w_{(4g,3)}^{(3,-1)}(\alpha_{12}, \alpha_{13}, \alpha_{23}) + w_{(12)(31)}(\alpha_{12}, \alpha_{13}, \alpha_{23}) + w_{(12)(31)}(\alpha_{13}, \alpha_{12}, \alpha_{23}) = \\
& \frac{1}{6} \frac{1}{(4\pi)^3} f^{abe} f^{cde} \{ \mathbf{T}_1^a, \mathbf{T}_1^d \} \mathbf{T}_2^b \mathbf{T}_3^c \\
& \times \left( \frac{1}{3} \log^5(\alpha_{12}) + \frac{1}{3} \log^5(\alpha_{13}) + \frac{2}{3} \log(\alpha_{23}) \log^4(\alpha_{12}) \right. \\
& + \frac{2}{3} \log^4(\alpha_{13}) \log(\alpha_{23}) - \frac{5}{3} \log(\alpha_{13}) \log^4(\alpha_{12}) - \frac{5}{3} \log^4(\alpha_{13}) \log(\alpha_{12}) \\
& - \frac{1}{3} \log^4(\alpha_{23}) \log(\alpha_{12}) - \frac{1}{3} \log(\alpha_{13}) \log^4(\alpha_{23}) \\
& + \frac{4}{3} \log(\alpha_{13}) \log(\alpha_{23}) \log^3(\alpha_{12}) + \frac{4}{3} \log^3(\alpha_{13}) \log(\alpha_{23}) \log(\alpha_{12}) \\
& - \frac{4}{3} \log(\alpha_{13}) \log^3(\alpha_{23}) \log(\alpha_{12}) - 2 \log^2(\alpha_{23}) \log^3(\alpha_{12}) \\
& - 2 \log^3(\alpha_{13}) \log^2(\alpha_{23}) + \frac{4}{3} \log^3(\alpha_{23}) \log^2(\alpha_{12}) \\
& + \frac{4}{3} \log^2(\alpha_{13}) \log^3(\alpha_{23}) + \frac{2}{3} \log^3(\alpha_{13}) \log^2(\alpha_{12}) \\
& + \frac{2}{3} \log^2(\alpha_{13}) \log^3(\alpha_{12}) - 4 \log^2(\alpha_{12}) \log(\alpha_{23}) \log^2(\alpha_{13}) \\
& + 2 \log(\alpha_{12}) \log^2(\alpha_{23}) \log^2(\alpha_{13}) + 2 \log^2(\alpha_{12}) \log^2(\alpha_{23}) \log(\alpha_{13}) \\
& + \zeta_4 (24 \log(\alpha_{23}) - 24 \log(\alpha_{12}) - 24 \log(\alpha_{13}) + 48) \\
& + \zeta_3 (8 \log(\alpha_{23}) \log(\alpha_{12}) + 8 \log(\alpha_{13}) \log(\alpha_{23}) - 32 \log(\alpha_{13}) \log(\alpha_{12}) \\
& - 8 \log^2(\alpha_{12}) - 8 \log^2(\alpha_{13}) + 48) + \zeta_2 (8 \log(\alpha_{13}) \log^2(\alpha_{12}) \\
& + 8 \log^2(\alpha_{13}) \log(\alpha_{12}) - 8 \log(\alpha_{13}) \log(\alpha_{23}) \log(\alpha_{12}) \\
& + 32 \log(\alpha_{13}) \log(\alpha_{12}) + 48) + (64 - 50.1 \pm 0.1) (\log(\alpha_{12}) + \log(\alpha_{13})) \\
& \left. - (128 + 25 \pm 1.25) \right). \tag{5.29}
\end{aligned}$$

Again, we see the expected overall symmetry in swapping  $\beta_2$  and  $\beta_3$ . It is also noteworthy that while there is significant internal cancellation between the fully connected diagrams, some terms with weight less than five do survive.

In the above, we have stated a result for two constants based on the numerical methods documented in [77]. The errors given are those of a single standard deviation of the Cuba implementation of the Vegas algorithm [97], as determined by adding in quadrature the corresponding errors of each contributing MB integral. All integration parameters used are the default parameters of the package described in [77]. In the end, we will be able to determine the analytic value of the numerical coefficient proportional to  $\log(\alpha_{12})$  in the above from symmetry considerations





(a) Representative diagram of  $w_{311}$ . (b) Representative diagram of  $w_{122}$ .

**Figure 5.5** Representative diagrams of three-line webs containing a single three-gluon vertex.

when we assemble  $\bar{H}_3$  in section 6.3. The numerical value we found above will then serve as a consistency check. Similarly, we will obtain an analytic value for the overall constant by considering collinear limits in chapter 8.

## 5.2.2 Webs Containing a Single Three Gluon Vertex

For the 311-web in fig. 5.5a, we have put the detailed calculation in Appendix E. After integrating over the relevant scales and expanding in  $\epsilon$ , we find the following representation

$$\bar{w}_{(311)} = \mathcal{C}_{(311)} \mathcal{F}_{(311)}(\alpha_{12}, \alpha_{13}) \quad (5.30)$$

$$\mathcal{C}_{(311)} \equiv f^{abe} f^{cde} \{ \mathbf{T}_1^a, \mathbf{T}_1^d \} \mathbf{T}_2^b \mathbf{T}_3^c \quad (5.31)$$

$$\begin{aligned} \mathcal{F}_{(311)}^{(3,-1)}(\alpha_{12}, \alpha_{13}) &= i \frac{2}{3} \frac{1}{(4\pi)^3} \gamma_{12} \hat{\beta}_2^\mu \hat{\beta}_3^\nu \hat{\beta}_3^\rho \int_0^1 \frac{db}{b(1-b)} \int_0^1 da \int dx_1 dx_2 dx_3 \\ &\times \delta \left( 1 - \sum_i x_i \right) \theta (bx_3 > (1-b)(1-a)) \theta ((1-b)(1-a) > bx_2) \\ &\times \left( -(a\beta_1 - (1-a)\beta_2)^2 + i0 \right)^{-1} \Gamma_{\mu\nu\rho} (\partial_{x_1\beta_3}, \partial_{x_2\beta_1}, \partial_{x_3\beta_1}) \\ &\times \frac{1}{\pi^2} \int d^d z \left( -(x_1\beta_3 - z)^2 + i0 \right)^{-1} \\ &\times \left( -(x_2\beta_1 - z)^2 + i0 \right)^{-1} \left( -(x_3\beta_1 - z)^2 + i0 \right)^{-1}. \end{aligned} \quad (5.32)$$

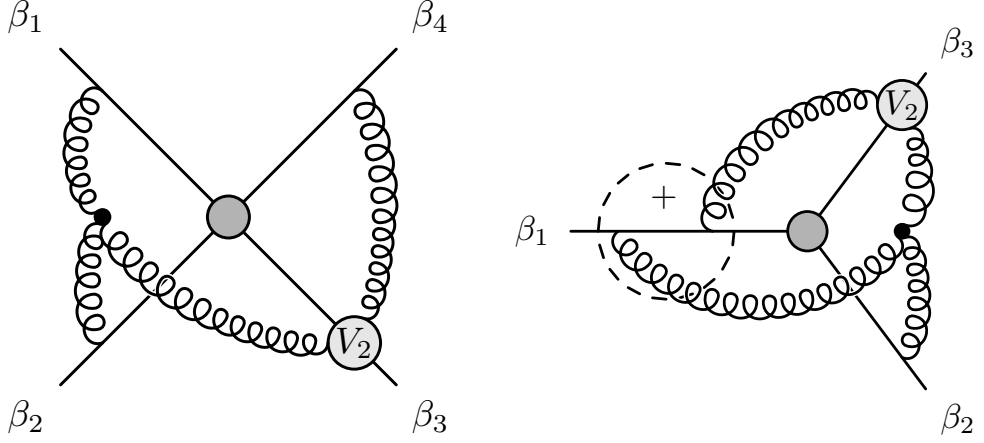


**Figure 5.6** Collinear reduction of  $w_{(1112)}$ , to  $w_{(221)}$

The integration over  $b$  can be performed, after which we find that the integral over  $a$  yields a MGEW basis function. It is notable that at this stage, the integration over the three-gluon vertex factorises completely from the single gluon exchange.

The vertex integration can be identified as a scalar triangle and we obtain

$$\begin{aligned}
\mathcal{F}_{(311)}^{(3,-1)}(\alpha_{12}, \alpha_{13}) &= -\frac{2}{3} \frac{1}{(4\pi)^3} r(\alpha_{12}) M_{0,0,0}(\alpha_{12}) \hat{\beta}_2^\mu \hat{\beta}_3^\nu \hat{\beta}_3^\rho \int dx_1 dx_2 dx_3 \\
&\times \delta \left( 1 - \sum_i x_i \right) \theta(x_3 > x_2) \frac{d}{da} \left( \frac{x_3}{x_2} \right)^a \Big|_{a=0} \\
&\times \Gamma_{\mu\nu\rho}(\partial_{x_1\beta_2}, \partial_{x_2\beta_1}, \partial_{x_3\beta_1}) T(\{p_i^2\}, \{1\}, 4)
\end{aligned} \tag{5.33}$$

The calculation now proceeds in the same way as it did for the three gluon vertex diagram in chapter 2. Taking the asymptotic light-like limit, we obtain

$$\begin{aligned}
\mathcal{F}_{(311),ll}^{(3,-1)}(\alpha_{12}, \alpha_{13}) &= -\frac{2}{3} \frac{1}{(4\pi)^3} \log(\alpha_{12}) \\
&\times \left( \frac{1}{3} \log^4(\alpha_{13}) + 4(\zeta_3 - 2\zeta_2)(1 + \log(\alpha_{13})) - 3\zeta_4 \right)
\end{aligned} \tag{5.34}$$

Next we consider the 221-web in fig. 5.5b. We will utilise collinear reduction of the 1112-web in fig. 5.2 to find its contribution to  $\Gamma^S$ . To obtain this, we must take  $\beta_4$  collinear to either  $\beta_1$  or  $\beta_2$ , which will produce permutations of the same diagram. We choose  $\beta_4 \parallel \beta_1$ , as depicted in fig. 5.6. We have

$$\begin{aligned} \mathcal{C}_{1112} &= f^{abe} f^{cde} \mathbf{T}_1^a \mathbf{T}_2^b \mathbf{T}_3^c \mathbf{T}_4^d \\ &\xrightarrow{4||1} \frac{1}{2} f^{abe} f^{cde} \{ \mathbf{T}_1^a, \mathbf{T}_1^d \} \mathbf{T}_2^b \mathbf{T}_3^c, \end{aligned} \quad (5.35)$$

$$\mathcal{F}_{(1112)}(\alpha_{12}, \alpha_{13}, \alpha_{23}; \alpha_{34}) \xrightarrow{4||1} \mathcal{F}_{(1112)}(\alpha_{12}, \alpha_{13}, \alpha_{23}; \alpha_{13}). \quad (5.36)$$

This is the only collinear reduction yielding this colour factor and this configuration of the diagram. It is therefore clear that prior to taking the light-like limit, we may write

$$\begin{aligned} w_{(122)} &= \left( f^{abe} f^{cde} \{ \mathbf{T}_1^a, \mathbf{T}_1^d \} \mathbf{T}_2^b \mathbf{T}_3^c \right) \left( \frac{1}{2} \mathcal{F}_{(1112)}(\alpha_{12}, \alpha_{13}, \alpha_{23}; \alpha_{13}) \right) \\ &\equiv C_{(122)} \mathcal{F}_{(122)}(\alpha_{12}, \alpha_{23}; \alpha_{13}) \end{aligned} \quad (5.37)$$

Inserting this into eq. (5.7) we obtain

$$\begin{aligned} \mathcal{F}_{(221)}^{(3,-1)}(\alpha_{12}, \alpha_{23}; \alpha_{13}) &= \frac{1}{6} \frac{1}{(4\pi)^3} (M_{0,0,0}(\alpha_{13}) t_1(\alpha_{12}, \alpha_{13}, \alpha_{23}) \\ &\quad - 2M_{1,0,0}(\alpha_{13}) t_0(\alpha_{12}, \alpha_{13}, \alpha_{23})) \end{aligned} \quad (5.38)$$

We observe that our calculation of  $t_1$  and  $t_0$  proceed as before, the only alteration being the argument of the MGEW basis function preceding it. Moreover, the fact that there is no dependence on  $\alpha_{14}$  in  $\mathcal{F}_{(1112)}$  means that we can safely take the light-like limit without incurring any conflict with the collinear reduction. Thus, we may simply change the argument of the MGEW basis function in our result

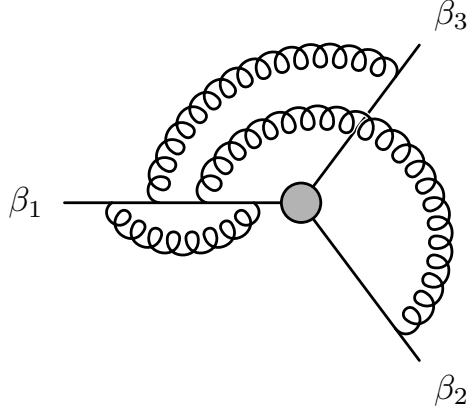


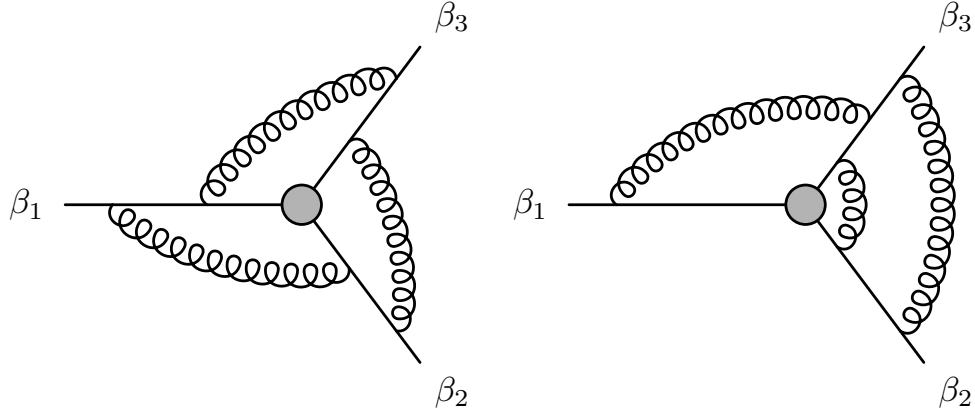
**Figure 5.7** Representative diagram of the 411-web:  $w_{(411)}$ .

for  $\mathcal{F}_{(1112)}$ , and obtain

$$\begin{aligned}
\mathcal{F}_{(221)}^{(3,-1)}(\alpha_{12}, \alpha_{23}; \alpha_{13}) &= \frac{1}{(4\pi)^3} \left[ -\frac{2}{9} \log^5(\alpha_{13}) + \frac{10}{9} \log(\alpha_{12}) \log^4(\alpha_{13}) \right. \\
&\quad - \frac{4}{9} \log(\alpha_{23}) \log^4(\alpha_{13}) + \frac{2}{9} \log^4(\alpha_{23}) \log(\alpha_{13}) \\
&\quad + \frac{2}{9} \log^2(\alpha_{13}) \log^3(\alpha_{12}) - \frac{2}{3} \log^3(\alpha_{13}) \log^2(\alpha_{12}) \\
&\quad - \frac{8}{9} \log^2(\alpha_{13}) \log^3(\alpha_{23}) + \frac{4}{3} \log^3(\alpha_{13}) \log^2(\alpha_{23}) \\
&\quad - \frac{2}{9} \log(\alpha_{13}) \log(\alpha_{23}) \log^3(\alpha_{12}) + \frac{2}{9} \log(\alpha_{13}) \log^3(\alpha_{23}) \log(\alpha_{12}) \\
&\quad - \frac{2}{3} \log^3(\alpha_{13}) \log(\alpha_{23}) \log(\alpha_{12}) \\
&\quad + \frac{4}{3} \zeta_2 \left( -\log^3(\alpha_{13}) + \log(\alpha_{12}) \log^2(\alpha_{13}) - \log(\alpha_{23}) \log^2(\alpha_{13}) \right. \\
&\quad \left. - \log^2(\alpha_{12}) \log(\alpha_{13}) + 2 \log^2(\alpha_{23}) \log(\alpha_{13}) - \log(\alpha_{12}) \log^2(\alpha_{23}) \right. \\
&\quad \left. + \log^2(\alpha_{12}) \log(\alpha_{23}) - \log(\alpha_{12}) \log(\alpha_{23}) \log(\alpha_{13}) \right) \\
&\quad \left. + \frac{8}{3} \zeta_3 \left( \log^2(\alpha_{13}) - \log(\alpha_{13}) \log(\alpha_{23}) \right) \right] \tag{5.39}
\end{aligned}$$

### 5.2.3 Webs with Vertex Corrections

On three legs, we have our first occurrence of a so-called boomerang graph, a vertex correction graph in which a gluon propagator has both legs attached to the same Wilson line, i.e.  $w_{(411)}$  in fig. 5.7. This web has been computed in [94]. In utilising it, we are forced to assume a sign error in order to obtain the required



(a) Representative diagram in  $w_{222}$ . (b) Representative diagram in  $w_{123}$ .

**Figure 5.8** Three-line MGEWs.

cancellation of lower-weight terms when the web is combined with the others. Thus, taking the opposite sign from [94], we have

$$w_{(411)}^{(3,-1)}(\alpha_{12}, \alpha_{13}) = -\frac{1}{6} \frac{1}{(4\pi)^3} f^{abe} f^{cde} \{ \mathbf{T}_1^a, \mathbf{T}_1^d \} \mathbf{T}_2^b \mathbf{T}_3^c (-16\zeta_2 M_{0,0,0}(\alpha_{12}) M_{0,0,0}(\alpha_{13})). \quad (5.40)$$

Taking the light-like limit, we then find

$$w_{(411),l}^{(3,-1)}(\alpha_{12}, \alpha_{13}) = -\frac{1}{6} \frac{1}{(4\pi)^3} f^{abe} f^{cde} \{ \mathbf{T}_1^a, \mathbf{T}_1^d \} \mathbf{T}_2^b \mathbf{T}_3^c (-64\zeta_2 \log(\alpha_{12}) \log(\alpha_{13})). \quad (5.41)$$

## 5.2.4 Three-line Multiple Gluon Exchange Webs

The web  $w_{(222)}$  in fig. 5.8a can be written as [95]

$$\begin{aligned}
w_{(222)}(\{\alpha_{ij}\}) &= f^{abe} f^{cde} \{\mathbf{T}_1^a, \mathbf{T}_1^d\} \mathbf{T}_2^b \mathbf{T}_3^c \mathcal{F}_{(222)}(\alpha_{12}, \alpha_{23}, \alpha_{13}) \\
&\quad - f^{abe} f^{cde} \mathbf{T}_1^a \{\mathbf{T}_2^b, \mathbf{T}_2^c\} \mathbf{T}_3^d \mathcal{F}_{(222)}(\alpha_{23}, \alpha_{13}, \alpha_{12}) \\
&\quad - f^{ade} f^{bce} \mathbf{T}_1^a \mathbf{T}_2^b \{\mathbf{T}_3^c, \mathbf{T}_3^d\} \mathcal{F}_{(222)}(\alpha_{13}, \alpha_{12}, \alpha_{23})
\end{aligned} \tag{5.42}$$

$$\begin{aligned}
\mathcal{F}_{(222)}^{(3,-1)}(\alpha_{12}, \alpha_{23}, \alpha_{13}) &= -\frac{1}{6} \frac{1}{(4\pi)^3} \frac{1}{3} r(\alpha_{12}) r(\alpha_{13}) r(\alpha_{23}) \\
&\quad \times \left[ M_{0,0,0}(\alpha_{12}) M_{0,0,0}(\alpha_{13}) \left( M_{0,2,0}(\alpha_{23}) - \frac{1}{4} M_{2,0,0}(\alpha_{23}) \right) \right. \\
&\quad + \frac{1}{8} M_{2,0,0}(\alpha_{12}) M_{0,0,0}(\alpha_{13}) M_{0,0,0}(\alpha_{23}) \\
&\quad + \frac{1}{8} M_{0,0,0}(\alpha_{12}) M_{2,0,0}(\alpha_{13}) M_{0,0,0}(\alpha_{23}) \\
&\quad - \frac{1}{2} M_{1,0,0}(\alpha_{12}) M_{1,0,0}(\alpha_{13}) M_{0,0,0}(\alpha_{23}) \\
&\quad + \frac{1}{4} M_{1,0,0}(\alpha_{12}) M_{0,0,0}(\alpha_{13}) M_{1,0,0}(\alpha_{23}) \\
&\quad \left. + \frac{1}{4} M_{0,0,0}(\alpha_{12}) M_{1,0,0}(\alpha_{13}) M_{1,0,0}(\alpha_{23}) \right]
\end{aligned} \tag{5.43}$$

$M_{0,2,0}$  is unaltered in the light-like limit, its full form is simply

$$M_{0,2,0}(\alpha) = \frac{2}{3} \log^3(\alpha) + 4\zeta_2 \log(\alpha). \tag{5.44}$$

Utilising this, along with eqs. (5.17) to (5.19), we obtain the following expression in the light-like limit

$$\begin{aligned}
\mathcal{F}_{(222),ll}^{(3,-1)}(\alpha_{12}, \alpha_{23}, \alpha_{13}) = & \frac{1}{(4\pi)^3} \left[ \frac{4}{9} \log^3(\alpha_{12}) \log(\alpha_{13}) \log(\alpha_{23}) \right. \\
& + \frac{4}{9} \log(\alpha_{12}) \log^3(\alpha_{13}) \log(\alpha_{23}) - \frac{4}{3} \log^2(\alpha_{12}) \log^2(\alpha_{13}) \log(\alpha_{23}) \\
& + \frac{2}{3} \log^2(\alpha_{12}) \log(\alpha_{13}) \log^2(\alpha_{23}) + \frac{2}{3} \log(\alpha_{12}) \log^2(\alpha_{13}) \log^2(\alpha_{23}) \\
& + \frac{5}{3} \zeta_4 (\log(\alpha_{12}) + \log(\alpha_{13}) - 2 \log(\alpha_{23})) \\
& - \frac{2}{3} \zeta_3 (\log(\alpha_{12}) \log(\alpha_{23}) + \log(\alpha_{13}) \log(\alpha_{23}) - 2 \log(\alpha_{12}) \log(\alpha_{13})) \\
& + \frac{2}{3} \zeta_2 (\log^2(\alpha_{13}) \log(\alpha_{12}) + \log^2(\alpha_{23}) \log(\alpha_{12}) + \log(\alpha_{13}) \log^2(\alpha_{23}) \\
& + \log(\alpha_{13}) \log^2(\alpha_{12}) - 2 \log(\alpha_{23}) \log^2(\alpha_{12}) - 2 \log^2(\alpha_{13}) \log(\alpha_{23}) \\
& \left. + 8 \log(\alpha_{12}) \log(\alpha_{13}) \log(\alpha_{23})) \right] \tag{5.45}
\end{aligned}$$

Next, we have  $w_{(123)}$ , depicted in fig. 5.8b. This web has also been computed in [95], neglecting tripole contributions, it is

$$\begin{aligned}
w_{(123)}(\alpha_{13}, \alpha_{23}) = & - f^{abe} f^{cde} \mathbf{T}_1^a \{ \mathbf{T}_2^b, \mathbf{T}_2^d \} \mathbf{T}_3^d \mathcal{F}_{(123),2}(\alpha_{13}, \alpha_{23}) \\
& + f^{ade} f^{bce} \mathbf{T}_1^a \mathbf{T}_2^b \{ \mathbf{T}_3^c, \mathbf{T}_3^d \} \mathcal{F}_{(123),3}(\alpha_{13}, \alpha_{23}) \tag{5.46}
\end{aligned}$$

$$\begin{aligned}
\mathcal{F}_{(123),2}^{(3,-1)}(\alpha_{13}, \alpha_{23}) = & - \frac{1}{6} \frac{1}{(4\pi)^3} \frac{1}{12} r(\alpha_{13}) r^2(\alpha_{23}) \left[ \frac{1}{2} M_{(2,0,0)}(\alpha_{13}) M_{0,0,0}^2(\alpha_{23}) \right. \\
& - \frac{1}{2} M_{0,0,0}(\alpha_{13}) M_{0,0,0}(\alpha_{23}) M_{2,0,0}(\alpha_{23}) + M_{0,0,0}(\alpha_{13}) M_{1,0,0}^2(\alpha_{23}) \\
& \left. - M_{1,0,0}(\alpha_{13}) M_{0,0,0}(\alpha_{23}) M_{1,0,0}(\alpha_{23}) \right] \tag{5.47}
\end{aligned}$$

$$\begin{aligned}
\mathcal{F}_{(123),3}^{(3,-1)}(\alpha_{13}, \alpha_{23}) = & \frac{1}{6} \frac{1}{(4\pi)^3} \frac{1}{12} r(\alpha_{13}) r^2(\alpha_{23}) \left[ -\frac{1}{2} M_{(2,0,0)}(\alpha_{13}) M_{0,0,0}^2(\alpha_{23}) \right. \\
& + \frac{1}{2} M_{0,0,0}(\alpha_{13}) M_{0,0,0}(\alpha_{23}) (M_{2,0,0}(\alpha_{23}) - 8M_{0,2,0}(\alpha_{23})) \\
& \left. - M_{0,0,0}(\alpha_{13}) M_{1,0,0}^2(\alpha_{23}) + M_{1,0,0}(\alpha_{13}) M_{0,0,0}(\alpha_{23}) M_{1,0,0}(\alpha_{23}) \right] \tag{5.48}
\end{aligned}$$

Taking the light-like limits, we obtain

$$\begin{aligned}
\mathcal{F}_{(123),2,ll}^{(3,-1)}(\alpha_{13}, \alpha_{23}) = & \frac{1}{(4\pi)^3} \left[ \frac{2}{9} \log(\alpha_{13}) \log^4(\alpha_{23}) - \frac{2}{3} \log^2(\alpha_{13}) \log^3(\alpha_{23}) \right. \\
& + \frac{4}{9} \log^3(\alpha_{13}) \log^2(\alpha_{23}) + \frac{5}{3} \zeta_4 (\log(\alpha_{13}) - \alpha_{23}) \\
& + \frac{2}{3} \zeta_3 (\log(\alpha_{13}) \log(\alpha_{23}) - \log^2(\alpha_{23})) \\
& + \frac{2}{3} \zeta_2 (2 \log(\alpha_{13}) \log^2(\alpha_{23}) \\
& \left. - \log^3(\alpha_{23}) - \log^2(\alpha_{13}) \log(\alpha_{23})) \right]
\end{aligned} \tag{5.49a}$$

$$\begin{aligned}
\mathcal{F}_{(123),3,ll}^{(3,-1)}(\alpha_{13}, \alpha_{23}) = & \frac{1}{(4\pi)^3} \left[ \frac{10}{9} \log(\alpha_{13}) \log^4(\alpha_{23}) - \frac{2}{3} \log^2(\alpha_{13}) \log^3(\alpha_{23}) \right. \\
& + \frac{4}{9} \log^3(\alpha_{13}) \log^2(\alpha_{23}) - \frac{5}{3} \zeta_4 (\log(\alpha_{23}) - \log(\alpha_{13})) \\
& + \frac{2}{3} \zeta_3 (\log(\alpha_{13}) \log(\alpha_{23}) - \log^2(\alpha_{23})) \\
& - \frac{2}{3} \zeta_2 (\log^3(\alpha_{23}) - 10 \log(\alpha_{13}) \log^2(\alpha_{23}) \\
& \left. + \log^2(\alpha_{13}) \log(\alpha_{23})) \right]
\end{aligned} \tag{5.49b}$$

## 5.3 Two-Line Webs

Finally, we consider the two-line webs contributing to  $H_2$  in eq. (3.20). As in the other sections, we start with the fully connected graphs.

### 5.3.1 Fully Connected Webs

As was the case with three-line webs, we have three fully connected web topologies to consider: one consisting of a four-gluon vertex exchange (fig. 5.9a), and two composed of two connected three-gluon vertices (figs. 5.9b and 5.9c). We begin with the four-gluon vertex web, our starting point is the following colour and



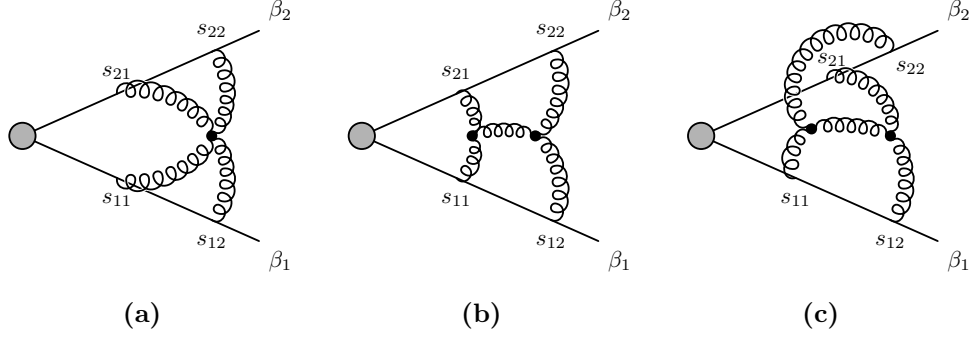


**Figure 5.9** Fully connected two-line webs.

kinematic factors

$$\mathcal{C}_{(4gv),2} = f^{ace} f^{bde} \{ \mathbf{T}_1^a, \mathbf{T}_1^b \} \{ \mathbf{T}_2^c, \mathbf{T}_2^d \} \quad (5.50)$$

$$\begin{aligned} \mathcal{F}_{(4gv),2}^{(3,-1)}(\alpha_{12}) &= -i g_s^6 \frac{1}{2} \left( \frac{\mu^2}{m^2} \right)^{3\epsilon} \mathcal{N}^4 \Gamma(6\epsilon) \left( 1 - \frac{\gamma_{12}^2}{4} \right) \\ &\times \int d^d z \prod_{\substack{i \in (1,2) \\ j \in (1,2)}} \left[ \int_0^\infty dy_{i,j} \frac{1}{[-(y_{i,j} \beta_i - z)^2 + i0]^{1-\epsilon}} \right] \\ &\times \delta \left( 1 - \sum_{\substack{i \in (1,2) \\ j \in (1,2)}} y_{i,j} \right) \theta(y_{1,1} < y_{1,2}) \theta(y_{2,1} < y_{2,2}). \end{aligned} \quad (5.51)$$

The calculation now proceeds in the same way as the preceding two calculations involving a four-gluon vertex. We obtain

$$\begin{aligned} \mathcal{F}_{(4gv),2,l}^{(3,-1)}(\alpha_{12}) &= -\frac{1}{6} \frac{1}{(4\pi)^3} \left[ (32 - 16\zeta_3) \log(\alpha_{12}) - 16 \log^2(\alpha_{12}) \right. \\ &\quad \left. + \frac{16}{3} \log^3(\alpha_{12}) - \frac{4}{3} \log^4(\alpha_{12}) + (0.22 \pm 0.01) \right]. \end{aligned} \quad (5.52)$$

As before, the error given is the result of numerically computing a constant coefficient using the methods given in [77]. It is a single standard deviation of the Vegas algorithm implemented in [97], using the default parameters implemented in [77].

Turning our attention to the double three gluon vertex diagrams in figs. 5.9b

and 5.9c, we obtain the following representation

$$\begin{aligned}
\mathcal{C}_{(3g)^2,2} &= f^{ace} f^{bde} \{ \mathbf{T}_1^a, \mathbf{T}_1^b \} \{ \mathbf{T}_2^c, \mathbf{T}_2^d \} & (5.53) \\
\mathcal{F}_{(3g)^2,2,1}(\alpha_{12}) + \mathcal{F}_{(3g)^2,2,2}(\alpha_{12}) &= -\frac{1}{4} \left( \frac{\mu}{m} \right)^{6\epsilon} g_s^6 \mathcal{N}^5 \Gamma(6\epsilon) \\
&\times \left( \prod_{\substack{i \in (1,2) \\ j \in (1,2)}} \int_0^\infty \beta_i^{\sigma_j} dy_{i,j} \right) \delta \left( 1 - \sum_{\substack{i \in (1,2) \\ j \in (1,2)}} y_{i,j} \right) \\
&\times \theta(y_{1,2} > y_{1,1}) (\theta(y_{1,2} > y_{1,1}) + \theta(y_{1,1} > y_{1,2})) \\
&\times \Gamma_{\sigma_1 \sigma_2 \tau} (\partial_{y_{1,1} \beta_1}, \partial_{y_{2,1} \beta_2}, -\partial_{y_{1,1} \beta_1} - \partial_{y_{2,1} \beta_2}) \\
&\times \Gamma_{\sigma_3 \sigma_4}^\tau (\partial_{y_{1,2} \beta_1}, \partial_{y_{2,2} \beta_2}, -\partial_{y_{1,2} \beta_2} - \partial_{y_{2,2} \beta_2}) \\
&\times \int d^d z d^d w (-(y_{1,1} \beta_1 - z)^2 + i0)^{\epsilon-1} \\
&\times (-(y_{2,1} \beta_2 - z)^2 + i0)^{\epsilon-1} (-(y_{1,2} \beta_1 - w)^2 + i0)^{\epsilon-1} \\
&\times (-(y_{2,2} \beta_2 - w)^2 + i0)^{\epsilon-1} (-(z - w)^2 + i0)^{\epsilon-1}. & (5.54)
\end{aligned}$$

We compute this integral as usual, and obtain

$$\begin{aligned}
\mathcal{F}_{(3g)^2,2,1}^{(3,-1)}(\alpha_{12}) + \mathcal{F}_{(3g)^2,2,2}(\alpha_{12}) &= -\frac{1}{3} \frac{1}{(4\pi)^3} \left[ -\frac{2}{3} \log^5(\alpha_{12}) + \frac{8}{3} \log^4(\alpha_{12}) \right. \\
&- \left( \frac{32}{3} - 8\zeta_2 \right) \log^3(\alpha_{12}) + (46.172 \pm 0.008) \log^2(\alpha_{12}) \\
&\left. - (23.75 \pm 0.13) \log(\alpha_{12}) - (31.6 \pm 3.3) \right]. & (5.55)
\end{aligned}$$

As was the case for the four-gluon vertex above, we have been forced to utilise numerics for the computation of some constant coefficients in the above result. The errors given here are the same as they were for the four-gluon vertex, i.e. single standard deviations as determined by the Vegas algorithm implemented in [97], using the default parameters of MB tools [77]. In the coming chapters we will see that we can obtain the analytic coefficients of both of the terms proportional to  $\log(\alpha_{12})$  from analytical considerations (see section 6.3), as well as the analytic value of the constant from collinear limit considerations (see chapter 8).

### 5.3.2 Webs Containing Three Gluon Vertices

On two lines, we have one web containing a three-gluon vertex: the 32-web in fig. 5.10. We wish to obtain it via collinear reduction from the 221-web in fig. 5.5b,

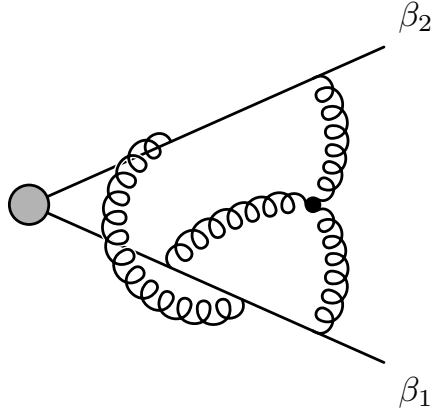


**Figure 5.10** *Representative diagram from the 32-web,  $w_{32}$ .*

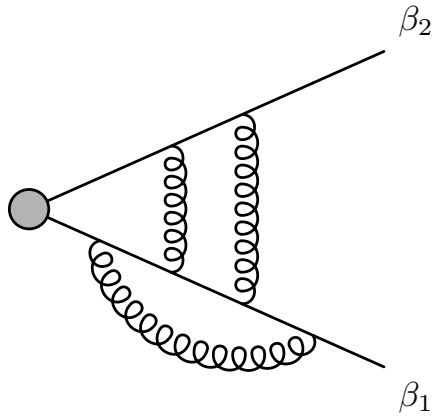


**Figure 5.11** *Representative diagram of the 24-web,  $w_{42}$*

however, we only have light-like results for  $w_{122}$ . The route we take to obtain this result is therefore somewhat circuitous: we use what we know about the analytic structure of the non-lightlike 1121-web to obtain the required collinear reduction. The derivation is given in full in Appendix F, the end result is

$$\mathcal{F}_{(32),ll}^{(3,-1)}(\alpha_{12}) = -\frac{1}{6} \frac{1}{(4\pi)^3} \left[ \frac{8}{3} \log^5(\alpha_{12}) + (32\zeta_3 - 64\zeta_2) \log^2(\alpha_{12}) \right. \quad (5.56)$$

$$\left. - (64\zeta_2 - 32\zeta_3 + 24\zeta_4) \log(\alpha_{12}) \right]. \quad (5.57)$$

### 5.3.3 Webs With Vertex Corrections

Considering the 24-web in fig. 5.11, we may obtain it from collinear reduction either of  $w_{(411)}$ , or from the combined reduction of  $w_{123}$  and  $w_{222}$ . We choose to

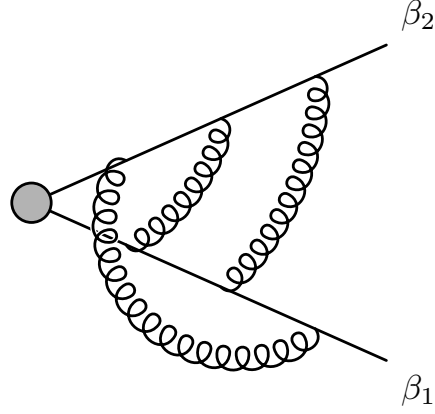


**Figure 5.12**  $w_{33}(\alpha_{12})$

reduce  $w_{(411)}$  and find

$$\mathcal{C}_{24} = f^{ace} f^{bde} \{ \mathbf{T}_1^a, \mathbf{T}_1^b \} \{ \mathbf{T}_2^c, \mathbf{T}_2^d \} \quad (5.58)$$

$$\begin{aligned} \mathcal{F}_{24}^{(3,-1)}(\alpha_{12}) &= -\frac{1}{2} \mathcal{F}_{411}(\alpha_{12}, \alpha_{12}) \\ &= -\frac{1}{6} \frac{1}{(4\pi)^3} 8\zeta_2 M_{(0,0,0)}^2(\alpha_{12}) \\ &= -\frac{1}{6} \frac{1}{(4\pi)^3} 32\zeta_2 \log^2(\alpha_{12}) \end{aligned} \quad (5.59)$$

### 5.3.4 Multiple Gluon Exchange Webs

At two legs, we only have a single MGEW to consider –  $w_{33}$  – it is depicted in fig. 5.12. We will obtain it entirely through collinear reduction. We desire a colour factor which contains an anticommutator on each leg, thus precluding any contributions from  $V_3$ . Furthermore, we need a fully connected colour factor, which means that in effective vertex notation, we are looking for the diagram depicted in fig. 5.13c.

The collinear reduction proceeds as outlined in fig. 5.13. We first take  $\beta_4 \parallel \beta_2$  and subsequently  $\beta_3 \parallel \beta_1$ . We note, however, that the final result has an additional symmetry compared to the intermediate  $w_{123}$ -web. This leads to the introduction

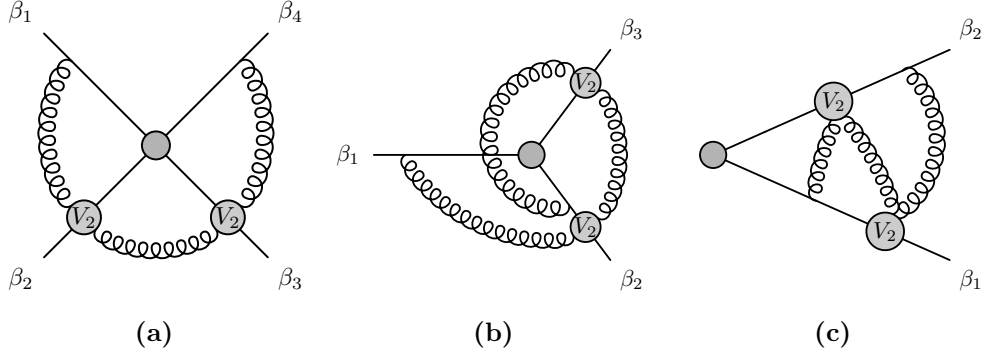


**Figure 5.13** Collinear reduction of  $w_{1221}$  to  $w_{33}$ , note the symmetry  $\beta_1 \leftrightarrow \beta_2$  in  $w_{33}$ , not present in  $w_{123}$ .

of a symmetry factor  $\frac{1}{2}$ . We obtain

$$\mathcal{C}_{33} = f^{ace} f^{bde} \{ \mathbf{T}_1^a, \mathbf{T}_1^b \} \{ \mathbf{T}_2^c, \mathbf{T}_2^d \} \quad (5.60)$$

$$\mathcal{F}_{33}^{(3,-1)}(\alpha_{12}) = \frac{1}{8} \mathcal{F}_{1221}^{(3,-1)}(\alpha_{12}, \alpha_{12}, \alpha_{12}) \quad (5.61)$$

$$= -\frac{1}{6} \frac{1}{(4\pi)^3} \left( -\frac{1}{2} \right) M_{0,0,0}(\alpha_{12}) M_{0,2,0}(\alpha_{12}) \quad (5.62)$$

Taking the asymptotic light-like limit, we obtain

$$\mathcal{F}_{(33),ll}^{(3,-1)}(\alpha_{12}) = -\frac{1}{6} \frac{1}{(4\pi)^3} \left( -8\zeta_2 \log^3(\alpha_{12}) - \frac{4}{3} \log^5(\alpha_{12}) \right) \quad (5.63)$$

# Chapter 6

## The Quadrupole Correction to the Soft Anomalous Dimension

We now turn to assembling all our results from chapter 5 with the aim of obtaining the final form of  $\Delta$ , as in eq. (3.31). To do this, we recall eq. (3.31):

$$\begin{aligned} \Delta(z, \bar{z}) = & \mathbf{T}_1^a \mathbf{T}_2^b \mathbf{T}_3^c \mathbf{T}_4^d \left( f^{abe} f^{cde} \bar{H}_4 [(1, 2); (3, 4)] \right. \\ & + f^{ace} f^{bde} \bar{H}_4 [(1, 3); (2, 4)] + f^{ade} f^{bce} \bar{H}_4 [(1, 4); (2, 3)] \Big) \\ & + C \sum_{\substack{(i,j,k) \in (1,2,3,4) \\ j < k}} f^{abe} f^{cde} \{ \mathbf{T}_i^a, \mathbf{T}_i^d \} \mathbf{T}_j^b \mathbf{T}_k^c. \end{aligned} \quad (6.1)$$

We will begin by assembling  $H_3$  and  $H_2$  (defined in eqs. (3.8) and (3.20), respectively).

### 6.1 Assembling all two-line diagrams

We recall that  $H_2(\{i, j\})$  is the coefficient of the colour factor  $f^{abe} f^{cde} \{ \mathbf{T}_i^a, \mathbf{T}_i^c \} \{ \mathbf{T}_j^b, \mathbf{T}_j^d \}$ . In terms of the kinematic factors in section 5.3, we then find

$$\begin{aligned} H_2(\{1, 2\}) = & -6 \left( \mathcal{F}_{(4gv), 2, l}(\alpha_{12}) + \mathcal{F}_{(3g)^2, 2, 1, l}(\alpha_{12}) \right. \\ & + \mathcal{F}_{(3g)^2, 2, 2, l}(\alpha_{12}) + 2\mathcal{F}_{(23), l}(\alpha_{12}) \\ & \left. + 2\mathcal{F}_{(33), l}(\alpha_{12}). \right) \end{aligned} \quad (6.2)$$

Explicitly, in terms of eqs. (5.52), (5.55), (5.59) and (5.63)

$$\begin{aligned}
H_2(\{\alpha_{12}\}) = & \frac{1}{(4\pi)^3} \left( -\frac{1}{3} \log^5(\alpha_{12}) - 4\zeta_2 \log^3(\alpha_{12}) \right. \\
& + 16\zeta_3 \log^2(\alpha_{12}) - 12\zeta_4 \log(\alpha_{12}) - 16\zeta_2 \log^2(\alpha_{12}) \\
& - 32\zeta_2 \log(\alpha_{12}) + (7.086 \pm 0.016) \log^2(\alpha_{12}) \\
& \left. + (20.12 \pm 0.26) \log(\alpha_{12}) - (15.6 \pm 6.7) \right)
\end{aligned} \tag{6.3}$$

Note the appearance of terms with transcendental weight less than five. Such terms cannot appear in  $\Delta(z, \bar{z})$  [35], and their cancellation will serve as a useful check of our result.

## 6.2 Assembling all three-line diagrams

In a similar fashion, we have for  $H_3$

$$\begin{aligned}
H_3(1, \{2, 3\}) = & -6 \left( \mathcal{F}_{(4g),3,l}(\alpha_{12}, \alpha_{13}; \alpha_{23}) + \mathcal{F}_{(3g)^2,3,l}(\alpha_{12}, \alpha_{13}; \alpha_{23}) \right. \\
& + \mathcal{F}_{(3g)^2,3,l}(\alpha_{13}, \alpha_{12}; \alpha_{23}) + \mathcal{F}_{(122),l}(\alpha_{12}, \alpha_{13}; \alpha_{23}) \\
& + \mathcal{F}_{(114),l}(\alpha_{12}, \alpha_{13}; \alpha_{23}) + \mathcal{F}_{(222),l}(\alpha_{12}, \alpha_{13}; \alpha_{23}) \\
& \left. + \mathcal{F}_{(123),2}(\alpha_{23}, \alpha_{13}) + \mathcal{F}_{(123),3}(\alpha_{13}, \alpha_{12}) \right)
\end{aligned} \tag{6.4}$$

Inserting the results from eqs. (5.29), (5.34), (5.39), (5.41), (5.45), (5.49a) and (5.49b) we obtain

$$\begin{aligned}
H_3(1, \{2, 3\}) = & \frac{1}{(4\pi)^3} \left( \frac{1}{3} \log^5(\alpha_{12}) + \frac{1}{3} \log^5(\alpha_{13}) \right. \\
& + \frac{1}{3} \log(\alpha_{13}) \log^4(\alpha_{12}) + \frac{1}{3} \log^4(\alpha_{13}) \log(\alpha_{12}) \\
& - \frac{1}{3} \log^4(\alpha_{23}) \log(\alpha_{12}) - \frac{1}{3} \log(\alpha_{13}) \log^4(\alpha_{23}) + 4\zeta_2 \log^3(\alpha_{12}) \\
& + 4\zeta_2 \log^3(\alpha_{13}) + 4\zeta_2 \log(\alpha_{13}) \log^2(\alpha_{12}) + 4\zeta_2 \log^2(\alpha_{13}) \log(\alpha_{12}) \quad (6.5) \\
& - 4\zeta_2 \log^2(\alpha_{23}) \log(\alpha_{12}) - 4\zeta_2 \log(\alpha_{13}) \log^2(\alpha_{23}) + 36\zeta_4 \log(\alpha_{13}) \\
& + 36\zeta_4 \log(\alpha_{12}) - 24\zeta_4 \log(\alpha_{23}) + 32\zeta_2 \log(\alpha_{12}) + 32\zeta_2 \log(\alpha_{13}) \\
& - 16\zeta_3 \log(\alpha_{12}) - 16\zeta_3 \log(\alpha_{13}) - (13.8 \pm 0.1) (\log(\alpha_{12}) + \log(\alpha_{13})) \\
& \left. - (34.76 \pm 1.25) \right)
\end{aligned}$$

### 6.3 Combining Two-Line and Three-Line Webs

We see immediately that when  $H_3$  is combined with  $H_2$  according to eq. (3.24), we will have significant cancellation, notably of the terms proportional to  $\log^5(\alpha_{ij})$ ,  $\zeta_2 \log^3(\alpha_{ij})$ . Due to the numerical coefficient, it is less clear that the mixed weight terms proportional to  $\log(\alpha_{ij})$  cancel, however, we find that when we construct  $\bar{H}_3$  we obtain

$$\begin{aligned}
\bar{H}_3(1, \{2, 3\}) = & \frac{1}{(4\pi)^3} \left( \frac{1}{3} \log(\alpha_{13}) \log^4(\alpha_{12}) + \frac{1}{3} \log^4(\alpha_{13}) \log(\alpha_{12}) \right. \\
& - \frac{1}{3} \log^4(\alpha_{23}) \log(\alpha_{12}) - \frac{1}{3} \log(\alpha_{13}) \log^4(\alpha_{23}) \\
& + 4\zeta_2 \log(\alpha_{13}) \log^2(\alpha_{12}) + 4\zeta_2 \log^2(\alpha_{13}) \log(\alpha_{12}) \quad (6.6) \\
& - 4\zeta_2 \log^2(\alpha_{23}) \log(\alpha_{12}) - 4\zeta_2 \log(\alpha_{13}) \log^2(\alpha_{23}) - 24\zeta_4 \log(\alpha_{23}) \\
& \left. + C_{l_2} (\log^2(\alpha_{12}) + \log^2(\alpha_{13})) + C_{l_1} (\log(\alpha_{12}) + \log(\alpha_{13})) + C_{l_0} \right),
\end{aligned}$$

where we have defined the numerically determined constants

$$C_{l_2} = 16\zeta_3 - 16\zeta_2 + 7.086 \pm 0.016, \quad (6.7a)$$

$$C_{l_1} = 24\zeta_4 - 16\zeta_3 + 6.25 \pm 0.36, \quad (6.7b)$$

$$C_{l_0} = -66.0 \pm 14.7. \quad (6.7c)$$



The numerical coefficients  $C_{l_0}$ ,  $C_{l_1}$  and  $C_{l_2}$  should now all be uniform weight five with reasonably simple rational prefactors. We can determine the value of  $C_{l_1}$  and  $C_{l_2}$  by comparing eq. (6.10) to the symmetry requirement imposed on  $\bar{H}_3$  by the requirement that tripole terms may only be proportional to a constant, as given in eq. (3.26). Inserting eq. (6.10) into eq. (3.26), we find that we must have

$$C_{l_2} = 0, \tag{6.8a}$$

$$C_{l_1} = 12\zeta_4. \tag{6.8b}$$

Comparing this to the numeric results we have obtained, we find

$$C_{l_2} = 0.000 \pm 0.016 \tag{6.9a}$$

$$C_{l_1} = 12\zeta_4 + (0.00 \pm 0.36) \tag{6.9b}$$

In other words, our numerical results are consistent with the requirements of eq. (3.26), and we find

$$\begin{aligned} \bar{H}_3(1, \{2, 3\}) = & \frac{1}{(4\pi)^3} \left( \frac{1}{3} \log(\alpha_{13}) \log^4(\alpha_{12}) + \frac{1}{3} \log^4(\alpha_{13}) \log(\alpha_{12}) \right. \\ & - \frac{1}{3} \log^4(\alpha_{23}) \log(\alpha_{12}) - \frac{1}{3} \log(\alpha_{13}) \log^4(\alpha_{23}) \\ & + 4\zeta_2 \log(\alpha_{13}) \log^2(\alpha_{12}) + 4\zeta_2 \log^2(\alpha_{13}) \log(\alpha_{12}) \\ & - 4\zeta_2 \log^2(\alpha_{23}) \log(\alpha_{12}) - 4\zeta_2 \log(\alpha_{13}) \log^2(\alpha_{23}) - 24\zeta_4 \log(\alpha_{23}) \\ & \left. + 12\zeta_4 (\log(\alpha_{12}) + \log(\alpha_{13})) + C_{l_0} \right). \end{aligned} \tag{6.10}$$

## 6.4 Four-line diagrams

Turning to  $H_4$ , our expectation for  $\Delta$  dictates that  $H_4$  must separate into two pieces: one which is polylogarithmic in  $z$  and  $\bar{z}$ , and one which depends only logarithmically on all angles. Since this term must combine eventually with  $\bar{H}_3$  to form only terms which depend on  $\log(\rho_{ijkl})$ ,  $H_4$  cannot contain any terms which are products of more than three angles. We will verify this explicitly by calculating  $H_4$ .

It is worth noting that our four-line colour basis obeys the Jacobi identity

$$f^{abe} f^{cde} - f^{ace} f^{bde} + f^{ade} f^{bce} = 0. \tag{6.11}$$

While applying this to our two-line or three-line colour factors would not make a difference, it will affect our results here. We will utilise the Jacobi identity to choose to work with kinematic functions which are explicitly Bose symmetric, as we did for  $H_4$  in chapter 3.

Thus, we define the following: for a reduced four-line web  $w_f(\{\alpha_{ij}\}) = C_f \mathcal{F}_f(\alpha_{ij})$ , define  $H_f$  by means of the sum over all permutations of webs of type  $f$  which contribute to colour factors in a manner compatible with the symmetries of  $H_4$ , schematically:

$$\begin{aligned} \sum_{\text{permutations}} \bar{w}_f &= f^{abe} f^{cde} H_f((1, 2); (3, 4)) \\ &+ f^{ace} f^{bde} H_f((1, 3); (2, 4)) + f^{ade} f^{bce} H_f((1, 4); (2, 3)), \end{aligned} \quad (6.12)$$

where we require as we did for  $H_4$  that  $H_{(i)}$  is antisymmetric under permutation of the legs within the round brackets, and symmetric in swapping the two brackets. We will then find linear combinations of the kinematic factors  $\mathcal{F}_{(i)}$  such that ultimately we have

$$H_4((1, 2); (3, 4)) = \sum_i H_{(i)}((1, 2); (3, 4)). \quad (6.13)$$

### 6.4.1 Combining all fully connected diagrams.

We first consider the fully connected diagrams. They contribute to  $\Gamma^S$  as a sum over permutations of  $z$  and  $\bar{z}$  (see section 1.2.4 for details):

$$\begin{aligned} \Gamma_{4c}(z, \bar{z}, \{\log(\alpha_{ij})\}) &\equiv \\ &-6 \left( \begin{array}{cccc} \text{Diagram 1} & + & \text{Diagram 2} & + & \text{Diagram 3} & + & \text{Diagram 4} \end{array} \right) \\ &= \bar{w}_{(4g)}(\{\alpha_{ij}\}) + \bar{w}_{(12)(34)}(\{\alpha_{ij}\}) + \bar{w}_{(13)(24)}(\{\alpha_{ij}\}) + \bar{w}_{(14)(23)}(\{\alpha_{ij}\}) \\ &= \mathbf{T}_1^a \mathbf{T}_2^b \mathbf{T}_3^c \mathbf{T}_4^d \left( f^{abe} f^{cde} f_0(z, \bar{z}, \{\alpha_{ij}\}) + f^{ace} f^{bde} f_0\left(\frac{1}{z}, \frac{1}{\bar{z}}, \{\alpha_{ij}\}\right)_{2\leftrightarrow 3} \right. \\ &\quad \left. + f^{ade} f^{bce} f_0(1-z, 1-\bar{z}, \{\alpha_{ij}\})_{2\leftrightarrow 4} \right). \end{aligned} \quad (6.14)$$

We observe the complete cancellation of  $f_1$ , which appears in each of the webs, but is absent in their sum. This can be understood as follows: in the momentum-conserving limit of  $z \rightarrow \bar{z}$ , the prefactor  $\frac{1}{z-\bar{z}}$  generates a derivative, causing  $f_1$  to be at most weight four, thus once again introducing results which would be inconsistent with the uniform weight seen in  $\mathcal{N} = 4$  Super Yang-Mills [35].

It is interesting to note that we now have all non-logarithmic contributions to  $\Delta(z, \bar{z})$ . None of the other webs, either MGEWs or webs connecting three or two lines depend independently on a set of  $\alpha_{ij}$  which may combine into a CICR. Thus all other webs can contribute at most logarithmically. A highly non-trivial check of our result thus far, then, would be the requirement that we be able to define a purely CICR-dependent quantity  $\Delta_P(z, \bar{z})$  and a logarithmic polynomial in  $\log(\alpha_{ij}) - R(\{\log(\alpha_{ij})\})$  – such that

$$\Gamma_{4c}(z, \bar{z}, \{\log(\alpha_{ij})\}) = \Delta_P(z, \bar{z}) + R(\{\log(\alpha_{ij})\}). \quad (6.15)$$

We find this to be the case after applying the Jacobi identity to eq. (6.14), with

$$\begin{aligned} \Delta_P(z, \bar{z}) = \frac{16}{(4\pi)^3} \mathbf{T}_1^a \mathbf{T}_2^b \mathbf{T}_3^c \mathbf{T}_4^d & \left[ f^{abe} f^{cde} \left( F\left(1 - \frac{1}{z}\right) - F\left(\frac{1}{z}\right) \right) \right. \\ & + f^{ace} f^{bde} (F(1-z) - F(z)) \\ & \left. + f^{ade} f^{bce} \left( F\left(\frac{1}{1-z}\right) - F\left(\frac{z}{z-1}\right) \right) \right], \end{aligned} \quad (6.16)$$

$$F(z) = \mathcal{L}_{10101}(z) + 2\zeta_2 (\mathcal{L}_{100}(z) + \mathcal{L}_{001}(z)), \quad (6.17)$$

where we have utilised the notation of single-valued harmonic polylogarithms we described in section 1.4.4. The expression above is final: since all other diagrams may only contribute logarithmically to  $\Delta$ , this polylogarithmic part will be a direct contribution with no further alterations. The logarithmic terms given by  $R$  in eq. (6.15) can be written as

$$\begin{aligned} R(\{\log(\alpha_{ij})\}) = \frac{1}{(4\pi)^3} \mathbf{T}_1^a \mathbf{T}_2^b \mathbf{T}_3^c \mathbf{T}_4^d & \left[ \right. \\ & f^{abe} f^{cde} (F_R(1, 2, 3, 4) - F_R(2, 1, 3, 4) - F_R(1, 2, 4, 3) + F_R(2, 1, 3, 4)) \\ & + f^{ace} f^{bde} (F_R(1, 3, 2, 4) - F_R(3, 1, 2, 4) - F_R(1, 3, 4, 2) - F_R(3, 1, 4, 2)) \\ & \left. - f^{ade} f^{bce} (F_R(1, 4, 2, 3) - F_R(4, 1, 2, 3) - F_R(1, 4, 3, 2) + F_R(4, 1, 3, 2)) \right], \end{aligned} \quad (6.18)$$

$$\begin{aligned}
F_R(1, 2, 3, 4) = & \\
& -8 \log(\alpha_{12}) \log(\alpha_{14}) \log(\alpha_{34}) \log^2(\alpha_{24}) \\
& -8 \log(\alpha_{12}) \log(\alpha_{23}) \log(\alpha_{34}) \log^2(\alpha_{24}) \\
& 16 \log(\alpha_{12}) \log^2(\alpha_{34}) \log^2(\alpha_{24}) - 8 \log(\alpha_{14}) \log^2(\alpha_{34}) \log^2(\alpha_{24}) \\
& -8 \log^2(\alpha_{12}) \log(\alpha_{23}) \log^2(\alpha_{24}) + 16 \log^2(\alpha_{12}) \log(\alpha_{34}) \log^2(\alpha_{24}) \\
& -16 \log^2(\alpha_{14}) \log^2(\alpha_{23}) \log(\alpha_{24}) + 8 \log(\alpha_{12}) \log^2(\alpha_{14}) \log^2(\alpha_{23}) \\
& +8 \log^2(\alpha_{14}) \log^2(\alpha_{23}) \log(\alpha_{34}) + \frac{16}{3} \log(\alpha_{12}) \log(\alpha_{23}) \log^3(\alpha_{24}) \\
& -\frac{16}{3} \log(\alpha_{12}) \log(\alpha_{34}) \log^3(\alpha_{24}) + \frac{16}{3} \log(\alpha_{14}) \log(\alpha_{34}) \log^3(\alpha_{24}) \\
& -\frac{8}{3} \log(\alpha_{14}) \log^3(\alpha_{23}) \log(\alpha_{24}) - \frac{8}{3} \log^3(\alpha_{14}) \log(\alpha_{23}) \log(\alpha_{24}) \\
& +\frac{8}{3} \log(\alpha_{12}) \log(\alpha_{14}) \log^3(\alpha_{23}) + \frac{8}{3} \log(\alpha_{14}) \log^3(\alpha_{23}) \log(\alpha_{34}) \\
& -\frac{4}{3} \log(\alpha_{12}) \log^4(\alpha_{24}) - \frac{4}{3} \log(\alpha_{34}) \log^4(\alpha_{24}) \\
& -32\zeta_2 \log(\alpha_{12}) \log(\alpha_{34}) \log(\alpha_{24}) + 32\zeta_3 \log(\alpha_{12}) \log(\alpha_{24}) \\
& +32\zeta_3 \log(\alpha_{34}) \log(\alpha_{24}) + 96\zeta_4 \log(\alpha_{24}).
\end{aligned} \tag{6.19}$$

We may thus define the sum over all connected diagrams in a manner consistent with the symmetries of  $H_4$ :  $H_C((1, 2); (3, 4)) \equiv H_{(4g)}((1, 2); (3, 4)) + H_{(3g)^2}((1, 2); (3, 4))$ , we find

$$\begin{aligned}
H_C((1, 2); (3, 4)) = & \frac{1}{(4\pi)^3} \left( 16F \left( 1 - \frac{1}{z} \right) - 16F \left( \frac{1}{z} \right) \right) \\
& + F_R(1, 2, 3, 4) - F_R(2, 1, 3, 4) \\
& - F_R(1, 2, 4, 3) + F_R(2, 1, 3, 4)
\end{aligned} \tag{6.20}$$

## 6.4.2 The 1221-web and the 1121-web

We wish to find the contribution of all webs to  $H_4$ . This means that we need to find a way of expressing the sum over permutations of each web in such a way as to explicitly satisfy Bose symmetry. In the case of both the 1221-web, and the 1121-web, we find that this is possible without having to consider the Jacobi identity. In the case of the 1221-web, we have 12 unique permutations of the

diagram, which combines in the following fashion:

$$\begin{aligned}
H_{(1221)}((1, 2), (3, 4)) \equiv & \mathcal{F}_{(1221),l}(\alpha_{12}, \alpha_{23}, \alpha_{34}) + \mathcal{F}_{(1221),l}(\alpha_{12}, \alpha_{14}, \alpha_{34}) \\
& - \mathcal{F}_{(1221),l}(\alpha_{12}, \alpha_{13}, \alpha_{34}) - \mathcal{F}_{(1221),l}(\alpha_{12}, \alpha_{24}, \alpha_{34}).
\end{aligned} \tag{6.21}$$

This linear combination thus contains the sum over all twelve permutations of 1221, with correct prefactors, and obeys the required symmetries of  $H_4$ .

The 1121-web also has 12 unique permutations. We note that the antisymmetry of the three gluon vertex yields the following relation for the kinematic factor

$$\mathcal{F}_{(1121),l}(\alpha_{12}, \alpha_{13}, \alpha_{23}, \alpha_{34}) = -\mathcal{F}_{(1121),l}(\alpha_{12}, \alpha_{23}, \alpha_{13}, \alpha_{34}). \tag{6.22}$$

Using this, we find that the following contribution to  $H_4$ :

$$\begin{aligned}
H_{(1121)}((1, 2), (3, 4)) \equiv & \\
& \mathcal{F}_{(1121),l}(\alpha_{12}, \alpha_{13}, \alpha_{23}, \alpha_{34}) - \mathcal{F}_{(1121),l}(\alpha_{12}, \alpha_{14}, \alpha_{24}, \alpha_{34}) \\
& + \mathcal{F}_{(1121),l}(\alpha_{34}, \alpha_{13}, \alpha_{14}, \alpha_{12}) - \mathcal{F}_{(1121),l}(\alpha_{34}, \alpha_{23}, \alpha_{24}, \alpha_{12}).
\end{aligned} \tag{6.23}$$

### 6.4.3 The 1113-web

The 1113-web has four unique permutations, corresponding to attaching the three gluon attachments to one of the four legs. We recall eq. (5.15), which gives us

$$\begin{aligned}
\bar{w}_{(1113)}^{(3)}(\alpha_{14}, \alpha_{24}, \alpha_{34}) \propto & \mathbf{T}_1^a \mathbf{T}_2^b \mathbf{T}_3^c \mathbf{T}_4^d (f^{ade} f^{bce} G_{(1113)}(\alpha_{14}, \alpha_{24}, \alpha_{34}) \\
& + f^{ace} f^{bde} G_{(1113)}(\alpha_{24}, \alpha_{14}, \alpha_{34})).
\end{aligned} \tag{6.24}$$

We further note that eq. (5.16) admits the following identities

$$G_{(1113)}(a, b, c) + G_{(1113)}(b, c, a) + G_{(1113)}(c, a, b) = 0, \tag{6.25}$$

$$G_{(1113)}(a, b, c) = G_{(1113)}(c, b, a). \tag{6.26}$$

The term  $G_{(1113)}(\alpha_{12}, \alpha_{13}, \alpha_{14})$  has colour factor  $f^{abe} f^{cde} \mathbf{T}_1^a \mathbf{T}_2^b \mathbf{T}_3^c \mathbf{T}_4^d$ , we use this fact to construct an ansatz for  $H_{(1113)}$  by constructing the only permissible linear

combination of  $G_{(1113)}$  which admits all the symmetries of  $H_4$ .

$$\begin{aligned}
H_{(1113)}((1, 2), (3, 4)) = & \\
& -C \left( G_{(1113)}(\alpha_{12}, \alpha_{13}, \alpha_{14}) + G_{(1113)}(\alpha_{12}, \alpha_{23}, \alpha_{24}) \right. \\
& + G_{(1113)}(\alpha_{12}, \alpha_{14}, \alpha_{13}) - G_{(1113)}(\alpha_{12}, \alpha_{24}, \alpha_{23}) \\
& - G_{(1113)}(\alpha_{34}, \alpha_{13}, \alpha_{23}) + G_{(1113)}(\alpha_{34}, \alpha_{14}, \alpha_{24}) \\
& \left. + G_{(1113)}(\alpha_{34}, \alpha_{23}, \alpha_{13}) - G_{(1113)}(\alpha_{34}, \alpha_{24}, \alpha_{14}) \right)
\end{aligned} \tag{6.27}$$

Where  $C$  is some constant to be determined. We then sum over all permutations of  $\bar{w}_{(1113)}$ , and apply the Jacobi identity of eq. (6.11) to both it and the ansatz with the aim of comparing the two. We find that setting  $C = \frac{1}{3}$  reproduces the sum over permutations of  $\bar{w}_{(1113)}$ , and we obtain

$$\begin{aligned}
H_{(1113)}((1, 2), (3, 4)) = & \\
& -\frac{1}{3}G_{(1113)}(\alpha_{12}, \alpha_{13}, \alpha_{14}) + \frac{1}{3}G_{(1113)}(\alpha_{12}, \alpha_{23}, \alpha_{24}) \\
& + \frac{1}{3}G_{(1113)}(\alpha_{12}, \alpha_{14}, \alpha_{13}) - \frac{1}{3}G_{(1113)}(\alpha_{12}, \alpha_{24}, \alpha_{23}) \\
& - \frac{1}{3}G_{(1113)}(\alpha_{34}, \alpha_{13}, \alpha_{23}) + \frac{1}{3}G_{(1113)}(\alpha_{34}, \alpha_{14}, \alpha_{24}) \\
& + \frac{1}{3}G_{(1113)}(\alpha_{34}, \alpha_{23}, \alpha_{13}) - \frac{1}{3}G_{(1113)}(\alpha_{34}, \alpha_{24}, \alpha_{14}).
\end{aligned} \tag{6.28}$$

### 6.4.4 Combining all Four-Line Diagrams

We may now assemble  $H_4$ . In terms of eqs. (6.20), (6.21), (6.23) and (6.28) we have

$$\begin{aligned}
H_4((1, 2), (3, 4)) &= \frac{1}{(4\pi)^3} \left( 16F \left( 1 - \frac{1}{z} \right) - 16F \left( \frac{1}{z} \right) \right) \\
&+ \frac{1}{(4\pi)^3} F_R(1, 2, 3, 4) - \frac{1}{(4\pi)^3} F_R(2, 1, 3, 4) \\
&- \frac{1}{(4\pi)^3} F_R(1, 2, 4, 3) + \frac{1}{(4\pi)^3} F_R(2, 1, 3, 4) \\
&+ \mathcal{F}_{(1121),u}(\alpha_{12}, \alpha_{13}, \alpha_{23}, \alpha_{34}) - \mathcal{F}_{(1121),u}(\alpha_{12}, \alpha_{14}, \alpha_{24}, \alpha_{34}) \\
&+ \mathcal{F}_{(1121),u}(\alpha_{34}, \alpha_{13}, \alpha_{14}, \alpha_{12}) - \mathcal{F}_{(1121),u}(\alpha_{34}, \alpha_{23}, \alpha_{24}, \alpha_{12}) \\
&+ \mathcal{F}_{(1221),u}(\alpha_{12}, \alpha_{23}, \alpha_{34}) + \mathcal{F}_{(1221),u}(\alpha_{12}, \alpha_{14}, \alpha_{34}) \\
&- \mathcal{F}_{(1221),u}(\alpha_{12}, \alpha_{13}, \alpha_{34}) - \mathcal{F}_{(1221),u}(\alpha_{12}, \alpha_{24}, \alpha_{34}) \\
&- \frac{1}{3} \frac{1}{(4\pi)^3} G_{(1113),u}(\alpha_{12}, \alpha_{13}, \alpha_{14}) + \frac{1}{3} \frac{1}{(4\pi)^3} G_{(1113),u}(\alpha_{12}, \alpha_{23}, \alpha_{24}) \\
&+ \frac{1}{3} \frac{1}{(4\pi)^3} G_{(1113),u}(\alpha_{12}, \alpha_{14}, \alpha_{13}) - \frac{1}{3} \frac{1}{(4\pi)^3} G_{(1113),u}(\alpha_{12}, \alpha_{24}, \alpha_{23}) \\
&- \frac{1}{3} \frac{1}{(4\pi)^3} G_{(1113),u}(\alpha_{34}, \alpha_{13}, \alpha_{23}) + \frac{1}{3} \frac{1}{(4\pi)^3} G_{(1113),u}(\alpha_{34}, \alpha_{14}, \alpha_{24}) \\
&+ \frac{1}{3} \frac{1}{(4\pi)^3} G_{(1113),u}(\alpha_{34}, \alpha_{23}, \alpha_{13}) - \frac{1}{3} \frac{1}{(4\pi)^3} G_{(1113),u}(\alpha_{34}, \alpha_{24}, \alpha_{14}).
\end{aligned} \tag{6.29}$$

Inserting eqs. (5.12), (5.20), (5.21) and (6.19) and ?? we obtain the following result:

$$\begin{aligned}
H_4((1, 2), (3, 4)) &= \frac{1}{(4\pi)^3} \left( 16F \left( 1 - \frac{1}{z} \right) - 16F \left( \frac{1}{z} \right) \right. \\
&+ \frac{4}{3} \log(\alpha_{12}) \log^4(\alpha_{13}) + \frac{4}{3} \log(\alpha_{34}) \log^4(\alpha_{13}) \\
&- \frac{4}{3} \log(\alpha_{12}) \log^4(\alpha_{14}) - \frac{4}{3} \log(\alpha_{12}) \log^4(\alpha_{23}) \\
&+ \frac{4}{3} \log(\alpha_{12}) \log^4(\alpha_{24}) - \frac{4}{3} \log^4(\alpha_{14}) \log(\alpha_{34}) \\
&- \frac{4}{3} \log^4(\alpha_{23}) \log(\alpha_{34}) + \frac{4}{3} \log^4(\alpha_{24}) \log(\alpha_{34}) \\
&+ 96\zeta_4 (\log(\alpha_{13}) - \log(\alpha_{14}) - \log(\alpha_{23}) + \log(\alpha_{24})) \\
&+ 16\zeta_2 (\log(\alpha_{12}) + \log(\alpha_{34})) \\
&\left. \times (\log^2(\alpha_{13}) - \log^2(\alpha_{14}) - \log^2(\alpha_{23}) + \log^2(\alpha_{24})) \right)
\end{aligned} \tag{6.30}$$

The result is remarkably simple, and belies a large amount of cancellation between different webs. Notably, we only have terms which depend on two angles, whereas a priori, products which depend on three angles would be permissible.

## 6.5 Assembling all diagrams

We now assemble  $\bar{H}_4$  according to eq. (3.27). Initially, this produces a large expression, however, after applying the Jacobi identity, we find that we may define

$$\bar{H}_4((1, 2); (3, 4)) = \frac{1}{(4\pi)^3} \left( 16F \left( 1 - \frac{1}{z} \right) - 16F \left( \frac{1}{z} \right) \right). \quad (6.31)$$

That is, we have complete cancellation of all angle-dependent terms, leaving behind a pure polylogarithmic function of  $z$  and  $\bar{z}$ , of weight five. Thus, we obtain a complete result for  $\Delta$  as follows

$$\begin{aligned} \Delta(z, \bar{z}) &= \frac{1}{(4\pi)^3} 16 \mathbf{T}_1^a \mathbf{T}_2^b \mathbf{T}_3^c \mathbf{T}_4^d \\ &\times \left[ f^{abe} f^{cde} \left( F \left( 1 - \frac{1}{z} \right) - F \left( \frac{1}{z} \right) \right) \right. \\ &\quad - f^{ace} f^{bde} (F(z) - F(1-z)) \\ &\quad \left. + f^{ade} f^{bce} \left( F \left( \frac{1}{1-z} \right) - F \left( \frac{z}{z-1} \right) \right) \right] \\ &+ \frac{1}{(4\pi)^3} C_{l0} \sum_{\substack{(i,j,k) \in (1,2,3,4) \\ j < k}} f^{abe} f^{cde} \{ \mathbf{T}_i^a, \mathbf{T}_i^d \} \mathbf{T}_j^b \mathbf{T}_k^c. \end{aligned} \quad (6.32)$$

Where  $F(z)$  is the same as in eq. (6.17), namely

$$F(z) = \mathcal{L}_{10101}(z) + 2\zeta_2 (\mathcal{L}_{100}(z) + \mathcal{L}_{001}(z)). \quad (6.33)$$

The analytic value of  $C_{l0}$  is clearly unknown at this point, however we will find in chapter 8 that it is uniquely determined by the requirement of collinear splitting factorisation. Hence, we will postpone any further discussion of  $C_{l0}$  until then.

The result for  $\Delta$  is strikingly simple, and has the manifest Bose symmetry outlined in section 1.2.4. Without further ado, let us now consider the Regge limit and collinear limits in the next two chapters.





# Chapter 7

## The Regge Limit

Having computed  $\Delta$ , we next consider the Regge limit. We recall from our discussion in section 1.2.8 that since the dipole formula is responsible for the leading and subleading logarithmic contributions in the Regge limit, we must have cancellation of superleading, leading and subleading logarithms when we take this limit of  $\Delta$  [62]. To verify this, we will have to analytically continue to the region of forward scattering, and impose momentum conservation. Our expectation is then that in the limit of the mandelstam invariants  $s \gg t$ , we should have no real contributions with powers higher than  $\log\left(\frac{s}{t}\right)$ , and no imaginary contributions with powers higher than  $i \log^2\left(\frac{s}{t}\right)$ .

Thus, we now consider the forward scattering region. That is, we take two of our Wilson lines to be incoming and two outgoing. The angles  $\gamma_{ij}$  then continue as follows [62]

$$\gamma_{ij} = |\gamma_{ij}| e^{-i\pi\lambda_{ij}}. \quad (7.1)$$

The phase is determined by  $\lambda_{ij} = 1$  if both partons are either incoming or outgoing, and  $\lambda_{ij} = 0$  otherwise. Thus, if we then pick a pair to be incoming or outgoing, the CICRs may acquire phases. Translating these phases to  $z$  and  $\bar{z}$  of eqs. (1.39a) and (1.39b), we observe that they always transform such that  $z \rightarrow \bar{z}$  and  $\bar{z} \rightarrow z$ , along contours which encircle, either clockwise or counterclockwise around one or both of the points  $z = 0$  and  $z = 1$ . The contours for the analytic continuation are detailed for  $\rho_{1234}$ ,  $\rho_{1432}$  (defined in eq. (1.34)),  $z$  and  $\bar{z}$  in table 7.1, an example contour for  $z$  and  $\bar{z}$  is shown in fig. 7.1. The problem of analytic continuation to

Incoming partons	$\rho_{1234}$	$\rho_{1432}$	$z$	$\bar{z}$
(1, 2) or (3, 4)	$-2\pi i$	1		c. around 0
(1, 3) or (2, 4)	$2\pi i$	$2\pi i$	c.c. around 0	c.c. around 1
(1, 4) or (2, 3)	1	$-2\pi i$	c. around 1	

**Table 7.1** Analytic continuation of  $u$ ,  $v$ ,  $z$ , and  $\bar{z}$  to the forward scattering region. We give the total phase change of  $u$  and  $v$ , and the corresponding transformation of  $z$  and  $\bar{z}$ , where we have abbreviated the direction of the contours as *c.* for clockwise and *c.c.* for counterclockwise.

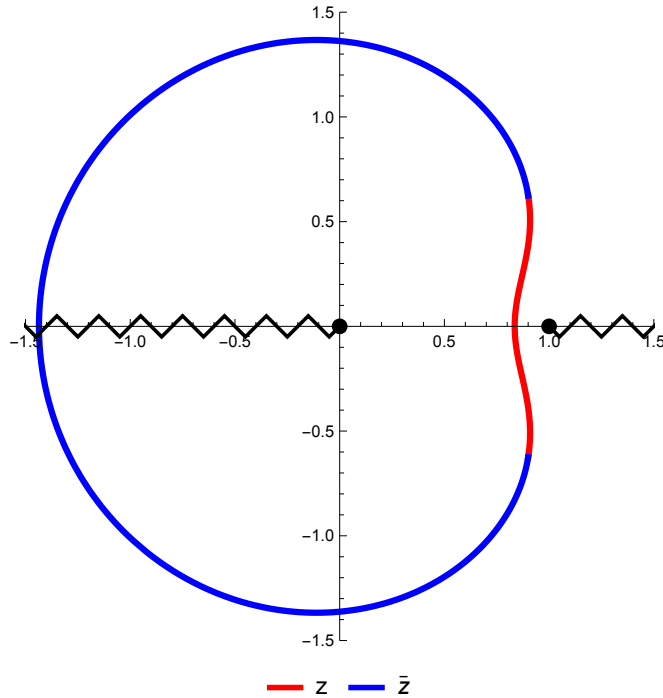


**Figure 7.1** Analytic continuation contours for  $z$  and  $\bar{z}$  for the case of  $\beta_1$  and  $\beta_2$  incoming, both contours are continuing in the clockwise direction.

forward scattering is thus reduced to that of taking monodromies of single-valued harmonic polylogarithms (SVHPLs) around the points  $z = 0$  and  $z = 1$ . These monodromies can be found by utilising the generating functionals outlined in [88, 98].

We define  $\Delta_{(1,2)}(z, \bar{z})$  as the  $\Delta$  of eq. (8.19) analytically continued to have legs 1

and 2 incoming. Performing the analytic continuation, we then find

$$\begin{aligned}
\Delta_{(1,2)}(z, \bar{z}) = & \frac{1}{(4\pi)^3} 16 \mathbf{T}_1^a \mathbf{T}_2^b \mathbf{T}_3^c \mathbf{T}_4^d [f^{abe} f^{cde} H_B(z, \bar{z}) \\
& + f^{ace} f^{bde} H_C(z, \bar{z}) + f^{ade} f^{bce} H_D(z, \bar{z})] \\
& + C_{l_0} \sum_{\substack{(i,j,k) \in (1,2,3,4) \\ j < k}} f^{abe} f^{cde} \{ \mathbf{T}_i^a, \mathbf{T}_i^d \} \mathbf{T}_j^b \mathbf{T}_k^c.
\end{aligned} \tag{7.2}$$

In the above we have retained the same colour factors as in eq. (8.19) and implicitly defined  $H_B$ ,  $H_C$  and  $H_D$  as the analytically continued coefficient of each four-line colour factor. For instance, defining  $F_{(1,2)}(z)$  as  $F(z)$  in eq. (6.33), analytically continued to legs 1 and 2 incoming, we have defined  $H_C(z, \bar{z}) \equiv$

$F_{(1,2)}(1-z) - F_{(1,2)}(z)$ , which is given by

$$\begin{aligned}
H_C(z, \bar{z}) = & -G(0, 1, 0, z)G(0, 1, \bar{z}) - G(0, 1, z)G(0, 1, 0, \bar{z}) \\
& + G(1, 0, 1, z)G(1, 0, \bar{z}) + G(1, 0, z)G(1, 0, 1, \bar{z}) \\
& - G(0, 1, 0, 1, z)G(0, \bar{z}) - G(0, z)G(0, 1, 0, 1, \bar{z}) \\
& + G(1, 0, 1, 0, z)G(1, \bar{z}) + G(1, z)G(1, 0, 1, 0, \bar{z}) \\
& - G(0, 1, 0, 1, 0, \bar{z}) + G(1, 0, 1, 0, 1, \bar{z}) \\
& - G(0, 1, 0, 1, 0, z) + G(1, 0, 1, 0, 1, z) \\
& + 2\zeta_2 \left( G(0, 0, z)G(1, \bar{z}) + G(1, z)G(0, 0, \bar{z}) \right. \\
& - G(0, 1, z)G(1, \bar{z}) - G(1, z)G(0, 1, \bar{z}) \\
& + G(1, 0, z)G(0, \bar{z}) + G(0, z)G(1, 0, \bar{z}) \\
& - G(1, 1, z)G(0, \bar{z}) - G(0, z)G(1, 1, \bar{z}) \\
& + G(0, 0, 1, \bar{z}) - G(0, 1, 1, \bar{z}) + G(1, 0, 0, \bar{z}) \\
& - G(1, 1, 0, \bar{z}) + G(0, 0, 1, z) - G(0, 1, 1, z) \\
& \left. + G(1, 0, 0, z) - G(1, 1, 0, z) \right) \\
& + 4\zeta_3 (G(0, 1, z) + G(0, 1, \bar{z}) - G(1, z)G(1, \bar{z})) \\
& - 60\zeta_4 (G(1, z) + G(1, \bar{z})) + 4(\zeta_5 + 2\zeta_2\zeta_3) \\
& + 2i\pi \left( G(0, 1, z)G(0, 1, \bar{z}) - G(1, 0, 1, z)G(1, \bar{z}) \right. \\
& - G(1, z)G(1, 0, 1, \bar{z}) + G(0, 1, 0, 1, \bar{z}) \\
& + G(0, 1, 0, 1, z) + 2\zeta_2 [-G(1, z)G(0, \bar{z}) - G(0, z)G(1, \bar{z}) \\
& \left. - G(1, 0, \bar{z}) + G(1, 1, \bar{z}) - G(1, 0, z) + G(1, 1, z)] \right).
\end{aligned} \tag{7.3}$$

The expressions for  $H_B$  and  $H_D$  are even lengthier, and we will not state them here, except in the relevant kinematic limits.

Having thus taken  $\beta_1$  and  $\beta_2$  incoming, we next need to impose momentum conservation. We wish to specialise to mandelstam invariants, and choose to do so by means of a clockwise labelling of our indices. An example  $t$ -channel diagram in this convention is shown in fig. 7.2.

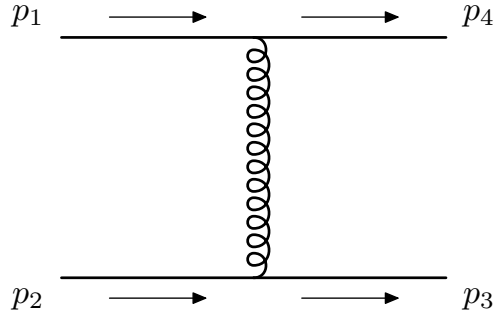


**Figure 7.2** *Example t-channel exchange in clockwise labelling convention.*

We recall eqs. (1.40a) and (1.40b).

$$z = 1 - \rho_{1234} + \rho_{1432} + \sqrt{\lambda(1, \rho_{1234}, \rho_{1432})}, \quad (7.4a)$$

$$\bar{z} = 1 - \rho_{1234} + \rho_{1432} - \sqrt{\lambda(1, \rho_{1234}, \rho_{1432})}, \quad (7.4b)$$

where  $\lambda$  is the Källén function

$$\lambda(a, b, c) = a^2 + b^2 + c^2 - 2ab - 2ac - 2bc. \quad (7.5)$$

In the momentum conserving limit, we have

$$\rho_{1234} = \frac{((\beta_1 + \beta_2)^2)^2}{((\beta_1 - \beta_3)^2)^2}, \quad (7.6a)$$

$$\rho_{1432} = \frac{((\beta_1 - \beta_4)^2)^2}{((\beta_1 - \beta_3)^2)^2}. \quad (7.6b)$$

Inserting this into eqs. (7.4a) and (7.4b), we find that momentum conservation yields  $\lambda(1, \rho_{1234}, \rho_{1432}) = 0$ , or equivalently  $z = \bar{z}$ . One important distinction is that  $z$  and  $\bar{z}$  still maintain a small (and opposite) imaginary part as per the  $i\epsilon$ -prescription. I.e. after analytic continuation and momentum conservation we have  $z - i\epsilon$  and  $\bar{z} + i\epsilon$ . This is important because we have a branch cut along  $\{z, \bar{z}\} \in [1, \infty)$ , and retaining the imaginary part thus affects from which side of the branch cut each variable approaches the Regge limit. Using the clockwise labelling convention, we obtain the Mandelstam invariants

$$s = -\gamma_{12} = -\gamma_{34} \quad (7.7)$$

$$t = \gamma_{14} = \gamma_{23} \quad (7.8)$$

$$u = \gamma_{13} = \gamma_{24} \quad (7.9)$$

We thus obtain the following relations

$$\left(\frac{s}{s+t}\right)^2 = z^2 \quad (7.10)$$

$$\left(\frac{t}{s+t}\right)^2 = (1-z)^2 \quad (7.11)$$

Solving for  $z$ , we find that in the limit of  $s \gg t$  we have

$$z = 1 + \mathcal{O}\left(\frac{-t}{s}\right). \quad (7.12)$$

We wish to expand  $\Delta$  around this limit. Considering each colour factor separately, we obtain

$$\begin{aligned} H_B(z, \bar{z})|_{z=1+\frac{-t}{s}-i\epsilon, \bar{z}=1+\frac{-t}{s}+i\epsilon} \underset{t \ll s}{\approx} & 120\zeta_4 \log\left(\frac{-t}{s}\right) + 40\zeta_2\zeta_3 - 4\zeta_5 \\ & + 4i\pi \left( 3\zeta_4 - 2\zeta_2 \log^2\left(\frac{-t}{s}\right) - 2\zeta_3 \log\left(\frac{-t}{s}\right) \right) \end{aligned} \quad (7.13)$$

$$\begin{aligned} H_C(z, \bar{z})|_{z=1+\frac{-t}{s}-i\epsilon, \bar{z}=1+\frac{-t}{s}+i\epsilon} \underset{t \ll s}{\approx} & -120\zeta_4 \log\left(\frac{-t}{s}\right) - 8\zeta_2\zeta_3 - 4\zeta_5 \\ & - 4i\pi \left( 3\zeta_4 - 2\zeta_2 \log^2\left(\frac{-t}{s}\right) - 2\zeta_3 \log\left(\frac{-t}{s}\right) \right) \end{aligned} \quad (7.14)$$

$$\begin{aligned} H_D(z, \bar{z})|_{z=1+\frac{-t}{s}-i\epsilon, \bar{z}=1+\frac{-t}{s}+i\epsilon} \underset{t \ll s}{\approx} & 120\zeta_4 \log\left(\frac{-t}{s}\right) - 8i\pi\zeta_2 \log^2\left(\frac{-t}{s}\right) - 76i\pi\zeta_4 \end{aligned} \quad (7.15)$$

The limit has real logarithmic contributions along with imaginary contributions of second order in  $\log(t/s)$ . However, applying the Jacobi identity, we find that we may write  $\Delta$  as

$$\begin{aligned} \Delta_{(1,2)}(z, \bar{z})|_{z=1+\frac{-t}{s}-i\epsilon, \bar{z}=1+\frac{-t}{s}+i\epsilon} \underset{t \ll s}{\approx} & \frac{1}{(4\pi)^3} 16 \mathbf{T}_1^a \mathbf{T}_2^b \mathbf{T}_3^c \mathbf{T}_4^d \left[ f^{abe} f^{cde} (32\zeta_2\zeta_3 - 8\zeta_5) \right. \\ & \left. - f^{ade} f^{bce} \left( 4\zeta_5 + 8\zeta_2\zeta_3 - 8i\pi\zeta_3 \log\left(\frac{-t}{s}\right) + 88i\pi\zeta_4 \right) \right] \\ & + \frac{1}{(4\pi)^3} C_{l_0} \sum_{\substack{(i,j,k) \in (1,2,3,4) \\ j < k}} f^{abe} f^{cde} \{ \mathbf{T}_i^a, \mathbf{T}_i^d \} \mathbf{T}_j^b \mathbf{T}_k^c \end{aligned} \quad (7.16)$$

Thus our result is compatible with the expectation that  $\Delta$  does not contribute above  $\mathcal{O}(\log(\frac{-t}{s}))$ , and no imaginary contributions with powers higher than  $\mathcal{O}(i \log^2(\frac{-t}{s}))$  in the Regge limit [62].





# Chapter 8

## Collinear Limits

We recall the definition of the splitting amplitude anomalous dimension (eq. (1.66)):

$$\Gamma_{\text{Sp}}(p_1, p_2) = \Gamma_n(p_1, p_2, \dots, p_n) - \Gamma_{n-1}(p_1 + p_2, p_3, \dots, \beta_n), \quad (8.1)$$

where  $\Gamma_n$  here refers to the complete soft anomalous dimension on  $n$  lines. Splitting  $\Gamma_4$  and  $\Gamma_3$  into dipole and non-dipole components, which we label  $\Gamma_n^{\text{dip}}$  and  $\Gamma_n^\Delta$ , respectively, the dipole part already obeys collinear splitting factorisation separately (for details, see [35]). We therefore consider

$$\Gamma_{\text{Sp}}^\Delta(P, p_1, p_2) \equiv \Gamma_n^\Delta(\beta_1, \beta_2, \dots, \beta_n) - \Gamma_{n-1}^\Delta(\beta_1 + \beta_2, \beta_3, \dots, \beta_n) \quad (8.2)$$

Our expectation is that  $\Gamma_{\text{Sp}}^\Delta$  may only depend on  $\mathbf{T}_1 + \mathbf{T}_2$ ,  $\mathbf{T}_1$  and  $\mathbf{T}_2$  in terms of colour, and only on  $p_1$  and  $p_2$  [32, 35, 69, 75].

Setting  $n = 4$ , we have  $\Gamma_4^\Delta = \Delta$ . We consider the limit of  $1 \parallel 2$ , we then have  $p_1 = zP$ ,  $p_2 = (1 - z)P$ , where  $P = p_1 + p_2$  is the total momentum carried by the two collinear partons, and we have momentum conservation, so  $p_1 + p_2 + p_3 + p_4 = 0$  [35]:

$$z\bar{z} = \frac{(p_3 \cdot p_4) P^2}{(P \cdot p_3)(P \cdot p_4)} \xrightarrow{P^2 \rightarrow 0} 0 \quad (8.3)$$

$$(1 - z)(1 - \bar{z}) = \frac{(p_3 \cdot P)(p_4 \cdot P)}{(p_3 \cdot P)(p_4 \cdot P)} = 1 \quad (8.4)$$

In other words, we wish to take the limit  $z, \bar{z} \rightarrow 0$ . We note that this limit is precisely the same limit we would obtain if we were to take  $3 \parallel 4$ . Taking this

limit, we obtain

$$\begin{aligned} \lim_{p_1 \parallel p_2} \Delta(z, \bar{z}) &= \frac{1}{(4\pi)^3} 64 \mathbf{T}_1^a \mathbf{T}_2^b \mathbf{T}_3^c \mathbf{T}_4^d (f^{ade} f^{bce} + f^{ace} f^{bde}) (\zeta_5 + 2\zeta_2 \zeta_3) \\ &+ \frac{1}{(4\pi)^3} C_{10} \sum_{\substack{(i,j,k) \in (1,2,3,4) \\ j < k}} f^{abe} f^{cde} \{ \mathbf{T}_i^a, \mathbf{T}_i^d \} \mathbf{T}_j^b \mathbf{T}_k^c. \end{aligned} \quad (8.5)$$

The collinear limit thus retains no kinematic dependence, however it does appear to have some non-trivial colour dependence. To shed some further light on this, consider the following four-line basis of colour tensors:

$$\mathbf{T}_A = \mathbf{T}_1 + \mathbf{T}_2, \quad (8.6)$$

$$\mathbf{T}_B = \mathbf{T}_1 - \mathbf{T}_2, \quad (8.7)$$

$$\mathbf{T}_C = \mathbf{T}_3 - \mathbf{T}_4, \quad (8.8)$$

$$\mathbf{T}_D = \mathbf{T}_3 + \mathbf{T}_4. \quad (8.9)$$

The above basis is useful since it captures the combined colour of the two partons going collinear. We would expect  $\Gamma_{\text{Sp}}(p_1, p_2)$  to only depend on  $\mathbf{T}_A$  and  $\mathbf{T}_B$ . Applying colour conservation  $\mathbf{T}_D = -\mathbf{T}_A$  to eq. (8.5) we then obtain

$$\begin{aligned} \lim_{p_1 \parallel p_2} \Delta(z, \bar{z}) &= \frac{1}{(4\pi)^3} f^{ace} f^{bde} \{ \mathbf{T}_A^a \mathbf{T}_A^b \} \{ \mathbf{T}_B^c \mathbf{T}_B^d \} \left( -2(\zeta_5 + 2\zeta_2 \zeta_3) + \frac{1}{4} C_{10} \right) \\ &+ \frac{1}{(4\pi)^3} f^{ace} f^{bde} \{ \mathbf{T}_D^a \mathbf{T}_D^b \} \{ \mathbf{T}_C^c \mathbf{T}_C^d \} \left( -2(\zeta_5 + 2\zeta_2 \zeta_3) + \frac{1}{4} C_{10} \right) \\ &+ \frac{1}{(4\pi)^3} f^{ace} f^{bde} \{ \mathbf{T}_B^a \mathbf{T}_B^b \} \{ \mathbf{T}_C^c \mathbf{T}_C^d \} \left( 2(\zeta_5 + 2\zeta_2 \zeta_3) + \frac{1}{8} C_{10} \right) \\ &+ \frac{1}{(4\pi)^3} N_c^2 (\mathbf{T}_A \cdot \mathbf{T}_A) \left( \zeta_5 + 2\zeta_2 \zeta_3 - \frac{5}{16} C_{10} \right). \end{aligned} \quad (8.10)$$

We now wish to do the same to  $\Gamma_3^\Delta$ . We recall its composition in terms of three-line and two-line webs from eq. (3.34):

$$\Gamma_3^\Delta(p_1, p_2, p_3) = \sum_{\substack{(i,j,k) \in (1,2,3) \\ j < k}} \mathbf{T}_i^a \mathbf{T}_i^d \mathbf{T}_j^b \mathbf{T}_k^c f^{abe} f^{cde} \bar{H}_3(i, \{j, k\}) \quad (8.11)$$

In order to calculate  $\Gamma_{\text{Sp}}^\Delta$ , we must promote  $\Gamma_3$  to a four-line object, this is done by taking  $\Gamma_3^\Delta(P, p_3, p_4)$ , where the colour of  $P = p_1 + p_2$  is given by  $\mathbf{T}_A = \mathbf{T}_1 + \mathbf{T}_2$  [32, 35]. Applying colour conservation to this, we obtain sums over cyclic

permutations of  $\bar{H}_3$ , leading to

$$\begin{aligned} \Gamma_3^\Delta(P, p_3, p_4) &= \frac{1}{(4\pi)^3} f^{ace} f^{bde} \{\mathbf{T}_D^a \mathbf{T}_D^b\} \{\mathbf{T}_C^c \mathbf{T}_C^d\} \frac{3}{8} C_{l_0} \\ &- \frac{3}{16} N_c^2 (\mathbf{T}_A \cdot \mathbf{T}_A) C_{l_0} \end{aligned} \quad (8.12)$$

Inserting this into eq. (8.2), we obtain  $\Gamma_{\text{Sp}}^\Delta$ :

$$\begin{aligned} \Gamma_{\text{Sp}}^\Delta(P, p_1, p_2) &= \frac{1}{(4\pi)^3} f^{ace} f^{bde} \{\mathbf{T}_A^a \mathbf{T}_A^b\} \{\mathbf{T}_B^c \mathbf{T}_B^d\} \left( -2(\zeta_5 + 2\zeta_2\zeta_3) + \frac{1}{4} C_{l_0} \right) \\ &+ \frac{1}{(4\pi)^3} f^{ace} f^{bde} \{\mathbf{T}_D^a \mathbf{T}_D^b\} \{\mathbf{T}_C^c \mathbf{T}_C^d\} \left( -2(\zeta_5 + 2\zeta_2\zeta_3) - \frac{1}{8} C_{l_0} \right) \\ &+ \frac{1}{(4\pi)^3} f^{ace} f^{bde} \{\mathbf{T}_B^a \mathbf{T}_B^b\} \{\mathbf{T}_C^c \mathbf{T}_C^d\} \left( 2(\zeta_5 + 2\zeta_2\zeta_3) + \frac{1}{8} C_{l_0} \right) \\ &+ \frac{1}{(4\pi)^3} N_c^2 (\mathbf{T}_A \cdot \mathbf{T}_A) \left( \zeta_5 + 2\zeta_2\zeta_3 - \frac{1}{8} C_{l_0} \right). \end{aligned} \quad (8.13)$$

The colour factor above is independent of  $\mathbf{T}_3$  and  $\mathbf{T}_4$  if and only if we have  $C_{l_0} = -16(\zeta_5 + 2\zeta_2\zeta_3)$ . We have

$$C_{l_0} = -(\zeta_5 + 2\zeta_2\zeta_3)(13.2 \pm 2.9). \quad (8.14)$$

Thus our numerical result for  $C_{l_0}$  is consistent with the deduction:

$$C_{l_0} = -16(\zeta_5 + 2\zeta_2\zeta_3). \quad (8.15)$$

We then obtain

$$\begin{aligned} \Gamma_{\text{Sp}}^\Delta(P, p_1, p_2) &= -\frac{1}{(4\pi)^3} 6 f^{ace} f^{bde} \{\mathbf{T}_A^a \mathbf{T}_A^b\} \{\mathbf{T}_B^c \mathbf{T}_B^d\} (\zeta_5 + 2\zeta_2\zeta_3) \\ &+ \frac{1}{(4\pi)^3} 3 N_c^2 (\mathbf{T}_A \cdot \mathbf{T}_A) (\zeta_5 + 2\zeta_2\zeta_3) \end{aligned} \quad (8.16)$$

Through a remarkable set of cancellations we have obtained a contribution to the splitting amplitude which is wholly independent of any kinematics, and which only depends on the colour structure internal to the pair going collinear. This is a strong indication that  $C_{l_0}$  is indeed given by eq. (8.15).

As discussed in chapter 3, the inclusion of a constant term was not anticipated in [32, 33]. Above we have direct evidence of such a term appearing, so it is worthwhile considering the reasons why such a term was excluded in previous

papers. In [32], two main arguments are given for why such constants cannot occur. The first is an argument based on collinear reduction: if such a constant term does occur in three-line graphs, it is shown that a corresponding term in the same two-line graph would cancel it upon applying colour conservation. This assumes, however, that graphs which are affected by the cusp anomaly do not generate further constant terms upon collinear reduction. We can see that this is not the case by comparing the results for two-line and three-line results for the same topology obtained in chapter 5.

The second argument made in [32] is that the constant term produced by the three-line graph has colour structures which are inconsistent with the collinear splitting amplitude. This is indeed true:  $C_{l0}$  contributes a term to  $\Gamma_{\text{Sp}}^\Delta$  which depends on all four colour factors. However, we see that this contribution is precisely cancelled by a constant produced by applying the collinear limit to  $\bar{H}_4$ . Thus, the non-constant terms in  $\bar{H}_4$  produce a constant upon collinear reduction which, when combined with  $C_{l0}$  produces a term consistent with collinear splitting factorisation. Thus, we have strong evidence that not only is  $C_{l0}$  a possible contribution, it is vital in order to consistently define  $\Gamma_{\text{Sp}}^\Delta$ .

One further consistency check can be performed by noting that  $\Gamma_{\text{Sp}}$  is universal, i.e. eq. (8.1) is independent of  $n$ . In order to consistently define  $\Gamma_{\text{Sp}}$ , we must then also be able to choose  $n = 3$  in eq. (8.1), which yields.

$$\Gamma_{\text{Sp}}^\Delta(P, p_1, p_2) = \Gamma_3^\Delta(\beta_1, \beta_2, \beta_3) - \Gamma_2^\Delta(\beta_1 + \beta_2, \beta_3). \quad (8.17)$$

By definition  $\Gamma^{\text{dip.}}$  is the sum over *all* two-line webs, we therefore have  $\Gamma_2^\Delta = 0$ . Inserting eq. (3.34), we find

$$\begin{aligned} \Gamma_{\text{Sp}}^\Delta(P, p_1, p_2) &= \Gamma_3^\Delta(\beta_1, \beta_2, \beta_3) \\ &= \frac{1}{(4\pi)^3} f^{ace} f^{bde} \{\mathbf{T}_A^a \mathbf{T}_A^b\} \{\mathbf{T}_B^c \mathbf{T}_B^d\} \frac{3}{8} C_{l0} \\ &\quad - \frac{1}{(4\pi)^3} (\mathbf{T}_A \cdot \mathbf{T}_A) \frac{3}{16} N_c^2 C_{l0} \end{aligned} \quad (8.18)$$

The above result is only consistent with eq. (8.2) if we choose  $C_{l0}$  according to

eq. (8.15). Thus, we obtain a complete result for  $\Delta(z, \bar{z})$ :

$$\begin{aligned}
\Delta(z, \bar{z}) &= \frac{1}{(4\pi)^3} 16 \mathbf{T}_1^a \mathbf{T}_2^b \mathbf{T}_3^c \mathbf{T}_4^d \\
&\times \left[ f^{abe} f^{cde} \left( F \left( 1 - \frac{1}{z} \right) - 16 F \left( \frac{1}{z} \right) \right) \right. \\
&\quad - f^{ace} f^{bde} (F(z) - F(1-z)) \\
&\quad \left. + f^{ade} f^{bce} \left( F \left( \frac{1}{1-z} \right) - F \left( \frac{z}{z-1} \right) \right) \right] \\
&- \frac{1}{(4\pi)^3} 16 (\zeta_5 + 2\zeta_2 \zeta_3) \sum_{\substack{(i,j,k) \in (1,2,3,4) \\ j < k}} f^{abe} f^{cde} \{ \mathbf{T}_i^a, \mathbf{T}_i^d \} \mathbf{T}_j^b \mathbf{T}_k^c.
\end{aligned} \tag{8.19}$$



# Chapter 9

## Concluding Remarks and Outlook

Infrared singularities are ubiquitous in any gauge theory containing massless gauge bosons. Having been properly treated, they still contribute logarithmic corrections to scattering amplitudes, which may grow large and threaten perturbativity. Apart from their phenomenological relevance, IR singularities also have a number of salient features which make them interesting from a more theoretical perspective.

Firstly, soft-collinear factorisation [11, 13, 14, 27, 33, 49, 50, 69] enables us to compute IR singularities in a general gauge theory. Furthermore, IR singularities are spin-independent, and exponentiate which ultimately allows us to directly compute a soft anomalous dimension  $\Gamma^S$  diagrammatically. Furthermore, this simplified structure has led to the formulation of a concise basis of functions of which all IR-singular contributions must be composed [26].

Prior to this work, a full calculation had only been performed at two loops [27–31], with partial results existing at three loops [26, 95]. In addition to this, factorisation constraints had yielded a set of constraint equations [32, 33, 37], ultimately resulting in an ansatz for the all-order structure of soft singularities with massless external partons: the so-called dipole formula. The first corrections to this dipole formula may be found at three loops, and in this thesis we have computed them explicitly.

In chapter 3 we presented a general picture of the colour structure of soft singularities at three loops on four legs. We then proceeded to calculate all relevant diagrams to compute the non-dipole contribution to soft singularities at three loops in chapters 4 to 6. It takes the form of a remarkably simple weight-five



function of single-valued harmonic polylogarithms of conformally invariant cross-ratios. We have furthermore shown that the result is compatible with expectations from Regge limits. Moreover: collinear splitting factorisation fixes a final constant,  $C_{10}$ , and we have shown by universality of the splitting function that this choice of constant is the only one which enables a consistent definition of the splitting function.

It is desirable to determine the analytic value of  $C_{10}$ . There are two potential methods for doing this: direct analytic computation or a numerical fit to rational multiples of possible weight five constants. Work on this is ongoing, though at present no clear method exists for achieving the required numerical precision from the associated MB integrals. Meanwhile, we have shown that collinear splitting factorisation is obeyed, in accordance with expectations [32, 35] and formal proofs [69, 75].

# Appendices



# Appendix A

## Full Calculation of the Four-Line Four-Gluon Vertex Diagram

We wish to calculate the diagram  $w_{4g}$  in fig. A.1, it can be factorised into a kinematic and a colour component as follows

$$w_{4g} \equiv \mathcal{C}_{4g}(\{\mathbf{T}_i\}, \{\beta_i\}) \mathcal{F}_{(4g)}(\{\beta_i\}, \epsilon), \quad (\text{A.1})$$

$$\begin{aligned} \mathcal{C}_{4g}(\{\mathbf{T}_i\}, \{\beta_i\}) \equiv & \frac{1}{(\beta_1 \cdot \beta_3)(\beta_2 \cdot \beta_4)} \mathbf{T}_1^{a_1} \mathbf{T}_2^{a_2} \mathbf{T}_3^{a_3} \mathbf{T}_4^{a_4} \beta_1^\mu \beta_2^\nu \beta_3^\rho \beta_4^\sigma \\ & \times [f^{a_1 a_2 e} f^{a_3 a_4 e} (g_{\mu\rho} g_{\nu\sigma} - g_{\mu\sigma} g_{\nu\rho}) \\ & + f^{a_1 a_3 e} f^{a_2 a_4 e} (g_{\mu\nu} g_{\rho\sigma} - g_{\mu\sigma} g_{\nu\rho}) \\ & + f^{a_1 a_4 e} f^{a_2 a_3 e} (g_{\mu\nu} g_{\rho\sigma} - g_{\mu\rho} g_{\nu\sigma})], \end{aligned} \quad (\text{A.2})$$

$$\begin{aligned} \mathcal{F}_{(4g)}(\{\beta_i\}, \epsilon) \equiv & -ig_s^6 \left(\frac{\mu^2}{m^2}\right)^{3\epsilon} \mathcal{N}^4(\beta_1 \cdot \beta_3)(\beta_2 \cdot \beta_4) \\ & \times \int d^d z \prod_{i=1}^4 \left[ \int_0^\infty ds_i \frac{e^{-ims_i \sqrt{\beta_i^2 - i0}}}{[-(s_i \beta_i - z)^2 + i0]^{1-\epsilon}} \right]. \end{aligned} \quad (\text{A.3})$$

The colour factor can be simplified further. Evaluating the dot products and introducing the canonical variables  $z$  and  $\bar{z}$  (eqs. (1.39a) and (1.39b)), we obtain

$$\begin{aligned} \mathcal{C}_{4g}(\{\mathbf{T}_i\}, z, \bar{z}) = & \mathbf{T}_1^{a_1} \mathbf{T}_2^{a_2} \mathbf{T}_3^{a_3} \mathbf{T}_4^{a_4} [f^{a_1 a_2 e} f^{a_3 a_4 e} (1 - (1-z)(1-\bar{z})) \\ & + f^{a_1 a_3 e} f^{a_2 a_4 e} (z\bar{z} - (1-z)(1-\bar{z})) + f^{a_1 a_4 e} f^{a_2 a_3 e} (z\bar{z} - 1)]. \end{aligned} \quad (\text{A.4})$$

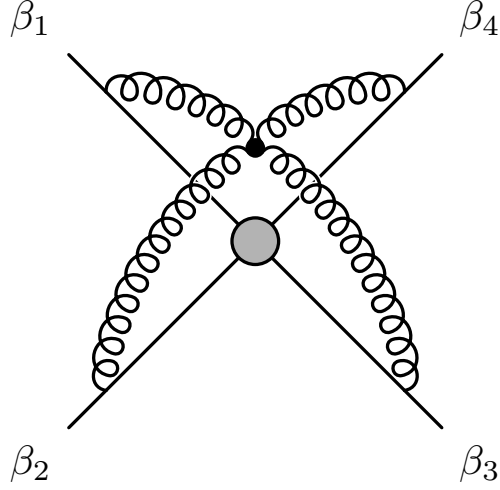


**Figure A.1** The four-gluon vertex web  $w_{4g}$

Examining the kinematic factor  $\mathcal{F}_{(4g)}$ , we may extract the leading singularity by means of the following reparametrisation

$$s_i \rightarrow \alpha y_i, \quad i = 1 \dots 3, \quad (\text{A.5})$$

$$s_4 \rightarrow \alpha \left( 1 - \sum_{i=1}^3 y_i \right), \quad (\text{A.6})$$

$$z \rightarrow \alpha z, \quad (\text{A.7})$$

yielding

$$\begin{aligned} \mathcal{F}_{(4g)}(\{\beta_i\}, \epsilon) &= -ig_s^6 \left( \frac{\mu^2}{m^2} \right)^{3\epsilon} \mathcal{N}^4 \frac{\gamma_{13}\gamma_{24}}{4} \Gamma(6\epsilon) \int d^d z \int_0^1 \left( \prod_{i=1}^4 dy_i \right) \\ &\times \delta \left( 1 - \sum_{i=1}^4 y_i \right) \prod_{i=1}^4 \left[ - \left( y_i \hat{\beta}_i - z \right)^2 + i0 \right]^{\epsilon-1}. \end{aligned} \quad (\text{A.8})$$

The remaining integrals are finite. Since we only require the leading pole we expand around  $\epsilon = 0$ . We define  $\mathcal{F}_{(4g)}(\{\beta_i\}, \epsilon) \equiv \alpha_s^3 \sum_i \epsilon^i \mathcal{F}_{(4g)}^{(3,i)}(\{\beta_i\})$ , then

$$\begin{aligned} \mathcal{F}_{(4g)}^{(3,-1)}(\{\beta_i\}) &= -i \frac{1}{(4\pi)^3} \gamma_{13}\gamma_{24} \frac{2}{3} \int_0^1 \left( \prod_{i=1}^4 dy_i \right) \delta \left( 1 - \sum_{i=1}^4 y_i \right) \\ &\times \int \frac{d^4 z}{\pi^2} \prod_{i=1}^4 \left[ - \left( y_i \hat{\beta}_i - z \right)^2 + i0 \right]^{-1}. \end{aligned} \quad (\text{A.9})$$

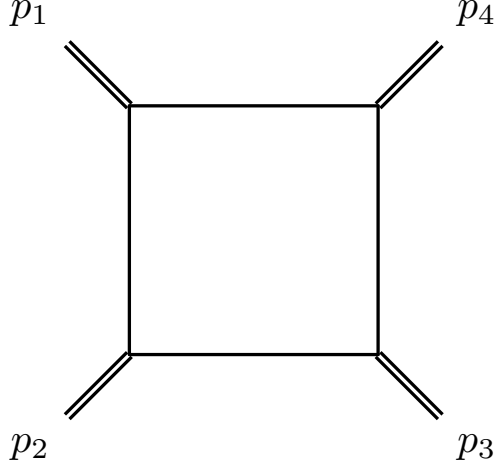


**Figure A.2** *The four mass box,  $\text{Box}(\{p_i\})$*

### Auxiliary momentum integral

The integral over the vertex  $z$  can now be recast as a dual momentum-space integral over a four mass box (fig. A.2),

$$\text{Box}(\{p_i\}, \{\nu_i\}, d) \equiv -i \int \frac{d^4 k}{\pi^2} \prod_{i=1}^4 \frac{1}{\left( (k + \sum_{j=1}^i p_j)^2 - i0 \right)^{\nu_i}}, \quad (\text{A.10})$$

where we have taken all external momenta to be incoming. Returning to  $\mathcal{F}_{(4g)}^{(3,-1)}$ , we define the auxiliary momenta

$$p_i = y_i \hat{\beta}_i - y_{i-1} \hat{\beta}_{i-1}, \quad y_0 \hat{\beta}_0 \equiv y_4 \hat{\beta}_4. \quad (\text{A.11})$$

Shifting the integrand  $z = k + y_4$  we obtain

$$\mathcal{F}_{(4g)}^{(3,-1)}(\{\beta_i\}) = \frac{1}{(4\pi)^3} \gamma_{13} \gamma_{24} \frac{2}{3} \int_0^1 \left( \prod_{i=1}^4 dy_i \right) \delta \left( 1 - \sum_{i=1}^4 y_i \right) \quad (\text{A.12})$$

$$\times \text{Box}(\{p_i\}, \{1\}, 4). \quad (\text{A.13})$$

The four-mass box has a well-known representation as a Mellin-Barnes integral [96]. Defining the mandelstam invariants  $s = (p_1 + p_2)^2$ ,  $t = (p_2 + p_3)^2$ , it is

$$\text{Box}(\{p_i\}) = -\frac{1}{st} \frac{1}{(2\pi i)^2} \int_{-i\infty}^{+i\infty} dz_1 dz_2 \left( \frac{p_2^2 p_4^2}{st} \right)^{z_1} \left( \frac{p_1^2 p_3^2}{st} \right)^{z_2} \times \Gamma^2(-z_1) \Gamma^2(-z_2) \Gamma^2(1 + z_1 + z_2). \quad (\text{A.14})$$

The overall minus sign stems from the  $i0$ -prescription we obtain for the momentum integral, which is the opposite of the one used in [96]. It is noteworthy that

the leading term in the  $\epsilon$ -expansion of the four-mass box in four dimensions is conformally invariant [96]. Hence we see the appearance of conformally invariant cross-ratios of the external momenta appear for the first time in eq. (A.14). Introducing the shorthand  $y_{ij} \equiv -(y_i \hat{\beta}_i - y_j \hat{\beta}_j)^2$ , we then obtain for  $\mathcal{F}_{(4g)}^{(3,-1)}$

$$\begin{aligned} \mathcal{F}_{(4g)}^{(3,-1)}(\{\beta_i\}) &= -\frac{1}{(4\pi)^3} \frac{2}{3} \gamma_{13} \gamma_{24} \frac{1}{(2\pi i)^2} \int_{-i\infty}^{+i\infty} dz_1 dz_2 \\ &\quad \times \Gamma^2(-z_1) \Gamma^2(-z_2) \Gamma^2(1+z_1+z_2) \\ &\quad \times \int_0^1 \left( \prod_{i=1}^4 dy_i \right) \delta \left( 1 - \sum_{i=1}^4 y_i \right) \\ &\quad \times (y_{12} y_{34})^{z_1} (y_{14} y_{23})^{z_2} (y_{13} y_{24})^{-1-z_1-z_2}. \end{aligned} \quad (\text{A.15})$$

Our aim now is to bring this integral to a form where we can perform an asymptotic expansion near the limit  $\gamma_{ij} \rightarrow -\infty$ . To this end, we wish to obtain a Mellin-Barnes representation of  $w_{4g}$  where the dependence on  $\gamma_{ij}$  is a pure power-dependence in the MB parameters. We therefore use the standard formula in eq. (1.67) to split  $y_{ij}$ :

$$\begin{aligned} y_{ij}^\lambda &= (y_i^2 + y_j^2 - y_i y_j \gamma_{ij})^\lambda \\ &= \frac{1}{\Gamma(-\lambda)} \frac{1}{2\pi i} \int_{-i\infty}^{+i\infty} dw_{ij} \Gamma(-w_{ij}) \Gamma(w_{ij} - \lambda) \frac{(-y_i y_j \gamma_{ij})^{w_{ij}}}{(y_i^2 + y_j^2)^{w_{ij} - \lambda}}. \end{aligned} \quad (\text{A.16})$$

Applying eq. (A.16) to eq. (A.15) yields

$$\begin{aligned} \mathcal{F}_{(4g)}^{(3,-1)}(\{\beta_i\}) &= -\frac{1}{(4\pi)^3} \frac{2}{3} \gamma_{13} \gamma_{24} \frac{1}{(2\pi i)^8} \int_{-i\infty}^{+i\infty} dz_1 dz_2 \\ &\quad \times \left( \prod_{i<j} \int_{-i\infty}^{i\infty} dw_{ij} \Gamma(-w_{ij}) (-\gamma_{ij})^{w_{ij}} \right) \\ &\quad \times \Gamma(w_{12} - z_1) \Gamma(w_{34} - z_1) \Gamma(w_{14} - z_2) \Gamma(w_{23} - z_2) \\ &\quad \times \Gamma(1 + w_{13} + z_1 + z_2) \Gamma(1 + w_{24} + z_1 + z_2) \\ &\quad \times \int_0^1 \left( \prod_{i=1}^4 dy_i \right) \delta \left( 1 - \sum_{i=1}^4 y_i \right) \\ &\quad \times y_1^{w_{12}+w_{13}+w_{14}} y_2^{w_{12}+w_{23}+w_{24}} y_3^{w_{13}+w_{23}+w_{34}} y_4^{w_{14}+w_{24}+w_{34}} \\ &\quad \times (y_1^2 + y_2^2)^{z_1 - w_{12}} (y_1^2 + y_3^2)^{-1 - w_{13} - z_1 - z_2} (y_1^2 + y_4^2)^{z_2 - w_{14}} \\ &\quad \times (y_2^2 + y_3^2)^{z_2 - w_{23}} (y_2^2 + y_4^2)^{-1 - w_{24} - z_1 - z_2} (y_3^2 + y_4^2)^{z_1 - w_{34}}. \end{aligned} \quad (\text{A.17})$$

We calculated the parameter integral associated with the Wilson lines in

section 4.2.2. Hence, inserting eq. (4.25) into eq. (A.17) yields

$$\begin{aligned}
\mathcal{F}_{(4g)}^{(3,-1)}(\{\beta_i\}) = & \\
& - \frac{1}{(4\pi)^3} \frac{2}{3} \gamma_{13} \gamma_{24} \frac{1}{8} \frac{1}{(2\pi i)^{11}} \left( \prod_{i=1}^5 \int_{-i\infty}^{+i\infty} dz_i \right) \\
& \times \left( \prod_{1 \leq i < j \leq 4} \int_{-i\infty}^{i\infty} dw_{ij} \Gamma(-w_{ij}) (-\gamma_{ij})^{w_{ij}} \right) \\
& \times \Gamma(-z_3) \Gamma(-z_4) \Gamma(-z_5) \Gamma(w_{14} - z_2 + z_5) \\
& \times \Gamma(w_{13} + z_1 + z_2 + z_3 + 1) \Gamma(w_{24} + z_1 + z_2 + z_4 + 1) \\
& \times \Gamma\left(\frac{w_{12}}{2} - \frac{w_{13}}{2} - \frac{w_{14}}{2} - z_1 - z_3 - z_5 - \frac{1}{2}\right) \\
& \times \Gamma\left(\frac{w_{12}}{2} + \frac{w_{13}}{2} + \frac{w_{14}}{2} + z_3 + z_5 + \frac{1}{2}\right) \\
& \times \Gamma\left(-\frac{w_{14}}{2} - \frac{w_{24}}{2} + \frac{w_{34}}{2} - z_1 - z_4 - z_5 - \frac{1}{2}\right) \\
& \times \Gamma\left(\frac{w_{14}}{2} + \frac{w_{24}}{2} + \frac{w_{34}}{2} + z_4 + z_5 + \frac{1}{2}\right) \\
& \times \Gamma\left(-\frac{w_{13}}{2} - \frac{w_{14}}{2} + \frac{w_{23}}{2} - \frac{w_{24}}{2} - z_1 - z_2 - z_3 - z_4 - z_5 - 1\right) \\
& \times \Gamma\left(\frac{w_{13}}{2} + \frac{w_{14}}{2} + \frac{w_{23}}{2} + \frac{w_{24}}{2} + z_1 + z_3 + z_4 + z_5 + 1\right)
\end{aligned} \tag{A.18}$$

## Asymptotics and MB integration

At this point it is possible to perform an asymptotic expansion in the limit  $\gamma_{ij} \rightarrow -\infty$ . Doing so and subsequently applying Barnes' lemma yields an expression of the following schematic form

$$\begin{aligned}
\mathcal{F}_{(4g)}^{(3,-1)}(\{\beta_i\}) = & - \frac{1}{(4\pi)^3} \frac{2}{3} \frac{1}{(2\pi i)^2} \int_{-i\infty}^{+i\infty} dz_1 dz_2 (\rho_{1234})^{z_1} (\rho_{1432})^{z_2} \\
& \times \Gamma^2(-z_1) \Gamma^2(-z_2) \Gamma^2(1 + z_1 + z_2) \mathcal{T}(\{z_i\}, \{\log(\gamma_{ij})\}).
\end{aligned} \tag{A.19}$$

The pole structure of the above MB integral is similar to that of the four-mass box, however, the order and residue of the poles is altered by the presence of  $\mathcal{T}$ . This is to be expected, since the four-mass box is of uniform transcendental weight two, and  $\mathcal{F}_{(4g)}^{(3,-1)}$  should have uniform transcendental weight five.  $\mathcal{T}$  serves the role of raising the transcendental weight of the MB integral. One clear indication of this is its dependence directly on  $\log(\gamma_{ij})$ , however its dependence on  $\{z_i\}$  also alters the weight of the integral. Specifically, we may assign a weight  $n + 1$  to



$\psi^{(n)}$ ,  $\mathcal{T}$  then takes the form

$$\mathcal{T}(\{z_i\}, \{\log(\gamma_{ij})\}) = \sum_i C_i \prod_a^{\text{Weight 3}} [a \in \{\psi^{(n)}(-z_1), \psi^{(n)}(-z_2), \psi^{(n)}(1+z_1+z_2), \gamma_E, \zeta_n, \log(\gamma_{ij})\}], \quad (\text{A.20})$$

where  $C_i$  are rational numbers. The assignment of weight to  $\psi^{(n)}$  is unconventional and specific to our integral. In general, MB integrals need not be transcendental functions, and certainly not functions of uniform weight. However, the presence of polygamma functions raises the maximal weight that an MB integral can attain, in accordance with the fact that an  $\epsilon$ -expansion under an MB integral results in polygamma functions of increasing weight, order by order in  $\epsilon$ .

**Final result for  $\mathcal{F}_{(4g)}^{(3,-1)}$**

Having obtained a much simpler MB representation, we now convert eq. (A.19) to parameter integrals utilising the techniques outlined in section 1.3.2. These parameter integrals can then be performed in terms of Goncharov polylogarithms using the methods outlined in section 1.4. The full result is rather lengthy, but has the generic form

$$\mathcal{F}_{(4g)}^{(3,-1)}(\{\beta_{ij}\}) = - \left( \frac{1}{4\pi} \right)^3 \frac{2}{3} \frac{1}{z - \bar{z}} f_1(z, \bar{z}, \gamma_{ij}). \quad (\text{A.21})$$

Where  $f_1$  is a pure weight five function. The full result is rather lengthy, so we have appended it electronically to this thesis.

## Appendix B

# Full Calculation of the Four-Line Double Three-Gluon Vertex Diagram

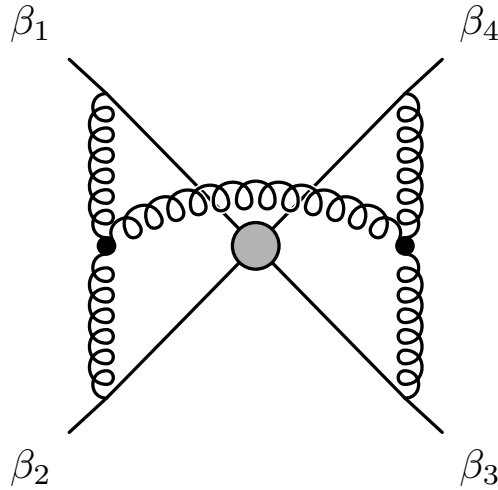


Figure B.1  $w_{(12)(34)}$

We now consider the diagram  $w_{(12)(34)}$ , depicted in fig. B.1. Our Feynman rules in

section 1.2.7 prescribe

$$\begin{aligned}
w_{(12)(34)}(\{\gamma_{ij}\}, \epsilon) &\equiv \mu^{6\epsilon} g_s^6 \mathcal{N}^5 \int d^d z d^d w \left( \prod_{j=1}^4 \mathbf{T}_j^{a_j} \int_0^\infty \beta_j^{\sigma_j} ds_j e^{-i(m-i0)s_j} \right) \\
&\times f^{a_1 a_2 e} \Gamma_{\sigma_1 \sigma_2 \tau} (\partial_{s_1 \beta_1 - z}, \partial_{s_2 \beta_2 - z}, \partial_{w-z}) \\
&\times f^{a_3 a_4 e} \Gamma_{\sigma_3 \sigma_4}{}^\tau (\partial_{s_3 \beta_3 - w}, \partial_{s_4 \beta_4 - w}, \partial_{z-w}) \\
&\times (-(s_1 \beta_1 - z)^2 + i0)^{\epsilon-1} (-(s_2 \beta_2 - z)^2 + i0)^{\epsilon-1} \\
&\times (-(s_3 \beta_3 - w)^2 + i0)^{\epsilon-1} (-(s_4 \beta_4 - w)^2 + i0)^{\epsilon-1} \\
&\times (-(z-w)^2 + i0)^{\epsilon-1}.
\end{aligned} \tag{B.1}$$

We will proceed in much the same way as we did in the previous chapter with  $w_{4g}$ , however there are some added complications. Notably, the derivatives associated with the three-gluon vertices will require some attention, and we will have to derive an MB representation for the two loop integrals over the vertices  $w$  and  $z$ .

As with  $w_{4g}$ , we define separate colour and kinematic factors

$$\mathcal{C}_{(12)(34)} \equiv f^{a_1 a_2 e} f^{a_3 a_4 e} \mathbf{T}_1^{a_1} \mathbf{T}_2^{a_2} \mathbf{T}_3^{a_3} \mathbf{T}_4^{a_4}, \tag{B.2}$$

$$\begin{aligned}
\mathcal{F}_{(12)(34)}(\{\gamma_{ij}\}, \epsilon) &\equiv \mu^{6\epsilon} g_s^6 \mathcal{N}^5 \int d^d z d^d w \left( \prod_{j=1}^4 \int_0^\infty \beta_j^{\sigma_j} ds_j e^{-i(m-i0)s_j} \right) \\
&\times \Gamma_{\sigma_1 \sigma_2 \tau} (\partial_{s_1 \beta_1 - z}, \partial_{s_2 \beta_2 - z}, \partial_{w-z}) \\
&\times \Gamma_{\sigma_3 \sigma_4}{}^\tau (\partial_{s_3 \beta_3 - w}, \partial_{s_4 \beta_4 - w}, \partial_{z-w}) \\
&\times (-(s_1 \beta_1 - z)^2 + i0)^{\epsilon-1} (-(s_2 \beta_2 - z)^2 + i0)^{\epsilon-1} \\
&\times (-(s_3 \beta_3 - w)^2 + i0)^{\epsilon-1} (-(s_4 \beta_4 - w)^2 + i0)^{\epsilon-1} \\
&\times (-(z-w)^2 + i0)^{\epsilon-1}.
\end{aligned} \tag{B.3}$$

We now proceed as we did previously to extract the UV pole by rescaling all integration variables according to eqs. (A.5) to (A.7). Subsequently, we wish to perform the loop integrals. We therefore need to extract the derivatives associated with the vertices. To do this, we utilise momentum conservation at each vertex to rewrite the derivatives with respect to  $(z-w)$  in terms of external parameters, yielding

$$\begin{aligned}
\mathcal{F}_{(12)(34)}(\{\gamma_{ij}\}, \epsilon) &= \left( \frac{\mu}{m} \right)^{6\epsilon} g_s^6 \mathcal{N}^5 \Gamma(6\epsilon) \left( \prod_{j=1}^4 \int_0^\infty \beta_j^{\sigma_j} dy_j \right) \delta \left( 1 - \sum_{i=1}^4 y_i \right) \\
&\times \Gamma_{\sigma_1 \sigma_2 \tau} (\partial_{y_1 \beta_1}, \partial_{y_2 \beta_2}, -\partial_{y_1 \beta_1} - \partial_{y_2 \beta_2}) \\
&\times \Gamma_{\sigma_3 \sigma_4}{}^\tau (\partial_{y_3 \beta_3}, \partial_{y_4 \beta_4}, -\partial_{y_3 \beta_3} - \partial_{y_4 \beta_4}) \\
&\times \int d^d z d^d w (-(y_1 \beta_1 - z)^2 + i0)^{\epsilon-1} (-(y_2 \beta_2 - z)^2 + i0)^{\epsilon-1} \\
&\times (-(y_3 \beta_3 - w)^2 + i0)^{\epsilon-1} (-(y_4 \beta_4 - w)^2 + i0)^{\epsilon-1} \\
&\times (-(z-w)^2 + i0)^{\epsilon-1}.
\end{aligned} \tag{B.4}$$

## Auxiliary momentum integral

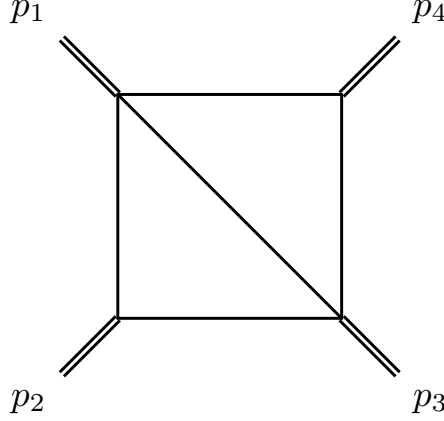


**Figure B.2** The slashed four mass box  $S(\{p_i^2\}, s, t)$

As previously, we may now relate the loop integral to an auxiliary momentum space integral. Since the remaining integrals are once again finite, we limit ourselves to the leading pole

$$\begin{aligned}
\mathcal{F}_{(12)(34)}^{(3,-1)}(\{\gamma_{ij}\}) &= \frac{1}{(4\pi)^3} \frac{2}{3} \left( \prod_{j=1}^4 \int_0^\infty \beta_j^{\sigma_j} dy_j \right) \delta \left( 1 - \sum_{i=1}^4 y_i \right) \\
&\times \Gamma_{\sigma_1 \sigma_2 \tau} (\partial_{y_1 \beta_1}, \partial_{y_2 \beta_2}, -\partial_{y_1 \beta_1} - \partial_{y_2 \beta_2}) \\
&\times \Gamma_{\sigma_3 \sigma_4}{}^\tau (\partial_{y_3 \beta_3}, \partial_{y_4 \beta_4}, -\partial_{y_3 \beta_3} - \partial_{y_4 \beta_4}) \\
&\times \frac{1}{\pi^4} \int d^4 z d^4 w (-y_1 \beta_1 - z)^{-1} (-y_2 \beta_2 - z)^{-1} \\
&\times (-y_3 \beta_3 - w)^{-1} (-y_4 \beta_4 - w)^{-1} (-z - w)^{-1}.
\end{aligned} \tag{B.5}$$

The two loop integrals have a slashed box (fig. B.2) as their dual diagram, we define

$$\begin{aligned}
S(\{p_i\}) &\equiv \frac{1}{\pi^4} \int \frac{d^4 k_1}{(-p_1 + k_1)^2 + i0} \frac{d^4 k_2}{(-p_1 + p_2 + k_1)^2 + i0} \\
&\times \int \frac{d^4 k_2}{(-(k_1 - k_2)^2 + i0) (-(k_2)^2 + i0) (-(p_1 + p_2 + p_3 + k_2)^2 + i0)}.
\end{aligned} \tag{B.6}$$

Identifying  $k_1 = z$ ,  $k_2 = w$ , and utilising the auxiliary momenta of eq. (A.11) we find

$$\begin{aligned}
\mathcal{F}_{(12)(34)}^{(3,-1)} &= \frac{1}{(4\pi)^3} \frac{2}{3} \left( \prod_{j=1}^4 \int_0^\infty \beta_j^{\sigma_j} dy_j \right) \delta \left( 1 - \sum_{i=1}^4 y_i \right) \\
&\times \Gamma_{\sigma_1 \sigma_2 \tau} (\partial_{y_1 \beta_1}, \partial_{y_2 \beta_2}, -\partial_{y_1 \beta_1} - \partial_{y_2 \beta_2}) \\
&\times \Gamma_{\sigma_3 \sigma_4}{}^\tau (\partial_{y_3 \beta_3}, \partial_{y_4 \beta_4}, -\partial_{y_3 \beta_3} - \partial_{y_4 \beta_4}) S(\{p_i(y_j \beta_j)\}).
\end{aligned} \tag{B.7}$$

In order to derive a Mellin-Barnes representation of  $S$ , we utilise the MB representation of the general one-loop  $N$ -point function  $J^{(N)}$  [99].

$$\begin{aligned}
J^{(N)}(\{\nu_j\}|\{q_j\}) &\equiv \int \frac{d^d r}{\prod_{j=1}^N [(q_j + r)^2 + i0]^{\nu_j}} \\
&= \pi^{\frac{d}{2}} i^{1-d} (k_{1N}^2)^{\frac{d}{2} - \sum \nu_i} \frac{1}{\Gamma(d - \sum \nu_i) \prod \Gamma(\nu_i)} \\
&\times \frac{1}{(2\pi i)^{L-1}} \int_{-i\infty}^{+i\infty} \cdots \int_{-i\infty}^{+i\infty} \prod_{\substack{j<l \\ (j,l) \neq (1,N)}} \left\{ ds_{jl} \left( \frac{k_{jl}^2}{k_{1N}^2} \right)^{s_{jl}} \Gamma(-s_{jl}) \right\} \\
&\times \Gamma \left( \sum \nu_i - \frac{d}{2} + \sum_{\substack{j<l \\ (j,l) \neq (1,N)}} s_{jl} \right) \Gamma \left( \frac{d}{2} - \sum \nu_i + \nu_N - \sum_{\substack{j<l \\ l \neq N}} s_{jl} \right) \\
&\times \Gamma \left( \frac{d}{2} - \sum \nu_i + \nu_1 - \sum_{\substack{j<l \\ j \neq 1}} s_{jl} \right) \prod_{i=2}^{N-1} \Gamma \left( \nu_i + \sum_{j<i} s_{ji} + \sum_{l>i} s_{il} \right),
\end{aligned} \tag{B.8}$$

with  $L = N(N-1)/2$ , and  $k_{ij} = q_i - q_j$ . Examining  $S$ , we see that the integral over  $k_2$  is a three-point function with  $\{q_i\} = \{0, -k_1, -p_4\}$ . We extract the minus signs from the propagators, this yields

$$\begin{aligned}
S(\{p_i\}) &= -\frac{1}{\pi^4} \int \frac{d^4 k_1}{((p_1 + k_1)^2 - i0)((p_1 + p_2 + k_1)^2 - i0)} \\
&\times J(\{1, 1, 1\}, \{0, -k_1, -p_4\}).
\end{aligned} \tag{B.9}$$

Inserting the identity in eq. (B.8) and accounting again for the difference in the  $i0$ -prescription between  $J$  and  $S$ , we observe that the integral over  $k_1$  is a four-point function. We parametrise it using the same formula, choosing  $p_1$  to carry the dimension of the integral over  $k_1$

$$\begin{aligned}
S(\{p_i\}) &= \frac{1}{(2\pi i)^7} \int_{-i\infty}^{+i\infty} ds_{12} ds_{23} dt_{12} dt_{13} dt_{23} dt_{24} dt_{34} \\
&\times \frac{\Gamma(-s_{12})\Gamma(-s_{23})\Gamma(1 + s_{12} + s_{23})^2}{\Gamma(2 + s_{12} + s_{23})} (p_4^2)^{-1} \left( \frac{p_2^2}{p_1^2} \right)^{t_{12}} \\
&\times \left( \frac{(p_2 + p_3)^2}{p_1^2} \right)^{t_{13}} \left( \frac{p_3^2}{p_1^2} \right)^{t_{23}} \left( \frac{(p_1 + p_2)^2}{p_1^2} \right)^{t_{24}} \left( \frac{p_4^2}{p_1^2} \right)^{t_{34} - s_{12} - s_{23}} \\
&\times \Gamma(-t_{12})\Gamma(-t_{13})\Gamma(-t_{23})\Gamma(-t_{24})\Gamma(-t_{34}) \\
&\times \Gamma(t_{12} + t_{13} + t_{23} + t_{24} + t_{34} - s_{12} - s_{23}) \\
&\times \Gamma(1 + t_{12} + t_{23} + t_{24})\Gamma(-s_{23} + t_{13} + t_{23} + t_{34}) \\
&\times \Gamma(1 + s_{12} + s_{23} - t_{23} - t_{24} - t_{34})\Gamma(s_{23} - t_{12} - t_{13} - t_{23}).
\end{aligned} \tag{B.10}$$

Applying Barnes' lemma causes the integration over  $s_{ij}$  to vanish and we obtain after some simplification

$$\begin{aligned}
S(\{p_i\}) &= (p_1^2)^{-1} \frac{1}{(2\pi i)^5} \int_{-i\infty}^{+i\infty} dt_{12} dt_{13} dt_{23} dt_{24} dt_{34} \\
&\times \left(\frac{p_2^2}{p_1^2}\right)^{t_{12}} \left(\frac{(p_2+p_3)^2}{p_1^2}\right)^{t_{13}} \left(\frac{p_3^2}{p_1^2}\right)^{t_{23}} \left(\frac{(p_1+p_2)^2}{p_1^2}\right)^{t_{24}} \left(\frac{p_4^2}{p_1^2}\right)^{t_{34}} \\
&\times \Gamma(-t_{12})\Gamma(-t_{13})\Gamma(-t_{23})\Gamma(-t_{24})\Gamma(-t_{34}) \\
&\times \Gamma(-t_{12}-t_{13}-t_{23})\Gamma(-t_{23}-t_{24}-t_{34})\Gamma(1+t_{12}+t_{23}+t_{24}) \\
&\times \Gamma(1+t_{13}+t_{23}+t_{34})\Gamma(1+t_{12}+t_{13}+t_{23}+t_{24}+t_{34}) \\
&\times \frac{\Gamma(t_{34}-t_{12})}{\Gamma(1+t_{34}-t_{12})} (\psi(-t_{12}) - \psi(-t_{34})).
\end{aligned} \tag{B.11}$$

Returning to eq. (B.7), we have

$$\begin{aligned}
\mathcal{F}_{(12)(34)}^{(3,-1)} &= \frac{1}{(4\pi)^3} \frac{2}{3} \left( \prod_{j=1}^4 \int_0^\infty \beta_j^{\sigma_j} dy_j \right) \delta \left( 1 - \sum_{i=1}^4 y_i \right) \\
&\times \Gamma_{\sigma_1\sigma_2\tau} (\partial_{y_1\beta_1}, \partial_{y_2\beta_2}, -\partial_{y_1\beta_1} - \partial_{y_2\beta_2}) \\
&\times \Gamma_{\sigma_3\sigma_4}{}^\tau (\partial_{y_3\beta_3}, \partial_{y_4\beta_4}, -\partial_{y_3\beta_3} - \partial_{y_4\beta_4}) \\
&\times \left( \prod_{\substack{i<j \\ (i,j)\neq(1,4)}} \frac{1}{(2\pi i)} \int_{-i\infty}^{i\infty} dt_{ij} \left(\frac{y_{ij}}{y_{14}}\right)^{t_{ij}} \Gamma(-t_{ij}) \right) \\
&\times \Gamma(-t_{12}-t_{13}-t_{23})\Gamma(-t_{23}-t_{24}-t_{34})\Gamma(1+t_{12}+t_{23}+t_{24}) \\
&\times \Gamma(1+t_{13}+t_{23}+t_{34})\Gamma(1+t_{12}+t_{13}+t_{23}+t_{24}+t_{34}) \\
&\times \frac{\Gamma(t_{34}-t_{12})}{\Gamma(1+t_{34}-t_{12})} (\psi(-t_{12}) - \psi(-t_{34})).
\end{aligned} \tag{B.12}$$

## Differentiating

The structure of the integral is now similar to eq. (A.17). Indeed, if we apply the derivatives, the remaining integrals over the Wilson lines are of the form of eq. (4.20). We apply the derivatives by observing that every term  $(y_{ij})^{t_{ij}}$  comes with a corresponding  $\Gamma(-t_{ij})$ , yielding

$$\partial_{y_i\beta_i}^\mu y_{ij}^{t_{ij}} \Gamma(-t_{ij}) = 2(y_i\beta_{i\mu} - y_j\beta_{j\mu}) y_{ij}^{t_{ij}-1} \Gamma(1-t_{ij}). \tag{B.13}$$

We note that these differentiations have the effect of shifting the poles of a gamma function away from the origin. Thus any contour chosen to satisfy the initial requirements imposed by the slashed box integral is still valid after differentiation. Indeed, the differentiation somewhat relaxes the requirement on the real part of

the contour, which will be required in order to perform the integration over the Wilson lines. Our integral is now of the schematic form

$$\begin{aligned}
\mathcal{F}_{(12)(34)}^{(3,-1)} &= \frac{1}{(4\pi)^3} \frac{2}{3} \left( \prod_{j=1}^4 \int_0^\infty \beta_j^{\sigma_j} dy_j \right) \delta \left( 1 - \sum_{i=1}^4 y_i \right) \\
&\times \left( \prod_{\substack{i < j \\ (i,j) \neq (1,4)}} \frac{1}{(2\pi i)} \int_{-i\infty}^{i\infty} dt_{ij} \left( \frac{y_{ij}}{y_{14}} \right)^{t_{ij}} \Gamma(-t_{ij}) \right) \\
&\times \Gamma(-t_{12} - t_{13} - t_{23}) \Gamma(-t_{23} - t_{24} - t_{34}) \\
&\times \Gamma(1 + t_{12} + t_{23} + t_{24}) \Gamma(1 + t_{13} + t_{23} + t_{34}) \\
&\times \Gamma(1 + t_{12} + t_{13} + t_{23} + t_{24} + t_{34}) \\
&\times \frac{\Gamma(t_{34} - t_{12})}{\Gamma(1 + t_{34} - t_{12})} (\psi(-t_{12}) - \psi(-t_{34})) \\
&\times \sum_i C_i P_i(\{\gamma_{ij}\}) \left( \prod_{\sigma_i} \frac{\Gamma(1 - t_{\sigma_i})}{\Gamma(-t_{\sigma_i})} \right), \tag{B.14}
\end{aligned}$$

where  $C_i$  are rational coefficients,  $P_i$  are polynomials of  $\gamma_{ij}$  and  $\sigma_i$  index the terms  $t_{kl}$  which were produced by the differentiations.

### Final Result for $w_{(12)(34)}$

The calculation now proceeds in entirely the same way as it did in Appendix A. Following asymptotic expansion, we obtain a large set of one-, two- and threefold MB integrals. Unlike what we had in the case of  $w_{4g}$ , these integrals do not appear to have a single form, and many of them are of mixed transcendental weight. Indeed, due to the differentiations associated with the vertices, we see appearances of weight six terms upon parametrising single MB integrals. In accordance with the requirement that  $w_{(12)(34)}$  can be at most weight five, we observe that all these terms cancel upon adding up all contributions to  $w_{(12)(34)}$ . Furthermore, we also observe the cancellation of all terms with weight strictly less than five, in accordance with expectations that the soft anomalous dimension has uniform weight.

The final result is of the form

$$\mathcal{F}_{(12)(34)}^{(3,-1)} \equiv \left( \frac{1}{4\pi} \right)^3 \frac{2}{3} \left( f_0(z, \bar{z}, \gamma_{ij}) + \frac{1 - (1-z)(1-\bar{z})}{z - \bar{z}} f_1(z, \bar{z}, \gamma_{ij}) \right), \tag{B.15}$$

where we note that  $f_1$  here is the same  $f_1$  as appears in eq. (A.21).

# Appendix C

## Full Calculation of the Three-Line Four-Gluon Vertex Diagram

In order to compute the diagram in fig. C.1 we proceed in much the same way as we did for the four-line equivalent. We have

$$w_{(4g),3}(\alpha_{12}, \alpha_{13}, \alpha_{23}, \epsilon) = \mathcal{C}_{(4g),3} \mathcal{F}_{(4g),3}(\alpha_{12}, \alpha_{13}, \alpha_{23}, \epsilon), \quad (\text{C.1})$$

$$\mathcal{C}_{(4g),3} \equiv \mathbf{T}_1^a \mathbf{T}_1^d \mathbf{T}_2^b \mathbf{T}_3^c (f^{abe} f^{cde} + f^{ace} f^{bde}), \quad (\text{C.2})$$

$$\begin{aligned} \mathcal{F}_{(4g),3}(\alpha_{12}, \alpha_{13}, \alpha_{23}, \epsilon) &\equiv -ig_s^6 \mu^{6\epsilon} \mathcal{N}^4 \left( \frac{\gamma_{12}\gamma_{13}}{4} + \frac{\gamma_{23}}{2} \right) \int d^d z \\ &\times \prod_{i=1}^4 \left[ \int_0^\infty ds_i \frac{e^{-ims_i \sqrt{|\beta_i|^2 - i0}}}{(-(s_i \beta_i - z)^2)^{1-\epsilon}} \right] \theta(s_4 < s_1). \end{aligned} \quad (\text{C.3})$$

We have taken the definition of  $\beta_1 = \beta_4$  as implicit in the above for brevity. We proceed as we did in the four-line case by first extracting the singular term through the rescaling  $s_i = \alpha y_i / |\beta_i|^2$ ,  $\sum y_i = 1$  and  $z \rightarrow \alpha z$

$$\begin{aligned} \mathcal{F}_{(4g),3}(\alpha_{12}, \alpha_{13}, \alpha_{23}, \epsilon) &\equiv -ig_s^6 \left( \frac{\mu^2}{m^2} \right)^{3\epsilon} \mathcal{N}^4 \Gamma(6\epsilon) \left( \frac{\gamma_{12}\gamma_{13}}{4} + \frac{\gamma_{23}}{2} \right) \\ &\times \int d^d z \prod_{i=1}^4 \left[ \int_0^\infty dy_i \frac{1}{(-(y_i \beta_i - z)^2)^{1-\epsilon}} \right] \\ &\times \theta(y_4 < y_1) \delta \left( 1 - \sum_{i=1}^4 y_i \right). \end{aligned} \quad (\text{C.4})$$



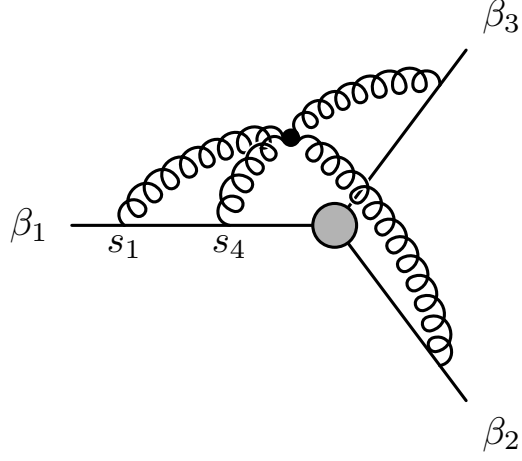


**Figure C.1** *Three-line four-gluon vertex  $w_{(4g),3}(\alpha_{12}, \alpha_{13}, \alpha_{23})$*

Next we proceed by inserting the MB representation of the box integral after expanding in  $\epsilon$ . Introducing the shorthand  $y_{ij} \equiv (y_i\beta_i - y_j\beta_j)^2$ , the result is

$$\begin{aligned}
\mathcal{F}_{(4g),3}^{(-1,3)}(\alpha_{12}, \alpha_{13}, \alpha_{23}, \epsilon) &= -\frac{1}{(4\pi)^3} \frac{2}{3} (\gamma_{12}\gamma_{13} + 2\gamma_{23}) \\
&\times \frac{1}{(2\pi i)^2} \int dz_1 dz_2 \left( \prod_{i=1}^4 \int dy_i \right) \\
&\times \Gamma^2(-z_1)\Gamma^2(-z_2)\Gamma^2(1+z_1+z_2) \\
&\times (y_{12}y_{34})^{z_1} (y_{14}y_{23})^{z_2} (y_{13}y_{24})^{-1-z_1-z_2} \\
&\times \delta\left(1 - \sum_{i=1}^4 y_i\right) \theta(y_4 < y_1).
\end{aligned} \tag{C.5}$$

Note that, since  $\beta_1 = \beta_4$ ,  $y_{14} = -(y_1 - y_4)^2$ . We split the other propagators using the standard MB parametrisation formula to isolate the term proportional to  $\gamma_{ij}$ :

$$\begin{aligned}
\mathcal{F}_{(4g),3}^{(-1,3)}(\alpha_{12}, \alpha_{13}, \alpha_{23}) &= -\frac{1}{(4\pi)^3} \frac{2}{3} (\gamma_{12}\gamma_{13} + 2\gamma_{23}) \frac{1}{(2\pi i)^7} \int dz_1 dz_2 \\
&\times \left( \prod_{\substack{1 \leq i < j \leq 4 \\ (i,j) \neq (1,4)}} \int dw_{ij} \Gamma(-w_{ij}) \right) \\
&\times \Gamma(-z_2) \Gamma(w_{12} - z_1) \Gamma(w_{34} - z_1) \Gamma(w_{23} - z_2) \\
&\times \Gamma(w_{13} + z_1 + z_2 - 1) \Gamma(w_{24} + z_1 + z_2 - 1) \\
&\times (-\gamma_{12})^{w_{12}+w_{24}} (-\gamma_{13})^{w_{13}+w_{34}} (-\gamma_{23})^{w_{23}} \\
&\times \left( \prod_{i=1}^4 \int dy_i \right) y_1^{w_{12}+w_{13}} y_2^{w_{12}+w_{23}+w_{24}} y_3^{w_{13}+w_{23}+w_{34}} \\
&\times y_4^{w_{24}+w_{34}} (y_1^2 + y_2^2)^{z_1-w_{12}} (y_3^2 + y_4^2)^{z_1-w_{34}} \\
&\times ((y_1 - y_4)^2)^{z_2} (y_2^2 + y_3^2)^{z_2-w_{23}} \\
&\times (y_1^2 + y_3^2)^{-w_{13}-z_1-z_2-1} (y_2^2 + y_4^2)^{-w_{24}-z_1-z_2-1} \\
&\times \delta \left( 1 - \sum_{i=1}^4 y_i \right) \theta(y_4 < y_1).
\end{aligned} \tag{C.6}$$

We now re-parametrise  $y_i$  to resolve the delta functions

$$\begin{pmatrix} y_1 \\ y_2 \\ y_3 \\ y_4 \end{pmatrix} = \begin{pmatrix} x(1-y) \\ (1-x)z \\ (1-x)(1-z) \\ xy \end{pmatrix} \tag{C.7}$$

The procedure from here on is similar to what we did in the four-line case. After switching to semi-infinite parameters of the form  $a = x/(1-x)$ , and rescaling

$a \rightarrow ac(1+b)/(1+c)$ , we obtain

$$\begin{aligned}
\mathcal{F}_{(4g),3}^{(-1,3)}(\alpha_{12}, \alpha_{13}, \alpha_{23}) &= -\frac{1}{(4\pi)^3} \frac{2}{3} (\gamma_{12}\gamma_{13} + 2\gamma_{23}) \frac{1}{(2\pi i)^7} \int dz_1 dz_2 \\
&\times \left( \prod_{\substack{1 \leq i < j \leq 4 \\ (i,j) \neq (1,4)}} \int dw_{ij} \Gamma(-w_{ij}) \right) \Gamma(-z_2) \Gamma(w_{12} - z_1) \\
&\times (-\gamma_{12})^{w_{12}+w_{24}} (-\gamma_{13})^{w_{13}+w_{34}} (-\gamma_{23})^{w_{23}} \\
&\times \Gamma(w_{34} - z_1) \Gamma(w_{23} - z_2) \Gamma(w_{13} + z_1 + z_2 - 1) \quad (C.8) \\
&\times \Gamma(w_{24} + z_1 + z_2 - 1) \int_0^\infty da \int_0^\infty db \int_0^\infty dc \\
&\times a^{w_{12}+w_{13}+w_{24}+w_{34}+2z_1+1} (1+a^2)^{z_2-w_{12}} \\
&\times b^{w_{24}+w_{34}} (1-b)^{2z_1} (a^2 b^2 + 1)^{-w_{24}-z_1-z_2-1} \\
&\times c^{w_{13}+w_{23}+w_{34}} (1+c^2)^{z_1-w_{23}} (a^2 b^2 c^2 + 1)^{z_2-w_{34}} \\
&\times (a^2 c^2 + 1)^{-w_{13}-z_1-z_2-1} \theta(b < 1)
\end{aligned}$$

Using the MB identity to split the brackets containing more than one integration variable, and performing the integrations, we obtain our final MB representation

$$\begin{aligned}
\mathcal{F}_{(4g),3}^{(-1,3)}(\alpha_{12}, \alpha_{13}, \alpha_{23}) &= -\frac{1}{(4\pi)^3} \frac{1}{6} (\gamma_{12}\gamma_{13} + 2\gamma_{23}) \frac{1}{(2\pi i)^{10}} \left( \prod_{i=1}^5 \int dz_i \right) \\
&\times \left( \prod_{\substack{1 \leq i < j \leq 4 \\ (i,j) \neq (1,4)}} \int dw_{ij} \Gamma(-w_{ij}) \right) (-\gamma_{12})^{w_{12}+w_{24}} (-\gamma_{13})^{w_{13}+w_{34}} (-\gamma_{23})^{w_{23}} \\
&\times \frac{\Gamma(-z_2) \Gamma(-z_3) \Gamma(-z_4) \Gamma(-z_5) \Gamma(1+2z_2)}{\Gamma(w_{24} + w_{34} + 2z_2 + 2z_3 + 2z_5 + 2)} \Gamma(w_{34} - z_1 + z_5) \\
&\times \Gamma(w_{24} + z_1 + z_2 + z_3 + 1) \Gamma(w_{13} + z_1 + z_2 + z_4 + 1) \quad (C.9) \\
&\times \Gamma\left(\frac{w_{23} - w_{13} - w_{34} - 1}{2} - z_2 - z_4 - z_5\right) \\
&\times \Gamma\left(\frac{w_{12} - w_{13} - w_{24} - w_{34}}{2} - z_1 - z_2 - z_3 - z_4 - z_5 - 1\right) \\
&\times \Gamma(w_{24} + w_{34} + 2z_3 + 2z_5 + 1) \Gamma\left(\frac{w_{13} + w_{23} + w_{34} + 1}{2} + z_4 + z_5\right) \\
&\times \Gamma\left(\frac{w_{12} + w_{13} + w_{24} + w_{34}}{2} + z_2 + z_3 + z_4 + z_5 + 1\right)
\end{aligned}$$

Upon performing the asymptotic expansion around  $\gamma_{ij} \rightarrow \infty$ , we obtain some unusual MB integrals of the form

$$\begin{aligned}
I \equiv & \int dz_1 dz_2 dz_3 \Gamma(-z_1) \Gamma(z_1 + 2) \Gamma(-z_1 - z_2 - 1) \Gamma(-z_2) \\
& \times \Gamma(-z_3)^2 \Gamma(z_2 + z_3) \Gamma(z_1 + z_2 + z_3 + 1) \\
& \times \frac{\Gamma(-z_1 - 2z_2 - 2z_3 - 1) \Gamma(2z_3 + 1)}{\Gamma(-z_1 - 2z_2)}
\end{aligned} \tag{C.10}$$

The main challenge in computing these integrals lies in handling the gamma function with multiples of  $z_i$ , we solve this by combining them into a single Beta function, which we subsequently insert the integral representation of and proceed as usual. This yields a parameter integral which is quadratic in some integration variables, but is ultimately manageable. We find

$$\begin{aligned}
\mathcal{F}_{(4g),3}^{(3,-1)} = & -\frac{1}{(4\pi)^3} \frac{1}{3} \left( -\frac{1}{3} \log^4(\alpha_{12}) - \frac{1}{3} \log^4(\alpha_{13}) - \log^2(\alpha_{12}) \log(\alpha_{13}) \log(\alpha_{23}) \right. \\
& - \log(\alpha_{12}) \log^2(\alpha_{13}) \log(\alpha_{23}) + 4 \log(\alpha_{12}) \log(\alpha_{13}) \log(\alpha_{23}) \\
& + 2 \log^2(\alpha_{12}) \log^2(\alpha_{13}) - \log^2(\alpha_{12}) \log^2(\alpha_{23}) - \log^2(\alpha_{13}) \log^2(\alpha_{23}) \\
& + \frac{1}{3} \log(\alpha_{12}) \log^3(\alpha_{23}) + \frac{1}{3} \log(\alpha_{13}) \log^3(\alpha_{23}) + \frac{2}{3} \log(\alpha_{13}) \log^3(\alpha_{12}) \\
& + \frac{2}{3} \log^3(\alpha_{13}) \log(\alpha_{12}) + \log(\alpha_{23}) \log^3(\alpha_{12}) + \log^3(\alpha_{13}) \log(\alpha_{23}) \\
& - 6 \log(\alpha_{13}) \log^2(\alpha_{12}) - 6 \log^2(\alpha_{13}) \log(\alpha_{12}) - 2 \log(\alpha_{23}) \log^2(\alpha_{12}) \\
& - 2 \log^2(\alpha_{13}) \log(\alpha_{23}) + 2 \log^2(\alpha_{23}) \log(\alpha_{12}) + 2 \log(\alpha_{13}) \log^2(\alpha_{23}) \\
& + \frac{2}{3} \log^3(\alpha_{12}) + \frac{2}{3} \log^3(\alpha_{13}) - \frac{2}{3} \log^3(\alpha_{23}) + 24 \log(\alpha_{12}) \log(\alpha_{13}) \\
& + 4 \log^2(\alpha_{12}) + 4 \log^2(\alpha_{13}) - 4 \log^2(\alpha_{23}) - 32 \log(\alpha_{12}) - 32 \log(\alpha_{13}) \\
& - 24 \zeta_4 + \zeta_3 (12 \log(\alpha_{12}) + 12 \log(\alpha_{13}) - 24) + \zeta_2 (-6 \log^2(\alpha_{12}) \\
& - 6 \log^2(\alpha_{13}) + 6 \log(\alpha_{23}) \log(\alpha_{12}) + 6 \log(\alpha_{13}) \log(\alpha_{23}) \\
& \left. + 12 \log(\alpha_{12}) + 12 \log(\alpha_{13}) - 12 \log(\alpha_{23}) - 24) + 64 \right)
\end{aligned} \tag{C.11}$$



## Appendix D

# Full Calculation of the Three-Line Double Three-Gluon Vertex Diagram

We now consider the diagram in fig. D.1, the set-up is similar to the previous diagram, we have

$$w_{(12),(31)}(\alpha_{12}, \alpha_{13}, \alpha_{23}, \epsilon) \equiv \mathcal{C}_{(12),(31)} \mathcal{F}_{(12),(31)}(\alpha_{12}, \alpha_{13}, \alpha_{23}, \epsilon) \quad (\text{D.1})$$

$$\mathcal{C}_{(12),(31)} \equiv \mathbf{T}_1^a \mathbf{T}_1^d \mathbf{T}_2^b \mathbf{T}_3^c f^{abe} f^{cde} \quad (\text{D.2})$$

$$\begin{aligned} \mathcal{F}_{(12),(31)}(\alpha_{12}, \alpha_{13}, \alpha_{23}, \epsilon) &\equiv \mu^{6\epsilon} g_s^6 \mathcal{N}^5 \int d^d z d^d w \int_0^\infty ds_1 ds_2 ds_3 ds_4 \\ &\times \beta_1^{\sigma_1} \beta_2^{\sigma_2} \beta_3^{\sigma_3} \beta_4^{\sigma_4} e^{-im \sum_i s_i \sqrt{|\beta_i|^2 - i0}} \\ &\times \Gamma_{\sigma_1 \sigma_2 \tau}(\partial_{s_1 \beta_1 - z}, \partial_{s_2 \beta_2 - z}, \partial_{w - z}) \\ &\times \Gamma_{\sigma_3 \sigma_4}{}^\tau(\partial_{s_3 \beta_3 - w}, \partial_{s_4 \beta_1 - w}, \partial_{z - w}) \\ &\times (-(s_1 \beta_1 - z)^2 + i0)^{\epsilon-1} (-(s_2 \beta_2 - z)^2 + i0)^{\epsilon-1} \\ &\times (-(s_3 \beta_3 - w)^2 + i0)^{\epsilon-1} (-(s_4 \beta_1 - w)^2 + i0)^{\epsilon-1} \\ &\times (-(z - w)^2 + i0)^{\epsilon-1} \theta(s_4 < s_1). \end{aligned} \quad (\text{D.3})$$

A brief note about the colour factor  $\mathcal{C}_{(12),(31)}$  is in order. We are interested in the coefficient of the colour factor  $f^{abe} f^{cde} \{\mathbf{T}_1^a, \mathbf{T}_1^d\} \mathbf{T}_2^b \mathbf{T}_2^c$ . This colour factor is

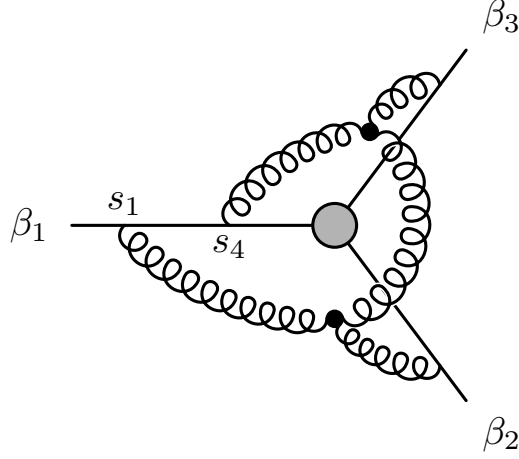


**Figure D.1** *Hard three-line double three gluon vertex*

produced by the symmetric combination of kinematic factors, i.e.

$$\begin{aligned}
& w_{(12),(31)}(\alpha_{12}, \alpha_{13}, \alpha_{23}, \epsilon) + w_{(12),(31)}(\alpha_{13}, \alpha_{12}, \alpha_{23}, \epsilon) \\
&= \frac{1}{2} f^{abe} f^{cde} \{ \mathbf{T}_1^a, \mathbf{T}_1^d \} \mathbf{T}_2^b \mathbf{T}_2^c \\
&\times \left( \mathcal{F}_{(12),(31)}(\alpha_{12}, \alpha_{13}, \alpha_{23}, \epsilon) + \mathcal{F}_{(12),(31)}(\alpha_{13}, \alpha_{12}, \alpha_{23}, \epsilon) \right) \quad (\text{D.4}) \\
&+ \frac{1}{2} f^{abe} f^{cde} [ \mathbf{T}_1^a, \mathbf{T}_1^d ] \mathbf{T}_2^b \mathbf{T}_2^c \\
&\times \left( \mathcal{F}_{(12),(31)}(\alpha_{12}, \alpha_{13}, \alpha_{23}, \epsilon) - \mathcal{F}_{(12),(31)}(\alpha_{13}, \alpha_{12}, \alpha_{23}, \epsilon) \right)
\end{aligned}$$

The symmetric kinematic combination holds some simplification in terms of computational time due to the cancellation of some terms in the MB integral we ultimately obtain. Therefore, we will proceed by calculating a single term  $\mathcal{F}_{(12),(31)}(\alpha_{12}, \alpha_{13}, \alpha_{23}, \epsilon)$  only until we perform the differentiations associated with the three-gluon vertices, after which we will only have results for the symmetric combination we require for our calculation.

As usual, we rescale the integration parameters by  $\alpha/|\beta_i^2|$  and rewrite the derivatives in terms of the Wilson line integration parameters to obtain

$$\begin{aligned}
\mathcal{F}_{(12),(31)}^{(3,-1)}(\alpha_{12}, \alpha_{13}, \alpha_{23}) &\equiv \frac{1}{(4\pi)^3} \frac{2}{3} \frac{1}{\pi^4} \int d^d z d^d w \int_0^\infty dy_1 dy_2 dy_3 dy_4 \\
&\times \beta_1^{\sigma_1} \beta_2^{\sigma_2} \beta_3^{\sigma_3} \beta_4^{\sigma_4} \delta \left( 1 - \sum_i y_i \right) \\
&\times \Gamma_{\sigma_1 \sigma_2 \tau} (\partial_{y_1 \beta_1}, \partial_{y_2 \beta_2}, -\partial_{y_1 \beta_1} - \partial_{y_2 \beta_2}) \\
&\times \Gamma_{\sigma_3 \sigma_4}{}^\tau (\partial_{y_3 \beta_3}, \partial_{y_4 \beta_4}, -\partial_{y_3 \beta_3} - \partial_{y_4 \beta_4}) \\
&\times (- (y_1 \beta_1 - z)^2 + i0)^{\epsilon-1} (- (y_2 \beta_2 - z)^2 + i0)^{\epsilon-1} \\
&\times (- (y_3 \beta_3 - w)^2 + i0)^{\epsilon-1} (- (y_4 \beta_4 - w)^2 + i0)^{\epsilon-1} \\
&\times (- (z - w)^2 + i0)^{\epsilon-1} \theta(y_4 < y_1). \quad (\text{D.5})
\end{aligned}$$

Next, we may insert our MB representation of the diagonal box and introduce  $y_{ij} \equiv (y_i \beta_i - y_j \beta_j)^2, \beta_4 = \beta_1$ , this yields

$$\begin{aligned}
\mathcal{F}_{(12),(31)}^{(3,-1)}(\alpha_{12}, \alpha_{13}, \alpha_{23}) &\equiv \frac{1}{(4\pi)^3} \frac{2}{3} \int_0^\infty dy_1 dy_2 dy_3 dy_4 \\
&\times \beta_1^{\sigma_1} \beta_2^{\sigma_2} \beta_3^{\sigma_3} \beta_1^{\sigma_4} \delta \left( 1 - \sum_i y_i \right) \theta(y_4 < y_1) \\
&\times \Gamma_{\sigma_1 \sigma_2 \tau}(\partial_{y_1 \beta_1}, \partial_{y_2 \beta_2}, -\partial_{y_1 \beta_1} - \partial_{y_2 \beta_2}) \\
&\times \Gamma_{\sigma_3 \sigma_4}{}^\tau(\partial_{y_3 \beta_3}, \partial_{y_4 \beta_1}, -\partial_{y_3 \beta_3} - \partial_{y_4 \beta_1}) \\
&\times \left( \prod_{\substack{i < j \\ (i,j) \neq (1,4)}} \frac{1}{(2\pi i)} \int_{-i\infty}^{i\infty} dt_{ij} \left( \frac{y_{ij}}{y_{14}} \right)^{t_{ij}} \Gamma(-t_{ij}) \right) \\
&\times \Gamma(-t_{12} - t_{13} - t_{23}) \Gamma(-t_{23} - t_{24} - t_{34}) \\
&\times \Gamma(1 + t_{12} + t_{23} + t_{24}) \Gamma(1 + t_{13} + t_{23} + t_{34}) \\
&\times \Gamma(1 + t_{12} + t_{13} + t_{23} + t_{24} + t_{34}) \\
&\times \frac{\Gamma(t_{34} - t_{12})}{\Gamma(1 + t_{34} - t_{12})} (\psi(-t_{12}) - \psi(-t_{34})).
\end{aligned} \tag{D.6}$$

We now apply the differentiation as we did in the four-line case. The parameter integration is then identical in form to the one we performed for the four-gluon vertex diagram in Appendix C.

After asymptotic expansion, we obtain a large set of MB integrals, most of which we perform analytically. However, we were unable to analytically evaluate the constant and the coefficient of a single logarithmic term. Performing numerical evaluations using the tools provided in [77], we obtain the following expression for



the required symmetric combination of diagrams.

$$\begin{aligned}
& \mathcal{F}_{(12),(31)}^{(3,-1)}(\alpha_{12}, \alpha_{13}, \alpha_{23}) + \mathcal{F}_{(12),(31)}^{(3,-1)}(\alpha_{13}, \alpha_{12}, \alpha_{23}) = \\
& -\frac{1}{6} \frac{1}{(4\pi)^3} \left[ -\frac{1}{3} \log^5(\alpha_{12}) - \frac{1}{3} \log^5(\alpha_{13}) \right. \\
& + \frac{2}{3} \log^4(\alpha_{13}) + \frac{2}{3} \log^4(\alpha_{12}) - \frac{4}{3} \log^3(\alpha_{12}) \\
& + \frac{4}{3} \log^3(\alpha_{23}) - \frac{4}{3} \log^3(\alpha_{13}) + 8 \log^2(\alpha_{23}) \\
& + \frac{5}{3} \log(\alpha_{13}) \log^4(\alpha_{12}) + \frac{5}{3} \log^4(\alpha_{13}) \log(\alpha_{12}) \\
& - \frac{2}{3} \log(\alpha_{23}) \log^4(\alpha_{12}) + \frac{1}{3} \log^4(\alpha_{23}) \log(\alpha_{12}) \\
& + \frac{1}{3} \log(\alpha_{13}) \log^4(\alpha_{23}) - \frac{2}{3} \log^2(\alpha_{13}) \log^3(\alpha_{12}) \\
& - \frac{2}{3} \log^3(\alpha_{13}) \log^2(\alpha_{12}) - \frac{4}{3} \log^3(\alpha_{23}) \log^2(\alpha_{12}) \\
& - \frac{4}{3} \log^2(\alpha_{13}) \log^3(\alpha_{23}) + 2 \log^2(\alpha_{23}) \log^3(\alpha_{12}) \\
& + 2 \log^3(\alpha_{13}) \log^2(\alpha_{23}) + \frac{4}{3} \log(\alpha_{13}) \log^3(\alpha_{23}) \log(\alpha_{12}) \\
& - \frac{4}{3} \log(\alpha_{13}) \log(\alpha_{23}) \log^3(\alpha_{12}) - \frac{4}{3} \log^3(\alpha_{13}) \log(\alpha_{23}) \log(\alpha_{12}) \\
& - 2 \log(\alpha_{13}) \log^2(\alpha_{23}) \log^2(\alpha_{12}) + 4 \log^2(\alpha_{13}) \log(\alpha_{23}) \log^2(\alpha_{12}) \\
& - 2 \log^2(\alpha_{13}) \log^2(\alpha_{23}) \log(\alpha_{12}) + 2 \log(\alpha_{13}) \log(\alpha_{23}) \log^2(\alpha_{12}) \quad (D.7) \\
& - \frac{4}{3} \log^3(\alpha_{13}) \log(\alpha_{12}) - \frac{2}{3} \log^3(\alpha_{23}) \log(\alpha_{12}) \\
& - \frac{4}{3} \log(\alpha_{13}) \log^3(\alpha_{12}) - \frac{2}{3} \log(\alpha_{13}) \log^3(\alpha_{23}) \\
& - \frac{2}{3} \log^4(\alpha_{13}) \log(\alpha_{23}) + 4 \log(\alpha_{23}) \log^2(\alpha_{12}) \\
& - 4 \log^2(\alpha_{23}) \log(\alpha_{12}) + 2 \log^2(\alpha_{23}) \log^2(\alpha_{12}) \\
& + 2 \log^2(\alpha_{13}) \log(\alpha_{23}) \log(\alpha_{12}) - 2 \log(\alpha_{23}) \log^3(\alpha_{12}) \\
& - 4 \log^2(\alpha_{13}) \log^2(\alpha_{12}) + 2 \log^2(\alpha_{13}) \log^2(\alpha_{23}) \\
& - 4 \log(\alpha_{13}) \log^2(\alpha_{23}) - 2 \log^3(\alpha_{13}) \log(\alpha_{23}) \\
& + 4 \log^2(\alpha_{13}) \log(\alpha_{23}) - 4(3\zeta_2 + 2\zeta_3) \log(\alpha_{13}) \log(\alpha_{23}) \\
& + \log(\alpha_{13})(12 - 8\zeta_2) \log^2(\alpha_{12}) \\
& + \log^2(\alpha_{13})(12\zeta_2 + 8\zeta_3 - 8) + 24(\zeta_2 - \zeta_4) \log(\alpha_{23}) \\
& + 8(\zeta_2 - 1) \log(\alpha_{13}) \log(\alpha_{23}) \log(\alpha_{12}) \\
& + \log^2(\alpha_{13})(12 - 8\zeta_2) \log(\alpha_{12}) \\
& - 4 \log(\alpha_{23})(3\zeta_2 + 2\zeta_3) \log(\alpha_{12}) \\
& - 16(2\zeta_2 - 2\zeta_3 + 3) \log(\alpha_{13}) \log(\alpha_{12}) \\
& + ((50.1 \pm 0.1) - 24\zeta_2 - 24\zeta_3 + 24\zeta_4) (\log(\alpha_{12}) \log(\alpha_{13})) \\
& \left. + (25.85 \pm 1.25) \right]
\end{aligned}$$

The result is clearly symmetric in interchanging  $\alpha_{12}$  and  $\alpha_{13}$ , as expected. We see a large number of terms of transcendental weight less than five, all of which must cancel in the final sum of all diagrams.



# Appendix E

## Full Calculation of the 311-Web

According to [16] (diagram A, in Appendix A.2.4), the full expression for this web is

$$\bar{w}_{(311)}(\alpha_{12}, \alpha_{13}) = \mathcal{C}_{(311)} \mathcal{F}_{(311)}(\alpha_{12}, \alpha_{13}) \quad (\text{E.1})$$

$$\mathcal{C}_{(311)} \equiv f^{ade} f^{bce} \{ \mathbf{T}_1^a, \mathbf{T}_1^d \} \mathbf{T}_2^b \mathbf{T}_3^c \quad (\text{E.2})$$

$$\begin{aligned} \mathcal{F}_{(311)} = & -\frac{i}{2} \mathcal{N}^4 (ig_s \mu^\epsilon)^6 (\beta_2 \cdot \beta_1) \beta_3^\mu \beta_1^\nu \beta_1^\rho \int d^d z \int_0^\infty ds_2 ds_3 ds_{1,1} ds_{1,2} ds_{1,3} \\ & \times \theta(s_{1,3} > s_{1,2}) \theta(s_{1,2} > s_{1,1}) \Gamma_{\mu\nu\rho} (\partial_{s_2 \beta_3 - z}, \partial_{s_{1,1} \beta_1 - z}, \partial_{s_{1,3} \beta_1 - z}) \\ & \times \left( -(s_2 \beta_2 - s_{1,2} \beta_1)^2 + i0 \right)^{\epsilon-1} \left( -(s_2 \beta_3 - z)^2 + i0 \right)^{\epsilon-1} \\ & \times \left( -(s_{1,1} \beta_1 - z)^2 + i0 \right)^{\epsilon-1} \left( -(s_{1,3} \beta_1 - z)^2 + i0 \right)^{\epsilon-1} \\ & \times e^{-im \left( s_2 \sqrt{\beta_2^2 - i0} + s_2 \sqrt{\beta_3^2 - i0} + (s_{1,1} + s_{1,2} + s_{1,3}) \sqrt{\beta_1^2 - i0} \right)} \end{aligned} \quad (\text{E.3})$$

As usual, we rescale our integration variables by  $s_i \rightarrow s_i / \sqrt{\beta_i^2}$  for normalisation, then we introduce the following rescalings

$$\begin{pmatrix} s_2 \\ s_{1,2} \end{pmatrix} = \lambda \begin{pmatrix} a \\ 1 - a \end{pmatrix}, \quad (\text{E.4})$$

$$\begin{pmatrix} s_2 \\ s_{1,1} \\ s_{1,3} \end{pmatrix} = \kappa \begin{pmatrix} x_1 \\ x_2 \\ x_3 \end{pmatrix}, \quad (\text{E.5})$$

with Jacobians  $\lambda$  and  $\kappa^2$  and the requirement  $\sum_i x_i = 1$ . This yields

$$\begin{aligned}
\mathcal{F}_{(311)} &= -i\mathcal{N}^4 (g_s \mu^\epsilon)^6 \frac{\gamma_{12}}{4} \hat{\beta}_2^\mu \hat{\beta}_3^\nu \hat{\beta}_3^\rho \int_0^\infty d\lambda \lambda^{2\epsilon-1} \int_0^\infty d\kappa \kappa^{4\epsilon-1} e^{-im(\kappa+\lambda)} \\
&\times \int_0^1 da \int dx_1 dx_2 dx_3 \times \delta \left( 1 - \sum_i x_i \right) \theta(\kappa x_3 > \lambda(1-a)) \\
&\times \theta(\lambda(1-a) > \kappa x_2) \left( -(a\beta_2 - (1-a)\beta_1)^2 + i0 \right)^{\epsilon-1} \\
&\times \Gamma_{\mu\nu\rho}(\partial_{x_1\beta_3}, \partial_{x_2\beta_1}, \partial_{x_3\beta_1}) \int d^d z \left( -(x_1\beta_3 - z)^2 + i0 \right)^{\epsilon-1} \\
&\times \left( -(x_2\beta_1 - z)^2 + i0 \right)^{\epsilon-1} \left( -(x_3\beta_1 - z)^2 + i0 \right)^{\epsilon-1}
\end{aligned} \tag{E.6}$$

We perform one more transformation in order to integrate over the exponential regulator, namely

$$\begin{pmatrix} \kappa \\ \lambda \end{pmatrix} = \eta \begin{pmatrix} b \\ 1-b \end{pmatrix}. \tag{E.7}$$

This transformation then yields

$$\begin{aligned}
\mathcal{F}_{(311)} &= -i\mathcal{N}^4 (g_s \mu^\epsilon)^6 \frac{\gamma_{12}}{4} \hat{\beta}_2^\mu \hat{\beta}_3^\nu \hat{\beta}_3^\rho \int_0^\infty d\eta \eta^{6\epsilon-1} e^{-im\eta} \int_0^1 db (b)^{4\epsilon-1} (1-b)^{2\epsilon-1} \\
&\times \int_0^1 da \int dx_1 dx_2 dx_3 \delta \left( 1 - \sum_i x_i \right) \theta(bx_3 > (1-b)(1-a)) \\
&\times \theta((1-b)(1-a) > bx_2) \left( -(a\beta_2 - (1-a)\beta_1)^2 + i0 \right)^{\epsilon-1} \\
&\times \Gamma_{\mu\nu\rho}(\partial_{x_1\beta_3}, \partial_{x_2\beta_1}, \partial_{x_3\beta_1}) \int d^d z \left( -(x_1\beta_3 - z)^2 + i0 \right)^{\epsilon-1} \\
&\times \left( -(x_2\beta_1 - z)^2 + i0 \right)^{\epsilon-1} \left( -(x_3\beta_1 - z)^2 + i0 \right)^{\epsilon-1}
\end{aligned} \tag{E.8}$$

The integral over  $\eta$  can now be performed, yielding an overall UV pole. Since the diagram does not have further subdivergences, we then simply expand in  $\epsilon$ , retaining only the pole term.

$$\begin{aligned}
\mathcal{F}_{(311)}^{(3,-1)} &= -i \frac{2}{3} \frac{1}{(4\pi)^3} \gamma_{12} \hat{\beta}_2^\mu \hat{\beta}_3^\nu \hat{\beta}_3^\rho \int_0^1 \frac{db}{b(1-b)} \int_0^1 da \int dx_1 dx_2 dx_3 \\
&\times \delta \left( 1 - \sum_i x_i \right) \theta(bx_3 > (1-b)(1-a)) \theta((1-b)(1-a) > bx_2) \\
&\times \left( -(a\beta_2 - (1-a)\beta_1)^2 + i0 \right)^{-1} \Gamma_{\mu\nu\rho}(\partial_{x_1\beta_3}, \partial_{x_2\beta_1}, \partial_{x_3\beta_1}) \\
&\times \frac{1}{\pi^2} \int d^d z \left( -(x_1\beta_3 - z)^2 + i0 \right)^{-1} \\
&\times \left( -(x_2\beta_1 - z)^2 + i0 \right)^{-1} \left( -(x_3\beta_1 - z)^2 + i0 \right)^{-1}.
\end{aligned} \tag{E.9}$$

The integral over  $b$  is now trivial to perform, we obtain

$$\begin{aligned}
\mathcal{F}_{(311)}^{(3,-1)} &= -i\gamma_{12}\hat{\beta}_2^\mu\hat{\beta}_3^\nu\hat{\beta}_3^\rho \int_0^1 da \int dx_1 dx_2 dx_3 \delta\left(1 - \sum_i x_i\right) \theta(x_3 > x_2) \\
&\times \log\left(\frac{x_3}{x_2}\right) \left(- (a\beta_2 - (1-a)\beta_1)^2 + i0\right)^{-1} \Gamma_{\mu\nu\rho}(\partial_{x_1\beta_3}, \partial_{x_2\beta_1}, \partial_{x_3\beta_1}) \\
&\times \int \frac{1}{\pi^2} d^d z \left(- (x_1\beta_3 - z)^2 + i0\right)^{-1} \left(- (x_2\beta_1 - z)^2 + i0\right)^{-1} \\
&\times \left(- (x_3\beta_1 - z)^2 + i0\right)^{-1}
\end{aligned} \tag{E.10}$$

Furthermore, the integral over  $a$  is an MGEW basis function, specifically  $\frac{r(\alpha_{12})}{\gamma_{12}}M_{0,0,0}(\alpha_{12})$ . We therefore find

$$\begin{aligned}
\mathcal{F}_{(311)}^{(-1)} &= -i\frac{2}{3}\frac{1}{(4\pi)^3}r(\alpha_{12})M_{0,0,0}(\alpha_{12})\hat{\beta}_2^\mu\hat{\beta}_3^\nu\hat{\beta}_3^\rho \int dx_1 dx_2 dx_3 \\
&\times \delta\left(1 - \sum_i x_i\right) \theta(x_3 > x_2) \log\left(\frac{x_3}{x_2}\right) \Gamma_{\mu\nu\rho}(\partial_{x_1\beta_3}, \partial_{x_2\beta_1}, \partial_{x_3\beta_1}) \\
&\times \frac{1}{\pi^2} \int d^d z \left(- (x_1\beta_3 - z)^2 + i0\right)^{-1} \left(- (x_2\beta_1 - z)^2 + i0\right)^{-1} \\
&\times \left(- (x_3\beta_1 - z)^2 + i0\right)^{-1}
\end{aligned} \tag{E.11}$$

Finally, looking at the  $z$ -integral it is a scalar triangle with dual momenta  $p_i$  defined as follows

$$\begin{pmatrix} p_1 \\ p_2 \\ p_3 \end{pmatrix} = \begin{pmatrix} x_1\beta_3 - x_3\beta_1 \\ x_2\beta_1 - x_1\beta_3 \\ x_3\beta_1 - x_2\beta_1 \end{pmatrix} \tag{E.12}$$

We therefore obtain

$$\begin{aligned}
\mathcal{F}_{(311)}^{(-1)} &= \frac{2}{3}\frac{1}{(4\pi)^3}r(\alpha_{12})M_{0,0,0}(\alpha_{12})\hat{\beta}_2^\mu\hat{\beta}_3^\nu\hat{\beta}_3^\rho \int dx_1 dx_2 dx_3 \\
&\times \delta\left(1 - \sum_i x_i\right) \theta(x_3 > x_2) \left.\frac{d}{da}\left(\frac{x_3}{x_2}\right)^a\right|_{a=0} \\
&\times \Gamma_{\mu\nu\rho}(\partial_{x_1\beta_3}, \partial_{x_2\beta_1}, \partial_{x_3\beta_1}) T(\{p_i^2\}, \{1\}, 4)
\end{aligned} \tag{E.13}$$

The calculation now proceeds in the same way as it did for the three gluon vertex diagram in chapter 2. Taking the asymptotic light-like limit, we obtain

$$\begin{aligned}
\mathcal{F}_{(311),ll}^{(3,-1)}(\alpha_{12}, \alpha_{13}) &= \frac{2}{3}\frac{1}{(4\pi)^3} \log(\alpha_{12}) \\
&\times \left(\frac{1}{3} \log^4(\alpha_{13}) + 4(\zeta_3 - 2\zeta_2)(1 + \log(\alpha_{13})) - 3\zeta_4\right)
\end{aligned} \tag{E.14}$$



# Appendix F

## Collinear reduction of the 23-Web

We wish to find an expression for  $w_{(23)}$ , as depicted in fig. F.1. Our main problem is that we only have light-like results for  $w_{(311)}$ , which we might have used to obtain  $w_{(23)}$ . However, we may attempt to use what we know about the structure of  $w_{1121}$  to obtain what we need.

We recall that  $w_{1121}$  may be written as in eq. (5.7):

$$\mathcal{C}_{1121} = f^{abe} f^{cde} \mathbf{T}_1^a \mathbf{T}_2^b \mathbf{T}_3^c \mathbf{T}_4^d \quad (\text{F.1})$$

$$\begin{aligned} \mathcal{F}_{1121}^{(3,-1)}(\alpha_{12}, \alpha_{13}, \alpha_{23}, \alpha_{34}) &= \frac{1}{3} \frac{1}{(4\pi)^3} (M_{0,0,0}(\alpha_{34}) t_1(\alpha_{12}, \alpha_{13}, \alpha_{23}) \\ &\quad - 2M_{1,0,0}(\alpha_{34}) t_0(\alpha_{12}, \alpha_{13}, \alpha_{23})). \end{aligned} \quad (\text{F.2})$$

Crucially,  $t_0$  is antisymmetric under the interchange of any two  $\beta_i$  in the light-like limit (it is the light-like limit of the three-gluon vertex diagram in eq. (2.22)).

If we consider the limit  $\beta_3 \rightarrow \beta_2$  of  $\mathcal{F}_{(1121)}$ , we find that we may recover the

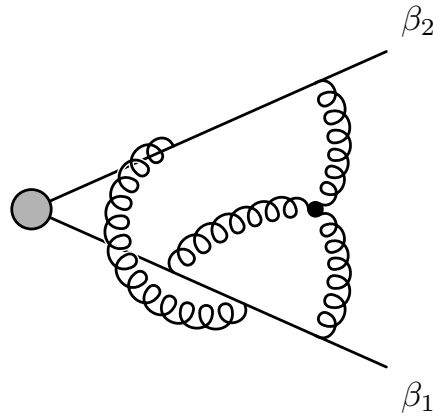


**Figure F.1** *Representative diagram of the 23-web.*



311-web:

$$\begin{aligned} w_{(311)}(\alpha_{24}, \alpha_{12}) &= w_{1121}(\alpha_{12}, \alpha_{12}, 1, \alpha_{24}) \\ &= -\frac{1}{2} f^{abe} f^{cde} \mathbf{T}_1^a \{ \mathbf{T}_2^b, \mathbf{T}_2^d \} \mathbf{T}_4^c M_{0,0,0}(\alpha_{24}) t_1(\alpha_{12}, \alpha_{12}, 1), \end{aligned} \quad (\text{F.3})$$

where we have used the fact that due to its antisymmetry,  $t_0(\alpha_{12}, \alpha_{12}, 1) = 0$ . This result is true without taking the light-like limit.

If we now wish to obtain  $w_{(32)}$ , we may consider the reduction  $4 \parallel 1$ , this yields

$$\begin{aligned} w_{(32)}(\alpha_{12}) &= w_{(311)}(\alpha_{12}, \alpha_{12}) \\ &= \frac{1}{4} f^{ace} f^{bde} \{ \mathbf{T}_1^a, \mathbf{T}_1^b \} \{ \mathbf{T}_2^c, \mathbf{T}_2^d \} M_{0,0,0}(\alpha_{12}) t_1(\alpha_{12}, \alpha_{12}, 1). \end{aligned} \quad (\text{F.4})$$

We can now obtain  $w_{(32)}$  by solving eq. (F.3) for  $t_1(\alpha_{12}, \alpha_{12}, 1)$ , we find

$$\mathcal{F}_{(32)}(\alpha_{12}) = -\frac{1}{2} \mathcal{F}_{(311)}(\alpha_{24}, \alpha_{12}) \frac{M_{0,0,0}(\alpha_{12})}{M_{0,0,0}(\alpha_{24})}. \quad (\text{F.5})$$

Taking the light-like limit and inserting eq. (5.34) we find

$$\begin{aligned} \mathcal{C}_{(32)} &= f^{ace} f^{bde} \{ \mathbf{T}_1^a, \mathbf{T}_1^b \} \{ \mathbf{T}_2^c, \mathbf{T}_2^d \} \\ \mathcal{F}_{(32),ll}^{(3,-1)}(\alpha_{12}) &= -\frac{1}{6} \frac{1}{(4\pi)^3} \left[ \frac{8}{3} \log^5(\alpha_{12}) + (32\zeta_3 - 64\zeta_2) \log^2(\alpha_{12}) \right. \\ &\quad \left. - (64\zeta_2 - 32\zeta_3 + 24\zeta_4) \log(\alpha_{12}) \right]. \end{aligned} \quad (\text{F.6}) \quad (\text{F.7})$$

# Bibliography

- [1] Ø. Almelid, C. Duhr, and E. Gardi, *Three-loop corrections to the soft anomalous dimension in multi-leg scattering*, arXiv:1507.00047.
- [2] K. G. Wilson and J. B. Kogut, *The Renormalization group and the epsilon expansion*, *Phys. Rept.* **12** (1974) 75–200.
- [3] B. Delamotte, *A Hint of renormalization*, *Am. J. Phys.* **72** (2004) 170–184, [hep-th/0212049].
- [4] M. E. Peskin and D. V. Schroeder, *An Introduction to quantum field theory*. 1995.
- [5] A. Zee, *Quantum field theory in a nutshell*. 2003.
- [6] S. Catani, *The Singular behavior of QCD amplitudes at two loop order*, *Phys. Lett.* **B427** (1998) 161–171, [hep-ph/9802439].
- [7] F. Bloch and A. Nordsieck, *Note on the Radiation Field of the electron*, *Phys. Rev.* **52** (1937) 54–59.
- [8] T. Kinoshita, *Mass singularities of Feynman amplitudes*, *J. Math. Phys.* **3** (1962) 650–677.
- [9] T. D. Lee and M. Nauenberg, *Degenerate Systems and Mass Singularities*, *Phys. Rev.* **133** (1964) B1549–B1562. [,25(1964)].
- [10] G. F. Sterman, *QCD and jets*, in *Physics in  $D \geq 4$ . Proceedings, Theoretical Advanced Study Institute in elementary particle physics, TASI 2004, Boulder, USA, June 6-July 2, 2004*, pp. 67–145, 2004. hep-ph/0412013.
- [11] G. F. Sterman, *Partons, factorization and resummation, TASI 95*, in *QCD and beyond. Proceedings, Theoretical Advanced Study Institute in Elementary Particle Physics, TASI-95, Boulder, USA, June 4-30, 1995*, 1995. hep-ph/9606312.
- [12] D. R. Yennie, S. C. Frautschi, and H. Suura, *The infrared divergence phenomena and high-energy processes*, *Annals Phys.* **13** (1961) 379–452.

- [13] J. C. Collins, D. E. Soper, and G. F. Sterman, *Factorization of Hard Processes in QCD*, *Adv. Ser. Direct. High Energy Phys.* **5** (1989) 1–91, [[hep-ph/0409313](#)].
- [14] A. Sen, *Asymptotic Behavior of the Wide Angle On-Shell Quark Scattering Amplitudes in Nonabelian Gauge Theories*, *Phys. Rev.* **D28** (1983) 860.
- [15] J. Frenkel and J. C. Taylor, *NONABELIAN EIKONAL EXPONENTIATION*, *Nucl. Phys.* **B246** (1984) 231.
- [16] E. Gardi, J. M. Smillie, and C. D. White, *The Non-Abelian Exponentiation theorem for multiple Wilson lines*, *JHEP* **06** (2013) 088, [[arXiv:1304.7040](#)].
- [17] E. Gardi, J. M. Smillie, and C. D. White, *On the renormalization of multiparton webs*, *JHEP* **09** (2011) 114, [[arXiv:1108.1357](#)].
- [18] G. P. Korchemsky and A. V. Radyushkin, *Renormalization of the Wilson Loops Beyond the Leading Order*, *Nucl. Phys.* **B283** (1987) 342–364.
- [19] G. F. Sterman, *Infrared divergences in perturbative QCD*, *AIP Conf. Proc.* **74** (1981) 22–40.
- [20] E. Gardi, E. Laenen, G. Stavenga, and C. D. White, *Webs in multiparton scattering using the replica trick*, *JHEP* **11** (2010) 155, [[arXiv:1008.0098](#)].
- [21] S. Catani and M. H. Seymour, *The Dipole formalism for the calculation of QCD jet cross-sections at next-to-leading order*, *Phys. Lett.* **B378** (1996) 287–301, [[hep-ph/9602277](#)].
- [22] J. G. M. Gatheral, *Exponentiation of Eikonal Cross-sections in Nonabelian Gauge Theories*, *Phys. Lett.* **B133** (1983) 90.
- [23] A. Mitov, G. Sterman, and I. Sung, *Diagrammatic Exponentiation for Products of Wilson Lines*, *Phys. Rev.* **D82** (2010) 096010, [[arXiv:1008.0099](#)].
- [24] M. Dukes, E. Gardi, H. McAslan, D. J. Scott, and C. D. White, *Webs and Posets*, *JHEP* **01** (2014) 024, [[arXiv:1310.3127](#)].
- [25] M. Dukes, E. Gardi, E. Steingrimsson, and C. D. White, *Web worlds, web-colouring matrices, and web-mixing matrices*, *J. Comb. Theory Ser.* **A120** (2013) 1012–1037, [[arXiv:1301.6576](#)].
- [26] E. Gardi, *From Webs to Polylogarithms*, *JHEP* **04** (2014) 044, [[arXiv:1310.5268](#)].
- [27] S. M. Aybat, L. J. Dixon, and G. F. Sterman, *The Two-loop soft anomalous dimension matrix and resummation at next-to-next-to leading pole*, *Phys. Rev.* **D74** (2006) 074004, [[hep-ph/0607309](#)].

- [28] A. Mitov, G. F. Sterman, and I. Sung, *The Massive Soft Anomalous Dimension Matrix at Two Loops*, *Phys. Rev.* **D79** (2009) 094015, [arXiv:0903.3241].
- [29] A. Mitov, G. F. Sterman, and I. Sung, *Computation of the Soft Anomalous Dimension Matrix in Coordinate Space*, *Phys. Rev.* **D82** (2010) 034020, [arXiv:1005.4646].
- [30] A. Ferroglia, M. Neubert, B. D. Pecjak, and L. L. Yang, *Two-loop divergences of scattering amplitudes with massive partons*, *Phys. Rev. Lett.* **103** (2009) 201601, [arXiv:0907.4791].
- [31] A. Ferroglia, M. Neubert, B. D. Pecjak, and L. L. Yang, *Two-loop divergences of massive scattering amplitudes in non-abelian gauge theories*, *JHEP* **11** (2009) 062, [arXiv:0908.3676].
- [32] T. Becher and M. Neubert, *On the Structure of Infrared Singularities of Gauge-Theory Amplitudes*, *JHEP* **06** (2009) 081, [arXiv:0903.1126]. [Erratum: JHEP11,024(2013)].
- [33] E. Gardi and L. Magnea, *Factorization constraints for soft anomalous dimensions in QCD scattering amplitudes*, *JHEP* **03** (2009) 079, [arXiv:0901.1091].
- [34] S. Caron-Huot, *When does the gluon reggeize?*, *JHEP* **05** (2015) 093, [arXiv:1309.6521].
- [35] L. J. Dixon, E. Gardi, and L. Magnea, *On soft singularities at three loops and beyond*, *JHEP* **02** (2010) 081, [arXiv:0910.3653].
- [36] M. Czakon, A. Mitov, and G. F. Sterman, *Threshold Resummation for Top-Pair Hadroproduction to Next-To-Next-To-Leading Log*, *Phys. Rev.* **D80** (2009) 074017, [arXiv:0907.1790].
- [37] T. Becher and M. Neubert, *Infrared Singularities of Scattering Amplitudes in Perturbative QCD*, *Phys. Rev. Lett.* **102** (2009) 162001, [arXiv:0901.0722]. [Erratum: Phys. Rev. Lett.111,no.19,199905(2013)].
- [38] T. Becher and M. Neubert, *Toward a Nnlo Calculation of the Anti-B  $\rightarrow$  X(S) Gamma Decay Rate with a Cut on Photon Energy: I. Two-Loop Result for the Soft Function*, *Phys. Lett.* **B633** (2006) 739–747, [hep-ph/0512208].
- [39] M. H. Seymour and M. Sjoedahl, *Symmetry of Anomalous Dimension Matrices Explained*, *JHEP* **12** (2008) 066, [arXiv:0810.5756].
- [40] N. Kidonakis and G. F. Sterman, *Resummation for QCD hard scattering*, *Nucl. Phys.* **B505** (1997) 321–348, [hep-ph/9705234].
- [41] L. J. Dixon, *Matter Dependence of the Three-Loop Soft Anomalous Dimension Matrix*, *Phys. Rev.* **D79** (2009) 091501, [arXiv:0901.3414].

- [42] T. Becher and M. Neubert, *Toward a Nnlo Calculation of the Anti-B  $\rightarrow$  X(S) Gamma Decay Rate with a Cut on Photon Energy. II. Two-Loop Result for the Jet Function*, *Phys. Lett.* **B637** (2006) 251–259, [hep-ph/0603140].
- [43] G. P. Korchemsky and G. Marchesini, *Structure Function for Large  $\times$  and Renormalization of Wilson Loop*, *Nucl. Phys.* **B406** (1993) 225–258, [hep-ph/9210281].
- [44] J. Botts and G. F. Sterman, *Hard Elastic Scattering in QCD: Leading Behavior*, *Nucl. Phys.* **B325** (1989) 62.
- [45] J.-y. Chiu, A. Fuhrer, R. Kelley, and A. V. Manohar, *Factorization Structure of Gauge Theory Amplitudes and Application to Hard Scattering Processes at the Lhc*, *Phys. Rev.* **D80** (2009) 094013, [arXiv:0909.0012].
- [46] G. P. Korchemsky, *Asymptotics of the Altarelli-Parisi-Lipatov Evolution Kernels of Parton Distributions*, *Mod. Phys. Lett.* **A4** (1989) 1257–1276.
- [47] M. Sjodahl, *Color Evolution of  $2 \rightarrow 3$  Processes*, *JHEP* **12** (2008) 083, [arXiv:0807.0555].
- [48] A. Kyrieleis and M. H. Seymour, *The Colour Evolution of the Process  $Q Q \rightarrow Q Q G$* , *JHEP* **01** (2006) 085, [hep-ph/0510089].
- [49] G. F. Sterman and M. E. Tejeda-Yeomans, *Multiloop amplitudes and resummation*, *Phys. Lett.* **B552** (2003) 48–56, [hep-ph/0210130].
- [50] L. J. Dixon, L. Magnea, and G. F. Sterman, *Universal structure of subleading infrared poles in gauge theory amplitudes*, *JHEP* **08** (2008) 022, [arXiv:0805.3515].
- [51] G. P. Korchemsky, *Sudakov Form-Factor in QCD*, *Phys. Lett.* **B220** (1989) 629.
- [52] S. V. Ivanov, G. P. Korchemsky, and A. V. Radyushkin, *Infrared Asymptotics of Perturbative QCD: Contour Gauges*, *Yad. Fiz.* **44** (1986) 230–240. [Sov. J. Nucl. Phys.44,145(1986)].
- [53] G. P. Korchemsky and A. V. Radyushkin, *Loop Space Formalism and Renormalization Group for the Infrared Asymptotics of QCD*, *Phys. Lett.* **B171** (1986) 459–467.
- [54] E. Gardi, *On the Quark Distribution in an On-Shell Heavy Quark and Its All-Order Relations with the Perturbative Fragmentation Function*, *JHEP* **02** (2005) 053, [hep-ph/0501257].
- [55] N. Kidonakis, *Two-Loop Soft Anomalous Dimensions and Nnll Resummation for Heavy Quark Production*, *Phys. Rev. Lett.* **102** (2009) 232003, [arXiv:0903.2561].

- [56] N. Kidonakis, G. Oderda, and G. F. Sterman, *Evolution of color exchange in QCD hard scattering*, *Nucl. Phys.* **B531** (1998) 365–402, [[hep-ph/9803241](#)].
- [57] E. Laenen, L. Magnea, and G. Stavenga, *On Next-To-Eikonal Corrections to Threshold Resummation for the Drell-Yan and Dis Cross Sections*, *Phys. Lett.* **B669** (2008) 173–179, [[arXiv:0807.4412](#)].
- [58] A. Ferroglia, M. Neubert, B. D. Pecjak, and L. L. Yang, *Infrared Singularities and Soft Gluon Resummation with Massive Partons*, *Nucl. Phys. Proc. Suppl.* **205-206** (2010) 98–103, [[arXiv:1006.4680](#)].
- [59] H. Contopanagos, E. Laenen, and G. F. Sterman, *Sudakov Factorization and Resummation*, *Nucl. Phys.* **B484** (1997) 303–330, [[hep-ph/9604313](#)].
- [60] I. A. Korchemskaya and G. P. Korchemsky, *High-Energy Scattering in QCD and Cross Singularities of Wilson Loops*, *Nucl. Phys.* **B437** (1995) 127–162, [[hep-ph/9409446](#)].
- [61] M. Beneke, P. Falgari, and C. Schwinn, *Soft Radiation in Heavy-Particle Pair Production: All-Order Colour Structure and Two-Loop Anomalous Dimension*, *Nucl. Phys.* **B828** (2010) 69–101, [[arXiv:0907.1443](#)].
- [62] L. Magnea, V. Del Duca, C. Duhr, E. Gardi, and C. D. White, *Infrared singularities in the high-energy limit*, *PoS LL2012* (2012) 008, [[arXiv:1210.6786](#)].
- [63] V. Del Duca, C. Duhr, E. Gardi, L. Magnea, and C. D. White, *Infrared Singularities and the High-Energy Limit*, [arXiv:1201.2841](#). [[PoSRADCOR2011,038\(2011\)](#)].
- [64] J. M. Henn and B. Mistlberger, *Four-gluon scattering at three loops, infrared structure and Regge limit*, [arXiv:1608.00850](#).
- [65] N. Kidonakis, G. Oderda, and G. F. Sterman, *Threshold resummation for dijet cross-sections*, *Nucl. Phys.* **B525** (1998) 299–332, [[hep-ph/9801268](#)].
- [66] T. Becher and X. Garcia i Tormo, *Factorization and resummation for transverse thrust*, *JHEP* **06** (2015) 071, [[arXiv:1502.04136](#)].
- [67] T. Becher, X. Garcia i Tormo, and J. Piclum, *Next-to-next-to-leading logarithmic resummation for transverse thrust*, *Phys. Rev.* **D93** (2016), no. 5 054038, [[arXiv:1512.00022](#)]. [Erratum: *Phys. Rev.* **D93**,no.7,079905(2016)].
- [68] T. Becher, M. Neubert, L. Rothen, and D. Y. Shao, *Factorization and Resummation for Jet Processes*, [arXiv:1605.02737](#).
- [69] I. Feige and M. D. Schwartz, *Hard-Soft-Collinear Factorization to All Orders*, *Phys. Rev.* **D90** (2014), no. 10 105020, [[arXiv:1403.6472](#)].
- [70] R. A. Brandt, F. Neri, and M.-a. Sato, *Renormalization of Loop Functions for All Loops*, *Phys. Rev.* **D24** (1981) 879.

- [71] A. Grozin, J. M. Henn, G. P. Korchemsky, and P. Marquard, *Three Loop Cusp Anomalous Dimension in QCD*, *Phys. Rev. Lett.* **114** (2015), no. 6 062006, [arXiv:1409.0023].
- [72] J. C. Collins, *Sudakov form-factors*, *Adv. Ser. Direct. High Energy Phys.* **5** (1989) 573–614, [hep-ph/0312336].
- [73] C. F. Berger, *Soft gluon exponentiation and resummation*. PhD thesis, SUNY, Stony Brook, 2003. hep-ph/0305076.
- [74] V. Del Duca, C. Duhr, E. Gardi, L. Magnea, and C. D. White, *The Infrared structure of gauge theory amplitudes in the high-energy limit*, *JHEP* **12** (2011) 021, [arXiv:1109.3581].
- [75] D. A. Kosower, *All order collinear behavior in gauge theories*, *Nucl. Phys.* **B552** (1999) 319–336, [hep-ph/9901201].
- [76] V. A. Smirnov, *Evaluating Feynman integrals*, *Springer Tracts Mod. Phys.* **211** (2004) 1–244.
- [77] M. Czakon, *Automatized analytic continuation of Mellin-Barnes integrals*, *Comput. Phys. Commun.* **175** (2006) 559–571, [hep-ph/0511200].
- [78] A. V. Smirnov and V. A. Smirnov, *On the Resolution of Singularities of Multiple Mellin-Barnes Integrals*, *Eur. Phys. J.* **C62** (2009) 445–449, [arXiv:0901.0386].
- [79] C. Anastasiou, C. Duhr, F. Dulat, and B. Mistlberger, *Soft triple-real radiation for Higgs production at N<sup>3</sup>LO*, *JHEP* **07** (2013) 003, [arXiv:1302.4379].
- [80] M. Czakon, “mbasymptotics.” <https://mbtools.hepforge.org/>.
- [81] A. B. Goncharov, *Galois symmetries of fundamental groupoids and noncommutative geometry*, *Duke Math. J.* **128** (2005) 209, [math/0208144].
- [82] C. Duhr, *Hopf algebras, coproducts and symbols: an application to Higgs boson amplitudes*, *JHEP* **08** (2012) 043, [arXiv:1203.0454].
- [83] C. Duhr, *Mathematical aspects of scattering amplitudes*, in *Theoretical Advanced Study Institute in Elementary Particle Physics: Journeys Through the Precision Frontier: Amplitudes for Colliders (TASI 2014) Boulder, Colorado, June 2-27, 2014*, 2014. arXiv:1411.7538.
- [84] A. B. Goncharov, *Multiple polylogarithms, cyclotomy and modular complexes*, *Math. Res. Lett.* **5** (1998) 497–516, [arXiv:1105.2076].
- [85] A. B. Goncharov, *Multiple polylogarithms and mixed Tate motives*, math/0103059.

- [86] S. Abreu, R. Britto, C. Duhr, and E. Gardi, *From multiple unitarity cuts to the coproduct of Feynman integrals*, *JHEP* **10** (2014) 125, [[arXiv:1401.3546](#)].
- [87] E. Panzer, *Feynman integrals and hyperlogarithms*. PhD thesis, Humboldt U., Berlin, Inst. Math., 2015. [arXiv:1506.07243](#).
- [88] F. C. Brown, *Polylogarithmes multiples uniformes en une variable*, *Comptes Rendus Mathematique* **338** (2004), no. 7 527 – 532.
- [89] F. Chavez and C. Duhr, *Three-mass triangle integrals and single-valued polylogarithms*, *JHEP* **11** (2012) 114, [[arXiv:1209.2722](#)].
- [90] L. J. Dixon, C. Duhr, and J. Pennington, *Single-valued harmonic polylogarithms and the multi-Regge limit*, *JHEP* **10** (2012) 074, [[arXiv:1207.0186](#)].
- [91] E. W. Barnes, *A new development of the theory of the hypergeometric functions.*, *Proc. Lond. Math. Soc. (2)* **6** (1908) 141–177.
- [92] E. W. Barnes, *A transformation of generalised hypergeometric series.*, *Quart. J.* **41** (1910) 136–140.
- [93] M. Harley, *Multiparton Webs in Non-abelian Gauge Theories at Three Loops and Beyond*. PhD thesis, University of Edinburgh, 2015.
- [94] R. Lodin, *Basis Functions for Webs with Boomerang Gluons*, Master’s thesis, University of Edinburgh, 2016.
- [95] G. Falcioni, E. Gardi, M. Harley, L. Magnea, and C. D. White, *Multiple Gluon Exchange Webs*, *JHEP* **10** (2014) 10, [[arXiv:1407.3477](#)].
- [96] N. I. Usyukina and A. I. Davydychev, *Exact results for three and four point ladder diagrams with an arbitrary number of rungs*, *Phys. Lett.* **B305** (1993) 136–143.
- [97] T. Hahn, *CUBA: A Library for multidimensional numerical integration*, *Comput. Phys. Commun.* **168** (2005) 78–95, [[hep-ph/0404043](#)].
- [98] H. N. Minh, M. Petitot, and J. Van der Hoeven, *Polylogarithms and shuffle algebra*, FPSAC, 1998.
- [99] A. I. Davydychev, *General results for massive  $N$  point Feynman diagrams with different masses*, *J. Math. Phys.* **33** (1992) 358–369.